

**Importance of the *TP53* Family and the DNA Damage  
Repair Machinery in Overcoming Targeted Therapy  
Resistance in Malignant Melanoma**

**Dissertation**

der Mathematisch-Naturwissenschaftlichen Fakultät

der Eberhard Karls Universität Tübingen

zur Erlangung des Grades eines

Doktors der Naturwissenschaften

(Dr. rer. nat.)

vorgelegt von

Lisa Marie Fröhlich

aus Kitzingen

Tübingen

2023

Gedruckt mit Genehmigung der Mathematisch-Naturwissenschaftlichen Fakultät der Eberhard Karls Universität Tübingen.

Tag der mündlichen Qualifikation:

26.10.2023

Dekan:

Prof. Dr. Thilo Stehle

1. Berichterstatterin:

Prof. Dr. Birgit Schitteck

2. Berichterstatter:

Prof. Dr. Robert Feil

## Table of Contents

Table of Contents .....	2
1. List of Figures .....	5
2. List of Abbreviations .....	6
3. Summary .....	12
4. Zusammenfassung .....	14
5. List of Publications in the Thesis .....	16
5.1. Accepted Publications .....	16
5.2. Submitted Publication .....	16
6. Personal Contribution .....	17
6.1. Accepted Publication I .....	17
6.2. Accepted Publication II .....	17
6.3. Submitted Publication I .....	17
7. Introduction.....	18
7.1. Melanoma.....	18
7.1.1. Development of Melanoma .....	18
7.1.2. Staging of Melanoma .....	19
7.2. Treatment of Malignant Melanoma .....	21
7.2.1. Surgery .....	21
7.2.2. Chemotherapy .....	22
7.2.3. Immunotherapy .....	22
7.2.4. Targeted Therapy .....	24
7.3. p53 family .....	31
7.3.1. Structure of the p53 Family Members .....	31
7.3.2. p53 Family Signaling.....	33
7.3.3. p53 Family in Cancer .....	36
7.3.4. Pharmacological Modulation of p53 Family Members.....	37
7.4. DNA Damage Response .....	38

---

7.4.1.	DNA Repair Pathways .....	39
7.4.2.	DNA Damage Repair in Tumor Predisposition Syndromes.....	45
7.4.3.	DNA Repair Pathways Involved in Melanoma Progression .....	46
7.4.4.	Targeting DDR as an Anti-Cancer Therapy .....	47
8.	Aim of the Thesis.....	52
9.	Results and Discussion .....	53
9.1.	Relevance of MDM2 Inhibitor Treatment in Melanoma Therapy .....	53
9.1.1.	<i>CDKN1A</i> /p21 Levels Correlate with MDM2 Inhibitor Sensitivity.....	53
9.1.2.	MDM2 Inhibitor Treatment Increases BRAF Inhibitor Sensitivity.....	55
9.1.3.	p21 Expression Levels Regulate Sensitivity to Targeted Therapies .....	56
9.2.	Crosstalk Between p53 Family Members and Targets in Melanoma Cells..	57
9.3.	Significance of PARP Inhibitor Treatment in Melanoma Therapy.....	58
9.3.1.	PARP Inhibitor Treatment Effectively Kills BRAF Inhibitor Resistant Melanoma Cells.....	59
9.3.2.	Significance of p53 in PARP Inhibitor Induced Melanoma Cell Death ..	60
9.3.3.	Relevance of ATM in Enhanced PARP Inhibitor Sensitivity of MAPK Inhibitor Resistant Melanoma Cells .....	61
9.3.4.	Synergistic Killing of Melanoma Cells by Combined MAPK Inhibitor and PARP Inhibitor Therapy.....	63
9.3.5.	MAPK Inhibitors Induce Synthetic Lethality in Combination with PARP Inhibitors in Melanoma Cells .....	64
9.3.6.	PARP1 Gene Expression as a Biomarker for PARP Inhibitor Therapy Response .....	66
9.3.7.	High PARP1 Gene Expression Levels Correlate with Metastatic Potential of Melanomas.....	67
9.3.8.	High PARP1 Gene Expression Levels Correlate with Poor Overall Survival of Melanoma Patients.....	68
10.	References .....	70
11.	Appendix.....	96

---

11.1. Accepted Publication I.....	96
11.2. Accepted Publication II.....	110
11.3. Submitted Publication I.....	132
12. Acknowledgments.....	157

## 1. List of Figures

Figure 1: Overview of melanoma development and progression.....	19
Figure 2: Schematic overview of the MAPK signaling pathway. ....	25
Figure 3: Graphical representation of MAPKi resistance mechanisms. ....	30
Figure 4: Structure of the p53 family genes. ....	32
Figure 5: Schematic illustration of p53 canonical signaling.....	35
Figure 6: Graphical representation of the repair of single strand damages. ....	42
Figure 7: Schematic overview of the repair of DSB. ....	45
Figure 8: Schematic illustration of the molecular mechanism of PARPi toxicity.....	50

## 2. List of Abbreviations

A	adenine
ADP	adenosine diphosphate
ALM	acral lentiginous melanoma
aNHEJ	alternative NHEJ
AP site	abasic site, apurinic/apyrimidinic site
APE1	apurinic endonuclease
APTX	aprataxin
ARF	ADP-ribosylation factor
AT	ataxia telangiectasia
ATM	ataxia telangiectasia mutated
ATR	ataxia telangiectasia and Rad3-related
BAP1	BRCA1-associated protein-1
BAP1-TPDS	BAP1 tumor predisposition syndrome
Bcl-2	B-cell lymphoma 2
BIR	break-induced replication
BLM	bloom-syndrome-protein
BOP1	block of proliferation 1
BRAF	v-raf murine sarcoma viral oncogene homolog B1
BRAF <sup>i</sup>	BRAF inhibitor
BRCA1	breast cancer 1
BRCA2	breast cancer 2
CAF	cancer associated fibroblasts
CDK	cyclin dependent kinase
CDKN1A	cyclin dependent kinase inhibitor 1A
CETN2	centrin 2
CHR	cell cycle genes homology region
cNHEJ	classical NHEJ
CNS	central nervous system
CPD	cyclobutane pyrimidine dimers
CS	Cockayne syndrome
CSA	Cockayne syndrome protein A
CSB	Cockayne syndrome protein A
CSD	chronic sun damage

---

CTLA-4	cytotoxic T lymphocyte-associated antigen 4
DBD	DNA binding domain
DDB1	damaged DNA binding protein 1
DDB2	damaged DNA binding protein 2
DDR	DNA damage response
DNA Pol	DNA polymerase
DNA-PK	DNA-dependent protein kinase
DNA-PKcs	DNA-dependent protein kinase, catalytic subunit
DSB	double strand break
DSBR	double strand break repair
dsDNA	double-stranded DNA
DTIC	dacarbazine
DUSP4	dual specificity phosphatase 4
DUSP6	dual specificity phosphatase 6
E	glutamic acid
E2F-1	E2 promoter binding factor 1
EMA	European Medicines Agency
ERCC1	excision repair cross-complementation group 1
ERK1/2	extracellular signal-regulated protein kinase 1/2
EXO1	exonuclease 1
FA	Fanconi anemia
FDA	U.S. Food and Drug Administration
FL	full length
G	guanine
GADD45 $\alpha$	growth arrest and DNA damage-inducible 45 $\alpha$
GAP	GTPase-activating protein
GDP	guanosine diphosphate
GF	growth factor
GGR	global genome repair
GLUT1	glucose transporter 1
GLUT3	glucose transporter 3
GLUT4	glucose transporter 4
GOF	gain of function
GRB2	growth factor receptor-bound protein 2

---

GTP	guanosine triphosphate
HDR	homology directed repair
HGF	hepatocyte growth factor
HIF1- $\alpha$	hypoxia-inducible factor 1 $\alpha$
HRR	homologous recombination repair
Hsp90	heat shock protein 90
ICB	immune checkpoint blockade
interleukin 2	IL-2
interleukin-10	IL-10
interleukin-6	IL-6
IR	ionizing radiation
irAE	immune-related adverse events
LMM	lentigo maligna melanoma
LOF	loss of function
LOH	loss of heterozygosity
LS	lynch syndrome
LST	large-scale state transition
MAP	MUTYH-associated polyposis
MAPK	mitogen-activated protein kinase
MAPKi	MAPK inhibitor
MAPKK	MAPK kinase
MAPKKK	MAPK kinase kinase
MEK1/2	MAP kinase/ERK kinase 1/2
MEKi	MEK inhibitor
MET	mesenchymal epithelial transition
MITF	melanocyte inducing transcription factor
MLH1	MutL homolog 2
MLH3	MutL homolog 2
MMC	mitomycin C
MMR	DNA mismatch repair
MRN	Mre11-Rad50-Nbs1
MSH2	MutS homolog 2
MSH3	MutS homolog 3
MSH6	MutS homolog 6

---

MSI	microsatellite instability
mTOR	mammalian target of rapamycin
N-3-MeA	<i>N</i> -3-methyladenine
N-7-MeG	<i>N</i> -7-methylguanine
NAD	nicotinamide adenine dinucleotide
NF-1	neurofibromin 1
NHEJ	non-homologous end joining
NM	nodular melanoma
NRG1	neuregulin-1
NSG	NOD scid gamma
OD	oligomerization domain
OS	overall survival
PAH	polycyclic aromatic hydrocarbon
PALB2	partner and localizer of BRCA2
panRAFi	panRAF inhibitor
PARP1	poly (ADP-ribose) polymerase 1
PARPi	PARP inhibitor
PARylation	poly-ADP-ribosylation
PCNA	proliferation cell nuclear antigen
PD-1	programmed cell death protein 1 pathway
PDX	patient derived xenograft
PFS	progression free survival
PI3K	phosphoinositide-3-kinase
PIP <sub>2</sub>	phosphatidylinositol 4,5-bisphosphate
PIP <sub>3</sub>	phosphatidylinositol 3,4,5-trisphosphate
PNKP	polynucleotide kinase 3'-phosphate
PR	proline-rich region
PRIMA-1	p53 reactivation and induction of massive apoptosis-1
PTEN	phosphatase and tensin homolog
RAC1	Ras-related C3 botulinum toxin substrate 1
RAF	rapidly accelerated fibrosarcoma
RAS	rat sarcoma
RB	retinoblastoma
RFC	replication factor C

---

RGP	radial growth phase
RHOB	Ras homolog gene family, member B
RNAPII $\alpha$	RNA Polymerase II
ROS	reactive oxygen species
RPA	replication protein A
RTK	receptor tyrosine kinase
SAM	sterile alpha motif
SDSA	synthesis-dependent strand annealing
SOS	son of sevenless
SSA	single strand annealing
SSB	single strand break
SSBR	single strand break repair
ssDNA	single-stranded DNA
SSM	superficial spreading melanoma
STAG2	stromal antigen 2
STAG3	stromal antigen 3
STR	short tandem repeat
T	thymine
TAD	transactivation domain
TAI	telomeric allelic imbalance
TAM	tumor associated macrophages
TCR	transcription coupled repair
TDP1	tyrosyl-DNA phosphodiesterase 1
TFIIH	transcription factor IIH
TGF- $\beta$	transforming growth factor $\beta$
TIGAR	TP53-induced glycolysis and apoptosis regulator
TME	tumor microenvironment
TMZ	temozolomide
TNF- $\alpha$	tumor necrosis factor $\alpha$
TOP1	topoisomerase 1
UV	ultraviolet
V	valine
VEGF	vascular endothelial growth factor
VGP	vertical growth phase

---

WRN	Werner syndrome ATP-dependent helicase
WT	wild-type
XLF	XRCC4-like factor
XP	xeroderma pigmentosum
XPB	xeroderma pigmentosum group B
XPC	xeroderma pigmentosum group C
XPD	xeroderma pigmentosum group D
XPG	xeroderma pigmentosum group G
XRCC1	X-ray repair cross complementing 1
XRCC4	X-ray repair cross complementing 4

### 3. Summary

The skin cancer melanoma is known for its aggressive nature and high mortality rate when metastasized. While there has been significant advancement in using mitogen-activated protein kinase (MAPK) inhibitors (MAPKi) to target melanoma cells and combat metastasis, most patients ultimately experience relapse due to different resistance mechanisms. Despite the positive impact of immunotherapy on the prognosis of melanoma patients, some individuals show no response to these therapeutic drugs. Consequently, it becomes crucial to unravel the molecular mechanisms behind acquired resistance to targeted treatments and explore innovative therapeutic approaches for these patients.

In the first part of our study, we aimed to uncover the role of the p53 target gene *CDKN1A/p21* in the response of melanoma cells to v-raf murine sarcoma viral oncogene homolog B1 (BRAF) inhibitors (BRAFi). Our findings reveal that activation of p53 enhances the sensitivity of melanoma cells to BRAFi in a synergistic manner, exclusively in cells exhibiting high expression levels of *CDKN1A/p21*. Similarly, high expression of *CDKN1A/p21* correlates with a more favorable response to the mouse double minute 2 (MDM2) inhibitor (MDM2i) Nutlin-3 compared to cells with low *CDKN1A/p21* expression. These results suggest that the effectiveness of targeted therapies (such as BRAFi and MDM2i) in melanoma cells correlates with the expression levels of the p21 protein in the cells. Furthermore, our study uncovers that p53 negatively regulates the expression of the p53 family member p73, however p73 does not appear to influence p53 expression. These discoveries offer new potential strategies for improving the treatment of melanoma patients with elevated basal p21 levels. Specifically, combination therapies utilizing p53 activators, which further increase p21 expression levels, can enhance the efficacy of BRAFi. Additionally, the data suggest that the expression and induction level of p21 could serve as a predictive biomarker in melanoma patients, enabling the prognosis of treatment outcomes with p53 activators and BRAFi.

In the second part of the project, the focus shifted towards targeting the DNA repair pathway as a potential therapy against melanoma, particularly in the case of melanoma cells resistant to MAPKi. We explored the use of poly adenosine diphosphate (ADP) ribose polymerase (PARP) inhibitors (PARPi) for this purpose. Our findings indicate that melanoma cells resistant to MAPKi exhibit increased sensitivity to PARPi

treatment, facilitated by decreased ataxia-telangiectasia mutated (ATM) basal expression, an important DNA damage sensor. As a result, these resistant melanoma cells demonstrate an impaired ability to detect and repair DNA double strand breaks through the homologous recombination repair (HRR) pathway, which can be induced by PARPi. Additionally, we discovered that inhibiting the MAPK pathway induces a state of HRR deficiency (HRD) in melanoma cells, regardless of their sensitivity to MAPKi. This led to a synthetic lethal interaction when combining MAPK inhibition with PARPi, resulting in a significant reduction in melanoma cell growth both *in vitro* and *in vivo*.

In the third part of the project, we were interested in the role of PARP1 as a predictive biomarker to forecast PARPi therapy response as well as progression and metastatic potential of melanomas. We could show that high PARP1 expressing melanoma cells are extremely sensitive to PARPi treatment due to a higher PARP trapping effect, and thereby increased cell death. Moreover, we found that PARP1 expression positively correlates with the invasiveness and metastatic potential of melanoma cells, and that PARP1 is low expressed in non-malignant skin cells. Most strikingly, we found that high PARP1 expression goes along with significantly decreased overall survival probability of metastasized late-stage melanoma patients. With this, we propose that PARP1 might be used as a potential biomarker to predict PARPi therapy response and that especially the late-stage melanoma patients would benefit from the therapy with PARPi.

## 4. Zusammenfassung

Das maligne Melanom ist eine sehr aggressive Form von Hautkrebs mit einer hohen Sterblichkeitsrate bei Patienten, die an Metastasen leiden. Trotz der großen Fortschritte, die bei der Bekämpfung des metastasierten Melanoms mit Hilfe von MAPK Inhibitoren (MAPKi) erzielt wurden, kommt es bei den meisten Patienten aufgrund verschiedener Resistenzmechanismen zu einem Rezidiv. Auch wenn der Einsatz der Immuntherapie die Prognose von metastasierten Melanompatienten verbessert hat, sprechen einige Patienten überhaupt nicht auf immuntherapeutische Medikamente an. Daher ist es von größter Bedeutung, die molekularen Mechanismen der erworbenen Resistenz gegen zielgerichtete Therapien zu entschlüsseln und neue therapeutische Strategien für diese Patienten zu finden.

Im ersten Teil dieser Studie haben wir versucht, die Rolle des p53 assoziierten Gens *CDKN1A/p21* in der Sensitivität von Melanomzellen auf BRAF Inhibitoren (BRAFi) zu entschlüsseln. Wir zeigen, dass die Aktivierung von p53 die Sensitivität gegenüber BRAFi auf synergistische Weise ausschließlich in Zellen mit einer hohen Expression von *CDKN1A/p21* erhöht. In ähnlicher Weise geht eine hohe Expression von p21 mit einer besseren Reaktion auf MDM2-Inhibitoren einher. Die Ergebnisse deuten darauf hin, dass die Sensitivität von Melanomzellen gegenüber zielgerichteten Therapien mit der Proteinexpression von p21 in den Zellen korreliert ist. Darüber hinaus haben wir festgestellt, dass p53 die Expression des p53 Familienmitglieds p73 negativ reguliert, p73 scheint jedoch keinen Einfluss auf die p53 Expression zu haben. Diese Ergebnisse bieten neue potenzielle Strategien für die Verbesserung der Behandlung von Melanompatienten mit hoher basaler p21 Expression mit BRAFi, indem die Wirksamkeit der Behandlung durch Kombinationstherapien mit p53 aktivierenden Substanzen erhöht wird, die in der Lage sind, die p21 Expression weiter zu steigern. Darüber hinaus deuten die Daten darauf hin, dass die Expressions- und Induktionswerte von p21 als prädiktiver Biomarker bei Melanompatienten verwendet werden könnten, um das Ergebnis einer Behandlung mit p53-aktivierenden Substanzen und BRAFi vorherzusagen.

Im zweiten Teil des Projekts konzentrierten wir uns auf die Regulation des DNA-Reparaturweg als Melanomtherapie, insbesondere bei MAPKi resistenten Melanomzellen, durch den Einsatz von PARP Inhibitoren (PARPi). Wir fanden heraus, dass MAPKi resistente Melanomzellen besonders empfindlich auf die Behandlung mit

PARPi reagieren, da sie eine geringere basale Expression des DNA-Schadenssensors ATM aufweisen. Folglich haben MAPKi resistente Melanomzellen eine verringerte Erkennung von DNA-Doppelstrangbrüchen, die durch PARPi verursacht werden. Darüber hinaus zeigen wir, dass die Hemmung des MAPK-Signalwegs in Melanomzellen unabhängig von ihrem Resistenzstatus gegenüber MAPKi einen homologen Rekombinationsreparatur defizienten (HRD) Phänotyp hervorruft. Die MAPK Inhibition in Kombination mit PARPi führt zu einer synthetisch letalen Interaktion, die das Wachstum von Melanomzellen *in vitro* und *in vivo* deutlich reduziert.

Im dritten Teil des Projekts interessierten wir uns für die Rolle von PARP1 als prädiktiver Biomarker zur Vorhersage des Ansprechens auf eine PARPi-Therapie sowie des Fortschreitens und des Metastasierungspotenzials von Melanomen. Wir konnten zeigen, dass Melanomzellen mit hoher PARP1 Expression sehr gut auf eine PARPi-Behandlung reagieren, da die Behandlung zu einem höheren PARP-Trapping-Effekt und damit einem erhöhten Zelltod führt. Darüber hinaus fanden wir heraus, dass die PARP1 Expression positiv mit der Invasivität und dem metastatischen Potenzial von Melanomzellen korreliert, und dass PARP1 in nicht-malignen Hautzellen nur gering exprimiert wird. Besonders auffallend ist, dass eine hohe PARP1 Expression mit einer deutlich geringeren Überlebenswahrscheinlichkeit von Patienten mit metastasiertem Melanom im Spätstadium einhergeht. Damit schlagen wir vor, dass PARP1 als potenzieller Biomarker für die Ansprechrate auf eine PARPi-Therapie verwendet werden könnte und dass insbesondere Melanompatienten im Spätstadium möglicherweise von einer PARPi-Therapie profitieren.

## 5. List of Publications in the Thesis

### 5.1. **Accepted Publications**

- I. Fröhlich, L. M., Makino, E., Sinnberg, T., & Schitteck, B. (2022). Enhanced expression of p21 promotes sensitivity of melanoma cells towards targeted therapies. *Experimental Dermatology*, 31(8), 1243-1252.
- II. Fröhlich L. M., Niessner H., Sauer B., Kämereit S., Chatziioannou E., Riel S., Sinnberg T., Schitteck B. (2023). PARP inhibitors effectively reduce MAPK inhibitor resistant melanoma cell growth and synergize with MAPK inhibitors through a synthetic lethal interaction *in vitro* and *in vivo*. *Cancer Research Communications*, 3 (9): 1743–1755.

### 5.2. **Submitted Publication**

- I. Fröhlich, L. M., Schitteck, B. PARP1 expression predicts PARP inhibitor sensitivity and correlates with metastatic potential and overall survival in melanoma. Submitted to *International Journal of Cancer* (Submitted August 17<sup>th</sup>, 2023)

## 6. Personal Contribution

### 6.1. **Accepted Publication I**

*Enhanced Expression of p21 Promotes Sensitivity of Melanoma Cells Towards Targeted Therapies.*

E. Makino and I performed all experiments. I performed the experiments of Figure 1 and Figure 3. B. Schitteck helped in the acquisition of data by administrative, technical, or material support. B. Schitteck and I wrote the manuscript. T. Sinnberg and E. Makino helped in proof-reading the manuscript. Together with B. Schitteck, E. Makino, and T. Sinnberg, I participated in the conception, design, and execution of the study.

### 6.2. **Accepted Publication II**

*PARP inhibitors Effectively Reduce MAPK inhibitor Resistant Melanoma Cell Growth and Synergize with MAPK inhibitors Through a Synthetic Lethal Interaction in vitro and in vivo.*

I performed all experiments with assistance of S. Kämereit (western blot, cell viability assay). H. Niessner and T. Sinnberg helped with the *in vivo* experiments, E. Chatziioannou helped with analyzing and presenting the GEO data, S. Riel helped with execution and analysis of the immunofluorescence and the comet assay, and W. Kempf helped with the FACS sorting experiment. B. Sauer performed the immunohistochemistry of the FFPE material. M. Eisele helped in performing a MUH cell viability assay. B. Schitteck helped in the acquisition of data by administrative, technical, or material support. I wrote the manuscript under the guidance of B. Schitteck. S. Kämereit, H. Niessner, T. Sinnberg, E. Chatziioannou helped in proof-reading the manuscript. Together with B. Schitteck and T. Sinnberg, I was involved in the conception, design, and execution of the study.

### 6.3. **Submitted Publication I**

*PARP1 Gene Expression as a Biomarker to Predict PARP inhibitor Sensitivity in Melanoma.*

I performed all experiments as well as database analysis. B. Schitteck helped in the acquisition of data by administrative, technical, or material support. I wrote the manuscript under the guidance of B. Schitteck. Together with B. Schitteck, I was involved in the conception, design, and execution of the study.

## 7. Introduction

### 7.1. Melanoma

Malignant melanoma is an extremely aggressive cancer with a high mortality rate, as it has a strong tendency to metastasize to distant organs <sup>1</sup>. The disease mostly affects Caucasians with light pigmentation compared to darker skin color populations, such as Hispanics, East Asians, or Africans <sup>2</sup>. As melanoma often develops earlier than other solid tumors and has a high metastatic potential, the disease accounts for most of the skin cancer related deaths <sup>3-5</sup>. In fact, in Australia, melanoma is the major source of cancer-related deaths in people aged 15 to 44 years <sup>5</sup>. The incidence of melanoma is steadily increasing with a much higher incidence in Australia (60 new cases per 100000 population) compared to Europe (<25 new cases per 100000 population) and a massive increase in people older than 60 years <sup>6</sup>. The major risk factors for developing melanoma are genetic predisposition, high sun exposure, a sensitive skin type, and high numbers of nevi <sup>4</sup>. Fortunately, melanoma incidence is decreasing in young people, a success that is achieved by prevention of melanoma development by proficient sun protection, as well as early recognition by regular examination of the skin by a dermatologist and the “**ABCDE**” melanoma detection rule, where **A** stands for asymmetry, **B** for border irregularity, **C** for color variability, **D** for diameters greater than 6 mm, and **E** for the evolution of the melanocytic lesion <sup>6,7</sup>.

#### 7.1.1. Development of Melanoma

The skin is composed of the epidermis and the dermis, separated by the basal layer <sup>8</sup>. Melanocytes, derived from neural crest cells, are mostly located in the epidermis and can produce melanin <sup>9</sup>. The development of melanoma is a multistep process that originates either from a nevus or *de novo* from melanocytes <sup>10</sup>. A benign nevus is characterized by limited cell growth, however, *BRAF* mutations can induce cell growth. Further genetic changes, such as, e.g., *CDKN2A* or phosphatase and tensin homolog (*PTEN*) loss can induce a premalignant dysplastic nevus and the atypical melanocytes then can form a melanoma *in situ* <sup>3</sup>. The melanoma *in situ* can evolve to invasive melanoma by decreased differentiation and clonal proliferation of the melanoma cells <sup>3,11</sup>. While melanomas in the radial growth phase (RGP) still grow locally, vertical growth phase (VGP) melanoma can cross the basement membrane and form local metastases <sup>3</sup>. In the last progression stage, the metastatic melanoma, cells enter the blood or lymphatic system, thereby spreading through the body and forming tumors in

distant organs, mainly in the brain, liver, and lungs <sup>12,13</sup>. Figure 1 summarizes the development and progression of melanoma cells.

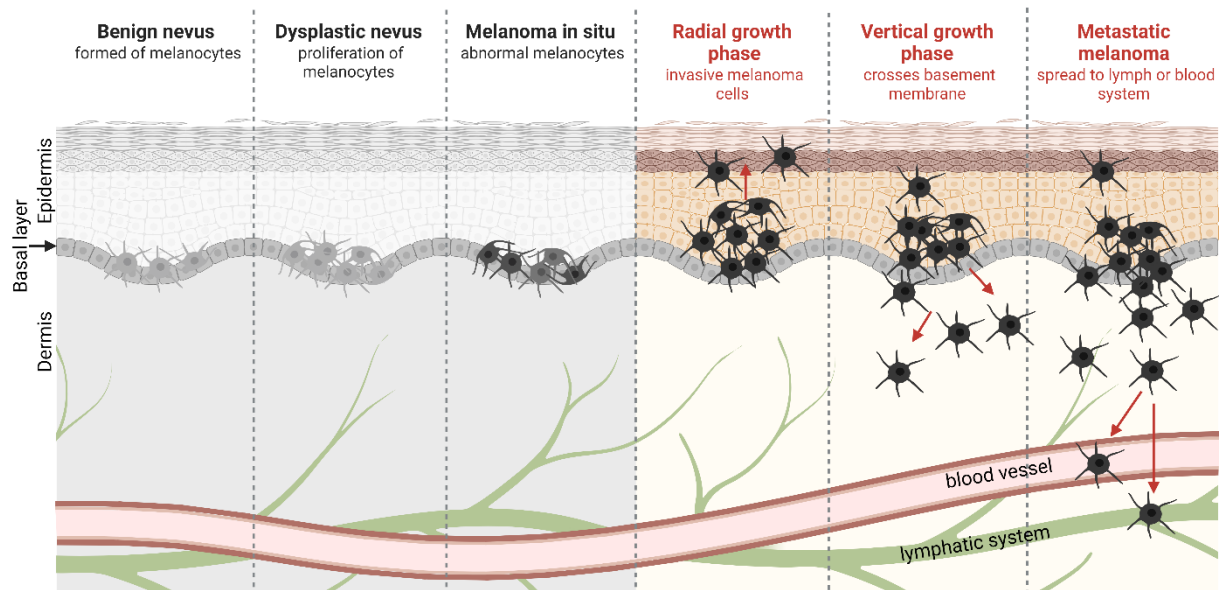


Figure 1: Overview of melanoma development and progression. A benign nevus transforms into a dysplastic nevus and further into a melanoma in situ, consisting of abnormal melanocytes. Melanoma in situ can transform into a melanoma in the radial growth phase (RGP). In the vertical growth phase (VGP), melanoma cells cross the basement membrane and thus have the potential to metastasize. The last stage represents metastatic melanoma, where the tumor cells spread via the blood or lymphatic system to distant organs, such as lung, liver, or brain. The illustration is adapted from <sup>3</sup> and was created with Biorender.com.

### 7.1.2. Staging of Melanoma

Depending on the histological features, melanoma can be classified into four major groups: superficial spreading melanoma (SSM), lentigo maligna melanoma (LMM), nodular melanoma (NM), and acral lentiginous melanoma (ALM) <sup>14</sup>. However, since these subgroups do not show clear clinical differences in terms of prognosis, an additional classification has been introduced, where melanomas are subdivided according to the primary location on the body <sup>15</sup>. The new classification includes melanoma on skin with chronic sun damage (CSD), melanoma on skin without chronic sun damage (non-CSD melanoma), melanoma on palms, soles, and nail bed (acral melanoma), and melanoma on mucous membranes (mucosal melanoma) <sup>14</sup>.

Moreover, in addition to the above-mentioned classification, the World Health Organization implemented the latest version of a classification in 2018, taking the sun damage into account. Nine different pathways on how melanocytic lesions can arise are now subdivided <sup>16,17</sup>:

- 1) **Superficial spreading melanomas** are arising in sun exposed skin. However, they show the molecular profile of low CSD and often harbor BRAF V600 mutations.
- 2) **High-CSD melanomas**, which include **LMM** and **high-CSD NM**, are characterized by mutations in the mitogen-activated protein kinase (MAPK) signaling pathway, such as neurofibromin 1 (*NF-1*), *NRAS*, or *BRAF* (other than V600) mutations.
- 3) **Desmoplastic melanomas** show mutations in the MAPK signaling pathway, in particular NF-1 inactivating mutations.
- 4) **Spitz melanomas** are associated with *HRAS* mutations, as well as kinase fusions, *CDKN2A* homozygous mutations and telomerase reverse transcriptase (*TERT*) promoter mutations.
- 5) **Acral melanomas** also include nodular melanoma in acral skin, and are characterized by *BRAF*, *NRAS*, and *KIT* mutations.
- 6) **Mucosal melanomas** show numerous copy number and structural variations.
- 7) **Melanomas arising from congenital nevi** are characterized by *BRAF* as well as *NRAS* mutations.
- 8) **Melanomas arising from blue nevi** are associated with mutations in the  $G\alpha q$  pathway.
- 9) **Uveal melanomas** typically also show mutations in the  $G\alpha q$  pathway, as well as mutations in genes involved in DNA repair.

Classes one, two, and three occur on chronic sun exposed skin, whereas the other classes are located at sun shielded sites <sup>16</sup>.

#### **7.1.2.1. AJCC Staging System**

The eighth edition of the AJCC staging is the latest version for melanoma, published in 2018, and utilizes the TNM classification to distinguish the different tumor stages, where T stands for the extent of the primary tumor, N represents the presence or absence of affected lymph nodes, and M indicates if the tumor has metastasized to other organs of the body <sup>18-21</sup>. The T category can be subdivided into T0, where no primary tumor is detectable, Tis, which refers to a melanoma in situ, T1a, where the tumor is smaller than 0.8 mm in thickness without ulceration, T1b, where the tumor is either smaller than 0.8 mm in thickness with ulceration, or between 0.8 mm and 1.0 mm without ulceration, or Tx, where the tumor thickness cannot be determined. According to this system, the T classification further includes T2, with a tumor thickness

between 1 and 2 mm, T3, with a tumor thickness between 2 and 4 mm, and T4, with a tumor thickness of more than 4 mm. The N category can be subdivided into N0, where no regional metastasis is detectable, and N1-3, where tumor involved lymph nodes and/or in-transit, satellite, or micrometastasis are found. The M category can be subdivided into M0, where no distant metastasis is detectable and M1, where distant metastases are identified. Moreover, M1 can be subclassified into M1a, where metastases are detected in skin or soft tissue, including muscle and non-regional lymph nodes, M1b, where metastases are identified in the lung tissue, M1c, where metastases are detected in non-central nervous system (CNS) visceral sites, and M1d, where metastases are identified in the CNS. In addition, M1a to M1c categories can be further subdivided into 0 and 1, where 0 indicates no elevated lactate dehydrogenase (LDH) levels, and 1 represents elevated LDH levels<sup>19,20</sup>.

To facilitate classification for clinical utility, a staging system ranging from stage 0 to stage IV was implemented. In this system, stage 0 represents carcinomas in situ (Tis, N0, M0). Stage I includes patients with localized tumors (T1-2, N0, M0). Stage II represents early stages of locally advanced tumors (T2-3, N0, M0), whereas stage III includes late stage locally advanced tumors with tumor involved lymph nodes (T1-4, N1-3, M0). The last level is stage IV and represents cancers metastasized to distant organs (T1-3, N1-3, M1)<sup>18</sup>.

## **7.2. Treatment of Malignant Melanoma**

Melanoma therapy consists of various treatment regimens and can range widely depending on the patient's genetic background. Continuous improvement of therapy has significantly increased the survival rate of advanced melanoma patients<sup>21</sup>.

### **7.2.1. Surgery**

Surgery is a highly effective method to treat localized melanoma in particular and is crucial for histological confirmation of the diagnosis. The outcome is critically dependent on the stage of the disease and often surgery is curative when a complete resection of the tumor tissue is possible<sup>22</sup>. To improve the outcome of surgery, other therapeutics such as targeted therapy or immunotherapy are applied as an adjuvant treatment<sup>23</sup>.

### 7.2.2. Chemotherapy

Chemotherapeutic agents that are used in melanoma therapy mainly include dacarbazine (DTIC) (see section 7.2.2), temozolomide (TMZ), platinum-based therapies (see section 7.2.2), such as cisplatin, and taxanes, such as paclitaxel <sup>24</sup>.

The taxane paclitaxel has the ability to induce G2/M mitotic arrest by polymerization of tubulin <sup>25</sup>. Numerous studies are underway to investigate the potential of paclitaxel in combination with various other anti-melanoma agents <sup>26</sup>. DTIC, an alkylating agent shows comparatively low response rates due to infrequent and short-termed complete responses in melanoma patients and is therefore mostly used in palliative care <sup>24,27</sup>. TMZ is another alkylating agent that shows a clinical advantage over DTIC due to its oral bioavailability <sup>28,29</sup>. Cisplatin and its analogue carboplatin are widely used as anti-cancer drugs of solid tumors, including melanoma, either as a monotherapy or as a combination therapy, especially with paclitaxel <sup>30</sup>. Overall, chemotherapeutic agents show modest response rates, and marked toxicity limit their therapeutic efficacy. Therefore, they are nowadays primarily used as a last-line therapeutic option <sup>31</sup>.

### 7.2.3. Immunotherapy

The era of immunotherapy for the treatment of melanoma was pioneered by high-dose interleukin-2 (IL-2). Even if only 5-10% of patients treated with high-dose IL-2 therapy showed a complete remission, it led to U.S. Food and Drug Administration (FDA) approval in 1998 due to the lack of alternatives for this patient group at that time <sup>32</sup>. In those days, despite the major toxicities, high-dose IL-2 was the only FDA approved drug besides DTIC for the systemic treatment of metastatic melanoma <sup>33</sup>.

The launch of the immune checkpoint blockade (ICB) therapy changed the landscape of melanoma treatment. Ipilimumab, a cytotoxic T lymphocyte-associated antigen 4 (CTLA-4) blocking antibody, was approved by the FDA in 2011, and since the programmed cell death protein 1 pathway (PD-1) blocking antibodies pembrolizumab and nivolumab showed better response than CTLA-4 inhibitors, they received FDA approval in 2014 for the treatment of metastatic melanoma <sup>34</sup>. CTLA-4 and PD-1 belong to the family of immune checkpoint receptors and are upregulated and presented on the cell surface upon T-cell activation to suppress T-cell function and sustain immunological homeostasis. Thereby, ICB therapy enables T-cells to kill the tumor <sup>35</sup>. Currently, melanoma patients receive CTLA-4 plus PD-1 blocking antibodies,

such as nivolumab plus ipilimumab, as the combined treatment showed superior effects to monotherapy in terms of response <sup>36</sup>.

A new target to direct the immune system to the tumor cells is the cell surface receptor lymphocyte activation gene 3 (LAG-3). The inhibitory molecule mediates immunosuppressive functions, and anti-LAG-3 inhibitors have been shown to effectively kill tumor cells <sup>37</sup>. The anti-LAG-3 inhibitor relatlimab was therefore approved by the FDA in March 2022 for the treatment of advanced melanoma, and in September 2022, the European Medicines Agency (EMA) approved the combination of nivolumab and relatlimab for the treatment of unresectable or metastatic melanoma in patients with less than 1% PD-L1 expression <sup>38</sup>.

Melanoma patients respond strongly to ICB compared to other solid tumors, since their high UV exposure and elevated tumor mutational burden (TMB) contribute to a high immunogenicity of the tumor, however, the effectiveness is constrained by two major issues, i.e., resistance mechanisms, as well as major toxicities associated with ICB <sup>39</sup>. Resistance to ICB occurs in about 40% of melanoma patients and can either be primary, meaning that patients do not respond to the drug from the start of therapy, or it develops during the treatment, thus termed acquired resistance <sup>40,41</sup>. Primary resistance mechanisms include amongst others a poor immunogenicity, high basal expression of the targeted checkpoint receptors, or upregulation of T-cells, whereas acquired resistance mechanisms rather comprise mutations of signaling pathways, resulting in upregulation of the targeted checkpoint receptors, or modification of the immune response <sup>42</sup>. To limit this clinical barrier, current research is focused on overcoming therapy resistance and exploring clinical biomarkers that could predict the response to ICB treatment as well as the management of adverse events. The major cancer ICB toxicities include immune-related adverse events (irAE), which are caused, for example, by autoreactive T cells, autoantibodies, or massive production of cytokines. Potentially fatal toxic events associated with immunotherapy include amongst others ulcerative colitis, hormone deregulation, hypophysitis, pneumonitis, hepatitis, diabetes mellitus, vitiligo, or myocarditis <sup>43,44</sup>.

Studies have shown that ICB in combination with targeted therapy leads to significant melanoma tumor regression, with ICB treatment as first-line treatment and MAPK inhibitor treatment as second-line treatment being the most effective application <sup>45</sup>.

### 7.2.4. Targeted Therapy

In cancer cells, many signaling pathways are overexpressed to enable rapid cell growth<sup>46</sup>. The triggering of these signaling pathways is often enabled by activating mutations of oncogenes, or suppression of tumor suppressor genes<sup>47</sup>. Targeted cancer therapies take advantage of these mutated signaling pathways and inhibit the altered signals to stop cancer cell growth<sup>48</sup>.

#### 7.2.4.1. *The MAPK Signaling Pathway*

A major breakthrough in melanoma therapy was the finding that the MAPK pathway is frequently overactivated in melanoma patients<sup>49</sup>. The classical MAPK pathway, on which we focus here, and which is also referred to as ERK pathway consists of three enzymes that mutually activate each other. At a glance, an extracellular mediated growth stimulus triggers a MAPK kinase kinase (MAPKKK) that activates a MAPK kinase (MAPKK), which in turn triggers a MAPK, resulting in the stimulation of substrates<sup>50</sup>. This eventually leads to proliferation, differentiation, and development of the cell<sup>51</sup>. In detail, upon binding of a ligand, such as growth factors (GF), the membrane spanning surface protein receptor tyrosine kinase (RTK) forms a dimer and is thereby activated<sup>52</sup>. Growth factor receptor-bound protein 2 (GRB2) is stimulated by the autophosphorylated intracellular domain of the RTK dimer and enables its interaction with son of sevenless (SOS)<sup>53</sup>. Next, SOS is translocated to the cell membrane, interacts with rat sarcoma (RAS) and enables nucleotide exchange from guanosine diphosphate (GDP) to guanosine triphosphate (GTP), which can be inhibited by NF-1, a GTPase-activating protein (GAP)<sup>54,55</sup>. Thereby, RAS phosphorylates the serine/threonine kinase family rapidly accelerated fibrosarcoma (RAF), which consists of ARAF, BRAF, and CRAF, ultimately triggering the MAPK cascade<sup>56</sup>. Activated RAF phosphorylates MAP kinase/ERK kinase 1/2 (MEK1/2), which in turn phosphorylates extracellular signal-regulated protein kinase 1/2 (ERK1/2), resulting in a phosphorylation of both cytoplasmic as well as nuclear target proteins and transcription factors<sup>57</sup>. The MAPK signaling pathway regulates various processes, including cell adhesion, cell cycle progression, migration, survival, differentiation, metabolism, proliferation, and transcription<sup>58</sup>. Interestingly, the MAPK signaling pathway may induce both pro- or antiapoptotic signals, according on the stimulus and the cell type<sup>59</sup>. Figure 2 depicts key elements in the MAPK signaling pathway.

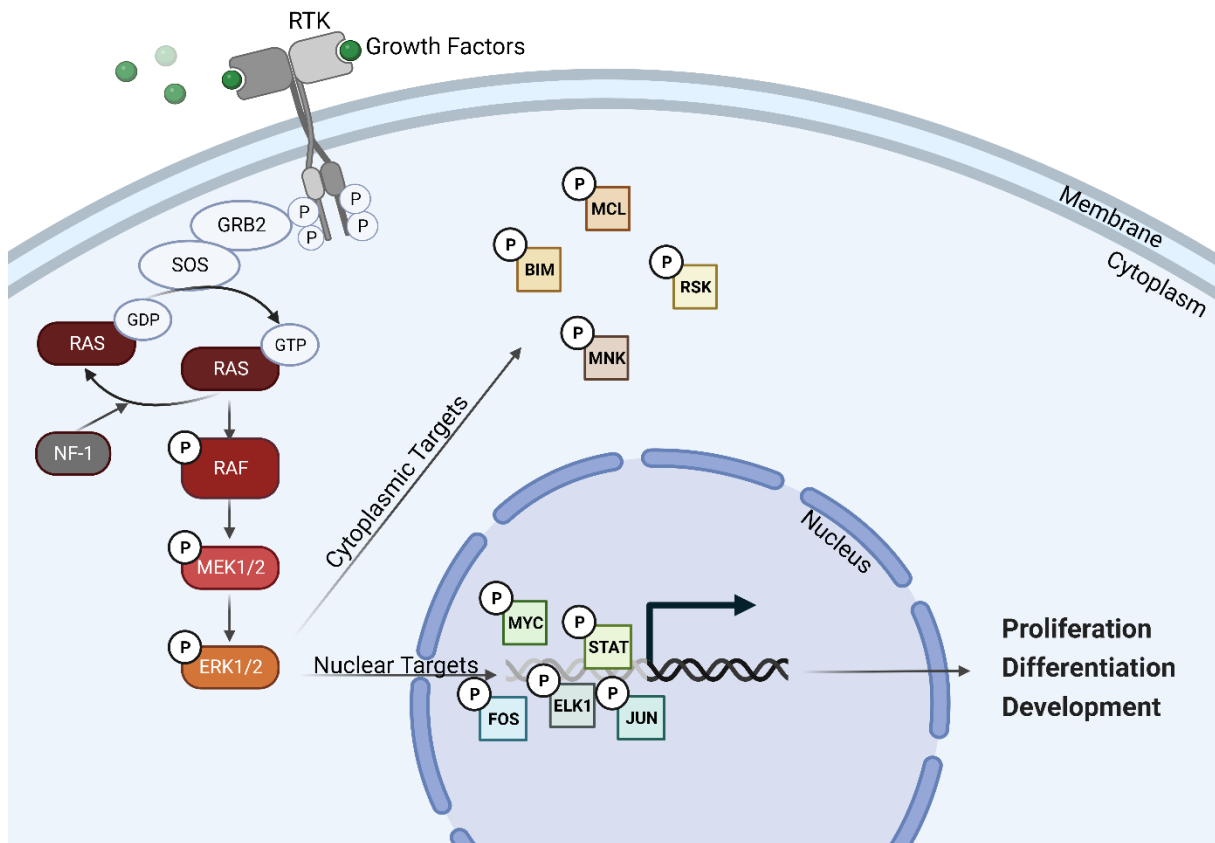


Figure 2: Schematic overview of the MAPK signaling pathway. A stimulus binds to the receptor tyrosine kinase (RTK) which results in the recruitment of the growth factor receptor-bound protein 2 (GRB2) and son of sevenless (SOS). This activates the small guanosine triphosphate (GTP)ase rat sarcoma (RAS) changing guanosine diphosphate (GDP) to GTP, which can be inhibited by neurofibromin 1 (NF-1). This in turn triggers the phosphorylation, and thereby activation of rapidly accelerated fibrosarcoma (RAF), phosphorylating the MAP kinase/ERK kinase 1/2 (MEK1/2). MEK1/2 then phosphorylates the extracellular signal-regulated protein kinase 1/2 (ERK1/2). ERK1/2 activation targets both nuclear, as well as cytoplasmic proteins, leading to proliferation, differentiation and development. The illustration was created with Biorender.com.

Various driver mutations may lead to massive overactivation of the MAPK signaling pathway. A dysregulation of the MAPK signaling pathway can result in malignant cells and may cause cancer, amongst others, melanoma<sup>60</sup>.

#### 7.2.4.2. Genomic Classification of Cutaneous Melanoma

After it was discovered that the MAPK signaling pathway has a great impact on melanoma development, a genomic classification of cutaneous melanoma according to the MAPK mutational status was introduced. Melanoma patients were classified in four major groups<sup>61</sup>:

- **BRAF mutated**
- **RAS mutated**
- **NF-1 mutated**
- **Triple Wild-Type (WT)**

The BRAF mutated subtype is the largest subgroup, since about 50% of melanoma patients show a mutation in the *BRAF* oncogene. Of these patients, more than 90% harbor a mutation at amino acid position 600, with a point mutation from valine (V) to glutamic acid (E) (*BRAF*<sup>V600E</sup>)<sup>62</sup>. The second largest group is the RAS mutated subtype, with the majority of mutations in *NRAS*, i.e., about 20% of melanoma cases. RAS mutated melanomas are known to be extremely aggressive and correlate with a worse prognosis<sup>63</sup>. Around 12-18% of all melanoma cases show an inactivating mutation in the *NF-1* gene, leading to the overactivation of the MAPK signaling pathway<sup>64</sup>. Melanoma patients classified into the Triple WT subtype do not harbor any of the aforementioned mutations in the MAPK signaling pathway. Interestingly, Triple WT subtype melanomas typically harbor many other driver mutations in genes such as *GNAQ*, *GNA11*, *KIT*, *CTNNB1*, and *EZH2*<sup>61</sup>.

#### **7.2.4.3. MAPK Inhibitor Therapy**

Having demonstrated the critical role of the MAPK signaling pathway in the development of melanoma, tremendous amount of research was conducted on inhibitors to suppress the overactivated MAPK pathway. The implementation of MAPK inhibitors (MAPKi) as a treatment option dramatically improved the survival of melanoma patients<sup>65</sup>. The rationale behind MAPKi therapy is to interfere with cell growth by affecting specific targets on which the tumor depends, but not the non-cancerous surrounding tissue. Melanoma patients treated with vemurafenib, an inhibitor of the mutated *BRAF*<sup>V600</sup>, showed high response rates, extended progression free survival (PFS), as well as improved median overall survival (OS). Therefore, it was the first targeted therapy for metastatic or unresectable BRAF mutated melanoma patients to be approved by the FDA in 2011 and the EMA in 2012<sup>66-68</sup>. Due to the great success of vemurafenib, two other BRAF inhibitors (BRAFi) were FDA and EMA approved for the same patient group, i.e., dabrafenib in 2013, and encorafenib in 2018<sup>69-71</sup>. In a second step, inhibitors targeting the downstream protein MEK were explored. The first FDA (2013) and EMA (2013) approved MEK1/2 inhibitor (MEKi), trametinib, is applied to treated BRAF mutated metastatic melanoma patients that did not receive BRAFi previously. Other MEKi used in melanoma therapy are cobimetinib and binimetinib<sup>72</sup>.

Since both ICB and MAPKi are effective treatment options for melanoma patients, their potential as a combination therapy was investigated<sup>73</sup>. Clinical studies focusing on the

triple therapy of BRAFi plus MEKi plus ICB in BRAF mutated melanoma patients showed mixed responses to this combination therapy <sup>74-78</sup>.

Novel treatment strategies for MAPKi resistant patients include treatment with LY3009120, a panRAF inhibitor (panRAFi) <sup>79</sup>. In a clinical study, LY3009120 showed potent tumor reducing activity, also in melanoma patients that developed resistance to MAPKi treatment <sup>80</sup>.

#### **7.2.4.4. Resistance Mechanisms to MAPK Inhibitors**

Even though a large number of melanoma patients benefit from targeted therapy, some patients do not respond to MAPKi treatment from the beginning, demonstrating the existence of intrinsic resistance <sup>81</sup>. Patients with intrinsic resistance to MAPKi therapy often harbor specific mutations that include amongst others PTEN loss, cyclin D1 activation, Ras-related C3 botulinum toxin substrate 1 (RAC1) activation, MEK1/2 activation, NF-1 loss, activation of the c-Jun/Ras homolog gene family, member B (RHOB) signaling axis, hepatocyte growth factor (HGF)/c-MET signaling axis activation, or hypoxia-inducible factor 1  $\alpha$  (HIF-1 $\alpha$ ) induced hypoxia <sup>82</sup>.

As already mentioned, targeted therapy eventually loses its effectiveness in killing melanoma tumor cells due to the very probable and rapid emergence of acquired resistance. Numerous resistance mechanisms have already been described, which will be discussed in more detail below <sup>83-85</sup>.

A major mechanism of MAPKi resistance is the **genetic reactivation of the MAPK signaling pathway**. The most obvious mechanism of BRAFi resistance is the mutant BRAF gene amplification, resulting in the reconstitution of the MAPK signaling pathway even under BRAFi therapy <sup>86-88</sup>. Aberrantly spliced BRAF variants leading to BRAF dimerization without activated RAS as well as secondary mutations in the BRAF oncogene have also been detected in BRAFi resistant cancers <sup>87,89-91</sup>. A paradoxical ectopic CRAF overexpression also showed to confer resistance to BRAFi treatment <sup>92,93</sup>. Furthermore, it was shown that not only mutations in the *BRAF* gene, but also other genes of the MAPK pathway advance the development of BRAFi resistance. Oncogenic *NRAS* mutations leading to a reactivation of the MAPK signaling pathway induce resistance to BRAFi therapy <sup>87,88,94-96</sup>. In addition, mutations activating the *MEK1* or *MEK2* genes are associated with BRAFi resistance development <sup>87,95,96</sup>. Increased RAS activation by BRAFi therapy associated mutations in the *NF-1* gene have also been related to BRAFi resistance <sup>97-100</sup>. Genetic mutations leading to an

upregulation of the RTK promote the MAPK signaling pathway without a stimulus and thereby confer resistance to BRAFi treatment <sup>94,101,102</sup>. In addition, enhanced abundance of growth factors that stimulate the RTK, such as for example HGF, show the same phenomenon <sup>103</sup>. Mutations leading to an activation of RAC1 have been shown to reactivate the MAPK signaling pathway and have been detected in patients that developed resistance to BRAFi therapy <sup>104-106</sup>. Moreover, loss of block of proliferation 1 (BOP1) or loss of stromal antigen 2 (STAG2) or stromal antigen 2 (STAG3), resulting in the downregulating of dual specificity phosphatase 4 (DUSP4) or dual specificity phosphatase 6 (DUSP6) activate ERK1/2, and thereby promote BRAFi resistance <sup>107,108</sup>. Overexpression of the MAPK downstream target melanocyte inducing transcription factor (MITF) occurs in a high number of melanoma patients treated with BRAFi or MEKi and has been shown to confer resistance to MAPKi therapy <sup>109</sup>.

In addition to the reactivation of the MAPK signaling pathway, **activation of alternative signaling pathways** also play a significant role in acquired MAPKi resistance. The phosphoinositide-3-kinase (PI3K)/AKT/mammalian target of rapamycin (mTOR) pathway is a key regulator of survival and may act independently of the MAPK signaling pathway. Briefly summarized, a GF stimulates the activation and phosphorylation of a RTK, which recruits PI3K to the membrane. Thereby phosphatidylinositol 3,4,5-trisphosphate (PIP<sub>3</sub>) is produced from phosphatidylinositol 4,5-bisphosphate (PIP<sub>2</sub>) which in turn phosphorylates AKT, that activates major downstream targets, such as mTOR, ultimately resulting in cell growth and downregulation of apoptosis <sup>110-112</sup>. A natural inhibitor of the PI3K pathway and thereby a tumor suppressor dephosphorylates PIP<sub>3</sub> resulting in PIP<sub>2</sub> and the inhibition of PI3K pathway downstream signaling <sup>113</sup>. Acquired mutations leading to the activation of the PI3K/AKT/mTOR pathway have been shown to promote the development of MAPKi resistance by stimulating cell growth and inhibiting apoptosis independently of the MAPK signaling pathway <sup>114</sup>. They mainly include genetic suppression of PTEN, or activation of AKT <sup>115,116</sup>. Another important pathway in MAPKi resistance is the Hippo signaling pathway, which promotes cell proliferation and survival <sup>117</sup>. Similar to the PI3K/AKT/mTOR signaling pathway, overactivation of the Hippo signaling pathway promotes cell survival even if the MAPK signaling pathway is suppressed due to MAPKi treatment. Activating mutations in the oncoprotein YAP, a transcriptional coactivator in

the Hippo signaling, have been found to confer resistance to BRAFi and MEKi therapy <sup>118-120</sup>.

The **tumor microenvironment** (TME) also has a major influence on the development of targeted therapy resistance <sup>121</sup>. A tumor can stimulate fibroblasts that surround the cancer cells to become cancer associated fibroblasts (CAF), and these CAF have the ability to induce tumorigenesis and metastasis <sup>122,123</sup>. Upon MAPKi treatment, tumor cells release transforming growth factor  $\beta$  (TGF- $\beta$ ), which leads to upregulation of neuregulin-1 (NRG1), ultimately inducing differentiation of the TME associated fibroblasts. Also, MAPKi treatment may trigger the MAPK signaling pathway in fibroblasts, resulting in the secretion of HGF which serves as a ligand for mesenchymal epithelial transition (MET) receptor, eventually resulting in the activation of the MAPK and PI3K signaling pathway in cancer cells, thereby conferring resistance to BRAFi treatment <sup>124,125</sup>. Integrin  $\alpha 5\beta 1$ , a fibronectin receptor, triggers the reactivation of the MAPK signaling pathway in the tumor cells, thereby promoting BRAFi resistance <sup>126</sup>. Interestingly, BRAFi treatment triggers the MAPK signaling pathway in tumor associated macrophages (TAM), causing tumor necrosis factor  $\alpha$  (TNF- $\alpha$ ) activation, which induces MITF, as well as vascular endothelial growth factor (VEGF) activation, eventually conferring BRAFi resistance and tumor growth in the cancer cells <sup>127</sup>. Moreover, it was shown that modulating the immune response may also promote MAPKi resistance. For example, the acquisition of PTEN loss upon BRAFi resistance creates a TME with low numbers of T and NK cells induces an immunosuppressive phenotype by upregulation of interleukin-6 (IL-6), interleukin-10 (IL-10), and VEGF <sup>128</sup>. The major molecular MAPKi resistance mechanisms are shown in Figure 3.

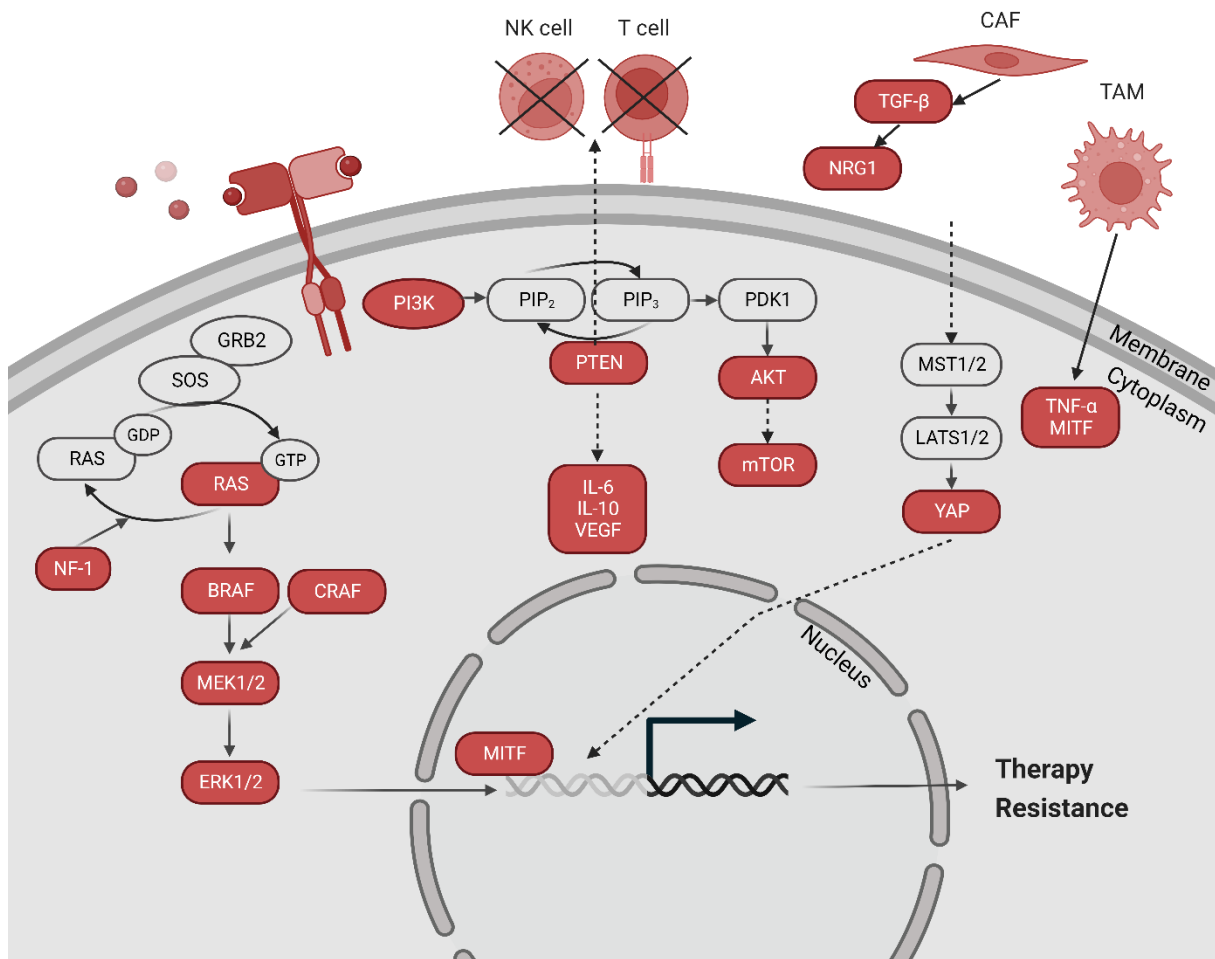


Figure 3: Graphical representation of MAPKi resistance mechanisms. Components colored in red are known to play a role in mitogen-activated protein kinase inhibitor (MAPKi) resistance. Reactivation of the MAPK signaling pathway, activation of the phosphoinositide-3-kinase (PI3K)/AKT/ mammalian target of rapamycin (mTOR) signaling pathway, or activation of the Hippo pathway induces MAPKi resistance. Also, modulation of the immune system, as well as cancer associated fibroblasts (CAF) and tumor associated macrophages (TAM) can induce MAPKi resistance. The illustration was created with Biorender.com.

#### 7.2.4.5. Possible Mechanisms in Overcoming Targeted Therapy Resistance

Since around half of the patients that received BRAFi show a progressive disease (PD) after half a year due to emerging resistance, approaches to combine BRAFi plus MEKi were studied hoping that the resistance development can be delayed. Interestingly, the combination studies showed a clear benefit compared to each monotherapies, especially in patients that were not pretreated with targeted therapy<sup>129</sup>. Not only the adverse events were dampened, but also the emergence of MAPKi resistance was significantly delayed with the combination of BRAFi plus MEKi compared to each monotherapy<sup>130-132</sup>. The combinations currently used in a clinical setting are vemurafenib plus cobimetinib, dabrafenib plus trametinib, and encorafenib plus binimetinib<sup>133</sup>. Currently, the combination of vemurafenib plus cobimetinib is licensed for treating unresectable BRAF mutated metastatic melanoma. As an adjuvant therapy,

this combination is approved for locally advanced BRAF mutated melanoma with tumor involved regional lymph nodes. The combination of vemurafenib plus cobimetinib and encorafenib plus binimetinib are approved for unresectable or metastatic BRAF mutated melanoma <sup>134</sup>.

Furthermore, various studies proposed a different treatment regimen, shifting from continuous treatment to an on-off schedule or possible drug holiday to overcome targeted therapy resistance <sup>135</sup>. However, a preclinical study showed no beneficial effects in the intermittent dosing schedule compared to continuous treatment regimen, but on the contrary, continuous treatment of melanoma patients showed statistically significant increased PFS compared to the on-off schedule <sup>136</sup>. Small molecule inhibitors that inhibit either pan-RAF or ERK have also been hypothesized to overcome MAPKi therapy resistance <sup>137-142</sup>. Since the heat shock protein 90 (Hsp90) is crucial for balancing the stability as well as degradation of BRAF<sup>V600E</sup> and CRAF, treatment with a Hsp90 inhibitor in combination with MAPKi showed clear prolongation of MAPKi response <sup>143,144</sup>. First preclinical studies show clinical activity of the combination <sup>145</sup>. It is obvious that inhibition of the PI3K pathway could stop MAPKi resistance and studies clearly showed that the combination could overcome therapy resistance <sup>146-148</sup>. However, due to massive toxicities, the clinical translation of this approach is exceedingly difficult <sup>149,150</sup>. Another promising target to overcome MAPKi resistance is reducing MITF overactivation by the HIV protease inhibitor nelfinavir <sup>109</sup>.

Taken together, it is crucial that further research will be conducted focusing on overcoming targeted therapy resistance in melanoma patients.

### **7.3. p53 family**

The p53 family is a group of transcription factors and comprises three proteins, p53 itself, p63, and p73 <sup>151</sup>. The *TP53* gene is located at chromosome 17p13.1, the *TP63* gene at chromosome 3q27-29 and the *TP73* gene at chromosome 1p36.3 <sup>152</sup>. The p53 family belongs to the most important tumor suppressors as they are major cell cycle regulators, deciding if a cell should further divide or enter cell death. Therefore, p53 is also named the “guardian of the genome” <sup>153</sup>.

#### **7.3.1. Structure of the p53 Family Members**

The gene structures of *TP53*, *TP63*, and *TP73* share high sequence homology. All genes encode a transactivation domain (TAD), a DNA binding domain (DBD), a proline-rich (PR) domain, as well as an oligomerization domain (OD) and *TP73* and

*TP63* also encode a sterile alpha motif (SAM) <sup>154</sup>. Due to alternative splicing and different promoters, the p53 family genes encode a large number of protein isoforms <sup>155</sup>. The  $\Delta N$  variants lack parts of the N-terminal TAD and are produced by activation of promoter 2, whereas the TA-variants contain the full TAD and are produced by activation of promoter 1. Alternative splicing or alternative translation results in the  $\Delta 40$  or  $\Delta 133$  isoforms of p53, as well as the  $\Delta$ exon2 and  $\Delta$ exon2/3 variants of p73. Further splicing allows many more isoforms, with p53 expressing the full length (FL), the  $\beta$ , as well as the  $\gamma$  isoform. Alternative splicing of the *TP63* and *TP73* genes allows the expression of an  $\alpha$ -isoform, containing the SAM, and the  $\beta$  and  $\gamma$  isoform, lacking the SAM. In contrast to the *TP63* gene, further alternative splicing of *TP73* can lead to  $\delta$ ,  $\epsilon$ ,  $\zeta$ , and  $\eta$  isoforms, which all are lacking the SAM <sup>156-162</sup>. The structure of the p53 family members is summarized in Figure 4.

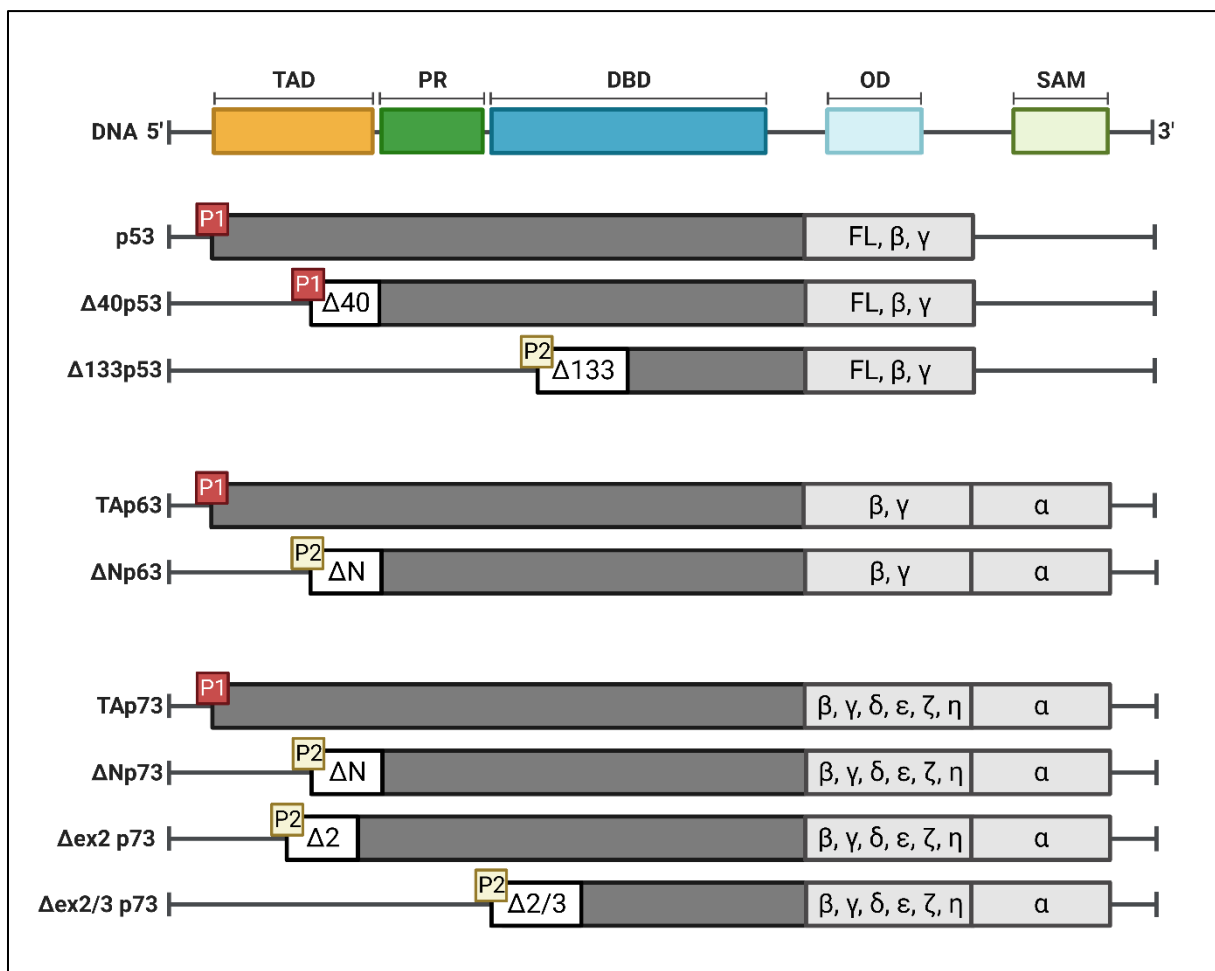


Figure 4: Structure of the p53 family genes. The p53 family genes encode a transactivation domain (TAD), a proline-rich (PR) domain, a DNA binding domain (DBD), an oligomerization domain and TP73 and TP63 also encode a sterile alpha motif (SAM). Full length, TA and  $\Delta 40$  isoforms are generated by promoter 1 (P1), whereas  $\Delta N$ ,  $\Delta 133$ ,  $\Delta$ exon2 ( $\Delta 2$ ), and  $\Delta$ exon2/3 ( $\Delta 2/3$ ) isoforms are produced by promoter 2 (P2). Alternative splicing results in various isoforms including full length (FL),  $\beta$ , and  $\gamma$  for TP53,  $\alpha$ ,  $\beta$ , and  $\gamma$  for TP63, and  $\alpha$ ,  $\beta$ ,  $\gamma$ ,  $\delta$ ,  $\epsilon$ ,  $\zeta$ , and  $\eta$  for TP73. The schematic overview was adapted from <sup>154-158,162</sup>. The illustration was created with Biorender.com.

The full length and TA isoforms of the p53 family members share similar functions, whereas the  $\Delta N$  isoforms rather exert their functions as negative regulators of the TA isoforms due to competitive binding of the same promoter, and thus inhibiting efficient translation of the TA isoforms <sup>158</sup>.

### 7.3.2. p53 Family Signaling

Since p53 exerts the crucial role of maintaining genomic stability of the cell, the p53 signaling pathway is mostly triggered in response to stress signals <sup>163,164</sup>. Under physiological conditions, that is, when the cell is not under stress, the p53-specific E3 ubiquitin ligase MDM2 keeps p53 suppressed by inducing proteasomal degradation via a negative feedback loop <sup>165,166</sup>.

Upon oncogenic signaling, the tumor suppressor gene ADP-ribosylation factor (*ARF*), encoding the protein p14<sup>ARF</sup>, a negative regulator of p53, is inhibited, resulting in the expression of p53 target genes, ultimately triggering cell cycle arrest or apoptosis <sup>167</sup>. The transcription factor E2 promoter binding factor 1 (E2F-1) can also stabilize p53 by triggering p14<sup>ARF</sup> expression <sup>168</sup>. Various genotoxic factors, such as hypoxia, reactive oxygen species (ROS), ionizing radiation (IR), UV-light, or chemotherapeutic agents induce DNA damage, which ultimately triggers p53-dependent DNA repair or cell death <sup>169</sup>. In detail, DNA damage induces DNA-dependent protein kinase (DNA-PK), Ataxia telangiectasia mutated (ATM) and ataxia telangiectasia and Rad3-related (ATR). ATM activation results in phosphorylation of checkpoint kinase 1 (CHK1) and ATR activation in phosphorylation of checkpoint kinase 2 (CHK2), which phosphorylate p53 through their serin/threonine kinase activity <sup>170-172</sup>.

A central downstream effect of p53 activation is the induction of apoptosis <sup>173</sup>. Mainly responsible for this process are the p53 targets genes *PUMA* and *NOXA* <sup>174</sup>. These genes belong to the BH3-only members of the B-cell lymphoma 2 (Bcl-2) protein family and induce apoptosis by inhibiting the pro-survival members of the Bcl-2 proteins <sup>175</sup>. Thus, the pro-apoptotic effectors BAX and BAK are activated. p53 can also directly activate BAX <sup>176</sup>. This ultimately leads to the formation of the apoptosome, activation of effector caspases, and the demolition of the cell <sup>173,177</sup>.

P53-mediated cell cycle arrest is mainly induced via the p53 target gene cyclin dependent kinase inhibitor 1A (*CDKN1A*), that encodes for the protein p21 <sup>178</sup>. P53 regulates various checkpoints of the cell cycle, including the transition from G1 to S phase, M phase entry as well as the G2/M checkpoint <sup>179</sup>. Cell cycle arrest via the p53-

p21-retinoblastoma (RB) signaling axis prevents the transition from G1 to S phase<sup>180,181</sup>. In detail, activation of p21 via p53 blocks different cyclin/cyclin dependent kinase (CDK) complexes, amongst others cyclin D – CDK4/6, cyclin A/E – CDK2, and cyclin B – CDK1, resulting in a hypophosphorylation of the tumor suppressor RB. This eventually leads to the formation of an RB-E2F complex and the transcription factor E2F cannot bind to the DNA anymore, resulting in inefficient expression of E2F regulated cell cycle genes, and ultimately G1 cell cycle arrest<sup>182,183</sup>. An overlapping mechanism in inducing cell cycle arrest is the p53-p21-DREAM signaling axis<sup>182</sup>. Activation of p21 leads to the hypophosphorylation of the core proteins p130 and p107, thereby triggering the formation of the DREAM complex, a transcriptional repressor with the ability to bind to the E2F as well as the cell cycle genes homology region (CHR) promoter complexes. Thus, this signaling axis has the ability to regulate cell cycle associated genes ranging from G1 to M phase<sup>182,184</sup>. Consistent with the p53-p21-RB signaling axis, repression of E2F regulated target genes results in G1 arrest, whereas the inhibition of cell cycle genes regulated by CHR promoter leads to a blockade in the G2/M phase of the cell cycle<sup>184,185</sup>. Interestingly, p53 can not only induce cell cycle arrest, but also senescence, which is a typical response to cellular stress for example by the induction of DNA damage and activation of ATM<sup>186</sup>. By activating the p53 signaling pathway, thereby triggering p21 expression, which subsequently leads to the inhibition of CDKs, the cell can also reach a senescent stage<sup>187</sup>.

Since the main task of the p53 family is to ensure genome maintenance, it is a key regulator in the activation of DNA damage repair pathways<sup>188</sup>. If the DNA damage is too severe, cell death is initiated. However, if there is a possibility that the cell can repair the defect, the repair of the DNA is initiated. With this, the p53 family plays a crucial role in the activation of both single strand break repair (SSBR), as well as the double strand break repair (DSBR)<sup>189</sup>.

Upon DNA damage, ATM and p53 is activated, triggering the expression of the p53 target protein growth arrest and DNA damage-inducible 45  $\alpha$  (GADD45 $\alpha$ )<sup>190</sup>. GADD45 $\alpha$  is known to induce cell cycle arrest at the S and G2/M checkpoint, as well as apoptosis. In addition to that, it was shown that p53 dependent induction of GADD45 $\alpha$  also plays a significant role in activating the repair of damaged DNA<sup>191,192</sup>. Figure 5 summarizes the canonical p53 signaling.

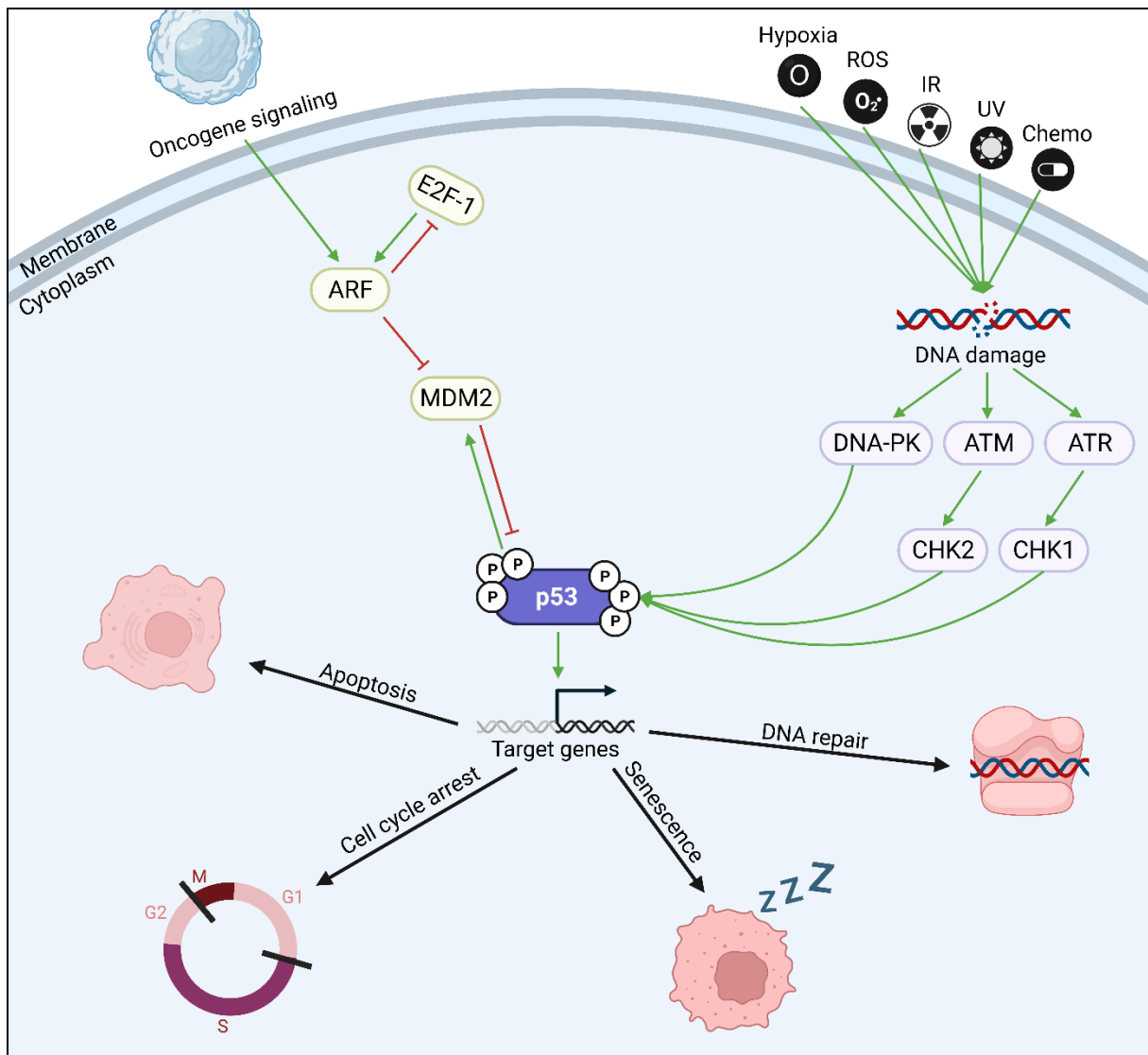


Figure 5: Schematic illustration of p53 canonical signaling. Oncogenic signaling induces p14/ADP-ribosylation factor (ARF) which inhibits murine double minute 2 (MDM2). E2 promoter binding factor 1 (E2F-1) negatively regulates ARF and is activated via ARF. MDM2 is a negative regulator of p53 and thus the oncogenic signaling results in phosphorylation and thereby activation of p53. Distinct factors, such as hypoxia, reactive oxygen species (ROS), ionizing radiation (IR), UV-light (UV), and chemotherapeutic treatment (Chemo.) induce DNA damage. This induces DNA-dependent protein kinase (DNA-PK), Ataxia telangiectasia–mutated (ATM), and Ataxia-telangiectasia mutated and Rad3-related (ATR). ATM activation results induces CHK2, and ATR activation induces CHK1, which in turn activate p53. P53 phosphorylation results mostly in apoptosis, cell cycle arrest, senescence, and DNA repair. The schematic overview was adapted from <sup>181,193,194</sup>. The illustration was created with Biorender.com.

The p53 targets discussed above are subject to the canonical p53 signaling. In contrast to canonical p53 signaling, various cellular processes, such as the tumor microenvironment, stem cell biology, metabolism, and cell death mechanisms are regulated via noncanonical p53 signaling <sup>195,196</sup>. Depending on the signal and the cell state, p53 can regulate the cellular metabolism to induce tumor prevention, or in the case of cancer cells trigger tumor suppression <sup>197</sup>. In the instance of tumor prevention, p53 exerts antioxidant functions, thereby avoiding DNA damage, whereas in the setting of tumor progression, p53 induces ROS, which ultimately triggers cancer cell death <sup>198</sup>.

Also, various p53 mediated noncanonical cell death mechanisms have been described, amongst others caspase-independent apoptosis, ferroptosis, necroptosis, autophagy, paraptosis, pyroptosis, efferocytosis, and mitotic catastrophe<sup>199</sup>. p53 also prevents cancer formation in a noncanonical manner by inducing differentiation of stem cells and suppressing stem cell self-renewal<sup>195</sup>. Moreover, due to the Warburg effect present in cancer cells, indicating that energy production is shifted towards glycolysis and not as usual mitochondrial oxidative phosphorylation, they massively rely on the production of energy in form of ATP via glycolysis<sup>200</sup>. Interestingly, it has been shown that p53 is able to both directly and indirectly downregulate the glucose transporter 1 (GLUT1), glucose transporter 3 (GLUT3), and glucose transporter 4 (GLUT4). In addition, TP53-induced glycolysis and apoptosis regulator (TIGAR) is activated. With this, p53 regulates energy production of cancer cells by suppressing glycolysis, ultimately slowing down cancer cell growth<sup>196,201</sup>.

### 7.3.3. p53 Family in Cancer

*TP53* is the most commonly mutated gene in human cancer, with about half of all cancer patients harboring an alteration in the *TP53* gene<sup>202</sup>. The majority of these mutations are missense mutations and lie in the DBD of the *TP53* gene<sup>203</sup>. *TP53* missense mutations can be divided into DNA contact mutations, meaning that p53 cannot bind the DNA anymore, and conformational mutations, changing the structure of the p53 protein<sup>195</sup>. *TP53* mutations often act as cancer drivers due to the loss of the crucial tumor suppressor function of p53<sup>204</sup>. But interestingly, p53 can not only lose its tumor suppressor functions by inactivating mutations, but also acquire oncogenic properties by gain of function (GOF) mutations<sup>205</sup>. Mutant p53 proteins exert their oncogenic functions via multiple modes of action<sup>206</sup>. By modifying the direct interaction between p53 and the DNA, mutant p53 may alter the efficiency of transcription. Another option is triggering transcription of oncogenic genes by complex formation of mutant p53 with cofactors and transcription factors. Conversely, mutant p53 can bind transcription factors, thus suppressing their ability to bind the promoter of crucial tumor suppressor genes. Also, mutant p53 can directly interact with proteins that are linked to transcriptional regulation of oncogenes and tumor suppressor genes<sup>207</sup>. Interestingly, mutant p53 has the ability to inhibit both p63 and p73, thereby resulting in cancer growth, invasion, and metastasis<sup>205,207</sup>. However, *TP63* and *TP73* are rarely mutated in cancers, but rather regulate cancer development and prevention by altered gene expression<sup>208,209</sup>. In general, overexpression of  $\Delta N$  isoforms is rather associated

with a poor clinical outcome, since this type of isoform acts as an oncogene, whereas downregulation of the TA isoforms tends to correlate with cancer formation <sup>210-212</sup>.

The aforementioned mechanisms show that mutations in the *TP53* gene are highly likely to promote cancer development. A good example is the well-known Li Fraumeni syndrome, in which patients suffer from various cancers already at an early age <sup>213</sup>. The familial clustering of predisposition to cancer formation in these patients is caused by germline mutations of the *TP53* gene <sup>214</sup>.

Interestingly, mutant p53 is very rare in melanoma, as studies revealed that 80-95% of melanoma patients harbor WT p53 expression <sup>215</sup>. Nevertheless, about 90% of melanoma patients show inactivated WT p53 independent of *TP53* genetic mutations, making p53 a potent target to limit melanoma growth <sup>216,217</sup>. Rather than *TP53* genetic mutations, melanoma cells decrease the p53 activity mostly by overexpressing the negative regulators MDM2 and MDM1, or deletions in the p53 activator *CDKN2A* <sup>218-220</sup>.

#### **7.3.4. Pharmacological Modulation of p53 Family Members**

Once elucidating the crucial role of p53 in cell homeostasis and thus cancer prevention, research focused on targeting p53 pharmacologically. Multiple approaches have shown promising results, amongst others p53 gene therapy, p53 based vaccines, targeting of p53 family proteins, restoration of mutant p53 to WT p53, elimination of mutant p53, or inhibition of p53-MDM2 interaction <sup>221</sup>. A method that has been studied for a long time is p53 gene therapy. A recombinant human p53 adenovirus tumor gene is injected into the patients, restoring p53's tumor suppressor function, thus resulting in cancer cell death <sup>222</sup>. Also, activation of the immune system by detecting p53 epitopes on the surface of cancer cells with the help of p53 peptide vaccines results in p53 mutant tumor cell death <sup>223</sup>. Several studies are ongoing focusing on activation of the p53 family proteins, p63 and p73. Possible treatment options include p63 and p73 activators as anti-cancer drugs in p53 mutated tumors, such as RETRA <sup>224</sup>. A promising method to target p53 mutant tumor cells is to interfere with the MDM2-p53 signaling axis <sup>225</sup>. By inhibiting MDM2 with a small molecule inhibitor, such as Nutlin-3 or AMG-232, the WT p53 activity can be restored, resulting in cell cycle arrest and subsequent apoptosis <sup>226,227</sup>. Multiple MDM2 inhibitors are currently being tested in clinical trials for the treatment of various cancer types <sup>228</sup>. By several molecular mechanisms, mutant p53 can be therapeutically restored to its WT activity <sup>229,230</sup>.

These compounds include p53 reactivation and induction of massive apoptosis-1 (PRIMA-1) and its methylated form PRIMA-1<sup>MET</sup>, which show great antitumor activity in various p53 mutant cancers, also in clinical trials <sup>231,232</sup>. Taken together, pharmacological modulation of p53 by multiple mechanisms showed potent antitumor activity both in preclinical and in clinical settings.

#### **7.4. DNA Damage Response**

Damaged DNA is a physiological situation in cells caused by constant endogenous and exogenous mutagens, with endogenous caused DNA damages being more common than exogenous <sup>233</sup>. During DNA replication, specific errors generated by the DNA polymerase (DNA Pol) can be detected and corrected by its 3' → 5' exonuclease proofreading function, thus reducing the number of replication-associated errors <sup>234</sup>. Endogenous metabolic processes can generate agents that function as mutagens. For example, ROS are constantly produced during mitochondrial respiration <sup>235</sup>. Cellular antioxidant defense mechanisms can resolve limited amounts of ROS, however oxidation of bases by endogenous ROS is a common process in the cell <sup>236</sup>. Physiological methylation of the DNA with the molecule *S*-adenosylmethionine is crucial for the regulation of gene expression, but also acts as an endogenous DNA alkylating agent <sup>237</sup>. Spontaneous, endogenous hydrolysis by cleavage of the glycosidic bond results in damaged DNA via the formation of abasic sites (AP sites) <sup>238</sup>.

Exogenous, environmental conditions, such as physical or chemical effects can also damage the DNA. Physical factors, as for example irradiation lead to the induction of reactive species, such as ROS, but can also induce single strand breaks (SSB) or even double strand breaks (DSB) <sup>239</sup>. Ultraviolet (UV)-light exposure causes DNA damage and contributes substantially to the emergence of melanoma and other skin cancers <sup>240</sup>. Via a photochemical reaction, high-energy UV-B radiation creates photoproducts, such as cyclobutane pyrimidine dimers (CPDs), which are covalent bonds between consecutive bases along the nucleotide chain, thus modifying the DNA helix conformation <sup>241</sup>. Alkylating agents can arise from tobacco smoke and commonly methylate the *N*-7 position of guanine (G), forming *N*-7-methylguanine (N-7-MeG) adducts, or methylate the *N*-3 position of adenine (A), forming *N*-3-methyladenine (N-3-MeA) <sup>242</sup>. Unlike the non-cytotoxic N-7-MeG, N-3-MeA is very mutagenic and causes many A-to-T transversions <sup>243</sup>. Exogenous crosslinking agents include for example

platinum-based chemotherapeutics, such as cisplatin, which form inter- and intrastrand crosslinks, mitomycin C (MMC), which produces interstrand crosslinks, or formaldehyde, which causes DNA-protein crosslinks<sup>244,245</sup>. Polycyclic aromatic hydrocarbons (PAHs), found in tobacco smoke and other sources, are known to induce DNA adducts and trigger the production of ROS<sup>246</sup>. Aromatic amines, for example aflatoxin B1 produced by some *Aspergillus* strains, cause DNA adducts, as well as SSB after being activated by Cytochrome P450<sup>246-248</sup>.

In general, DNA damage can lead to cell death, however, unrepaired DNA mutations that activate oncogenes or inactivate tumor suppressor genes can also result in carcinogenesis. Thus, it is crucial for the cell to preserve genomic integrity by using various molecular mechanisms to repair the DNA damages caused by endogenous or exogenous mutations<sup>249</sup>.

#### **7.4.1. DNA Repair Pathways**

In general, the DNA repair pathway can be divided into the repair of single strand damages, including DNA mismatch repair (MMR), base excision repair (BER), nucleotide excision repair (NER), SSBR, and the repair of double strand damages, including HDR and NHEJ<sup>246</sup>.

##### **7.4.1.1. DNA damage response**

The DNA damage response (DDR) is a complex consisting of various sensors, transducers, and effectors, deciding the fate of the cell. The DDR can either initiate the repair of the damage via specific DNA repair pathways, or guide the cell into cell death<sup>250</sup>. ATM, ATR, and DNA-dependent protein kinase, catalytic subunit (DNA-PKcs) show high structural similarities and are crucial for the DDR. ATM is activated by the Mre11-Rad50-Nbs1 (MRN) complex in response to DSB which are to be repaired via homologous recombination repair (HRR), whereas DNA-PKcs shows Ku-dependent activation upon DSB which are to be repaired via non-homologous end joining (NHEJ). Single strands resulting from single SSB are quickly coated by replication protein A (RPA), which then recruit ATR, enabling SSBR<sup>251</sup>.

##### **7.4.1.2. Repair of Single Strand Damages**

###### **7.4.1.2.1. DNA Mismatch Repair**

MMR is a post replicative DNA repair mechanism correcting errors that occurred during the replication process and escaped the proofreading function of the DNA-Pol. These errors mainly include base mismatches, but also strand slippage errors leading to

insertion-deletion mismatches <sup>252</sup>. In humans, MutS homolog 2 (MSH2) forming a heterodimer with either MutS homolog 6 (MSH6) or MutS homolog 3 (MSH3), recognizes the base mismatch. MutL homolog 1 (MLH1) forming a heterodimer with either MutL homolog 3 (MLH3), PMS1, or PMS2 activates the mismatch repair machinery. A proliferating cell nuclear antigen (PCNA) and replication factor C (RFC) dependent endonuclease inserts a nick in the DNA, which allows exonuclease 1 (EXO1) to perform further excision. DNA Pol  $\delta$  fills the gap, which is then closed by the Ligase I <sup>253</sup>.

#### 7.4.1.2.2. *Base Excision Repair*

BER is capable to correct minor damages in the DNA, such as small base lesions caused by endogenous or exogenous factors leading to oxidation, deamination, or alkylation of bases <sup>254</sup>. In detail, the BER process begins with a DNA-glycosylase, which locates the modified base and subsequently cuts the N-glycosyl bond at this site, thereby creating an AP site by a missing base. An apurinic endonuclease (APE1) further cleaves at the AP site causing overhangs. The DBD of poly (ADP-ribose) polymerase 1 (PARP1) then binds to the damaged DNA<sup>255</sup>. With the binding of nicotinamide adenine dinucleotide (NAD)<sup>+</sup> to the NAD<sup>+</sup> binding pocket of PARP1, proteins of the BER complex are poly-ADP-ribosylated and thereby recruited to the DNA damage. Poly-ADP-ribosylation (PARylation) of PARP1 itself (also called auto-PARylation) negatively charges the molecule, leading to its dissociation from the DNA <sup>256,257</sup>. The polymerase (Pol) then bound at the overhang inserts the missing base(s), and lastly the DNA-ligase III complexed to X-ray repair cross complementing 1 (XRCC1) rejoins the gaps created <sup>258</sup>. The BER system can replace a single base, referred to as short-patch BER, or substitute at least two bases, named long-patch BER <sup>259</sup>.

#### 7.4.1.2.3. *Nucleotide Excision Repair*

NER repairs more complex DNA damages, such as bulky, helix distorting DNA lesions. They are mainly induced by CPDs from UV-irradiation or chemical agents, such as PAHs or cisplatin <sup>260</sup>. Recognition of the DNA damage, which is to be repaired by NER can be divided into global genome repair (GGR) and transcription coupled repair (TCR). GGR detects DNA damage in an actively transcribed gene, while GGR repairs defects throughout the genome, regardless of the transcription status <sup>261</sup>. TCR is promoted by RNA Polymerase II (RNAPII), which remains attached to the damaged DNA. The Cockayne syndrome protein B (CSB) interacts with the RNAPII and recruits

the Cockayne syndrome protein A (CSA) complex. This in turn triggers the recruitment of XAB2 and HMGN1, which are critical for chromatin remodeling, leading to cleavage of the nascent mRNA by the RNAPII $\alpha$  so that the transcription can continue after the damage is repaired<sup>262</sup>. In GGR, the damage is recognized by damaged DNA binding protein 2 (DDB2) and damaged DNA binding protein 1 (DDB1), which in turn is detected by xeroderma pigmentosum group C (XPC) complexed with HR23B and centrin 2 (CETN2)<sup>263</sup>. After the recognition of the DNA damage site, both subtypes of the NER proceed in the same way. Xeroderma pigmentosum group B (XPB) and xeroderma pigmentosum group D (XPD), part of the multiunit complex transcription factor IIH (TFIIH), bind to the damage and unwind the DNA to form a bubble. RPA bind the single-stranded DNA (ssDNA) on the opposite side of the damage to prevent the strand from degradation, while XPC is released from the DNA. Next, XPA binds near the 5' position of the DNA bubble, and both xeroderma pigmentosum group G (XPG) and excision repair cross-complementation group 1 (ERCC1)-XPF associate with the TFIIH complex. XPG and ERCC1-XPF now incise into the DNA at their specific positions. Then, DNA Pol  $\delta$  or  $\epsilon$  recruits the helper proteins PCNA as well as RFC and synthesizes the new DNA strand. Lastly, either Ligase I or Ligase III $\alpha$ -XRCC1 religate the DNA strands<sup>264</sup>.

#### 7.4.1.2.4. *Single Strand Break Repair*

SSBR can be activated by direct SSB, such as sugar damages, or by indirect SSB, like for example AP sites<sup>265</sup>. Also, DNA topoisomerase 1 (TOP1) can trigger SSB<sup>266</sup>. The SSBR can be classified into long patch SSBR, short patch SSBR, and TOP1-SSBR<sup>246</sup>. In the long patch SSBR, PARP1 recognizes the SSB and activates its poly-ADP-ribosylation activity, recruiting key SSBR proteins<sup>267</sup>. Next, APE1, polynucleotide kinase 3'-phosphate (PNKP) and aprataxin (APTX) perform end resection, and FEN1 creates a ssDNA gap by removing the damaged 5'-terminus. The gap is then filled with the help of Pol  $\beta$ , Pol  $\delta$ , and Pol  $\epsilon$  and ligase I with the helper proteins PCNA and XRCC1 joins the DNA strands. SSB that need to be repaired via the short patch SSBR are generated during BER. APE1 detects the SSB, and the end processing is performed in the same way as for the long patch SSBR. Pol  $\beta$  fills the gap and ligase 3 religates the DNA strands<sup>268</sup>. As already mentioned, TOP1 can trigger SSB that must be repaired via TOP1-SSBR. In detail, the process is similar to the PARP1-dependent long patch SSBR, with one major difference. The end processing is conducted by the tyrosyl-DNA phosphodiesterase 1 (TDP1) that can remove the

trapped TOP1 from the 3' end of the DNA. Gap filling and re-ligation works in the same way as in long patch SSBR<sup>269</sup>. In Figure 6 MMR, BER, NER, and SSBR are graphically summarized. The similarities and differences between MMR, BER, NER, and SSBR are illustrated in Figure 6.

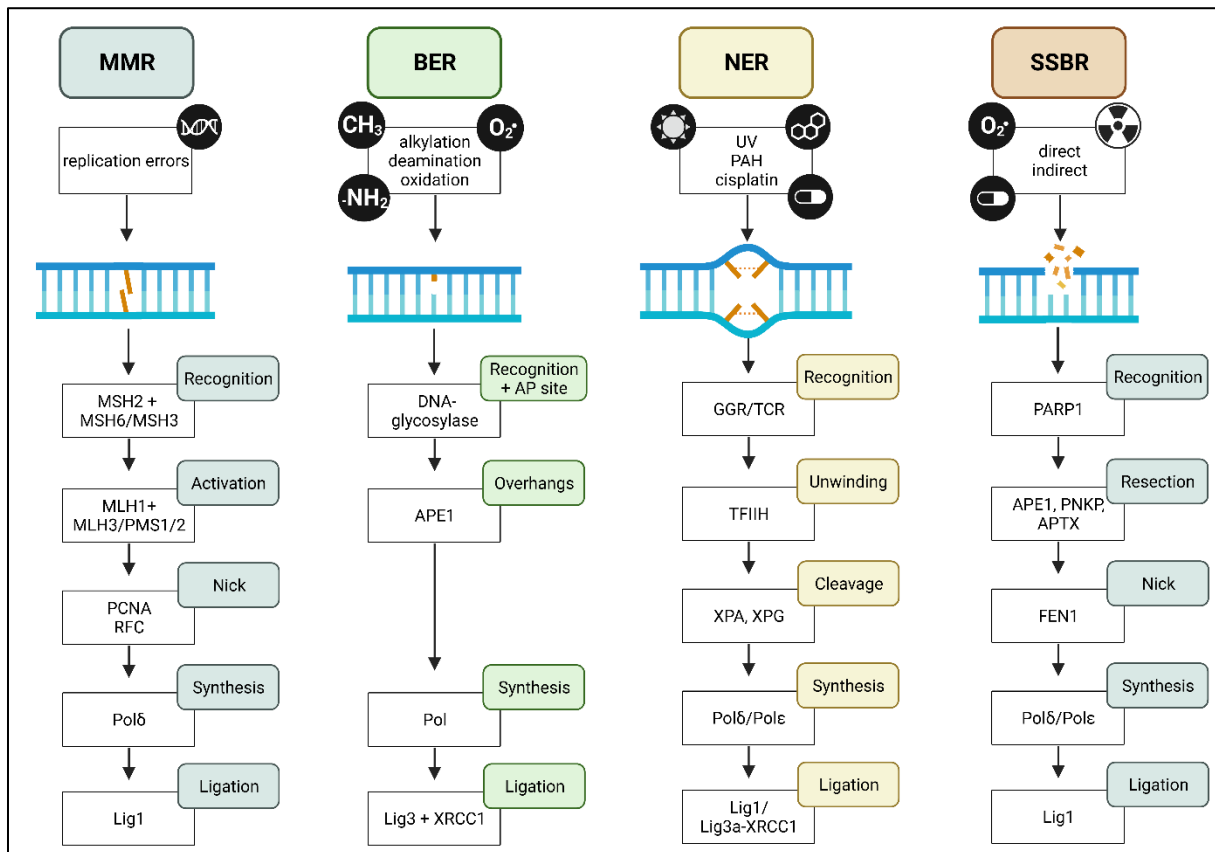


Figure 6: Graphical representation of the repair of single strand damages. DNA mismatch repair (MMR) repairs replication errors. Base excision repair (BER) corrects base mismatches induced by, e.g., alkylation, deamination, or oxidation. Nucleotide excision repair (NER) corrects bulky lesion induced by, e.g., UV light, polycyclic aromatic hydrocarbons (PAH), or platinum-based chemotherapeutics. Single strand break repair (SSBR) corrects single strand breaks that are directly or indirectly induced. All repair pathways can be subdivided into recognition of error, repair, and re-ligation. The illustration was created with BioRender.com.

#### 7.4.1.3. Repair of Double Strand Damages

DSB are even more toxic to the cell than SSB and can be divided into one-ended and two-ended DSB<sup>270</sup>. For example, irradiation induces two-ended DSB, whereas the replication of a SSB can result in a one-ended DSB<sup>271</sup>. The DSBR is a very complex mechanism and can be performed by homology directed repair (HDR) or NHEJ<sup>249</sup>.

##### 7.4.1.3.1. Homology Directed Repair

HDR is an overarching term for all DSBR pathways using homologous sequences to repair the damage in a very precise way. This includes HRR, synthesis-dependent strand annealing (SDSA), break-induced recombination (BIR), and single strand annealing (SSA)<sup>272</sup>. All HDR pathways must undergo an initial end resection to allow

efficient repair. For this, the MRN complex gets activated upon DNA damage. Mre11 has a ssDNA endonuclease activity, as well as a double strand DNA (dsDNA) exonuclease activity, and Rad50 and Nbs1 enhance its function. Next, ATM and CtIP are recruited to the DNA damage<sup>273,274</sup>. The initiation of the end resection is then completed and a short 3' ssDNA overhang is formed, that is of great importance for the extension of the end resection, which is indispensable for HDR. EXO1 is the major protein and indispensable for extensive end resection, as is it able to generate large overhangs<sup>275</sup>. The protein DNA2 harboring a ssDNA endonuclease activity combined with the helicase activity of the bloom-syndrome-protein (BLM) and the Werner syndrome ATP-dependent helicase (WRN) further mediate end resection. RPA coating of the ssDNA strand is of major importance for helicase activity of BLM to facilitate extended end resection<sup>276-278</sup>.

The most important HDR pathway is **HRR**. Since it requires a template in form of the sister chromatid to repair the break, HRR can only be performed when the sister chromatids are in close proximity to each other, namely in the S and G2 phases of the cell cycle<sup>279,280</sup>. The 3' tail that is generated by end resection invades the intact homologous sequence and forms a heteroduplex with the sister chromatid. In detail, breast cancer 1 (BRCA1) is both crucial for the end resection by colocalization with the MRN complex and loading of the Rad51 recombinase to promote HRR. Partner and localizer of BRCA2 (PALB2) is recruited by BRCA1 to the 3' overhang, which in turn recruits breast cancer 2 (BRCA2), essential for binding of Rad51 to ssDNA<sup>281</sup>. With the activation via ATP, Rad51 proteins displace RPA at the 3' tail and coat the ssDNA, termed the presynaptic filament. This allows the homology search to be initiated and a synaptic complex is formed by short base-pairing between the invaded 3' tail and the ssDNA of the homologous sequence. By displacing the second strand of the sister chromatid so that the Rad51 coated 3' tail can enter and form a heteroduplex with the complementary strand, the so-called D-loop is created<sup>282</sup>. The DNA sequence that was lost due to the double-strand break and subsequent end resection can now be restored by the DNA Pol. To ensure the recovery of the entire sequence, the just created Holliday junction needs to migrate. For the branch migration, Rad54, a helper protein of Rad51 steps in<sup>283</sup>. RFC, PCNA, and DNA Pol  $\delta$  mainly mediate extending the D-loop. Unwinding the heteroduplex with a helicase disrupts the D-loop and frees the newly synthesized, invaded ssDNA. To avoid degradation, RPA coats the ssDNA and as a last step, Rad52 anneals the matching strands<sup>284</sup>.

In **SDSA** the D-loop formation is followed by the synthesis of only a short DNA sequence and immediate reannealing with the other end of the DSB <sup>285</sup>. Thereby, SDSA always results in non-crossover products, making this repair mechanism highly attractive for somatic cells <sup>286</sup>.

**BIR** is a pathway that repairs one-ended DSB. These errors occur for example, if accidentally replication is not stopped, even if there is a DNA lesion, which ultimately results in replication fork collapse <sup>287-289</sup>. Since BIR copies the entire distal part of the chromosome, it always results in a translocation or a loss of heterozygosity (LOH) <sup>290</sup>.

Unlike the above presented HDR pathways, **SSA** does not require strand invasion of the homologous sequence, but only repairs damages with direct repeats flanking the DSB. SSA is therefore independent of Rad51 <sup>272,291</sup>. Upon end resection, ERCC1 complexes with XPF and is responsible for cleavage of the 3' ssDNA tails coated with RPA. Rad52 then binds the DNA and promotes the annealing of the matching single strands <sup>292</sup>. The cleavage and the immediate rejoining leads to deletion mutations of these direct repeats. Thus, the SSA pathway leads to deletion mutations <sup>293</sup>.

#### 7.4.1.3.2. *Non-Homologous End Joining*

In comparison to HDR, NHEJ does not require a homologous sequence to repair the DSB, but directly religates the broken ends. With this, NHEJ is a very error prone mechanism and is therefore a major source of genomic instability <sup>294</sup>. In general, NHEJ can be divided into classical NHEJ (cNHEJ) and alternative NHEJ (aNHEJ) <sup>295</sup>. In detail, in cNHEJ, a Ku heterodimer consisting of Ku70 and Ku80 bind the DNA ends at the damage and protect them from resection <sup>296</sup>. Next, DNA-PKcs binds the damaged DNA and phosphorylates crucial substrates, such as Artemis. The activated endonuclease Artemis performs short resection to provide the necessary ssDNA ends for ligation <sup>297</sup>. Finally, a complex of X-ray repair cross complementing 4 (XRCC4), ligase IV, and XRCC4-like factor (XLF) religate the gap between the two matching DNA ends <sup>298</sup>. In comparison to the cNHEJ pathway, where no end resection is needed, the mechanism of aNHEJ, which is also referred to as microhomology mediated end joining (MMEJ) requires initial end resection in a manner that is similar to HDR <sup>272</sup>. Interestingly, MMEJ is independent of Ku, and PARP1 competes for DNA binding with Ku proteins to enable MMEJ <sup>299</sup>. Next, the microhomologous regions are annealed, resulting in heterologous 3' flaps, which are then removed by the XPF/ERCC1

complex. Together with the cofactor XRCC1, ligase 3 and ligase 1 finally join the DNA strands <sup>300,301</sup>.

The decision whether to repair the defect via HRR or cNHEJ is determined by the end resection, which is only activated when the cells are in S or G2 phase of the cell cycle, thus ensuring that the homologous sequence needed as a template is in spatial proximity <sup>302</sup>. The DSBR is summarized in Figure 7.

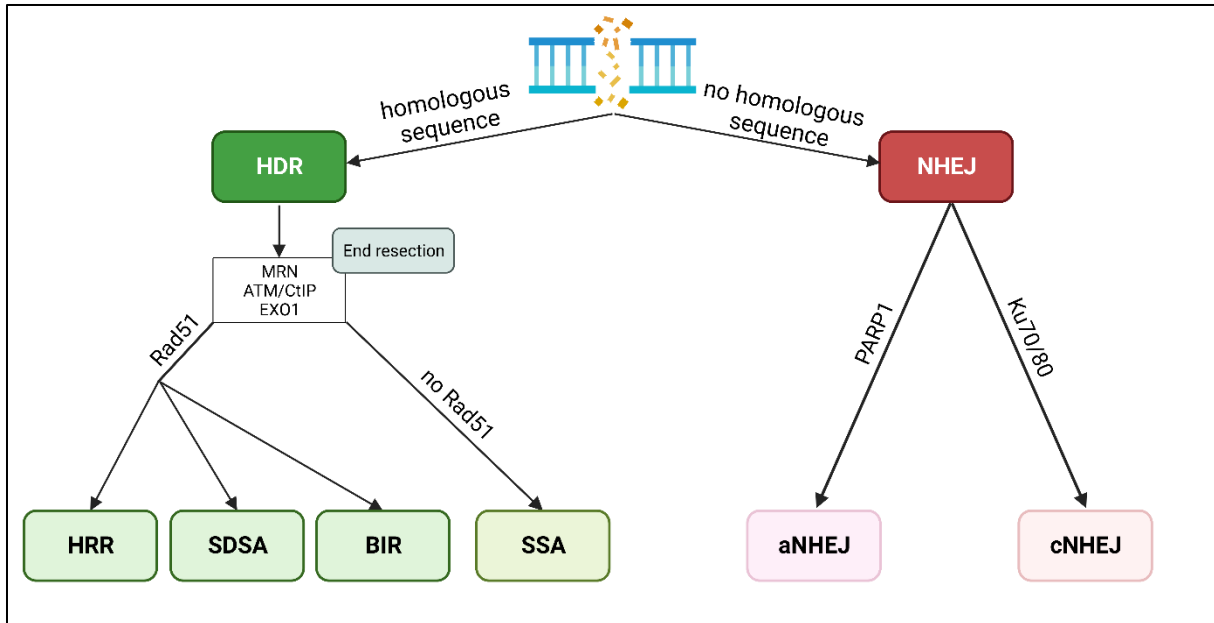


Figure 7: Schematic overview of the repair of DSBR. The DNA double strand break repair (DSBR) can be divided into homology directed repair (HDR) and non-homologous end joining (NHEJ). When HDR can be further separated into homologous recombination repair (HRR), synthesis-dependent strand annealing (SDSA), break induced replication (BIR) and single strand annealing (SSA). NHEJ can be further divided into alternative NHEJ (aNHEJ) and classical NHEJ (cNHEJ). The illustration is adapted from <sup>272</sup> and was created with BioRender.com.

#### 7.4.2. DNA Damage Repair in Tumor Predisposition Syndromes

Aberrant DDR can lead to genomic instability and patients harboring defects in DNA repair pathways are frequently predisposed for various cancers <sup>250,303</sup>.

For instance, defects in the MMR pathway are connected with high microsatellite instability (MSI) i.e. short tandem repeats (STR), and frequently lead to colorectal cancer <sup>304</sup>. Lynch syndrome (LS) is a genetic disorder that harbors mutations in MMR-associated genes, making patients likely to develop tumors <sup>305</sup>. Loss of function (LOF) mutations in the BER-associated gene *MUTYH* also predisposes patients for colorectal cancer and is termed *MUTYH*-associated polyposis (MAP) <sup>306</sup>.

Xeroderma pigmentosum (XP) and Cockayne syndrome (CS), diseases associated with defective DDR, are caused by different mutations in key genes of the NER pathway <sup>307</sup>. The disorders are linked to developmental delay and accelerated ageing,

and most importantly, high risk of skin cancer development<sup>308</sup>. Protection from sunlight is crucial for these patients, since they cannot repair UV-irradiation induced DNA damages<sup>309</sup>.

Ataxia telangiectasia (AT) is a DDR deficiency caused by LOF mutations in the *ATM* gene. The mutation in *ATM* leads to inefficient DDR of DSB<sup>310</sup>. Patients suffer from cerebellar degeneration, and are very susceptible to cancer development, primarily hematological tumors, as well as radiation<sup>311</sup>. Mutations in at least 20 DNA repair genes resulting in the inability to repair interstrand crosslinks give rise to Fanconi anemia (FA), a disease linked to bone marrow failure and cancer susceptibility<sup>312,313</sup>.

Mutations in *BRCA1/BRCA2* genes causing inefficient BRCA1/BRCA2 activity sensitizes especially female patients to breast, ovarian, fallopian tube, peritoneal, and other cancers<sup>314</sup>. The BRCA1/BRCA2 susceptibility results in inappropriate error-free DSBR during S and G2 phase, which ultimately leads to chromosomal instability<sup>315</sup>.

BRCA1-associated protein-1 (BAP1) is a tumor suppressor that is involved in the DNA damage repair via HRR<sup>316</sup>. The BAP1 tumor predisposition syndrome (BAP1-TPDS) is a hereditary cancer syndrome, where patients have germline mutations in the *BAP1* gene, predisposing them to various malignancies, amongst others uveal melanoma, cutaneous melanoma, renal cell carcinoma, and malignant mesothelioma<sup>317</sup>. BAP1-TPDS is associated with very aggressive cancers and early disease onset<sup>318</sup>. Around 40% of patients with uveal melanoma show a mutation in the *BAP1* gene and in more than 80% of metastatic uveal melanoma cells a *BAP1* mutation could be detected<sup>319</sup>.

Taken together, this paragraph shows that mutations causing ineffective DNA damage repair in any of the DNA repair pathways promote tumorigenesis by increasing genomic instability.

#### **7.4.3. DNA Repair Pathways Involved in Melanoma Progression**

Consistent with the above-mentioned importance of maintaining genomic stability to prevent cancer development, DNA repair defects are known to promote melanoma progression.

As discussed in section 7.4, melanoma is often induced by UV-associated DNA damage, that need to be repaired via NER<sup>240,260</sup>. Thus, mutations leading to defective NER machinery have been shown to increase melanoma progression, since the cell is

unable to fix the UV-induced DNA damage<sup>320</sup>. Also, many melanoma patients harbor mutations in the HRR leading to an HRD, ultimately causing genomic instability and thereby cancer development. Studies show that the frequency of HRR mutations in melanoma patients is as high as 18%-41%<sup>321</sup>.

On the other hand, an overexpression of DNA repair genes was shown to be associated with higher metastatic potential, relapse, and decreased overall survival in melanoma patients<sup>322-325</sup>. Activation of the DNA repair machinery is associated with genomic stability throughout the entire genome, ensuring a complete genetic repertoire, and with this the capacity of melanoma cells to invade and metastasize<sup>326</sup>. Massive DNA damage repair is additionally associated with higher resistance to chemotherapeutic or radiotherapy, as the DNA damage induced can be efficiently repaired. This might be one reason, why many metastatic melanomas show increased resistance to chemotherapeutic or radiotherapeutic treatment<sup>322</sup>. Interestingly, Makino et al. showed that upon MAPKi resistance, melanoma cells express reduced NER gene expression, sensitizing these cells to the chemotherapeutic treatment cisplatin<sup>327</sup>.

However, it can be summarized that the DNA repair machinery is not well studied in melanoma. Therefore, it is of main importance to further unravel the role of the DNA repair machinery in melanoma progression and therapy resistance.

#### **7.4.4. Targeting DDR as an Anti-Cancer Therapy**

##### **7.4.4.1. Chemotherapy and Radiotherapy**

In general, chemotherapeutic agents act by inducing DNA damage and thereby particularly targeting rapidly dividing cells, such as cancer cells<sup>328</sup>. In the following, the most prominent groups of chemotherapeutics as anti-cancer agents will be discussed.

Platinum-based chemotherapeutics, such as cisplatin or carboplatin mediate cancer cell toxicity by forming complexes with the DNA via binding of platinum to the N<sup>7</sup> position of purine bases, thereby producing intrastrand crosslinks. In addition, platinum-based therapeutics can also induce interstrand crosslinks, but to a lesser extent<sup>329</sup>. The damages caused in this way must be repaired via NER and to a minor degree via MMR, and unrepaired platinum-DNA adducts lead to cancer cell death<sup>330</sup>. Specific side effects promoted by platinum-based drugs include amongst others nephrotoxicity, myelosuppression, as well as neurotoxicity<sup>331,332</sup>.

Nucleoside analogues are chemotherapeutic agents applied both for solid and hematological cancers<sup>333</sup>. They act by mimicking nucleosides and can therefore be incorporated into the DNA strand during replication instead of the endogenous bases<sup>334</sup>. The integration of nucleoside analogues into the replicating DNA leads to stalled replication forks, thereby activating checkpoints for either cell cycle arrest or the repair of the DNA damage<sup>335</sup>.

As abovementioned, alkylation of DNA results in cross bridges in the DNA, that disturb the helical structure. Alkylating agents act precisely by this molecular mechanism and thereby promote cytotoxicity to fast dividing cells, such as cancer cells<sup>336</sup>.

The severe adverse events of chemotherapeutic agents caused by a high systemic toxicity limit their use as anti-cancer therapeutics. The side effects are mostly directed against rapidly proliferating tissues such as the mucous membranes of the mouth and stomach, leading to gastrointestinal problems, against the bone marrow, leading to decreased blood cell production, and also against the hair follicles, leading to hair loss<sup>337</sup>.

Radiotherapy is based on the principle that irradiation induces DSB, the most toxic form of DNA damage as described before<sup>338</sup>. The inability to repair the DSB or the excess of DSB causes cell cycle arrest and subsequent apoptosis to avoid genomic instability<sup>339</sup>. Targeting the DDR machinery with specific inhibition of major DDR proteins is a way to further sensitize cancers cells to radiation therapy<sup>340</sup>.

#### **7.4.4.2. PARPi Therapy**

Due to the massive off-target effects of classical chemotherapeutic agents, substantial research has been carried out to exploit specific interactions between cancer cells and the DNA damage repair. This should specifically target cancer cells and reduce the side effects on normal tissue. With this, the FDA and EMA approved PARP inhibitors (PARPi), the first anti-cancer therapeutics to directly target the DNA damage repair<sup>341</sup>.

PARP1 and to a lesser extend PARP2 and PARP3 play a central role in BER, since they can detect and bind to SSB, as described in section 7.4.1.2.2.

After binding of the SSB, PARP performs PARylation with the help of NAD<sup>+</sup>, transferring several ADP-ribose groups onto the acceptor protein, thereby enabling posttranscriptional modification of acceptor proteins<sup>342,343</sup>. PARP can auto-PARylate itself, resulting in dissociation from the damaged DNA so that the SSB can be repaired

by the recruited proteins and PARP can detect and bind to the next SSB<sup>344</sup>. Auto-PARylation of PARP also enables XRCC1 to bind to the SSB, which is indispensable for SSBR via BER<sup>345</sup>.

PARPi are NAD<sup>+</sup> analogues that fit into the NAD<sup>+</sup> binding pocket of PARP and thereby competitively bind to PARP<sup>346</sup>. Binding of a PARPi to PARP prevents the PARylation activity of PARP resulting in the inability to repair the SSB via BER. Interestingly, knockout of PARP compared to PARPi treatment has been shown not to cause the same level of cytotoxicity to cells<sup>347</sup>. The inability of NAD<sup>+</sup> to bind in the binding pocket of PARP does not only result in ineffective BER, but the non-functional auto-PARylation results in PARP trapped on the damaged DNA, also referred to as PARP trapping. Consequently, PARP can no longer dissociate from the DNA, which ultimately leads to replication fork collapse or blocking replication fork reversal<sup>348,349</sup>. The resulting DSB poses a strong cytotoxic effect to the cell and must now be repaired via HRR or NHEJ, otherwise the cell dies<sup>350</sup>. PARPi can bind to the NAD<sup>+</sup> binding pocket and thereby inhibit PARP1 and PARP2<sup>347</sup>.

PARPi in a physiological setting show limited cytotoxicity to cancer cells, however, in cancers cells lacking efficient HRR by genetic mutations, PARPi treatment results in massive cancer cell killing. This effect is referred to as synthetic lethality<sup>351</sup>. When cells are deficient in HRR, the DSB induced by PARPi treatment is either repaired with the error prone NHEJ mechanism, or cannot be repaired, leading to cell death induction in either case. Tumors with a mutation in either *BRCA1/BRCA2*, or tumors expressing so called BRCAness, sharing features of BRCA mutated tumors, i.e., ineffective HRR, are therefore particularly sensitive to PARPi therapy<sup>352</sup>. Inactivating mutations of the following genes have shown to contribute amongst others to an HRD: *ARID1A*, *ATM*, *ATRX*, *BAP1*, *BARD1*, *BLM*, *BRCA1/2*, *BRIP1*, *CHEK1/2*, *FANCA/C/D2/E/F/G/L*, *MRE11A*, *NBN*, *PALB2*, *RAD50*, *RAD51*, *RAD51B*, and *WRN*<sup>353</sup>. Moreover, a HRD score has been created, including 3 factors, which predicts the level of HRD, and thereby can forecast the sensitivity of a patient to PARPi therapy. It includes a LOH score, a telomeric allelic imbalance (TAI) score, as well as a large-scale state transition (LST) score. The higher these values, which correlate with the degree of impaired DNA double strand break repair, the higher the expected sensitivity to PARPi therapy<sup>354-356</sup>. The molecular mechanism of PARPi therapy on cancer cells is depicted in Figure 8.

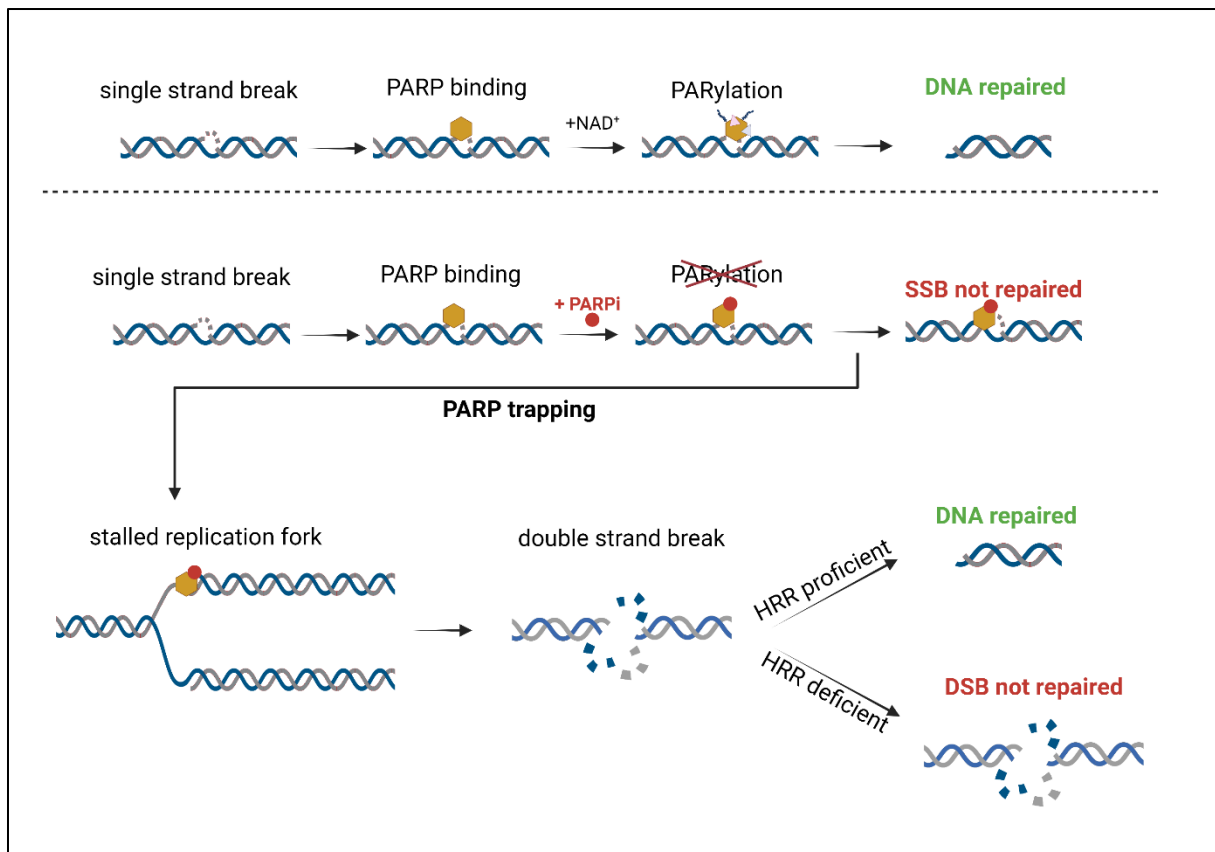


Figure 8: Schematic illustration of the molecular mechanism of PARPi toxicity. Above the dashed line: Role of poly (ADP-ribose) polymerase (PARP) in single strand break repair (SSBR) via base excision repair (BER). Under the dashed line: Mechanism of PARP inhibitor (PARPi) therapy, PARP trapping effect and the role of homologous recombination repair (HRR) in PARPi toxicity. PARPi therapy suppresses the poly-ADP-ribosylation (PARylation) process of PARP, which results in trapped PARP on the DNA, leading to stalled replication forks and the induction of double strand breaks (DSB). In a HRR proficient setting, the DSB can be repaired, however, in a HRR deficient setting, the DSB is not repaired, resulting in cell death. The illustration was created with BioRender.com.

Although PARPi have specific effects compared to chemotherapeutic agents, they still show side effects that can vary widely between the different PARPi. Common adverse events include hematological toxicities, mainly anemia, renal defects causing increased creatinine concentrations, nausea, or fatigue <sup>357</sup>.

**Olaparib** (tradename Lynparza) was the first PARPi to be approved by the FDA and is also approved by the EMA for the treatment of high grade ovarian, fallopian tube and peritoneal cancers, with initial sensitivity to chemotherapeutic treatment and/or HRD positivity <sup>358,359</sup>. In addition, it is used for the treatment of HER2-negative breast cancer with *BRCA1* or *BRCA2* gene mutations, as well as for the management of *BRCA1* or *BRCA2* mutated metastatic pancreatic cancer. Olaparib is also used in metastatic castrate resistant prostate cancer (mCRPC) patients with no response to castration and with *BRCA1* or *BRCA2* gene mutations or without the possibility of chemotherapeutic treatment <sup>359</sup>. Olaparib has shown effective antitumor efficacy in combination with for example the vascular endothelial growth factor (VEGF) inhibitor

bevacizumab in HRD positive ovarian cancer patients, or with abiraterone plus prednisone/prednisolone in HRD positive mCRPC patients <sup>360,361</sup>.

**Rucaparib** (tradename Rubraca) is approved by the EMA for the treatment of high grade ovarian, fallopian tube, and peritoneal cancers either as a maintenance therapy in patients responding to platinum-based chemotherapeutics, or for patients that do no longer respond to platinum-based chemotherapeutics and at best show a *BRCA1/BRCA2* gene mutation <sup>362,363</sup>.

**Niraparib** (tradename Zejula) is approved by the EMA for the treatment of advanced ovarian, fallopian tube, and peritoneal cancer patients who have either responded to platinum-based chemotherapy or whose cancer has relapsed after initial sensitivity to platinum-based chemotherapeutic treatment <sup>364</sup>.

**Talazoparib** (tradename Talzenna) is approved by the EMA for the treatment of HER2-negative *BRCA1/BRCA2* mutated breast cancer patients whose tumors have spread from the primary site, who show previous therapy resistance or when other treatments are not suitable <sup>365</sup>. Compared to the other EMA approved PARPi, talazoparib shows significantly higher antitumor efficacy due to a much higher PARP trapping effect <sup>366</sup>.

According to various reports including different cohorts, the frequency of mutations in the HRR pathway in melanoma patients is as high as 18-41% <sup>367</sup>. After promising *in vitro* and mouse *in vivo* data suggesting that PARPi might be an effective treatment option for melanoma patients, several clinical trials have been and are still being conducted in which PARPi are studied either as monotherapy or as a combination therapy <sup>321</sup>. The results of initial clinical trials using PARPi in melanoma patients did not look promising, but this was due to the fact that all patients were included, regardless of their HRD status. Now, several clinical trials include melanoma patients with HRD positive cancers to evaluate PARPi either as a monotherapy or in combination with immunotherapeutic agents, such as Nivolumab or Pembrolizumab (NCT03207347, NCT03925350, NCT04633902, NCT05482074, NCT04187833, NCT05169437).

Interestingly, preclinical, and clinical investigations of PARPi therapy in combination with other anti-cancer drugs are currently underway. In these studies, PARPi were mostly combined with chemotherapy, radiation therapy, targeted therapy, or with immunotherapeutic agents <sup>368</sup>.

## 8. Aim of the Thesis

Because of the high mortality of advanced melanoma patients, mostly due to limited therapy options and resistance mechanisms to anti-cancer therapeutics, the overall aim of this study was to improve the therapy of melanoma patients by understanding the molecular mechanisms of targeted therapy resistance and deciphering ways to overcome this. Our goal was to unravel the complex interplay of the p53 family members and to enhance the comprehension of the crucial role of the DNA damage response in melanoma therapy.

The specific aims for the included publications were the following:

**Accepted Publication I:** The aim of this publication was to (I) assess the impact of the p53 target p21 in the sensitivity to MDM2i and to (II) investigate the role of MDM2i sensitivity in the response to targeted therapy. Also, the goal of this publication was to (III) understand the interplay between p53 and its family member p73 in melanoma cells.

**Accepted Publication II:** The aim of this publication was to (I) assess the role of the BRAFi sensitivity status to PARPi responsiveness and to (II) understand the molecular mechanism behind the elevated sensitivity of BRAFi resistant melanoma cells to PARPi therapy. Also, the goal of this publication was to (III) study the role of the p53 family in PARPi associated melanoma cell death and to (IV) decipher the synthetic lethal interaction underlying the combinational therapy of MAPKi and PARPi treatment in melanoma cells.

**Submitted Publication I:** The aim of this publication was to (I) understand the role of PARP1 as a predictive biomarker for PARPi therapy response and to (II) assess the expression of PARP1 in melanoma samples and non-malignant skin cells. Also, the goal of this publication was to (III) unravel the role of PARP1 in the progression of melanoma samples as well as the overall survival of melanoma patients.

## 9. Results and Discussion

Given the constraints imposed by the emergence of MAPKi resistance, the investigation of alternative therapies capable of overcoming this challenge became the central focus of the thesis. The aim was to explore and assess potential solutions that could effectively address MAPKi resistance and expand the therapeutic options available to melanoma patients (see section 7.2.4.4 and 7.2.4.5)<sup>83-85</sup>.

### 9.1. *Relevance of MDM2 Inhibitor Treatment in Melanoma Therapy*

Even though *TP53* is the most commonly mutated tumor suppressor gene in human cancers, up to 80% of melanoma patients express WT p53 (see section 7.3.3)<sup>202,215</sup>. Surprisingly, however approximately 90% of melanomas show inactivated p53 function due to factors, such as deletions in the *CDKN2A* locus or the overexpression of MDM2, a negative regulator of p53 activity (see section 7.3.2 and 7.3.3)<sup>165,216-220</sup>. The rationale of targeting p53 in cancer cells is to restore its WT activity, thereby inducing cell cycle arrest via the p53-p21 axis, and also triggering the activation of p53-dependent apoptosis (see section 7.3.4)<sup>173,179</sup>. Based on these observations, we hypothesized that despite the absence of *TP53* mutations and because of the high frequency of overexpression of MDM2 in melanoma patients, MDM2i therapy could be a beneficial treatment strategy for this patient group. Additionally, we explored the potential interplay between MAPKi and MDM2i, particularly in MAPKi resistant melanoma cells.

#### 9.1.1. *CDKN1A/p21 Levels Correlate with MDM2 Inhibitor Sensitivity*

To assess the potential role of MDM2i in melanoma therapy, we used a diverse set of cell lines with WT p53, mutant p53 leading to a partial functionality of p53, and mutant p53 resulting in non-functional p53 activity. We could show that MDM2 inhibition via Nutlin-3 or AMG-232 treatment reduced the cell viability in a dose-dependent manner (Accepted Publication I, Figure 1A and 1B). This goes in line with previous publications, showing that p53 rescue by MDM2 inhibition suppresses melanoma cell growth in a large cohort of melanoma samples including patient derived xenograft (PDX) models<sup>369,370</sup>. We found that while some melanoma cell lines responded well to MDM2i treatment, others had a much lower sensitivity. This allowed us to split the different melanoma cells into two groups: MDM2i sensitive and MDM2i resistant. Interestingly, the MDM2i sensitivity status did not correlate with the *TP53* mutational status (Accepted Publication I, Table 1). Several other publications rejected the common

assumption that the *TP53* mutational status determines the sensitivity to MDM2i and thus investigated in alternative predictive biomarkers to forecast the MDM2i response rates<sup>371,372</sup>. In addition, no clear association between the *TP53* mutational status and p53 transcript expression could be determined, suggesting that altered p53 activity in melanoma cells is independent of the p53 mutational status<sup>373</sup>.

We therefore checked for other p53 targets, that might have an influence on MDM2i sensitivity. We found that the basal gene expression of *CDKN1A*, and in line with this the basal protein expression of p21, was elevated in MDM2i sensitive compared to MDM2i resistant cells (Accepted Publication I, Figure 1C and 1D). It is well known that p21 mediates p53-induced G1 cell cycle arrest, thereby ultimately triggering cell death (see section 7.3.2)<sup>182,183,374,375</sup>. Interestingly, we discovered that treatment with Nutlin-3 exclusively in MDM2i sensitive melanoma cell lines resulted in a massive increase in p21 protein levels (Accepted Publication I, Figure 2C). Consistent with that, additional publications revealed that MDM2i therapy enhances p21 expression leading to p21-mediated cell cycle arrest and subsequent apoptosis<sup>376,377</sup>. In contrast, in MDM2i resistant cell lines, no p21 protein expression was triggered, causing less cancer cell killing (Accepted Publication I, Figure 2C).

In recent years, it has become increasingly clear that p21 can also be regulated and induced independently of p53 to exert its tumor suppressor functions<sup>378,379</sup>. However, when p21 is present in the nucleus, it may exert oncogenic functions, such as activation of proliferation and migration<sup>380</sup>. A study showed that p53-independent upregulation of p21 in the initial phase acts as a senescence inducer, but the remaining proliferating p21 expressing cells tend to act more oncogenic by increasing genomic instability, thereby promoting aggressiveness and chemoresistance of these tumor cells<sup>381</sup>. This suggests that the particularly aggressive and thus difficult-to-treat melanoma cells that express high levels of p53-independent p21 may benefit from the treatment with MDM2i.

Taken together, we suggest that irrespective of the *TP53* mutational status, high p21 levels emerge as a critical determinant for a favorable response of melanoma cells to MDM2i treatment. These findings not only underscore the significance of p21 in therapeutic outcomes but also shed light on potential strategies for enhancing the efficacy of MDM2i therapy in melanoma patients.

Interestingly, we did not see significant differences in MDM2i sensitivity between MAPKi sensitive and BRAFi resistant melanoma cells, suggesting that the BRAFi resistance status is not decisive for the MDM2i sensitivity status (Accepted Publication I, Figure 1A and 1B). Therefore, we propose that melanoma patients suffering from BRAFi resistance, and thus have limited targeted therapeutic options, may profit from MDM2i treatment.

### 9.1.2. MDM2 Inhibitor Treatment Increases BRAF Inhibitor Sensitivity

Since the aim of this study was to find effective treatment options for BRAFi resistant melanoma patients, we were interested in whether MDM2i could potentially enhance the response to BRAFi therapy in BRAFi resistant melanoma cell lines. Interestingly, compared to the single treatment, combined treatment with BRAFi and MDM2i decreased the cell viability of MDM2i sensitive cell lines in a synergistic manner (Accepted Publication I, Figure 2A and 2B). This goes in line with a variety of previous other publications stating that MDM2i treatment potentiates BRAFi therapy in melanoma<sup>369,370,382-384</sup>. Promising results also show that a large number of clinical trials focus now on the combination of MAPKi plus MDM2i therapy in melanoma patients. The combination showed marked improvement in response rates, PFS, and OS which were superior to BRAFi treatment alone and in addition, side effects associated with the development of MAPKi resistance were lower<sup>385</sup>.

However, only an additive effect of combined BRAFi and MDM2i therapy was achieved in MDM2i resistant cells (Accepted Publication I, Figure 2A and 2B). The combined treatment induced the p53 targets *CDKN1A*, *MDM2*, and *BAX* in MDM2i sensitive cells (Accepted Publication I, Supplementary Figure 1A and 1B). Surprisingly, the single MDM2i therapy as well as combined BRAFi plus MDM2i treatment resulted in a massive induction of p21 solely in MDM2i sensitive cells (Accepted Publication I, Figure 2C). Another study showed similar results, proving a clear induction of p21 and further p53 target genes after MDM2i treatment in melanoma cells that were susceptible to MDM2 inhibition<sup>386</sup>. For the first time, we could show that the combinatorial treatment of BRAFi plus MDM2i induces a synergistic effect in some BRAFi resistant cells, but not in all. More precisely, MDM2i resistant melanoma cells, that did not respond to a combinational BRAFi plus MDM2i therapy, also did not show a p53 signaling transduction, suggesting that the p53 activation and thereby the direct induction of p53 target genes is of great importance for the synergistic effect.

Consistent with existing literature, our findings demonstrate that the combinatorial treatment of BRAFi plus MDM2i elicits a favorable response, particularly in the difficult-to-treat MAPKi resistant melanoma cells<sup>387</sup>.

With this, we conclude that the MDM2i treatment confers high sensitivity to BRAFi treatment in BRAFi resistant, MDM2i sensitive melanoma cells. These data unveil a promising treatment synergy that has the potential to pave the way for new treatment combinations for patients suffering from BRAFi resistance.

### 9.1.3. p21 Expression Levels Regulate Sensitivity to Targeted Therapies

Next, our aim was to further investigate whether p21 plays a role in the sensitivity of melanoma cells to targeted therapies. We were able to show that upon knockout of p53, and with this the absence of p53 target gene induction, MDM2i treatment has a lesser effect on decreasing melanoma cell viability (Accepted Publication I, Figure 3A-C). However, the effect of MDM2i treatment on melanoma cell viability was not completely attenuated, leading to the conclusion that a mechanism independent of p53 itself plays a critical role in the therapeutic response of melanoma cells to MDM2i. Supporting this hypothesis, various publications showed that MDM2i treatment induces cell death even in p53 deficient cancer cells<sup>388,389</sup>.

By ectopic overexpression of *CDKN1A*, and thereby the induction of p21 protein levels, we were able to sensitize both BRAFi sensitive as well as BRAFi resistant, MDM2i sensitive melanoma cells to both MDM2i and BRAFi treatment (Accepted Publication I, Figure 3F, 3H, and 3J). In accordance with that, a siRNA mediated knockdown of *CDKN1A* decreased the response to both MDM2i and BRAFi targeted therapies (Accepted Publication I, Figure 3E, 3G, and 3I).

These findings align with additional publications indicating that the effectiveness of MDM2i treatment relies on the induction of p21. Notably, the absence of p21 prevents the induction of growth arrest and senescence upon Nutlin-3 therapy<sup>390</sup>. Moreover, p21 was shown to be regulated by MDM2 independently of p53, pointing to a questionable role of p53 in MDM2i sensitivity of melanoma cells<sup>391</sup>.

In summary, our findings illustrate that the induction of p21 upon MDM2i treatment and subsequent cell death can occur independently of p53, highlighting that the levels of p21 induction, rather than the mutational status of p53, dictate the sensitivity of melanoma cells to MDM2i.

In a previous publication from our research group, it was demonstrated that cells resistant to BRAFi exhibit heightened sensitivity to the chemotherapeutic agent cisplatin<sup>327</sup>. Interestingly, this increased sensitivity was not attributed to p53 activation but rather to a decreased expression of the TAp73 isoform. Hence, our prior findings, coupled with the outcomes of this study, suggest that different members of the p53 family confer distinct sensitivities to anti-melanoma substances.

## **9.2. Crosstalk Between p53 Family Members and Targets in Melanoma Cells**

Considering the interesting observation, that p21 levels rather than the *TP53* mutational status plays a role in the response of melanoma cells to targeted therapy, we were interested in the crosstalk between the p53 family members and p53 targets. We found that siRNA induced knockdown of *CDKN1A* resulted in a decreased p53 protein expression, however p73 protein levels were increased (Accepted Publication I, Figure 3D). This suggests that, conversely, p21 positively regulates p53 signaling. Indeed, publications show that p21 induces p53 signaling in a positive loop across the ATM-p21 axis<sup>392</sup>. Because no direct interactions between p21 and p73 expression have been described, we proposed that the upregulation of p73 after knockdown of p21 resulted from p53 protein expression downregulation.

Based on these results, we postulated a potential negative cross-regulation of p53 and p73 in melanoma cells. We could show that p53 negatively regulates the protein expression of p73. A p53 overexpression decreased p73 protein expression in BRAFi sensitive and resistant melanoma cells, and vice versa, siRNA induced p53 knockdown enhanced total p73 protein (Accepted Publication I, Figure 4A). Surprisingly, the gene expressions of *TP73* and *TATP73* were not decreased after p53 knockdown, indicating a posttranscriptional regulation of p73 expression by p53 (Accepted Publication I, Figure 4B). Unexpectedly, MDM2 inhibition by siRNA or MDM2i treatment reduced both protein and gene expression of p73/*TP73*/*TATP73* (Accepted Publication I, Figure 4 C, Supplementary Figure 1J).

Various publications revealed that p53 can bind to the promoter of *TP73*, thereby inducing p73 expression upon cellular stress<sup>393,394</sup>. However, we show for the first time a negative regulation of p53 on p73 expression. Interestingly, it has been demonstrated that p53 is unable to trigger apoptosis upon DNA damage, if p63 and p73 are not expressed<sup>395</sup>. As p53 acts not only as a tumor suppressor gene (see section 7.3.2)

but also as an oncogene, downregulation of p73 following p53 induction may prevent p53-mediated cell death, consequently promoting the survival of cancer cells<sup>396</sup>. These observations go in line with further findings indicating that TAp73 functions as a tumor suppressor, and its downregulation results in increased invasion and migration of tumor cells<sup>397</sup>. Taken together, we propose that p53 paradoxically negatively regulates p73 to dampen the tumor suppressor signaling and to promote the oncogenic signature by inhibiting cell death in metastatic melanoma cells.

Given that p53 alteration did not affect the gene expression of *TP73* but negatively regulated p73 protein expression, while MDM2i treatment influenced both the gene expression of *TP73* and the protein expression of p73, we hypothesized that these mechanisms are distinct from each other. Indeed, MDM2 has been shown to bind directly to the promoter of *TP73* independent of p53 and induces TAp73 protein expression<sup>398,399</sup>. Thus, our findings demonstrate that MDM2i exhibit a similar effect than direct p53 overexpression, namely inhibition of p73 protein expression, but likely operate through distinct signaling pathways.

Of interest, based on our data, in turn, p73 has no effect on the expression of p53/*TP53* (Accepted Publication I, Figure 4D and 4E). This suggests that p73 plays a minor role compared to p53 and thus does not have the potential to regulate p53 expression.

To summarize, we were able to unravel a novel crosstalk between the p53 family members in metastatic melanoma cell lines, specifically highlighting the negative regulation of p73 by p53 to maintain cancer cell growth.

### **9.3. Significance of PARP Inhibitor Treatment in Melanoma Therapy**

Melanoma is associated with a high mutational load by massive DNA damage due to unrepaired sunlight associated DNA damages (see section 7.4)<sup>240,400</sup>. Also, maintaining genomic integrity by efficient repair of the DNA damages is of utmost significance to prevent cancer cell growth (see section 7.4.2)<sup>250,303</sup>. PARPi are the first FDA and EMA approved drugs to specifically target the DDR<sup>341</sup>. They act by inhibiting BER and additionally the PARP trapping effect induces DSB, that cause the main cytotoxicity<sup>347-349</sup>. Especially in cancer cells that show an HRD, PARPi demonstrate strong antitumor responses by a synthetic lethal interaction (see section 7.4.4.2)<sup>351</sup>. In this project, a possible application of PARPi therapy for melanoma patients was to be

assessed. Moreover, potential combination strategies of PARPi with other typical anti-melanoma agents, such as MAPKi were investigated. In the last part of the project, the role of PARP1 as a potential biomarker to forecast PARPi response and the influence of PARP1 on metastatic potential and overall survival of melanoma patients was to be identified.

### **9.3.1. PARP Inhibitor Treatment Effectively Kills BRAF Inhibitor Resistant Melanoma Cells**

In the first part, we investigated whether melanoma cells respond to PARPi therapy and checked for differences in PARPi response between MAPKi sensitive and MAPKi resistant melanoma cell lines. We were able to show that melanoma cells can be killed by PARPi treatment. Recent reviews focusing on the influence of DDR inhibitors in melanoma therapy summarized that PARPi treatment might serve as an appropriate therapy approach for certain melanoma patients, as both *in vitro* as well as *in vivo* experiments showed promising results<sup>321,401</sup>.

Interestingly, we found a significant enhanced PARPi response in MAPKi resistant melanoma cells compared to their sensitive counterpart (Accepted Publication II, Figure 1A). We could confirm this effect in a PDX cell line of a melanoma patient who developed clinical acquired resistance towards the BRAFi vemurafenib and the MEKi dabrafenib (Accepted Publication II, Figure 1A). In an *in vivo* experiment, we were able to confirm the killing effect of PARPi treatment, as the tumor growth of a MAPKi resistant melanoma cell line was nearly completely blocked in NOD scid gamma (NSG) mice that were treated with the PARPi talazoparib (Accepted Publication II, Figure 1B-1D). Additional studies also indicate that melanoma cells resistant to BRAFi are more effectively eradicated by PARPi treatment in comparison to their sensitive counterparts<sup>402</sup>. Nevertheless, the underlying molecular mechanism responsible for this effect has remained elusive.

In addition, we were able to show that PARPi treatment might decrease the metastatic potential of MAPKi resistant melanoma cells, as treatment with talazoparib clearly reduced the migration capability as well as the invasion potential of a metastatic melanoma cell line (Accepted Publication II, Figure 2A). Additional publications corroborate our data by indicating that PARPi treatment suppresses the migration, invasion, and colonization of distant organs by metastatic melanoma cells<sup>402,403</sup>.

Taken together, these findings suggest that PARPi treatment may not only cause a reduction in the size of the primary tumor but also diminish the metastatic capabilities of melanoma cells.

### **9.3.2. Significance of p53 in PARP Inhibitor Induced Melanoma Cell Death**

Based on the results indicating that PARPi induced massive cell death, especially of MAPKi resistant melanoma cell lines, we further aimed to unravel the molecular mechanism underlying this clear anti-melanoma effect. We could show that after talazoparib treatment, a massive G2/M arrest with a subsequent induction of G1 arrested cells was triggered (Accepted Publication II, Figure 2B, Figure 2C). To avoid genomic instability, the entry into mitosis is prevented and cells are arrested the G2/M if DSB are detected <sup>404</sup>. Indeed, it has been demonstrated that PARP depletion or inhibition results in mitotic defects, and PARPi treatment triggers a stress-induced cell death mechanism, termed mitotic catastrophe <sup>405,406</sup>. Cells that have evaded the G2/M checkpoint and entered mitosis despite being damaged may potentially exhibit a polyploid phenotype. Subsequently, these cells could now face arrest at the postmitotic G1 cell cycle phase, as the p53-dependent polyploidy checkpoint is triggered and thereby cell death via apoptosis is induced <sup>407,408</sup>.

To prove our hypothesis, we checked for p53-associated gene expression after PARPi treatment. Indeed, genes associated with p53-dependent activation of cell cycle arrest as well as apoptosis were clearly enhanced in melanoma cells treated with talazoparib (Accepted Publication II, Figure 2D, Supplementary Table ST1). Certainly, p53 is known to be crucial for DNA damage induced regulation of cell death <sup>409</sup>. Interestingly, the induction of p53 signaling in response to PARPi therapy has not been extensively studied. However, as stated above, PARPi treatment induces DNA damage, that directly can activate p53 signaling to either trigger the repair of the DNA or induce cell death (see section 7.3.2) <sup>163,164,169,172</sup>.

Further analysis revealed a potent induction of *CDKN1A* transcripts, a classical p53 target gene responsible for cell cycle arrest and apoptosis (Accepted Publication II, Figure 2F and 2E, Supplementary Figure S1A). Indeed, the activation of p21 via p53 signaling is well-established as a key mechanism for both G2/M and G1 checkpoint arrest in response to DNA damage <sup>410-412</sup>.

To sum up, we could show that PARPi treatment induces massive DNA damage, leading to G2/M arrest and mitotic catastrophe as well as subsequent G1 arrest and apoptosis. This mechanism is mainly mediated by induction of p53 and its targets, such as p21, in MAPKi resistant melanoma cells.

### **9.3.3. Relevance of ATM in Enhanced PARP Inhibitor Sensitivity of MAPK Inhibitor Resistant Melanoma Cells**

Considering that initial experiments revealed that MAPKi resistant melanoma cells are more susceptible to PARPi therapy in comparison to their treatment naïve counterpart, we aimed to understand the molecular mechanism behind this effect. Therefore, we compared treatment naïve and MAPKi resistant cells and found increased pH2AX levels, indicating elevated DNA damage in the MAPKi resistant cells (Accepted Publication II, Figure 3A, Supplementary Figure S1B) <sup>413,414</sup>. Since the PARP trapping induces DSB (see section 7.4.4.2) <sup>348,349</sup>, we hypothesized that a higher PARP trapping effect correlates with the induced DNA damage in MAPKi resistant melanoma cells.

Surprisingly, the PARP trapping was not enhanced in MAPKi resistant cells compared to MAPKi sensitive cells (Accepted Publication II, Figure 2B). We therefore concluded, that MAPKi resistant cells potentially have an impaired DNA damage repair activity. We thus checked for the expression of multiple DNA repair associated genes and found that ATM, a major sensor of DNA double strand breaks was reduced in MAPKi resistant cells and patient samples compared to their sensitive counterparts both on RNA and protein level (Accepted Publication II, Figure 3C, 3D, 3E, 3F, Supplementary Figure S1C, S1D). A cell viability assay of melanoma cells from a patient that has truncated ATM due to a genetic mutation reinforced our hypothesis, that ATM regulates PARPi response in melanoma cells (Accepted Publication II, Figure 3G).

As ATM is the most upstream DDR kinase of HRR and acts as a DSB sensor mediating the phosphorylation of HRR proteins and thereby triggering the repair of a DSB via HRR, it has been shown to have an impact on PARPi therapy response (see section 7.4.1) <sup>415,416</sup>. Indeed, numerous studies have provided evidence that cancer cells lacking functional ATM exhibit impaired HRR due to inefficient DNA damage sensing. Consequently, these cells are particularly vulnerable to treatment with PARPi as they act synthetic lethal <sup>417-419</sup>. Furthermore, due to the encouraging preclinical findings, clinical trials are currently being conducted to assess the effectiveness of PARPi treatment in cancer patients showing somatic or germline ATM gene mutations. These

trials encompass various cancer types, including melanoma patients (NCT03925350, NCT04633902) <sup>401</sup>.

A potential mechanism through which MAPKi resistant melanoma cells downregulate ATM gene and protein levels is by the paradoxical reactivation of the MAPK pathway during the development of resistance. This reactivation is often accompanied by the upregulation of the mTOR pathway, which is known to exert a negative effect on ATM expression <sup>420,421</sup>. Moreover, our research group showed that MAPKi resistance is associated with downregulated TAp73 levels <sup>327</sup>. Preliminary experiments indicate that the TAp73 isoform may positively influence ATM regulation levels (data not shown). Consequently, the development of MAPKi resistance leads to decreased TAp73 and ATM.

The use of an ATM inhibitor unveiled that MAPKi sensitive cells exhibit a significantly greater dependency on ATM activity compared to MAPKi resistant cells, as Ku-55933 demonstrated a lack of efficacy in inducing cell death in MAPKi resistant melanoma cells; however, the inhibitor demonstrated significant toxicity in MAPKi sensitive cells (Accepted Publication II, Figure 3H). These findings suggest that the downregulation of ATM during the emergence of MAPKi resistance leads to a diminished reliance on ATM signaling in MAPKi resistant cells, distinguishing them from MAPKi sensitive cells. This observation is consistent with a publication indicating that ATM-deficient cells do not exhibit a response to the ATM inhibitor Ku-55933 <sup>422</sup>.

Most strikingly, the pretreatment of MAPKi sensitive melanoma cells with the ATM inhibitor to reduce ATM activity resulted in enhanced response to the PARPi talazoparib (Accepted Publication II, Figure 3I). With this we were able to resemble the MAPKi resistance development in MAPKi sensitive cells and identified that low ATM levels confer the high sensitivity of MAPKi resistant melanoma cells to PARPi treatment.

Collectively, our compelling findings underscore the potential benefits of PARPi therapy for difficult-to-treat MAPKi resistant melanoma patients. Remarkably, these patients exhibit lower ATM levels, rendering them highly susceptible to PARPi treatment through a powerful synthetic lethal interaction.

### 9.3.4. Synergistic Killing of Melanoma Cells by Combined MAPK Inhibitor and PARP Inhibitor Therapy

Extensive investigations have focused on exploring the use of PARPi in combination with chemotherapy, ionizing radiation, or immunotherapies, both in preclinical and clinical settings (see section 7.4.4.2)<sup>341,344,368</sup>. Nevertheless, the potential of combining PARPi with targeted therapies, particularly with MAPKi, remains an area that requires further research.

To determine the clinical therapeutic benefit of PARPi more precisely for melanoma patients, we co-treated MAPKi sensitive, BRAFi resistant, as well as BRAFi plus MEKi double resistant melanoma cells with PARPi in combination with MAPKi. In MAPKi sensitive cells, a synergistic combinatorial effect between the PARPi talazoparib or olaparib and the BRAFi vemurafenib was observed (Accepted Publication II, Figure 4D, 4E, and 4F, Supplementary Figure S1C and S1D). While no combinatorial effect of the PARPi talazoparib and the BRAFi vemurafenib in BRAFi resistant melanoma cells was detected, a synergistic reduction of cell viability in BRAFi resistant cells was seen after combined treatment of talazoparib and the MEKi trametinib (Accepted Publication II, Figure 4A and 4B, Supplementary Figure S1A). In line with this the panRAFi LY3009120 enhanced talazoparib treatment in a synergistic manner in BRAFi plus MEKi double resistant melanoma cells (Accepted Publication II, Figure 4C, Supplementary Figure 1B). The *in vitro* data could be confirmed in an *in vivo* mouse model, where BRAFi sensitive melanoma cells were injected into NSG mice, and treated with either control, the monotherapies, or the combination of talazoparib and vemurafenib. Most strikingly, the monotherapies as well as the control showed increased tumor size over time, while the tumor volume of mice treated with the combination was even reduced (Accepted Publication II, Figure 4G and 4H).

In line with our results, Sun et al. demonstrated a synthetic lethal interaction between PARPi and MEKi or ERKi in a variety of Ras mutated MAPKi sensitive cell lines. Furthermore, they could show that suppressing the MAPK pathway can reverse acquired PARPi resistance, a phenomenon commonly observed in patients undergoing PARPi treatment<sup>423-425</sup>. An additional publication supports this hypothesis, revealing that the combination of the BRAFi dabrafenib, the MEKi trametinib, and the PARPi olaparib induced a synthetic lethal interaction in MAPKi sensitive melanoma cells<sup>426</sup>. Most remarkably, these highly encouraging findings paved the way for an exciting clinical trial (NCT03162627), wherein the potential of the combination therapy

involving the PARPi olaparib and the MEKi selumetinib will be assessed. The trial aims to evaluate its effectiveness in treating endometrial, ovarian, and other solid tumors harboring a Ras mutation, as well as ovarian tumors with PARPi resistance <sup>427</sup>.

Interestingly, we found that the combination treatment is specific to melanoma cells, as the same treatment resulted in significantly lower cytotoxicity in primary human fibroblasts (Accepted Publication II, Supplementary Figure S2E).

By suppressing the MAPK signaling pathway in BRAF mutated melanoma cell lines, a synergistic reduction of cell viability in combination with PARPi is only achieved, if the cell shows overactivated MAPK pathway activation and thereby responds to MAPKi therapy. In contrast to melanoma cells, a negative feedback loop ensures that the MAPK pathway activation remains at a physiological level in non-malignant skin cells <sup>428</sup>. Thus, the massive cytotoxic effect of the combined treatment is exclusively induced in tumor cells. This remarkable effect holds immense promise for clinical applications, as it suggests that the combination therapy selectively targets cancer cells while sparing healthy cells <sup>429</sup>. Consequently, the potential for general side effects is significantly reduced, presenting a highly advantageous prospect in the pursuit of effective and well-tolerated treatments.

Through our research, we have successfully unraveled promising treatment strategies for melanoma patients, unveiling the potential of combining PARPi with various MAPKi. The most advantageous combinations emerged, tailored to different patient groups: MAPKi sensitive patients profit from a combination of PARPi paired with a BRAFi. BRAFi resistant patients do not profit from this treatment, but the combination of PARPi with MEKi showed remarkable potential. In line with this, the combination of PARPi with panRAFi demonstrated promising efficacy in BRAFi plus MEKi double resistant melanoma patients. These novel treatment approaches offer a new treatment strategy to target melanoma and present enhanced therapeutic possibilities.

### **9.3.5. MAPK Inhibitors Induce Synthetic Lethality in Combination with PARP Inhibitors in Melanoma Cells**

As a next step, the molecular mechanisms underlying the synergistic effect between MAPKi and PARPi were to be assessed. Initially, our primary objective was to comprehend whether the combination therapy leads to a higher level of DNA damage in comparison to the individual monotherapies. Unexpectedly, we did not observe enhanced DNA damage accumulation in the combined treatment group (Accepted

Publication II, Figure 5A and 5B). Based on this, we concluded that the combination does not induce DNA damage, and therefore we suggested that the ability to repair DSB induced by the PARPi therapy is reduced by MAPKi therapy. To prove this hypothesis, we checked for gene expression of main HRR-associated genes, *BRCA1*, *BRCA2*, *RAD51*, and *EXO1*. In MAPKi sensitive melanoma cells, the BRAFi vemurafenib, the MEKi trametinib and the panRAFi LY3009120 significantly decreased the expression of these genes, suggesting an ineffective HRR in the MAPKi treated cells. Interestingly, the HRR-associated gene expression in BRAFi resistant cells was induced with the MEKi and the panRAFi, but not with the BRAFi. Consistent with this, exclusively the panRAFi treated BRAFi plus MEKi resistant melanoma cells showed decreased *BRCA1*, *BRCA2*, *RAD51*, and *EXO1* gene expression (Accepted Publication II, Figure 5C).

The data presented here show the pivotal role of the MAPK signaling pathway in regulating DDR gene expression, and consequently, the efficacy of the HRR machinery. Indeed, the MAPK pathway is known to play a crucial role in activating the DDR machinery<sup>430</sup>. Moreover, corroborating these findings, both our research team and other publications recently have demonstrated that inhibiting the MAPK pathway leads to a decrease in HRR in MAPKi sensitive cells, which is facilitated by the transcription factor ELK1<sup>425</sup>.

Since BRAFi plus MEKi double resistant patients do not profit from BRAFi or MEKi treatment, the recently developed panRAFi LY3009120 has demonstrated the capability to downregulate the MAPK pathway within these specific tumor types<sup>142,431</sup>.

MAPKi treatment is known to induce G1 cell cycle arrest in melanoma cells<sup>432</sup>. To study if the effect of downregulated HRR gene expression is exclusively due to checkpoint arrest, we FACS sorted MAPKi treated cells according to their cell cycle phase. Interestingly, the mechanism of HRR downregulation was independent of which cell cycle phase the melanoma cells were in (Accepted Publication II, Supplementary Figure S1F). This reinforces our hypothesis, that MAPK suppression results in decreased HRR gene expression.

Given the pivotal role of the MAPK signaling pathway in facilitating cell growth, we postulate that its activation, which drives accelerated cell division, would necessitate heightened HRR activity<sup>50</sup>. Consequently, we propose that the regulation of HRR genes is orchestrated by the MAPK signaling pathway.

With the data of Accepted Publication II, we support to the concept that PARPi therapy should be extended beyond BRCA mutated patients. Our findings illuminate the potential benefits of PARPi treatment in non-BRCA-mutant tumors that exhibit BRCAness but a HRD phenotype<sup>433-435</sup>. Excitingly, numerous ongoing clinical trials are actively investigating the efficacy of PARPi therapy in HRD cancer cases, including melanoma patients (NCT03207347, NCT03925350, NCT04633902, CT05482074, NCT04187833, NCT05169437). Remarkably, olaparib has even received approval for HRD prostate cancer patients with mutations in at least one of 14 HRR related genes. However, these studies focus on patients with germline or somatic HRR mutations<sup>436</sup>. Our data align with the findings of another study, which suggests that patients need not necessarily harbor mutations in the HRR pathway to experience a favorable response to PARPi treatment<sup>426</sup>. Instead, our evidence indicates that targeted therapy-induced suppression of the MAPK pathway results in reduced HRR gene expression, consequently inducing an HRD phenotype. This effect broadens the horizons of PARPi therapy, opening new possibilities for treating a wider spectrum of patients with the possibility of enhanced efficacy and improved outcomes.

### **9.3.6. PARP1 Gene Expression as a Biomarker for PARP Inhibitor Therapy Response**

Currently, good response to PARPi therapy is predicted by the presence of HRD in cancer patients<sup>437</sup>. Nevertheless, not all HRD cancers respond to PARPi therapy, suggesting the importance of further biomarkers to more accurately forecast the effectiveness of PARPi therapy<sup>438</sup>.

By correlating PARP1 levels of various melanoma cells with the sensitivity to the PARPi olaparib and talazoparib, we found that PARP1 gene expression levels positively correlate with the PARPi sensitivity (Submitted Publication I, Figure 1D, Supplementary Figure 1A, 1B). Further publications support our hypothesis, and a PET imaging radiotracer has even been manufactured to quantify PARP1 expression in the tumor, thus selecting patients eligible for PARPi therapy in a noninvasive manner<sup>439-441</sup>.

PARPi are known to exert its major cytotoxic functions not by inhibiting the BER, but by inducing DSB via PARP trapping (see section 7.4.4.2)<sup>341,348,349</sup>. We thus hypothesized that higher PARP1 levels lead to increased levels of PARP1 trapped on the DNA, which ultimately results in enhanced DSB induction. Indeed, low PARP1

expressing SKMel28 melanoma cells show reduced PARP trapping compared to high PARP1 expressing A375 melanoma cells. In SKMel28 cells, MMS + talazoparib treatment did not result in increased chromatin bound PARP, whereas in A375 cells, the MMS + talazoparib massively induced PARP trapped on the chromatin bound fraction (Submitted Publication I, Figure 2A). Consistent with this, siRNA induced downregulation of PARP1 in high PARP1 expressing A375 melanoma cells led to a clear desensitization to PARPi treatment (Submitted Publication I, Figure 2B). Conversely, upregulation of PARP1 in low PARP1 expressing SKMel28 melanoma cells resulted in a significant sensitization to PARPi treatment (Submitted Publication I, Figure 2C).

Thus, we propose that in addition to HRD testing, PARP1 gene expression should be assessed in patients eligible for PARPi therapy to allow a more accurate selection of patients suitable for PARPi therapy.

### **9.3.7. High PARP1 Gene Expression Levels Correlate with Metastatic Potential of Melanomas**

To discover, whether PARP1 might play a role in the development and progression of melanoma, we checked for PARP1 gene expression in non-malignant skin cells compared to melanoma cells. Interestingly, fibroblasts and melanocytic nevi show significantly lower PARP1 levels compared to melanoma cells (Submitted Publication I, Figure 1E). This goes in line with further publications stating that PARP1 levels are lower in non-malignant cells than in cancer cells, including melanoma <sup>442-444</sup>.

Moreover, an increase in PARP1 gene expression in the melanoma stages between RGP, VGP, and metastatic melanoma could be detected (Submitted Publication I, Figure 1E, 1F). Consistent with this, a previous publication showed that high PARP1 levels are associated with increased tumor size in uveal melanoma <sup>445</sup>. When further analyzing primary melanomas vs. metastatic melanomas, a significant increase in PARP1 gene expression levels could be seen in the metastatic melanoma samples (Submitted Publication I, Figure 3A). In addition, we found a positive trend between the relative metastatic potential and the PARP1 expression in melanoma samples (Submitted Publication I, Figure 3B). In line with this, we could show that the higher the PARP1 expression levels in melanoma samples, the higher the metastatic penetrance of these cells (Submitted Publication, Figure 3C). Further studies reinforce our data, showing that inhibition of PARP1 resulted in reduced metastatic features in various

cancers, including melanoma<sup>403,446</sup>. Also, PARP1 expression could be correlated with an increased aggressive phenotype of high PARP1 expressing cancer cells<sup>403,443,447</sup>.

Next, we aimed to understand if PARP1 has an influence on the progression of melanoma. We therefore checked for the invasive and migratory capacity of these cells, an important ability of cancer cells to metastasize. We could show that the migratory and invasive potential was significantly enhanced in high PARP1 expressing A375 melanoma cells compared to low PARP1 expressing SKMel28 melanoma cells (Submitted Publication, Figure 3D, 3E). Previous publications go in line with our results stating that high PARP1 levels correlate with an invasive clinical phenotype of cells from various cancer types<sup>403,443,447</sup>.

Taken together, these data indicate that high PARP1 gene expression levels are associated with increased cancerous potential, and further elevated metastatic potential in melanoma cell lines and patient samples. These results strengthen the hypothesis that PARP1 is a driver of cancer genesis and metastasis formation across various cancer types.

### **9.3.8. High PARP1 Gene Expression Levels Correlate with Poor Overall Survival of Melanoma Patients**

Since we found that PARP1 expression correlates with increased metastatic potential in melanomas, we were interested, if PARP1 also has an impact on the overall survival of melanoma patients. By using the TCGA 470 dataset, we analyzed the overall survival probability of 459 melanoma patients that were divided into high PARP1 expression and low PARP1 expression. Strikingly, patients with high PARP1 expression had a significantly lower overall survival probability compared to patients with low PARP1 expression (Submitted Publication I, Figure 1A). A wide variety of publications show the same trend, indicating that the association between high PARP1 levels and poor overall survival as well as disease free survival is a universal effect in various cancer types<sup>443,445-451</sup>.

When splitting all melanoma patients of the TCGA 470 dataset into patients in an early melanoma stage (stage 0-II) and patients suffering from late stage metastasized melanoma (stage III-IV) an interesting effect becomes evident. In the early melanoma stage melanoma cohort, no significant difference in overall survival between high PARP1 and low PARP1 expressing melanoma patients was observed (Submitted Publication I, Figure 1B). However, high PARP1 expressing late stage metastasized

melanoma patients have a significantly worse overall survival rate than low PARP1 expressing late stage metastasized melanoma (Submitted Publication I, Figure 1C).

Taken together, our data indicate that in particular patients with elevated PARP1 levels possibly profit from PARPi therapy. Interestingly, especially the late stage metastasized melanoma patients with a poor overall survival rate have high PARP1 levels, and thereby potentially respond well to PARPi therapy with minor side effects in low PARP1 expressing non-malignant tissue. Summarizing our data, we propose that stage III and IV metastasized melanoma patients should be screened for PARP1 expression. High PARP1 expressing patients should then further be screened for HRD. Patients with high PARP1 expression and a HRD should receive PARPi therapy. However, patients with high PARP1 expression but a proficiency in HRR should receive a combination of PARPi therapy and MAPKi therapy, as MAPKi therapy induces a HRD phenotype in BRAF mutated melanomas and therefore acts synthetic lethal in combination with PARPi therapy (Submitted Publication I, Graphical Abstract).

## 10. References

- 1 Saginala, K., Barsouk, A., Aluru, J. S., Rawla, P. & Barsouk, A. Epidemiology of Melanoma. *Med Sci (Basel)* **9** (2021). <https://doi.org:10.3390/medsci9040063>
- 2 Houghton, A. N. & Polsky, D. Focus on melanoma. *Cancer Cell* **2**, 275-278 (2002). [https://doi.org:10.1016/s1535-6108\(02\)00161-7](https://doi.org:10.1016/s1535-6108(02)00161-7)
- 3 Miller, A. J. & Mihm, M. C., Jr. Melanoma. *N Engl J Med* **355**, 51-65 (2006). <https://doi.org:10.1056/NEJMra052166>
- 4 Raimondi, S., Suppa, M. & Gandini, S. Melanoma Epidemiology and Sun Exposure. *Acta Derm Venereol* **100**, adv00136 (2020). <https://doi.org:10.2340/00015555-3491>
- 5 Carr, S., Smith, C. & Wernberg, J. Epidemiology and Risk Factors of Melanoma. *Surg Clin North Am* **100**, 1-12 (2020). <https://doi.org:10.1016/j.suc.2019.09.005>
- 6 Conforti, C. & Zalaudek, I. Epidemiology and Risk Factors of Melanoma: A Review. *Dermatol Pract Concept* **11**, e2021161S (2021). <https://doi.org:10.5826/dpc.11S1a161S>
- 7 Abbasi, N. R. *et al.* Early diagnosis of cutaneous melanoma: revisiting the ABCD criteria. *JAMA* **292**, 2771-2776 (2004). <https://doi.org:10.1001/jama.292.22.2771>
- 8 Bouwstra, J. A. & Honeywell-Nguyen, P. L. Skin structure and mode of action of vesicles. *Adv Drug Deliv Rev* **54 Suppl 1**, S41-55 (2002). [https://doi.org:10.1016/s0169-409x\(02\)00114-x](https://doi.org:10.1016/s0169-409x(02)00114-x)
- 9 Cichorek, M., Wachulska, M., Stasiewicz, A. & Tyminska, A. Skin melanocytes: biology and development. *Postepy Dermatol Alergol* **30**, 30-41 (2013). <https://doi.org:10.5114/pdia.2013.33376>
- 10 Bevona, C., Goggins, W., Quinn, T., Fullerton, J. & Tsao, H. Cutaneous melanomas associated with nevi. *Arch Dermatol* **139**, 1620-1624; discussion 1624 (2003). <https://doi.org:10.1001/archderm.139.12.1620>
- 11 Higgins, H. W., 2nd, Lee, K. C., Galan, A. & Leffell, D. J. Melanoma in situ: Part I. Epidemiology, screening, and clinical features. *J Am Acad Dermatol* **73**, 181-190, quiz 191-182 (2015). <https://doi.org:10.1016/j.jaad.2015.04.014>
- 12 Braeuer, R. R. *et al.* Why is melanoma so metastatic? *Pigment Cell Melanoma Res* **27**, 19-36 (2014). <https://doi.org:10.1111/pcmr.12172>
- 13 Seyfried, T. N. & Huysentruyt, L. C. On the origin of cancer metastasis. *Crit Rev Oncog* **18**, 43-73 (2013). <https://doi.org:10.1615/critrevoncog.v18.i1-2.40>
- 14 Takata, M., Murata, H. & Saida, T. Molecular pathogenesis of malignant melanoma: a different perspective from the studies of melanocytic nevus and acral melanoma. *Pigment Cell Melanoma Res* **23**, 64-71 (2010). <https://doi.org:10.1111/j.1755-148X.2009.00645.x>
- 15 Weyers, W., Euler, M., Diaz-Cascajo, C., Schill, W. B. & Bonczkowitz, M. Classification of cutaneous malignant melanoma: a reassessment of histopathologic criteria for the distinction of different types. *Cancer* **86**, 288-299 (1999). [https://doi.org:10.1002/\(sici\)1097-0142\(19990715\)86:2<288::aid-cncr13>3.0.co;2-s](https://doi.org:10.1002/(sici)1097-0142(19990715)86:2<288::aid-cncr13>3.0.co;2-s)
- 16 Ferrara, G. & Argenziano, G. The WHO 2018 Classification of Cutaneous Melanocytic Neoplasms: Suggestions From Routine Practice. *Front Oncol* **11**, 675296 (2021). <https://doi.org:10.3389/fonc.2021.675296>
- 17 Teixido, C., Castillo, P., Martinez-Vila, C., Arance, A. & Alos, L. Molecular Markers and Targets in Melanoma. *Cells* **10** (2021). <https://doi.org:10.3390/cells10092320>
- 18 Rosen, R. D. & Sapa, A. in *StatPearls* (2023).

- 19 Ogata, D., Namikawa, K., Takahashi, A. & Yamazaki, N. A review of the AJCC melanoma staging system in the TNM classification (eighth edition). *Jpn J Clin Oncol* **51**, 671-674 (2021). <https://doi.org:10.1093/jjco/hyab022>
- 20 Scolyer, R. A., Rawson, R. V., Gershenwald, J. E., Ferguson, P. M. & Prieto, V. G. Melanoma pathology reporting and staging. *Mod Pathol* **33**, 15-24 (2020). <https://doi.org:10.1038/s41379-019-0402-x>
- 21 Curti, B. D. & Faries, M. B. Recent Advances in the Treatment of Melanoma. *N Engl J Med* **384**, 2229-2240 (2021). <https://doi.org:10.1056/NEJMra2034861>
- 22 Joyce, K. M. Surgical Management of Melanoma. *Cutaneous Melanoma: Etiology and Therapy*, 91-100 (2017). <https://doi.org:10.15586/codon.cutaneoumelanoma.2017.ch7>
- 23 van Zeijl, M. C. T., van den Eertwegh, A. J., Haanen, J. B. & Wouters, M. W. J. M. (Neo)adjuvant systemic therapy for melanoma. *Ejso-Eur J Surg Onc* **43**, 534-543 (2017). <https://doi.org:10.1016/j.ejso.2016.07.001>
- 24 Atallah, E. & Flaherty, L. Treatment of metastatic malignant melanoma. *Curr Treat Options Oncol* **6**, 185-193 (2005). <https://doi.org:10.1007/s11864-005-0002-5>
- 25 Horwitz, S. B. Taxol (paclitaxel): mechanisms of action. *Ann Oncol* **5 Suppl 6**, S3-6 (1994).
- 26 Agarwala, S. S. Current systemic therapy for metastatic melanoma. *Expert Rev Anticanc* **9**, 587-595 (2009). <https://doi.org:10.1586/Era.09.25>
- 27 Middleton, M. R. *et al.* Randomized phase III study of temozolomide versus dacarbazine in the treatment of patients with advanced metastatic malignant melanoma. *J Clin Oncol* **18**, 158-166 (2000). <https://doi.org:10.1200/JCO.2000.18.1.158>
- 28 Quirt, I., Verma, S., Petrella, T., Bak, K. & Charette, M. Temozolomide for the treatment of metastatic melanoma: a systematic review. *Oncologist* **12**, 1114-1123 (2007). <https://doi.org:10.1634/theoncologist.12-9-1114>
- 29 Kuryk, L. *et al.* From Conventional Therapies to Immunotherapy: Melanoma Treatment in Review. *Cancers* **12** (2020). <https://doi.org:ARTN 3057>
- 10.3390/cancers12103057
- 30 Maeda, T. *et al.* The efficacy of platinum-based chemotherapy for immune checkpoint inhibitor-resistant advanced melanoma. *Acta Oncol* **58**, 379-381 (2019). <https://doi.org:10.1080/0284186X.2018.1541252>
- 31 Gupta, A., Gomes, F. & Lorigan, P. The role for chemotherapy in the modern management of melanoma. *Melanoma Manag* **4**, 125-136 (2017). <https://doi.org:10.2217/mmt-2017-0003>
- 32 Haanen, J. B. Immunotherapy of melanoma. *EJC Suppl* **11**, 97-105 (2013). <https://doi.org:10.1016/j.ejcsup.2013.07.013>
- 33 Kaufman, H. L. *et al.* The Society for Immunotherapy of Cancer consensus statement on tumour immunotherapy for the treatment of cutaneous melanoma. *Nat Rev Clin Oncol* **10**, 588-598 (2013). <https://doi.org:10.1038/nrclinonc.2013.153>
- 34 Huang, A. C. & Zappasodi, R. A decade of checkpoint blockade immunotherapy in melanoma: understanding the molecular basis for immune sensitivity and resistance. *Nat Immunol* **23**, 660-670 (2022). <https://doi.org:10.1038/s41590-022-01141-1>
- 35 Postow, M. A., Callahan, M. K. & Wolchok, J. D. Immune Checkpoint Blockade in Cancer Therapy. *J Clin Oncol* **33**, 1974-1982 (2015). <https://doi.org:10.1200/JCO.2014.59.4358>

- 36 Lazaroff, J. & Bolotin, D. Targeted Therapy and Immunotherapy in Melanoma. *Dermatol Clin* **41**, 65-77 (2023). <https://doi.org:10.1016/j.det.2022.07.007>
- 37 Chocarro, L. *et al.* Understanding LAG-3 Signaling. *Int J Mol Sci* **22** (2021). <https://doi.org:10.3390/ijms22105282>
- 38 Albrecht, L. J., Livingstone, E., Zimmer, L. & Schadendorf, D. The Latest Option: Nivolumab and Relatlimab in Advanced Melanoma. *Curr Oncol Rep* (2023). <https://doi.org:10.1007/s11912-023-01406-4>
- 39 Kang, K., Xie, F., Mao, J., Bai, Y. & Wang, X. Significance of Tumor Mutation Burden in Immune Infiltration and Prognosis in Cutaneous Melanoma. *Front Oncol* **10**, 573141 (2020). <https://doi.org:10.3389/fonc.2020.573141>
- 40 Sharma, P., Hu-Lieskovan, S., Wargo, J. A. & Ribas, A. Primary, Adaptive, and Acquired Resistance to Cancer Immunotherapy. *Cell* **168**, 707-723 (2017). <https://doi.org:10.1016/j.cell.2017.01.017>
- 41 Elia, A. R., Caputo, S. & Bellone, M. Immune Checkpoint-Mediated Interactions Between Cancer and Immune Cells in Prostate Adenocarcinoma and Melanoma. *Front Immunol* **9**, 1786 (2018). <https://doi.org:10.3389/fimmu.2018.01786>
- 42 Gide, T. N., Wilmott, J. S., Scolyer, R. A. & Long, G. V. Primary and Acquired Resistance to Immune Checkpoint Inhibitors in Metastatic Melanoma. *Clin Cancer Res* **24**, 1260-1270 (2018). <https://doi.org:10.1158/1078-0432.CCR-17-2267>
- 43 Kennedy, L. B. & Salama, A. K. S. A review of cancer immunotherapy toxicity. *CA Cancer J Clin* **70**, 86-104 (2020). <https://doi.org:10.3322/caac.21596>
- 44 Young, A., Quandt, Z. & Bluestone, J. A. The Balancing Act between Cancer Immunity and Autoimmunity in Response to Immunotherapy. *Cancer Immunol Res* **6**, 1445-1452 (2018). <https://doi.org:10.1158/2326-6066.CIR-18-0487>
- 45 Bari, S., Muzaffar, J. & Eroglu, Z. Combination targeted and immune therapy in the treatment of advanced melanoma: a valid treatment option for patients? *Ther Adv Med Oncol* **14**, 17588359221090306 (2022). <https://doi.org:10.1177/17588359221090306>
- 46 Bianco, R., Melisi, D., Ciardiello, F. & Tortora, G. Key cancer cell signal transduction pathways as therapeutic targets. *Eur J Cancer* **42**, 290-294 (2006). <https://doi.org:10.1016/j.ejca.2005.07.034>
- 47 Kontomanolis, E. N. *et al.* Role of Oncogenes and Tumor-suppressor Genes in Carcinogenesis: A Review. *Anticancer Res* **40**, 6009-6015 (2020). <https://doi.org:10.21873/anticancer.14622>
- 48 Sawyers, C. Targeted cancer therapy. *Nature* **432**, 294-297 (2004). <https://doi.org:10.1038/nature03095>
- 49 Fecher, L. A., Amaravadi, R. K. & Flaherty, K. T. The MAPK pathway in melanoma. *Curr Opin Oncol* **20**, 183-189 (2008). <https://doi.org:10.1097/CCO.0b013e3282f5271c>
- 50 Zhang, W. & Liu, H. T. MAPK signal pathways in the regulation of cell proliferation in mammalian cells. *Cell Res* **12**, 9-18 (2002). <https://doi.org:10.1038/sj.cr.7290105>
- 51 Seger, R. & Krebs, E. G. The MAPK signaling cascade. *FASEB J* **9**, 726-735 (1995).
- 52 McKay, M. M. & Morrison, D. K. Integrating signals from RTKs to ERK/MAPK. *Oncogene* **26**, 3113-3121 (2007). <https://doi.org:10.1038/sj.onc.1210394>
- 53 Pudewell, S., Wittich, C., Kazeminejad, N. S., Bazgir, F. & Ahmadian, M. R. Accessory proteins of the RAS-MAPK pathway: moving from the side line to

- the front line. *Commun Biol* **4**, 696 (2021). <https://doi.org:10.1038/s42003-021-02149-3>
- 54 Pierre, S., Bats, A. S. & Coumoul, X. Understanding SOS (Son of Sevenless). *Biochem Pharmacol* **82**, 1049-1056 (2011). <https://doi.org:10.1016/j.bcp.2011.07.072>
- 55 Helfferich, J. *et al.* Neurofibromatosis type 1 associated low grade gliomas: A comparison with sporadic low grade gliomas. *Crit Rev Oncol Hematol* **104**, 30-41 (2016). <https://doi.org:10.1016/j.critrevonc.2016.05.008>
- 56 Meister, M., Tomasovic, A., Banning, A. & Tikkanen, R. Mitogen-Activated Protein (MAP) Kinase Scaffolding Proteins: A Recount. *Int J Mol Sci* **14**, 4854-4884 (2013). <https://doi.org:10.3390/ijms14034854>
- 57 Braicu, C. *et al.* A Comprehensive Review on MAPK: A Promising Therapeutic Target in Cancer. *Cancers (Basel)* **11** (2019). <https://doi.org:10.3390/cancers11101618>
- 58 Roskoski, R., Jr. ERK1/2 MAP kinases: structure, function, and regulation. *Pharmacol Res* **66**, 105-143 (2012). <https://doi.org:10.1016/j.phrs.2012.04.005>
- 59 Yue, J. & Lopez, J. M. Understanding MAPK Signaling Pathways in Apoptosis. *Int J Mol Sci* **21** (2020). <https://doi.org:10.3390/ijms21072346>
- 60 Burotto, M., Chiou, V. L., Lee, J. M. & Kohn, E. C. The MAPK pathway across different malignancies: a new perspective. *Cancer* **120**, 3446-3456 (2014). <https://doi.org:10.1002/cncr.28864>
- 61 Cancer Genome Atlas, N. Genomic Classification of Cutaneous Melanoma. *Cell* **161**, 1681-1696 (2015). <https://doi.org:10.1016/j.cell.2015.05.044>
- 62 Ito, T. *et al.* BRAF Heterogeneity in Melanoma. *Curr Treat Options Oncol* **22**, 20 (2021). <https://doi.org:10.1007/s11864-021-00818-3>
- 63 Munoz-Couselo, E., Adelantado, E. Z., Ortiz, C., Garcia, J. S. & Perez-Garcia, J. NRAS-mutant melanoma: current challenges and future prospect. *Onco Targets Ther* **10**, 3941-3947 (2017). <https://doi.org:10.2147/OTT.S117121>
- 64 Kiuru, M. & Busam, K. J. The NF1 gene in tumor syndromes and melanoma. *Lab Invest* **97**, 146-157 (2017). <https://doi.org:10.1038/labinvest.2016.142>
- 65 Vennepureddy, A., Thumallapally, N., Motilal Nehru, V., Atallah, J. P. & Terjanian, T. Novel Drugs and Combination Therapies for the Treatment of Metastatic Melanoma. *J Clin Med Res* **8**, 63-75 (2016). <https://doi.org:10.14740/jocmr2424w>
- 66 Flaherty, K. T., Yasothan, U. & Kirkpatrick, P. Vemurafenib. *Nat Rev Drug Discov* **10**, 811-812 (2011). <https://doi.org:10.1038/nrd3579>
- 67 Garbe, C. & Eigentler, T. K. Vemurafenib. *Recent Results Cancer Res* **211**, 77-89 (2018). [https://doi.org:10.1007/978-3-319-91442-8\\_6](https://doi.org:10.1007/978-3-319-91442-8_6)
- 68 Garbe, C., Abusaif, S. & Eigentler, T. K. Vemurafenib. *Recent Results Cancer Res* **201**, 215-225 (2014). [https://doi.org:10.1007/978-3-642-54490-3\\_13](https://doi.org:10.1007/978-3-642-54490-3_13)
- 69 Trinh, V. A., Davis, J. E., Anderson, J. E. & Kim, K. B. Dabrafenib therapy for advanced melanoma. *Ann Pharmacother* **48**, 519-529 (2014). <https://doi.org:10.1177/1060028013513009>
- 70 Ballantyne, A. D. & Garnock-Jones, K. P. Dabrafenib: first global approval. *Drugs* **73**, 1367-1376 (2013). <https://doi.org:10.1007/s40265-013-0095-2>
- 71 Davis, J. & Wayman, M. Encorafenib and Binimetinib Combination Therapy in Metastatic Melanoma. *J Adv Pract Oncol* **13**, 450-455 (2022). <https://doi.org:10.6004/jadpro.2022.13.4.7>
- 72 Grimaldi, A. M. *et al.* MEK Inhibitors in the Treatment of Metastatic Melanoma and Solid Tumors. *Am J Clin Dermatol* **18**, 745-754 (2017). <https://doi.org:10.1007/s40257-017-0292-y>

- 73 Rager, T. *et al.* Treatment of Metastatic Melanoma with a Combination of Immunotherapies and Molecularly Targeted Therapies. *Cancers (Basel)* **14** (2022). <https://doi.org:10.3390/cancers14153779>
- 74 Ascierto, P. A. *et al.* Dabrafenib, trametinib and pembrolizumab or placebo in BRAF-mutant melanoma. *Nat Med* **25**, 941-946 (2019). <https://doi.org:10.1038/s41591-019-0448-9>
- 75 Ribas, A. *et al.* Combined BRAF and MEK inhibition with PD-1 blockade immunotherapy in BRAF-mutant melanoma. *Nat Med* **25**, 936-940 (2019). <https://doi.org:10.1038/s41591-019-0476-5>
- 76 Ribas, A. *et al.* Publisher Correction: Combined BRAF and MEK inhibition with PD-1 blockade immunotherapy in BRAF-mutant melanoma. *Nat Med* **25**, 1319 (2019). <https://doi.org:10.1038/s41591-019-0535-y>
- 77 Dummer, R. *et al.* Randomized Phase III Trial Evaluating Spartalizumab Plus Dabrafenib and Trametinib for BRAF V600-Mutant Unresectable or Metastatic Melanoma. *J Clin Oncol* **40**, 1428-1438 (2022). <https://doi.org:10.1200/JCO.21.01601>
- 78 Gutzmer, R. *et al.* Atezolizumab, vemurafenib, and cobimetinib as first-line treatment for unresectable advanced BRAF(V600) mutation-positive melanoma (IMspire150): primary analysis of the randomised, double-blind, placebo-controlled, phase 3 trial. *Lancet* **395**, 1835-1844 (2020). [https://doi.org:10.1016/S0140-6736\(20\)30934-X](https://doi.org:10.1016/S0140-6736(20)30934-X)
- 79 Singh, A. K., Kumar, A., Thareja, S. & Kumar, P. Current Insights into the Role of BRAF Inhibitors in Treatment of Melanoma. *Anticancer Agents Med Chem* **23**, 278-297 (2023). <https://doi.org:10.2174/1871520622666220624164152>
- 80 Sullivan, R. J. *et al.* A Phase I Study of LY3009120, a Pan-RAF Inhibitor, in Patients with Advanced or Metastatic Cancer. *Mol Cancer Ther* **19**, 460-467 (2020). <https://doi.org:10.1158/1535-7163.MCT-19-0681>
- 81 Konieczkowski, D. J. *et al.* A melanoma cell state distinction influences sensitivity to MAPK pathway inhibitors. *Cancer Discov* **4**, 816-827 (2014). <https://doi.org:10.1158/2159-8290.CD-13-0424>
- 82 Tangella, L. P., Clark, M. E. & Gray, E. S. Resistance mechanisms to targeted therapy in BRAF-mutant melanoma - A mini review. *Biochim Biophys Acta Gen Subj* **1865**, 129736 (2021). <https://doi.org:10.1016/j.bbagen.2020.129736>
- 83 Proietti, I. *et al.* Mechanisms of Acquired BRAF Inhibitor Resistance in Melanoma: A Systematic Review. *Cancers (Basel)* **12** (2020). <https://doi.org:10.3390/cancers12102801>
- 84 Czarnecka, A. M., Bartnik, E., Fiedorowicz, M. & Rutkowski, P. Targeted Therapy in Melanoma and Mechanisms of Resistance. *Int J Mol Sci* **21** (2020). <https://doi.org:10.3390/ijms21134576>
- 85 Patel, M. *et al.* Resistance to Molecularly Targeted Therapies in Melanoma. *Cancers (Basel)* **13** (2021). <https://doi.org:10.3390/cancers13051115>
- 86 Villanueva, J. *et al.* Concurrent MEK2 mutation and BRAF amplification confer resistance to BRAF and MEK inhibitors in melanoma. *Cell Rep* **4**, 1090-1099 (2013). <https://doi.org:10.1016/j.celrep.2013.08.023>
- 87 Rizos, H. *et al.* BRAF inhibitor resistance mechanisms in metastatic melanoma: spectrum and clinical impact. *Clin Cancer Res* **20**, 1965-1977 (2014). <https://doi.org:10.1158/1078-0432.CCR-13-3122>
- 88 Monsma, D. J. *et al.* Melanoma patient derived xenografts acquire distinct Vemurafenib resistance mechanisms. *Am J Cancer Res* **5**, 1507-1518 (2015).

- 89 Poulidakos, P. I. *et al.* RAF inhibitor resistance is mediated by dimerization of aberrantly spliced BRAF(V600E). *Nature* **480**, 387-390 (2011). <https://doi.org:10.1038/nature10662>
- 90 Wang, J. *et al.* A Secondary Mutation in BRAF Confers Resistance to RAF Inhibition in a BRAF(V600E)-Mutant Brain Tumor. *Cancer Discov* **8**, 1130-1141 (2018). <https://doi.org:10.1158/2159-8290.CD-17-1263>
- 91 Hoogstraat, M. *et al.* Detailed imaging and genetic analysis reveal a secondary BRAF(L505H) resistance mutation and extensive inpatient heterogeneity in metastatic BRAF mutant melanoma patients treated with vemurafenib. *Pigm Cell Melanoma R* **28** (2015). <https://doi.org:10.1111/pcmr.12347>
- 92 Antony, R., Emery, C. M., Sawyer, A. M. & Garraway, L. A. C-RAF mutations confer resistance to RAF inhibitors. *Cancer Res* **73**, 4840-4851 (2013). <https://doi.org:10.1158/0008-5472.CAN-12-4089>
- 93 Montagut, C. *et al.* Elevated CRAF as a potential mechanism of acquired resistance to BRAF inhibition in melanoma. *Cancer Res* **68**, 4853-4861 (2008). <https://doi.org:10.1158/0008-5472.CAN-07-6787>
- 94 Nazarian, R. *et al.* Melanomas acquire resistance to B-RAF(V600E) inhibition by RTK or N-RAS upregulation. *Nature* **468**, 973-977 (2010). <https://doi.org:10.1038/nature09626>
- 95 Van Allen, E. M. *et al.* The genetic landscape of clinical resistance to RAF inhibition in metastatic melanoma. *Cancer Discov* **4**, 94-109 (2014). <https://doi.org:10.1158/2159-8290.CD-13-0617>
- 96 Long, G. V. *et al.* Increased MAPK reactivation in early resistance to dabrafenib/trametinib combination therapy of BRAF-mutant metastatic melanoma. *Nat Commun* **5**, 5694 (2014). <https://doi.org:10.1038/ncomms6694>
- 97 Whittaker, S. R. *et al.* A genome-scale RNA interference screen implicates NF1 loss in resistance to RAF inhibition. *Cancer Discov* **3**, 350-362 (2013). <https://doi.org:10.1158/2159-8290.CD-12-0470>
- 98 Gibney, G. T. & Smalley, K. S. An unholy alliance: cooperation between BRAF and NF1 in melanoma development and BRAF inhibitor resistance. *Cancer Discov* **3**, 260-263 (2013). <https://doi.org:10.1158/2159-8290.CD-13-0017>
- 99 Nissan, M. H. *et al.* Loss of NF1 in cutaneous melanoma is associated with RAS activation and MEK dependence. *Cancer Res* **74**, 2340-2350 (2014). <https://doi.org:10.1158/0008-5472.CAN-13-2625>
- 100 Maertens, O. *et al.* Elucidating distinct roles for NF1 in melanomagenesis. *Cancer Discov* **3**, 338-349 (2013). <https://doi.org:10.1158/2159-8290.CD-12-0313>
- 101 Sun, C. *et al.* Reversible and adaptive resistance to BRAF(V600E) inhibition in melanoma. *Nature* **508**, 118-122 (2014). <https://doi.org:10.1038/nature13121>
- 102 Amaral, T. *et al.* MAPK pathway in melanoma part II-secondary and adaptive resistance mechanisms to BRAF inhibition. *Eur J Cancer* **73**, 93-101 (2017). <https://doi.org:10.1016/j.ejca.2016.12.012>
- 103 Wilson, T. R. *et al.* Widespread potential for growth-factor-driven resistance to anticancer kinase inhibitors. *Nature* **487**, 505-509 (2012). <https://doi.org:10.1038/nature11249>
- 104 Lionarons, D. A. *et al.* RAC1(P29S) Induces a Mesenchymal Phenotypic Switch via Serum Response Factor to Promote Melanoma Development and Therapy Resistance. *Cancer Cell* **36**, 68-83 e69 (2019). <https://doi.org:10.1016/j.ccell.2019.05.015>

- 105 Watson, I. R. *et al.* The RAC1 P29S hotspot mutation in melanoma confers resistance to pharmacological inhibition of RAF. *Cancer Res* **74**, 4845-4852 (2014). <https://doi.org:10.1158/0008-5472.CAN-14-1232-T>
- 106 Bagheri-Yarmand, R. *et al.* RAC1 Alterations Induce Acquired Dabrafenib Resistance in Association with Anaplastic Transformation in a Papillary Thyroid Cancer Patient. *Cancers (Basel)* **13** (2021). <https://doi.org:10.3390/cancers13194950>
- 107 Gupta, R. *et al.* Loss of BOP1 confers resistance to BRAF kinase inhibitors in melanoma by activating MAP kinase pathway. *Proc Natl Acad Sci U S A* **116**, 4583-4591 (2019). <https://doi.org:10.1073/pnas.1821889116>
- 108 Shen, C. H. *et al.* Loss of cohesin complex components STAG2 or STAG3 confers resistance to BRAF inhibition in melanoma. *Nat Med* **22**, 1056-1061 (2016). <https://doi.org:10.1038/nm.4155>
- 109 Smith, M. P. *et al.* Inhibiting Drivers of Non-mutational Drug Tolerance Is a Salvage Strategy for Targeted Melanoma Therapy. *Cancer Cell* **29**, 270-284 (2016). <https://doi.org:10.1016/j.ccell.2016.02.003>
- 110 Porta, C., Paglino, C. & Mosca, A. Targeting PI3K/Akt/mTOR Signaling in Cancer. *Front Oncol* **4**, 64 (2014). <https://doi.org:10.3389/fonc.2014.00064>
- 111 Markman, B., Dienstmann, R. & Tabernero, J. Targeting the PI3K/Akt/mTOR pathway--beyond rapalogs. *Oncotarget* **1**, 530-543 (2010). <https://doi.org:10.18632/oncotarget.101012>
- 112 Yap, T. A. *et al.* Targeting the PI3K-AKT-mTOR pathway: progress, pitfalls, and promises. *Curr Opin Pharmacol* **8**, 393-412 (2008). <https://doi.org:10.1016/j.coph.2008.08.004>
- 113 Papa, A. & Pandolfi, P. P. The PTEN(-)PI3K Axis in Cancer. *Biomolecules* **9** (2019). <https://doi.org:10.3390/biom9040153>
- 114 Manzano, J. L. *et al.* Resistant mechanisms to BRAF inhibitors in melanoma. *Ann Transl Med* **4**, 237 (2016). <https://doi.org:10.21037/atm.2016.06.07>
- 115 Shi, H. *et al.* A novel AKT1 mutant amplifies an adaptive melanoma response to BRAF inhibition. *Cancer Discov* **4**, 69-79 (2014). <https://doi.org:10.1158/2159-8290.CD-13-0279>
- 116 Shi, H. *et al.* Acquired resistance and clonal evolution in melanoma during BRAF inhibitor therapy. *Cancer Discov* **4**, 80-93 (2014). <https://doi.org:10.1158/2159-8290.CD-13-0642>
- 117 Pan, D. The hippo signaling pathway in development and cancer. *Dev Cell* **19**, 491-505 (2010). <https://doi.org:10.1016/j.devcel.2010.09.011>
- 118 Nguyen, C. D. K. & Yi, C. YAP/TAZ Signaling and Resistance to Cancer Therapy. *Trends Cancer* **5**, 283-296 (2019). <https://doi.org:10.1016/j.trecan.2019.02.010>
- 119 Lin, L. & Bivona, T. G. The Hippo effector YAP regulates the response of cancer cells to MAPK pathway inhibitors. *Mol Cell Oncol* **3**, e1021441 (2016). <https://doi.org:10.1080/23723556.2015.1021441>
- 120 Lin, L. *et al.* The Hippo effector YAP promotes resistance to RAF- and MEK-targeted cancer therapies. *Nat Genet* **47**, 250-256 (2015). <https://doi.org:10.1038/ng.3218>
- 121 Falcone, I. *et al.* Tumor Microenvironment: Implications in Melanoma Resistance to Targeted Therapy and Immunotherapy. *Cancers (Basel)* **12** (2020). <https://doi.org:10.3390/cancers12102870>
- 122 Xing, F., Saidou, J. & Watabe, K. Cancer associated fibroblasts (CAFs) in tumor microenvironment. *Front Biosci (Landmark Ed)* **15**, 166-179 (2010). <https://doi.org:10.2741/3613>

- 123 Liao, D., Luo, Y., Markowitz, D., Xiang, R. & Reisfeld, R. A. Cancer associated fibroblasts promote tumor growth and metastasis by modulating the tumor immune microenvironment in a 4T1 murine breast cancer model. *PLoS One* **4**, e7965 (2009). <https://doi.org:10.1371/journal.pone.0007965>
- 124 Fedorenko, I. V., Wargo, J. A., Flaherty, K. T., Messina, J. L. & Smalley, K. S. M. BRAF Inhibition Generates a Host-Tumor Niche that Mediates Therapeutic Escape. *J Invest Dermatol* **135**, 3115-3124 (2015). <https://doi.org:10.1038/jid.2015.329>
- 125 Straussman, R. *et al.* Tumour micro-environment elicits innate resistance to RAF inhibitors through HGF secretion. *Nature* **487**, 500-504 (2012). <https://doi.org:10.1038/nature11183>
- 126 Hirata, E. *et al.* Intravital imaging reveals how BRAF inhibition generates drug-tolerant microenvironments with high integrin beta1/FAK signaling. *Cancer Cell* **27**, 574-588 (2015). <https://doi.org:10.1016/j.ccell.2015.03.008>
- 127 Hu, W. *et al.* Tumor-associated macrophages in cancers. *Clin Transl Oncol* **18**, 251-258 (2016). <https://doi.org:10.1007/s12094-015-1373-0>
- 128 Cetintas, V. B. & Batada, N. N. Is there a causal link between PTEN deficient tumors and immunosuppressive tumor microenvironment? *J Transl Med* **18**, 45 (2020). <https://doi.org:10.1186/s12967-020-02219-w>
- 129 Mackiewicz, J. & Mackiewicz, A. BRAF and MEK inhibitors in the era of immunotherapy in melanoma patients. *Contemp Oncol (Pozn)* **22**, 68-72 (2018). <https://doi.org:10.5114/wo.2018.73890>
- 130 Subbiah, V., Baik, C. & Kirkwood, J. M. Clinical Development of BRAF plus MEK Inhibitor Combinations. *Trends Cancer* **6**, 797-810 (2020). <https://doi.org:10.1016/j.trecan.2020.05.009>
- 131 Paraiso, K. H. *et al.* Recovery of phospho-ERK activity allows melanoma cells to escape from BRAF inhibitor therapy. *Br J Cancer* **102**, 1724-1730 (2010). <https://doi.org:10.1038/sj.bjc.6605714>
- 132 Arozarena, I. & Wellbrock, C. Overcoming resistance to BRAF inhibitors. *Ann Transl Med* **5**, 387 (2017). <https://doi.org:10.21037/atm.2017.06.09>
- 133 Sibaud, V. *et al.* [Management of toxicities of BRAF inhibitors and MEK inhibitors in advanced melanoma]. *Bull Cancer* **108**, 528-543 (2021). <https://doi.org:10.1016/j.bulcan.2020.12.014>
- 134 Gouda, M. A. & Subbiah, V. Precision oncology for BRAF-mutant cancers with BRAF and MEK inhibitors: from melanoma to tissue-agnostic therapy. *ESMO Open* **8**, 100788 (2023). <https://doi.org:10.1016/j.esmoop.2023.100788>
- 135 Lim, S. Y., Menzies, A. M. & Rizos, H. Mechanisms and strategies to overcome resistance to molecularly targeted therapy for melanoma. *Cancer* **123**, 2118-2129 (2017). <https://doi.org:10.1002/cncr.30435>
- 136 Algazi, A. P. *et al.* Continuous versus intermittent BRAF and MEK inhibition in patients with BRAF-mutated melanoma: a randomized phase 2 trial. *Nat Med* **26**, 1564-1568 (2020). <https://doi.org:10.1038/s41591-020-1060-8>
- 137 Hatzivassiliou, G. *et al.* ERK inhibition overcomes acquired resistance to MEK inhibitors. *Mol Cancer Ther* **11**, 1143-1154 (2012). <https://doi.org:10.1158/1535-7163.MCT-11-1010>
- 138 Herrero, A. *et al.* Small Molecule Inhibition of ERK Dimerization Prevents Tumorigenesis by RAS-ERK Pathway Oncogenes. *Cancer Cell* **28**, 170-182 (2015). <https://doi.org:10.1016/j.ccell.2015.07.001>
- 139 Morris, E. J. *et al.* Discovery of a novel ERK inhibitor with activity in models of acquired resistance to BRAF and MEK inhibitors. *Cancer Discov* **3**, 742-750 (2013). <https://doi.org:10.1158/2159-8290.CD-13-0070>

- 140 Zhang, C. *et al.* RAF inhibitors that evade paradoxical MAPK pathway activation. *Nature* **526**, 583-586 (2015). <https://doi.org:10.1038/nature14982>
- 141 Atefi, M. *et al.* Combination of pan-RAF and MEK inhibitors in NRAS mutant melanoma. *Mol Cancer* **14**, 27 (2015). <https://doi.org:10.1186/s12943-015-0293-5>
- 142 Peng, S. B. *et al.* Inhibition of RAF Isoforms and Active Dimers by LY3009120 Leads to Anti-tumor Activities in RAS or BRAF Mutant Cancers. *Cancer Cell* **28**, 384-398 (2015). <https://doi.org:10.1016/j.ccell.2015.08.002>
- 143 Acquaviva, J. *et al.* Overcoming acquired BRAF inhibitor resistance in melanoma via targeted inhibition of Hsp90 with ganetespib. *Mol Cancer Ther* **13**, 353-363 (2014). <https://doi.org:10.1158/1535-7163.MCT-13-0481>
- 144 Paraiso, K. H. *et al.* The HSP90 inhibitor XL888 overcomes BRAF inhibitor resistance mediated through diverse mechanisms. *Clin Cancer Res* **18**, 2502-2514 (2012). <https://doi.org:10.1158/1078-0432.CCR-11-2612>
- 145 Eroglu, Z. *et al.* Combined BRAF and HSP90 Inhibition in Patients with Unresectable BRAF (V600E)-Mutant Melanoma. *Clin Cancer Res* **24**, 5516-5524 (2018). <https://doi.org:10.1158/1078-0432.CCR-18-0565>
- 146 Sweetlove, M. *et al.* Inhibitors of pan-PI3K Signaling Synergize with BRAF or MEK Inhibitors to Prevent BRAF-Mutant Melanoma Cell Growth. *Front Oncol* **5**, 135 (2015). <https://doi.org:10.3389/fonc.2015.00135>
- 147 Greger, J. G. *et al.* Combinations of BRAF, MEK, and PI3K/mTOR inhibitors overcome acquired resistance to the BRAF inhibitor GSK2118436 dabrafenib, mediated by NRAS or MEK mutations. *Mol Cancer Ther* **11**, 909-920 (2012). <https://doi.org:10.1158/1535-7163.MCT-11-0989>
- 148 Atefi, M. *et al.* Reversing melanoma cross-resistance to BRAF and MEK inhibitors by co-targeting the AKT/mTOR pathway. *PLoS One* **6**, e28973 (2011). <https://doi.org:10.1371/journal.pone.0028973>
- 149 Tolcher, A. W. *et al.* Phase I study of the MEK inhibitor trametinib in combination with the AKT inhibitor afuresertib in patients with solid tumors and multiple myeloma. *Cancer Chemother Pharmacol* **75**, 183-189 (2015). <https://doi.org:10.1007/s00280-014-2615-5>
- 150 Bedard, P. L. *et al.* A phase Ib dose-escalation study of the oral pan-PI3K inhibitor buparlisib (BKM120) in combination with the oral MEK1/2 inhibitor trametinib (GSK1120212) in patients with selected advanced solid tumors. *Clin Cancer Res* **21**, 730-738 (2015). <https://doi.org:10.1158/1078-0432.CCR-14-1814>
- 151 Kaelin, W. G., Jr. The p53 gene family. *Oncogene* **18**, 7701-7705 (1999). <https://doi.org:10.1038/sj.onc.1202955>
- 152 Belyi, V. A. *et al.* The origins and evolution of the p53 family of genes. *Cold Spring Harb Perspect Biol* **2**, a001198 (2010). <https://doi.org:10.1101/cshperspect.a001198>
- 153 Efeyan, A. & Serrano, M. p53: guardian of the genome and policeman of the oncogenes. *Cell Cycle* **6**, 1006-1010 (2007). <https://doi.org:10.4161/cc.6.9.4211>
- 154 Pietsch, E. C., Sykes, S. M., McMahon, S. B. & Murphy, M. E. The p53 family and programmed cell death. *Oncogene* **27**, 6507-6521 (2008). <https://doi.org:10.1038/onc.2008.315>
- 155 Murray-Zmijewski, F., Lane, D. P. & Bourdon, J. C. p53/p63/p73 isoforms: an orchestra of isoforms to harmonise cell differentiation and response to stress. *Cell Death Differ* **13**, 962-972 (2006). <https://doi.org:10.1038/sj.cdd.4401914>

- 156 Bourdon, J. C. p53 Family isoforms. *Curr Pharm Biotechnol* **8**, 332-336 (2007). <https://doi.org:10.2174/138920107783018444>
- 157 Stiewe, T. The p53 family in differentiation and tumorigenesis. *Nat Rev Cancer* **7**, 165-168 (2007). <https://doi.org:10.1038/nrc2072>
- 158 Wei, J., Zaika, E. & Zaika, A. p53 Family: Role of Protein Isoforms in Human Cancer. *J Nucleic Acids* **2012**, 687359 (2012). <https://doi.org:10.1155/2012/687359>
- 159 Khoury, M. P. & Bourdon, J. C. p53 Isoforms: An Intracellular Microprocessor? *Genes Cancer* **2**, 453-465 (2011). <https://doi.org:10.1177/1947601911408893>
- 160 Hall, C. & Muller, P. A. J. The Diverse Functions of Mutant 53, Its Family Members and Isoforms in Cancer. *Int J Mol Sci* **20** (2019). <https://doi.org:10.3390/ijms20246188>
- 161 Ferraiuolo, M., Di Agostino, S., Blandino, G. & Strano, S. Oncogenic Intra-p53 Family Member Interactions in Human Cancers. *Front Oncol* **6**, 77 (2016). <https://doi.org:10.3389/fonc.2016.00077>
- 162 Wolter, J., Angelini, P. & Irwin, M. p53 family: Therapeutic targets in neuroblastoma. *Future Oncol* **6**, 429-444 (2010). <https://doi.org:10.2217/fon.09.176>
- 163 Jeggo, P. A., Pearl, L. H. & Carr, A. M. DNA repair, genome stability and cancer: a historical perspective. *Nat Rev Cancer* **16**, 35-42 (2016). <https://doi.org:10.1038/nrc.2015.4>
- 164 Levine, A. J., Hu, W. & Feng, Z. The P53 pathway: what questions remain to be explored? *Cell Death Differ* **13**, 1027-1036 (2006). <https://doi.org:10.1038/sj.cdd.4401910>
- 165 Moll, U. M. & Petrenko, O. The MDM2-p53 interaction. *Mol Cancer Res* **1**, 1001-1008 (2003).
- 166 Meek, D. W. The p53 response to DNA damage. *DNA Repair (Amst)* **3**, 1049-1056 (2004). <https://doi.org:10.1016/j.dnarep.2004.03.027>
- 167 Sherr, C. J. Divorcing ARF and p53: an unsettled case. *Nat Rev Cancer* **6**, 663-673 (2006). <https://doi.org:10.1038/nrc1954>
- 168 Bell, L. A. & Ryan, K. M. Life and death decisions by E2F-1. *Cell Death Differ* **11**, 137-142 (2004). <https://doi.org:10.1038/sj.cdd.4401324>
- 169 Murray, D. & Mirzayans, R. Cellular Responses to Platinum-Based Anticancer Drugs and UVC: Role of p53 and Implications for Cancer Therapy. *Int J Mol Sci* **21** (2020). <https://doi.org:10.3390/ijms21165766>
- 170 Ronco, C., Martin, A. R., Demange, L. & Benhida, R. ATM, ATR, CHK1, CHK2 and WEE1 inhibitors in cancer and cancer stem cells. *Medchemcomm* **8**, 295-319 (2017). <https://doi.org:10.1039/c6md00439c>
- 171 Smith, J., Tho, L. M., Xu, N. & Gillespie, D. A. The ATM-Chk2 and ATR-Chk1 pathways in DNA damage signaling and cancer. *Adv Cancer Res* **108**, 73-112 (2010). <https://doi.org:10.1016/B978-0-12-380888-2.00003-0>
- 172 Ou, Y. H., Chung, P. H., Sun, T. P. & Shieh, S. Y. p53 C-terminal phosphorylation by CHK1 and CHK2 participates in the regulation of DNA-damage-induced C-terminal acetylation. *Mol Biol Cell* **16**, 1684-1695 (2005). <https://doi.org:10.1091/mbc.e04-08-0689>
- 173 Aubrey, B. J., Kelly, G. L., Janic, A., Herold, M. J. & Strasser, A. How does p53 induce apoptosis and how does this relate to p53-mediated tumour suppression? *Cell Death Differ* **25**, 104-113 (2018). <https://doi.org:10.1038/cdd.2017.169>

- 174 Yu, J. & Zhang, L. The transcriptional targets of p53 in apoptosis control. *Biochem Biophys Res Commun* **331**, 851-858 (2005). <https://doi.org/10.1016/j.bbrc.2005.03.189>
- 175 Bouillet, P. & Strasser, A. BH3-only proteins - evolutionarily conserved proapoptotic Bcl-2 family members essential for initiating programmed cell death. *J Cell Sci* **115**, 1567-1574 (2002). <https://doi.org/10.1242/jcs.115.8.1567>
- 176 Wu, X. & Deng, Y. Bax and BH3-domain-only proteins in p53-mediated apoptosis. *Front Biosci* **7**, d151-156 (2002). <https://doi.org/10.2741/A772>
- 177 Haupt, S., Berger, M., Goldberg, Z. & Haupt, Y. Apoptosis - the p53 network. *J Cell Sci* **116**, 4077-4085 (2003). <https://doi.org/10.1242/jcs.00739>
- 178 Kreis, N. N., Louwen, F. & Yuan, J. The Multifaceted p21 (Cip1/Waf1/CDKN1A) in Cell Differentiation, Migration and Cancer Therapy. *Cancers (Basel)* **11** (2019). <https://doi.org/10.3390/cancers11091220>
- 179 Rizzotto, D., Englmaier, L. & Villunger, A. At a Crossroads to Cancer: How p53-Induced Cell Fate Decisions Secure Genome Integrity. *Int J Mol Sci* **22** (2021). <https://doi.org/10.3390/ijms221910883>
- 180 Sherr, C. J. & McCormick, F. The RB and p53 pathways in cancer. *Cancer Cell* **2**, 103-112 (2002). [https://doi.org/10.1016/s1535-6108\(02\)00102-2](https://doi.org/10.1016/s1535-6108(02)00102-2)
- 181 Harris, S. L. & Levine, A. J. The p53 pathway: positive and negative feedback loops. *Oncogene* **24**, 2899-2908 (2005). <https://doi.org/10.1038/sj.onc.1208615>
- 182 Engeland, K. Cell cycle regulation: p53-p21-RB signaling. *Cell Death Differ* **29**, 946-960 (2022). <https://doi.org/10.1038/s41418-022-00988-z>
- 183 Chen, J. The Cell-Cycle Arrest and Apoptotic Functions of p53 in Tumor Initiation and Progression. *Cold Spring Harb Perspect Med* **6**, a026104 (2016). <https://doi.org/10.1101/cshperspect.a026104>
- 184 Engeland, K. Cell cycle arrest through indirect transcriptional repression by p53: I have a DREAM. *Cell Death Differ* **25**, 114-132 (2018). <https://doi.org/10.1038/cdd.2017.172>
- 185 Fischer, M., Quaas, M., Steiner, L. & Engeland, K. The p53-p21-DREAM-CDE/CHR pathway regulates G2/M cell cycle genes. *Nucleic Acids Res* **44**, 164-174 (2016). <https://doi.org/10.1093/nar/gkv927>
- 186 Rufini, A., Tucci, P., Celardo, I. & Melino, G. Senescence and aging: the critical roles of p53. *Oncogene* **32**, 5129-5143 (2013). <https://doi.org/10.1038/onc.2012.640>
- 187 Mijit, M., Caracciolo, V., Melillo, A., Amicarelli, F. & Giordano, A. Role of p53 in the Regulation of Cellular Senescence. *Biomolecules* **10** (2020). <https://doi.org/10.3390/biom10030420>
- 188 Nicolai, S. *et al.* DNA repair and aging: the impact of the p53 family. *Aging (Albany NY)* **7**, 1050-1065 (2015). <https://doi.org/10.18632/aging.100858>
- 189 Williams, A. B. & Schumacher, B. p53 in the DNA-Damage-Repair Process. *Cold Spring Harb Perspect Med* **6** (2016). <https://doi.org/10.1101/cshperspect.a026070>
- 190 Zhan, Q. Gadd45a, a p53- and BRCA1-regulated stress protein, in cellular response to DNA damage. *Mutat Res* **569**, 133-143 (2005). <https://doi.org/10.1016/j.mrfmmm.2004.06.055>
- 191 Niehrs, C. & Schafer, A. Active DNA demethylation by Gadd45 and DNA repair. *Trends Cell Biol* **22**, 220-227 (2012). <https://doi.org/10.1016/j.tcb.2012.01.002>
- 192 Tamura, R. E. *et al.* GADD45 proteins: central players in tumorigenesis. *Curr Mol Med* **12**, 634-651 (2012). <https://doi.org/10.2174/156652412800619978>
- 193 Marei, H. E. *et al.* p53 signaling in cancer progression and therapy. *Cancer Cell Int* **21**, 703 (2021). <https://doi.org/10.1186/s12935-021-02396-8>

- 194 Hernandez Borrero, L. J. & El-Deiry, W. S. Tumor suppressor p53: Biology, signaling pathways, and therapeutic targeting. *Biochim Biophys Acta Rev Cancer* **1876**, 188556 (2021). <https://doi.org:10.1016/j.bbcan.2021.188556>
- 195 Wang, M. & Attardi, L. D. A Balancing Act: p53 Activity from Tumor Suppression to Pathology and Therapeutic Implications. *Annu Rev Pathol* **17**, 205-226 (2022). <https://doi.org:10.1146/annurev-pathol-042320-025840>
- 196 Hager, K. M. & Gu, W. Understanding the non-canonical pathways involved in p53-mediated tumor suppression. *Carcinogenesis* **35**, 740-746 (2014). <https://doi.org:10.1093/carcin/bgt487>
- 197 Bensaad, K. & Vousden, K. H. p53: new roles in metabolism. *Trends Cell Biol* **17**, 286-291 (2007). <https://doi.org:10.1016/j.tcb.2007.04.004>
- 198 Cheung, E. C. & Vousden, K. H. The role of p53 in glucose metabolism. *Curr Opin Cell Biol* **22**, 186-191 (2010). <https://doi.org:10.1016/j.ceb.2009.12.006>
- 199 Ranjan, A. & Iwakuma, T. Non-Canonical Cell Death Induced by p53. *Int J Mol Sci* **17** (2016). <https://doi.org:10.3390/ijms17122068>
- 200 Potter, M., Newport, E. & Morten, K. J. The Warburg effect: 80 years on. *Biochem Soc Trans* **44**, 1499-1505 (2016). <https://doi.org:10.1042/BST20160094>
- 201 Itahana, Y. & Itahana, K. Emerging Roles of p53 Family Members in Glucose Metabolism. *Int J Mol Sci* **19** (2018). <https://doi.org:10.3390/ijms19030776>
- 202 Duffy, M. J. *et al.* p53 as a target for the treatment of cancer. *Cancer Treat Rev* **40**, 1153-1160 (2014). <https://doi.org:10.1016/j.ctrv.2014.10.004>
- 203 Soussi, T. & Lozano, G. p53 mutation heterogeneity in cancer. *Biochem Biophys Res Commun* **331**, 834-842 (2005). <https://doi.org:10.1016/j.bbrc.2005.03.190>
- 204 Hassin, O. & Oren, M. Drugging p53 in cancer: one protein, many targets. *Nat Rev Drug Discov* **22**, 127-144 (2023). <https://doi.org:10.1038/s41573-022-00571-8>
- 205 Liu, J., Zhang, C. & Feng, Z. Tumor suppressor p53 and its gain-of-function mutants in cancer. *Acta Biochim Biophys Sin (Shanghai)* **46**, 170-179 (2014). <https://doi.org:10.1093/abbs/gmt144>
- 206 Kasthuber, E. R. & Lowe, S. W. Putting p53 in Context. *Cell* **170**, 1062-1078 (2017). <https://doi.org:10.1016/j.cell.2017.08.028>
- 207 Muller, P. A. & Vousden, K. H. p53 mutations in cancer. *Nat Cell Biol* **15**, 2-8 (2013). <https://doi.org:10.1038/ncb2641>
- 208 Graziano, V. & De Laurenzi, V. Role of p63 in cancer development. *Biochim Biophys Acta* **1816**, 57-66 (2011). <https://doi.org:10.1016/j.bbcan.2011.04.002>
- 209 Deyoung, M. P. & Ellisen, L. W. p63 and p73 in human cancer: defining the network. *Oncogene* **26**, 5169-5183 (2007). <https://doi.org:10.1038/sj.onc.1210337>
- 210 Inoue, K. & Fry, E. A. Alterations of p63 and p73 in human cancers. *Subcell Biochem* **85**, 17-40 (2014). [https://doi.org:10.1007/978-94-017-9211-0\\_2](https://doi.org:10.1007/978-94-017-9211-0_2)
- 211 Maas, A. M., Bretz, A. C., Mack, E. & Stiewe, T. Targeting p73 in cancer. *Cancer Lett* **332**, 229-236 (2013). <https://doi.org:10.1016/j.canlet.2011.07.030>
- 212 Bergholz, J. & Xiao, Z. X. Role of p63 in Development, Tumorigenesis and Cancer Progression. *Cancer Microenviron* **5**, 311-322 (2012). <https://doi.org:10.1007/s12307-012-0116-9>
- 213 Zhou, R. *et al.* Li-Fraumeni Syndrome Disease Model: A Platform to Develop Precision Cancer Therapy Targeting Oncogenic p53. *Trends Pharmacol Sci* **38**, 908-927 (2017). <https://doi.org:10.1016/j.tips.2017.07.004>

- 214 Correa, H. Li-Fraumeni Syndrome. *J Pediatr Genet* **5**, 84-88 (2016). <https://doi.org:10.1055/s-0036-1579759>
- 215 Jochemsen, A. G. Reactivation of p53 as therapeutic intervention for malignant melanoma. *Curr Opin Oncol* **26**, 114-119 (2014). <https://doi.org:10.1097/CCO.0000000000000033>
- 216 Box, N. F., Vukmer, T. O. & Terzian, T. Targeting p53 in melanoma. *Pigment Cell Melanoma Res* **27**, 8-10 (2014). <https://doi.org:10.1111/pcmr.12180>
- 217 Hodis, E. *et al.* A landscape of driver mutations in melanoma. *Cell* **150**, 251-263 (2012). <https://doi.org:10.1016/j.cell.2012.06.024>
- 218 Polsky, D. *et al.* HDM2 protein overexpression, but not gene amplification, is related to tumorigenesis of cutaneous melanoma. *Cancer Res* **61**, 7642-7646 (2001).
- 219 Gembarska, A. *et al.* MDM4 is a key therapeutic target in cutaneous melanoma. *Nat Med* **18**, 1239-1247 (2012). <https://doi.org:10.1038/nm.2863>
- 220 Lu, M., Miller, P. & Lu, X. Restoring the tumour suppressive function of p53 as a parallel strategy in melanoma therapy. *FEBS Lett* **588**, 2616-2621 (2014). <https://doi.org:10.1016/j.febslet.2014.05.008>
- 221 Hong, B., van den Heuvel, A. P., Prabhu, V. V., Zhang, S. & El-Deiry, W. S. Targeting tumor suppressor p53 for cancer therapy: strategies, challenges and opportunities. *Curr Drug Targets* **15**, 80-89 (2014). <https://doi.org:10.2174/1389450114666140106101412>
- 222 Sun, W. *et al.* Advances in the techniques and methodologies of cancer gene therapy. *Discov Med* **27**, 45-55 (2019).
- 223 Zhou, S., Fan, C., Zeng, Z., Young, K. H. & Li, Y. Clinical and Immunological Effects of p53-Targeting Vaccines. *Front Cell Dev Biol* **9**, 762796 (2021). <https://doi.org:10.3389/fcell.2021.762796>
- 224 Cai, B. H. *et al.* P63 and P73 Activation in Cancers with p53 Mutation. *Biomedicines* **10** (2022). <https://doi.org:10.3390/biomedicines10071490>
- 225 Vassilev, L. T. MDM2 inhibitors for cancer therapy. *Trends Mol Med* **13**, 23-31 (2007). <https://doi.org:10.1016/j.molmed.2006.11.002>
- 226 Secchiero, P., Bosco, R., Celeghini, C. & Zauli, G. Recent advances in the therapeutic perspectives of Nutlin-3. *Curr Pharm Des* **17**, 569-577 (2011). <https://doi.org:10.2174/138161211795222586>
- 227 Konopleva, M. *et al.* MDM2 inhibition: an important step forward in cancer therapy. *Leukemia* **34**, 2858-2874 (2020). <https://doi.org:10.1038/s41375-020-0949-z>
- 228 Wang, S. & Chen, F. E. Small-molecule MDM2 inhibitors in clinical trials for cancer therapy. *Eur J Med Chem* **236**, 114334 (2022). <https://doi.org:10.1016/j.ejmech.2022.114334>
- 229 Wiman, K. G. Pharmacological reactivation of mutant p53: from protein structure to the cancer patient. *Oncogene* **29**, 4245-4252 (2010). <https://doi.org:10.1038/onc.2010.188>
- 230 Duffy, M. J., Synnott, N. C. & Crown, J. Mutant p53 as a target for cancer treatment. *Eur J Cancer* **83**, 258-265 (2017). <https://doi.org:10.1016/j.ejca.2017.06.023>
- 231 Perdrix, A. *et al.* PRIMA-1 and PRIMA-1(Met) (APR-246): From Mutant/Wild Type p53 Reactivation to Unexpected Mechanisms Underlying Their Potent Anti-Tumor Effect in Combinatorial Therapies. *Cancers (Basel)* **9** (2017). <https://doi.org:10.3390/cancers9120172>

- 232 Nishikawa, S. & Iwakuma, T. Drugs Targeting p53 Mutations with FDA Approval and in Clinical Trials. *Cancers (Basel)* **15** (2023). <https://doi.org:10.3390/cancers15020429>
- 233 De Bont, R. & van Larebeke, N. Endogenous DNA damage in humans: a review of quantitative data. *Mutagenesis* **19**, 169-185 (2004). <https://doi.org:10.1093/mutage/geh025>
- 234 Khare, V. & Eckert, K. A. The proofreading 3'→5' exonuclease activity of DNA polymerases: a kinetic barrier to translesion DNA synthesis. *Mutat Res* **510**, 45-54 (2002). [https://doi.org:10.1016/s0027-5107\(02\)00251-8](https://doi.org:10.1016/s0027-5107(02)00251-8)
- 235 Pelicano, H., Carney, D. & Huang, P. ROS stress in cancer cells and therapeutic implications. *Drug Resist Updat* **7**, 97-110 (2004). <https://doi.org:10.1016/j.drup.2004.01.004>
- 236 Hanukoglu, I. Antioxidant protective mechanisms against reactive oxygen species (ROS) generated by mitochondrial P450 systems in steroidogenic cells. *Drug Metab Rev* **38**, 171-196 (2006). <https://doi.org:10.1080/03602530600570040>
- 237 Sedgwick, B., Bates, P. A., Paik, J., Jacobs, S. C. & Lindahl, T. Repair of alkylated DNA: recent advances. *DNA Repair (Amst)* **6**, 429-442 (2007). <https://doi.org:10.1016/j.dnarep.2006.10.005>
- 238 Marnett, L. J. & Plataras, J. P. Endogenous DNA damage and mutation. *Trends Genet* **17**, 214-221 (2001). [https://doi.org:10.1016/s0168-9525\(01\)02239-9](https://doi.org:10.1016/s0168-9525(01)02239-9)
- 239 Lomax, M. E., Folkes, L. K. & O'Neill, P. Biological consequences of radiation-induced DNA damage: relevance to radiotherapy. *Clin Oncol (R Coll Radiol)* **25**, 578-585 (2013). <https://doi.org:10.1016/j.clon.2013.06.007>
- 240 Craig, S., Earnshaw, C. H. & Viros, A. Ultraviolet light and melanoma. *J Pathol* **244**, 578-585 (2018). <https://doi.org:10.1002/path.5039>
- 241 Vink, A. A. & Roza, L. Biological consequences of cyclobutane pyrimidine dimers. *J Photochem Photobiol B* **65**, 101-104 (2001). [https://doi.org:10.1016/s1011-1344\(01\)00245-7](https://doi.org:10.1016/s1011-1344(01)00245-7)
- 242 Klapacz, J. *et al.* Contributions of DNA repair and damage response pathways to the non-linear genotoxic responses of alkylating agents. *Mutat Res Rev Mutat Res* **767**, 77-91 (2016). <https://doi.org:10.1016/j.mrrev.2015.11.001>
- 243 Fronza, G. & Gold, B. The biological effects of N3-methyladenine. *J Cell Biochem* **91**, 250-257 (2004). <https://doi.org:10.1002/jcb.10698>
- 244 Merk, O. & Speit, G. Detection of crosslinks with the comet assay in relationship to genotoxicity and cytotoxicity. *Environ Mol Mutagen* **33**, 167-172 (1999). [https://doi.org:10.1002/\(sici\)1098-2280\(1999\)33:2<167::aid-em9>3.0.co;2-d](https://doi.org:10.1002/(sici)1098-2280(1999)33:2<167::aid-em9>3.0.co;2-d)
- 245 Malinge, J. M., Giraud-Panis, M. J. & Leng, M. Interstrand cross-links of cisplatin induce striking distortions in DNA. *J Inorg Biochem* **77**, 23-29 (1999). [https://doi.org:10.1016/s0162-0134\(99\)00148-8](https://doi.org:10.1016/s0162-0134(99)00148-8)
- 246 Chatterjee, N. & Walker, G. C. Mechanisms of DNA damage, repair, and mutagenesis. *Environ Mol Mutagen* **58**, 235-263 (2017). <https://doi.org:10.1002/em.22087>
- 247 Barnes, J. L., Zubair, M., John, K., Poirier, M. C. & Martin, F. L. Carcinogens and DNA damage. *Biochem Soc Trans* **46**, 1213-1224 (2018). <https://doi.org:10.1042/BST20180519>
- 248 Bedard, L. L. & Massey, T. E. Aflatoxin B1-induced DNA damage and its repair. *Cancer Lett* **241**, 174-183 (2006). <https://doi.org:10.1016/j.canlet.2005.11.018>

- 249 Torgovnick, A. & Schumacher, B. DNA repair mechanisms in cancer development and therapy. *Front Genet* **6**, 157 (2015). <https://doi.org:10.3389/fgene.2015.00157>
- 250 Alhmoud, J. F., Woolley, J. F., Al Moustafa, A. E. & Malki, M. I. DNA Damage/Repair Management in Cancers. *Cancers (Basel)* **12** (2020). <https://doi.org:10.3390/cancers12041050>
- 251 Blackford, A. N. & Jackson, S. P. ATM, ATR, and DNA-PK: The Trinity at the Heart of the DNA Damage Response. *Mol Cell* **66**, 801-817 (2017). <https://doi.org:10.1016/j.molcel.2017.05.015>
- 252 Kunkel, T. A. & Erie, D. A. DNA mismatch repair. *Annu Rev Biochem* **74**, 681-710 (2005). <https://doi.org:10.1146/annurev.biochem.74.082803.133243>
- 253 Li, G. M. Mechanisms and functions of DNA mismatch repair. *Cell Res* **18**, 85-98 (2008). <https://doi.org:10.1038/cr.2007.115>
- 254 Krokan, H. E. & Bjoras, M. Base excision repair. *Cold Spring Harb Perspect Biol* **5**, a012583 (2013). <https://doi.org:10.1101/cshperspect.a012583>
- 255 Rouleau, M., Patel, A., Hendzel, M. J., Kaufmann, S. H. & Poirier, G. G. PARP inhibition: PARP1 and beyond. *Nat Rev Cancer* **10**, 293-301 (2010). <https://doi.org:10.1038/nrc2812>
- 256 Zong, W., Gong, Y., Sun, W., Li, T. & Wang, Z. Q. PARP1: Liaison of Chromatin Remodeling and Transcription. *Cancers (Basel)* **14** (2022). <https://doi.org:10.3390/cancers14174162>
- 257 Ko, H. L. & Ren, E. C. Functional Aspects of PARP1 in DNA Repair and Transcription. *Biomolecules* **2**, 524-548 (2012). <https://doi.org:10.3390/biom2040524>
- 258 Wallace, S. S., Murphy, D. L. & Sweasy, J. B. Base excision repair and cancer. *Cancer Lett* **327**, 73-89 (2012). <https://doi.org:10.1016/j.canlet.2011.12.038>
- 259 Robertson, A. B., Klungland, A., Rognes, T. & Leiros, I. DNA repair in mammalian cells: Base excision repair: the long and short of it. *Cell Mol Life Sci* **66**, 981-993 (2009). <https://doi.org:10.1007/s00018-009-8736-z>
- 260 de Boer, J. & Hoeijmakers, J. H. Nucleotide excision repair and human syndromes. *Carcinogenesis* **21**, 453-460 (2000). <https://doi.org:10.1093/carcin/21.3.453>
- 261 Hanawalt, P. C. Subpathways of nucleotide excision repair and their regulation. *Oncogene* **21**, 8949-8956 (2002). <https://doi.org:10.1038/sj.onc.1206096>
- 262 Foustieri, M. & Mullenders, L. H. Transcription-coupled nucleotide excision repair in mammalian cells: molecular mechanisms and biological effects. *Cell Res* **18**, 73-84 (2008). <https://doi.org:10.1038/cr.2008.6>
- 263 Spivak, G. Nucleotide excision repair in humans. *DNA Repair (Amst)* **36**, 13-18 (2015). <https://doi.org:10.1016/j.dnarep.2015.09.003>
- 264 de Laat, W. L., Jaspers, N. G. & Hoeijmakers, J. H. Molecular mechanism of nucleotide excision repair. *Genes Dev* **13**, 768-785 (1999). <https://doi.org:10.1101/gad.13.7.768>
- 265 Caldecott, K. W. DNA single-strand break repair and human genetic disease. *Trends Cell Biol* **32**, 733-745 (2022). <https://doi.org:10.1016/j.tcb.2022.04.010>
- 266 Pommier, Y., Sun, Y., Huang, S. N. & Nitiss, J. L. Roles of eukaryotic topoisomerases in transcription, replication and genomic stability. *Nat Rev Mol Cell Biol* **17**, 703-721 (2016). <https://doi.org:10.1038/nrm.2016.111>
- 267 Godon, C. *et al.* PARP inhibition versus PARP-1 silencing: different outcomes in terms of single-strand break repair and radiation susceptibility. *Nucleic Acids Res* **36**, 4454-4464 (2008). <https://doi.org:10.1093/nar/gkn403>

- 268 Caldecott, K. W. Single-strand break repair and genetic disease. *Nat Rev Genet* **9**, 619-631 (2008). <https://doi.org:10.1038/nrg2380>
- 269 Plo, I. *et al.* Association of XRCC1 and tyrosyl DNA phosphodiesterase (Tdp1) for the repair of topoisomerase I-mediated DNA lesions. *DNA Repair (Amst)* **2**, 1087-1100 (2003). [https://doi.org:10.1016/s1568-7864\(03\)00116-2](https://doi.org:10.1016/s1568-7864(03)00116-2)
- 270 Helleday, T., Lo, J., van Gent, D. C. & Engelward, B. P. DNA double-strand break repair: from mechanistic understanding to cancer treatment. *DNA Repair (Amst)* **6**, 923-935 (2007). <https://doi.org:10.1016/j.dnarep.2007.02.006>
- 271 Shibata, A. Regulation of repair pathway choice at two-ended DNA double-strand breaks. *Mutat Res* **803-805**, 51-55 (2017). <https://doi.org:10.1016/j.mrfmmm.2017.07.011>
- 272 Blasiak, J. Single-Strand Annealing in Cancer. *Int J Mol Sci* **22** (2021). <https://doi.org:10.3390/ijms22042167>
- 273 van den Bosch, M., Bree, R. T. & Lowndes, N. F. The MRN complex: coordinating and mediating the response to broken chromosomes. *EMBO Rep* **4**, 844-849 (2003). <https://doi.org:10.1038/sj.embor.embor925>
- 274 Lamarche, B. J., Orazio, N. I. & Weitzman, M. D. The MRN complex in double-strand break repair and telomere maintenance. *FEBS Lett* **584**, 3682-3695 (2010). <https://doi.org:10.1016/j.febslet.2010.07.029>
- 275 Tran, P. T., Erdeniz, N., Symington, L. S. & Liskay, R. M. EXO1-A multi-tasking eukaryotic nuclease. *DNA Repair (Amst)* **3**, 1549-1559 (2004). <https://doi.org:10.1016/j.dnarep.2004.05.015>
- 276 Symington, L. S. & Gautier, J. Double-strand break end resection and repair pathway choice. *Annu Rev Genet* **45**, 247-271 (2011). <https://doi.org:10.1146/annurev-genet-110410-132435>
- 277 Mimitou, E. P. & Symington, L. S. DNA end resection--unraveling the tail. *DNA Repair (Amst)* **10**, 344-348 (2011). <https://doi.org:10.1016/j.dnarep.2010.12.004>
- 278 Zhao, F., Kim, W., Kloeber, J. A. & Lou, Z. DNA end resection and its role in DNA replication and DSB repair choice in mammalian cells. *Exp Mol Med* **52**, 1705-1714 (2020). <https://doi.org:10.1038/s12276-020-00519-1>
- 279 Dudas, A. & Chovanec, M. DNA double-strand break repair by homologous recombination. *Mutat Res* **566**, 131-167 (2004). <https://doi.org:10.1016/j.mrrev.2003.07.001>
- 280 Mao, Z., Bozzella, M., Seluanov, A. & Gorbunova, V. DNA repair by nonhomologous end joining and homologous recombination during cell cycle in human cells. *Cell Cycle* **7**, 2902-2906 (2008). <https://doi.org:10.4161/cc.7.18.6679>
- 281 Prakash, R., Zhang, Y., Feng, W. & Jasin, M. Homologous recombination and human health: the roles of BRCA1, BRCA2, and associated proteins. *Cold Spring Harb Perspect Biol* **7**, a016600 (2015). <https://doi.org:10.1101/cshperspect.a016600>
- 282 Laurini, E. *et al.* Role of Rad51 and DNA repair in cancer: A molecular perspective. *Pharmacol Ther* **208**, 107492 (2020). <https://doi.org:10.1016/j.pharmthera.2020.107492>
- 283 Mazin, A. V., Mazina, O. M., Bugreev, D. V. & Rossi, M. J. Rad54, the motor of homologous recombination. *DNA Repair (Amst)* **9**, 286-302 (2010). <https://doi.org:10.1016/j.dnarep.2009.12.006>
- 284 Wright, W. D., Shah, S. S. & Heyer, W. D. Homologous recombination and the repair of DNA double-strand breaks. *J Biol Chem* **293**, 10524-10535 (2018). <https://doi.org:10.1074/jbc.TM118.000372>

- 285 Li, X. & Heyer, W. D. Homologous recombination in DNA repair and DNA damage tolerance. *Cell Res* **18**, 99-113 (2008). <https://doi.org:10.1038/cr.2008.1>
- 286 Scully, R., Panday, A., Elango, R. & Willis, N. A. DNA double-strand break repair-pathway choice in somatic mammalian cells. *Nat Rev Mol Cell Biol* **20**, 698-714 (2019). <https://doi.org:10.1038/s41580-019-0152-0>
- 287 Kramara, J., Osia, B. & Malkova, A. Break-Induced Replication: The Where, The Why, and The How. *Trends Genet* **34**, 518-531 (2018). <https://doi.org:10.1016/j.tig.2018.04.002>
- 288 Malkova, A. & Ira, G. Break-induced replication: functions and molecular mechanism. *Curr Opin Genet Dev* **23**, 271-279 (2013). <https://doi.org:10.1016/j.gde.2013.05.007>
- 289 Sakofsky, C. J. & Malkova, A. Break induced replication in eukaryotes: mechanisms, functions, and consequences. *Crit Rev Biochem Mol Biol* **52**, 395-413 (2017). <https://doi.org:10.1080/10409238.2017.1314444>
- 290 Li, J. *et al.* Pathways and assays for DNA double-strand break repair by homologous recombination. *Acta Biochim Biophys Sin (Shanghai)* **51**, 879-889 (2019). <https://doi.org:10.1093/abbs/qmz076>
- 291 Ramakrishnan, S., Kockler, Z., Evans, R., Downing, B. D. & Malkova, A. Single-strand annealing between inverted DNA repeats: Pathway choice, participating proteins, and genome destabilizing consequences. *PLoS Genet* **14**, e1007543 (2018). <https://doi.org:10.1371/journal.pgen.1007543>
- 292 Bhargava, R., Onyango, D. O. & Stark, J. M. Regulation of Single-Strand Annealing and its Role in Genome Maintenance. *Trends Genet* **32**, 566-575 (2016). <https://doi.org:10.1016/j.tig.2016.06.007>
- 293 Vu, T. V., Das, S., Nguyen, C. C., Kim, J. & Kim, J. Y. Single-strand annealing: Molecular mechanisms and potential applications in CRISPR-Cas-based precision genome editing. *Biotechnol J* **17**, e2100413 (2022). <https://doi.org:10.1002/biot.202100413>
- 294 Weterings, E. & van Gent, D. C. The mechanism of non-homologous end-joining: a synopsis of synapsis. *DNA Repair (Amst)* **3**, 1425-1435 (2004). <https://doi.org:10.1016/j.dnarep.2004.06.003>
- 295 Deriano, L. & Roth, D. B. Modernizing the nonhomologous end-joining repertoire: alternative and classical NHEJ share the stage. *Annu Rev Genet* **47**, 433-455 (2013). <https://doi.org:10.1146/annurev-genet-110711-155540>
- 296 Zahid, S. *et al.* The Multifaceted Roles of Ku70/80. *Int J Mol Sci* **22** (2021). <https://doi.org:10.3390/ijms22084134>
- 297 van Gent, D. C. & van der Burg, M. Non-homologous end-joining, a sticky affair. *Oncogene* **26**, 7731-7740 (2007). <https://doi.org:10.1038/sj.onc.1210871>
- 298 Dueva, R. & Iliakis, G. Alternative pathways of non-homologous end joining (NHEJ) in genomic instability and cancer. *Transl Cancer Res* **2**, 163-177 (2013). <https://doi.org:10.3978/j.issn.2218-676X.2013.05.02>
- 299 Wang, H. & Xu, X. Microhomology-mediated end joining: new players join the team. *Cell Biosci* **7**, 6 (2017). <https://doi.org:10.1186/s13578-017-0136-8>
- 300 Sinha, S., Villarreal, D., Shim, E. Y. & Lee, S. E. Risky business: Microhomology-mediated end joining. *Mutat Res* **788**, 17-24 (2016). <https://doi.org:10.1016/j.mrfmmm.2015.12.005>
- 301 Sfeir, A. & Symington, L. S. Microhomology-Mediated End Joining: A Back-up Survival Mechanism or Dedicated Pathway? *Trends Biochem Sci* **40**, 701-714 (2015). <https://doi.org:10.1016/j.tibs.2015.08.006>

- 302 Ceccaldi, R., Rondinelli, B. & D'Andrea, A. D. Repair Pathway Choices and Consequences at the Double-Strand Break. *Trends Cell Biol* **26**, 52-64 (2016). <https://doi.org:10.1016/j.tcb.2015.07.009>
- 303 Kerzendorfer, C. & O'Driscoll, M. Human DNA damage response and repair deficiency syndromes: linking genomic instability and cell cycle checkpoint proficiency. *DNA Repair (Amst)* **8**, 1139-1152 (2009). <https://doi.org:10.1016/j.dnarep.2009.04.018>
- 304 Vilar, E. & Gruber, S. B. Microsatellite instability in colorectal cancer-the stable evidence. *Nat Rev Clin Oncol* **7**, 153-162 (2010). <https://doi.org:10.1038/nrclinonc.2009.237>
- 305 Li, S. K. H. & Martin, A. Mismatch Repair and Colon Cancer: Mechanisms and Therapies Explored. *Trends Mol Med* **22**, 274-289 (2016). <https://doi.org:10.1016/j.molmed.2016.02.003>
- 306 Cheadle, J. P. & Sampson, J. R. MUTYH-associated polyposis--from defect in base excision repair to clinical genetic testing. *DNA Repair (Amst)* **6**, 274-279 (2007). <https://doi.org:10.1016/j.dnarep.2006.11.001>
- 307 Lehmann, A. R., McGibbon, D. & Stefanini, M. Xeroderma pigmentosum. *Orphanet J Rare Dis* **6**, 70 (2011). <https://doi.org:10.1186/1750-1172-6-70>
- 308 Cleaver, J. E. Cancer in xeroderma pigmentosum and related disorders of DNA repair. *Nat Rev Cancer* **5**, 564-573 (2005). <https://doi.org:10.1038/nrc1652>
- 309 Black, J. O. Xeroderma Pigmentosum. *Head Neck Pathol* **10**, 139-144 (2016). <https://doi.org:10.1007/s12105-016-0707-8>
- 310 Amirifar, P., Ranjouri, M. R., Yazdani, R., Abolhassani, H. & Aghamohammadi, A. Ataxia-telangiectasia: A review of clinical features and molecular pathology. *Pediatr Allergy Immunol* **30**, 277-288 (2019). <https://doi.org:10.1111/pai.13020>
- 311 Rothblum-Oviatt, C. et al. Ataxia telangiectasia: a review. *Orphanet J Rare Dis* **11**, 159 (2016). <https://doi.org:10.1186/s13023-016-0543-7>
- 312 Niraj, J., Farkkila, A. & D'Andrea, A. D. The Fanconi Anemia Pathway in Cancer. *Annu Rev Cancer Biol* **3**, 457-478 (2019). <https://doi.org:10.1146/annurev-cancerbio-030617-050422>
- 313 Fiesco-Roa, M. O., Giri, N., McReynolds, L. J., Best, A. F. & Alter, B. P. Genotype-phenotype associations in Fanconi anemia: A literature review. *Blood Rev* **37**, 100589 (2019). <https://doi.org:10.1016/j.blre.2019.100589>
- 314 Liede, A., Karlan, B. Y. & Narod, S. A. Cancer risks for male carriers of germline mutations in BRCA1 or BRCA2: a review of the literature. *J Clin Oncol* **22**, 735-742 (2004). <https://doi.org:10.1200/JCO.2004.05.055>
- 315 Venkitaraman, A. R. Cancer susceptibility and the functions of BRCA1 and BRCA2. *Cell* **108**, 171-182 (2002). [https://doi.org:10.1016/s0092-8674\(02\)00615-3](https://doi.org:10.1016/s0092-8674(02)00615-3)
- 316 Carbone, M. et al. Biological Mechanisms and Clinical Significance of BAP1 Mutations in Human Cancer. *Cancer Discov* **10**, 1103-1120 (2020). <https://doi.org:10.1158/2159-8290.CD-19-1220>
- 317 Rai, K., Pilarski, R., Cebulla, C. & Abdel-Rahman, M. Comprehensive review of BAP1 tumor predisposition syndrome with report of two new cases. *Clinical genetics* **89**, 285-294 (2016).
- 318 Pilarski, R., Carlo, M., Cebulla, C. & Abdel-Rahman, M. BAP1 tumor predisposition syndrome. (2022).
- 319 Masoomian, B., Shields, J. A. & Shields, C. L. Overview of BAP1 cancer predisposition syndrome and the relationship to uveal melanoma. *J Curr Ophthalmol* **30**, 102-109 (2018). <https://doi.org:10.1016/j.joco.2018.02.005>

- 320 Povey, J. E. *et al.* DNA repair gene polymorphisms and genetic predisposition to cutaneous melanoma. *Carcinogenesis* **28**, 1087-1093 (2007). <https://doi.org:10.1093/carcin/bgl257>
- 321 Maresca, L., Stecca, B. & Carrassa, L. Novel Therapeutic Approaches with DNA Damage Response Inhibitors for Melanoma Treatment. *Cells* **11** (2022). <https://doi.org:10.3390/cells11091466>
- 322 Kauffmann, A. *et al.* High expression of DNA repair pathways is associated with metastasis in melanoma patients. *Oncogene* **27**, 565-573 (2008). <https://doi.org:10.1038/sj.onc.1210700>
- 323 Jewell, R. *et al.* Patterns of expression of DNA repair genes and relapse from melanoma. *Clin Cancer Res* **16**, 5211-5221 (2010). <https://doi.org:10.1158/1078-0432.CCR-10-1521>
- 324 Winnepeninckx, V. *et al.* Gene expression profiling of primary cutaneous melanoma and clinical outcome. *J Natl Cancer Inst* **98**, 472-482 (2006). <https://doi.org:10.1093/jnci/djj103>
- 325 Makino, E. *et al.* Targeting Rad51 as a strategy for the treatment of melanoma cells resistant to MAPK pathway inhibition. *Cell Death Dis* **11**, 581 (2020). <https://doi.org:10.1038/s41419-020-2702-y>
- 326 Francisco, G., Cirilo, P. D. R., Gonçalves, F. T., Junior, T. C. T. & Chammas, R. in *Melanoma-From Early Detection to Treatment* (IntechOpen, 2013).
- 327 Makino, E. *et al.* Melanoma cells resistant towards MAPK inhibitors exhibit reduced TAp73 expression mediating enhanced sensitivity to platinum-based drugs. *Cell Death Dis* **9**, 930 (2018). <https://doi.org:10.1038/s41419-018-0952-8>
- 328 Woods, D. & Turchi, J. J. Chemotherapy induced DNA damage response: convergence of drugs and pathways. *Cancer Biol Ther* **14**, 379-389 (2013). <https://doi.org:10.4161/cbt.23761>
- 329 Basu, A. & Krishnamurthy, S. Cellular responses to Cisplatin-induced DNA damage. *J Nucleic Acids* **2010** (2010). <https://doi.org:10.4061/2010/201367>
- 330 Martin, L. P., Hamilton, T. C. & Schilder, R. J. Platinum resistance: The role of DNA repair pathways. *Clin Cancer Res* **14**, 1291-1295 (2008). <https://doi.org:10.1158/1078-0432.Ccr-07-2238>
- 331 Oun, R., Moussa, Y. E. & Wheate, N. J. Correction: The side effects of platinum-based chemotherapy drugs: a review for chemists. *Dalton Trans* **47**, 7848 (2018). <https://doi.org:10.1039/c8dt90088d>
- 332 Oun, R., Moussa, Y. E. & Wheate, N. J. The side effects of platinum-based chemotherapy drugs: a review for chemists. *Dalton Trans* **47**, 6645-6653 (2018). <https://doi.org:10.1039/c8dt00838h>
- 333 Galmarini, C. M., Mackey, J. R. & Dumontet, C. Nucleoside analogues and nucleobases in cancer treatment. *Lancet Oncol* **3**, 415-424 (2002). [https://doi.org:10.1016/s1470-2045\(02\)00788-x](https://doi.org:10.1016/s1470-2045(02)00788-x)
- 334 Jordheim, L. P., Durantel, D., Zoulim, F. & Dumontet, C. Advances in the development of nucleoside and nucleotide analogues for cancer and viral diseases. *Nat Rev Drug Discov* **12**, 447-464 (2013). <https://doi.org:10.1038/nrd4010>
- 335 Sampath, D., Rao, V. A. & Plunkett, W. Mechanisms of apoptosis induction by nucleoside analogs. *Oncogene* **22**, 9063-9074 (2003). <https://doi.org:10.1038/sj.onc.1207229>
- 336 Ralhan, R. & Kaur, J. Alkylating agents and cancer therapy. *Expert Opin Ther Pat* **17**, 1061-1075 (2007). <https://doi.org:10.1517/13543776.17.9.1061>

- 337 Perez-Herrero, E. & Fernandez-Medarde, A. Advanced targeted therapies in cancer: Drug nanocarriers, the future of chemotherapy. *Eur J Pharm Biopharm* **93**, 52-79 (2015). <https://doi.org:10.1016/j.ejpb.2015.03.018>
- 338 Borchiellini, D., Etienne-Grimaldi, M. C., Thariat, J. & Milano, G. The impact of pharmacogenetics on radiation therapy outcome in cancer patients. A focus on DNA damage response genes. *Cancer Treat Rev* **38**, 737-759 (2012). <https://doi.org:10.1016/j.ctrv.2012.02.004>
- 339 Pawlik, T. M. & Keyomarsi, K. Role of cell cycle in mediating sensitivity to radiotherapy. *Int J Radiat Oncol Biol Phys* **59**, 928-942 (2004). <https://doi.org:10.1016/j.ijrobp.2004.03.005>
- 340 Huang, R. X. & Zhou, P. K. DNA damage response signaling pathways and targets for radiotherapy sensitization in cancer. *Signal Transduct Target Ther* **5**, 60 (2020). <https://doi.org:10.1038/s41392-020-0150-x>
- 341 Rose, M., Burgess, J. T., O'Byrne, K., Richard, D. J. & Bolderson, E. PARP Inhibitors: Clinical Relevance, Mechanisms of Action and Tumor Resistance. *Front Cell Dev Biol* **8**, 564601 (2020). <https://doi.org:10.3389/fcell.2020.564601>
- 342 Barkauskaite, E., Jankevicius, G. & Ahel, I. Structures and Mechanisms of Enzymes Employed in the Synthesis and Degradation of PARP-Dependent Protein ADP-Ribosylation. *Mol Cell* **58**, 935-946 (2015). <https://doi.org:10.1016/j.molcel.2015.05.007>
- 343 Hottiger, M. O. Nuclear ADP-Ribosylation and Its Role in Chromatin Plasticity, Cell Differentiation, and Epigenetics. *Annu Rev Biochem* **84**, 227-263 (2015). <https://doi.org:10.1146/annurev-biochem-060614-034506>
- 344 Min, A. & Im, S. A. PARP Inhibitors as Therapeutics: Beyond Modulation of PARylation. *Cancers* **12** (2020). <https://doi.org:ARTN 39410.3390/cancers12020394>
- 345 Caldecott, K. W. Protein ADP-ribosylation and the cellular response to DNA strand breaks. *DNA Repair (Amst)* **19**, 108-113 (2014). <https://doi.org:10.1016/j.dnarep.2014.03.021>
- 346 Curtin, N. J. PARP inhibitors for cancer therapy. *Expert Rev Mol Med* **7**, 1-20 (2005). <https://doi.org:10.1017/S146239940500904X>
- 347 Murai, J. *et al.* Trapping of PARP1 and PARP2 by Clinical PARP Inhibitors. *Cancer Res* **72**, 5588-5599 (2012). <https://doi.org:10.1158/0008-5472.CAN-12-2753>
- 348 Erratum for the Perspective: "Laying a trap to kill cancer cells: PARP inhibitors and their mechanisms of action" by Y. Pommier, M. J. O'Connor, J. de Bono. *Sci Transl Med* **8**, 368er367 (2016). <https://doi.org:10.1126/scitranslmed.aal4973>
- 349 Pommier, Y., O'Connor, M. J. & de Bono, J. Laying a trap to kill cancer cells: PARP inhibitors and their mechanisms of action. *Sci Transl Med* **8**, 362ps317 (2016). <https://doi.org:10.1126/scitranslmed.aaf9246>
- 350 Yi, M. *et al.* Advances and perspectives of PARP inhibitors. *Exp Hematol Oncol* **8**, 29 (2019). <https://doi.org:10.1186/s40164-019-0154-9>
- 351 O'Neil, N. J., Bailey, M. L. & Hieter, P. Synthetic lethality and cancer. *Nat Rev Genet* **18**, 613-623 (2017). <https://doi.org:10.1038/nrg.2017.47>
- 352 Lord, C. J. & Ashworth, A. BRCAness revisited. *Nat Rev Cancer* **16**, 110-120 (2016). <https://doi.org:10.1038/nrc.2015.21>
- 353 Heeke, A. L. *et al.* Prevalence of Homologous Recombination-Related Gene Mutations Across Multiple Cancer Types. *JCO Precis Oncol* **2018** (2018). <https://doi.org:10.1200/PO.17.00286>

- 354 Timms, K. M. *et al.* Association of BRCA1/2 defects with genomic scores predictive of DNA damage repair deficiency among breast cancer subtypes. *Breast Cancer Res* **16**, 475 (2014). <https://doi.org:10.1186/s13058-014-0475-x>
- 355 Hoppe, M. M., Sundar, R., Tan, D. S. P. & Jeyasekharan, A. D. Biomarkers for Homologous Recombination Deficiency in Cancer. *J Natl Cancer Inst* **110**, 704-713 (2018). <https://doi.org:10.1093/jnci/djy085>
- 356 Frey, M. K. & Pothuri, B. Homologous recombination deficiency (HRD) testing in ovarian cancer clinical practice: a review of the literature. *Gynecol Oncol Res Pract* **4**, 4 (2017). <https://doi.org:10.1186/s40661-017-0039-8>
- 357 LaFargue, C. J., Dal Molin, G. Z., Sood, A. K. & Coleman, R. L. Exploring and comparing adverse events between PARP inhibitors. *Lancet Oncology* **20**, E15-E28 (2019). [https://doi.org:Doi 10.1016/S1470-2045\(18\)30786-1](https://doi.org:Doi 10.1016/S1470-2045(18)30786-1)
- 358 Foo, T., George, A. & Banerjee, S. PARP inhibitors in ovarian cancer: An overview of the practice-changing trials. *Genes Chromosomes Cancer* **60**, 385-397 (2021). <https://doi.org:10.1002/gcc.22935>
- 359 EMA. *Lynparza*, <https://www.ema.europa.eu/en/medicines/human/EPAR/lynparza> (2018).
- 360 Paik, J. Olaparib: A Review as First-Line Maintenance Therapy in Advanced Ovarian Cancer. *Target Oncol* **16**, 847-856 (2021). <https://doi.org:10.1007/s11523-021-00842-1>
- 361 Saad, F. *et al.* Patient-reported outcomes with olaparib plus abiraterone versus placebo plus abiraterone for metastatic castration-resistant prostate cancer: a randomised, double-blind, phase 2 trial. *Lancet Oncol* **23**, 1297-1307 (2022). [https://doi.org:10.1016/S1470-2045\(22\)00498-3](https://doi.org:10.1016/S1470-2045(22)00498-3)
- 362 EMA. *Rubraca*, <https://www.ema.europa.eu/en/medicines/human/EPAR/rubraca> (2022).
- 363 Syed, Y. Y. Rucaparib: First Global Approval. *Drugs* **77**, 585-592 (2017). <https://doi.org:10.1007/s40265-017-0716-2>
- 364 EMA. *Zejula*, <https://www.ema.europa.eu/en/medicines/human/EPAR/zejula> (2018).
- 365 EMA. *Talzenna*, <https://www.ema.europa.eu/en/medicines/human/EPAR/talzenna> (
- 366 Murai, J. *et al.* Stereospecific PARP trapping by BMN 673 and comparison with olaparib and rucaparib. *Mol Cancer Ther* **13**, 433-443 (2014). <https://doi.org:10.1158/1535-7163.MCT-13-0803>
- 367 Chan, W. Y., Brown, L. J., Reid, L. & Joshua, A. M. PARP Inhibitors in Melanoma-An Expanding Therapeutic Option? *Cancers (Basel)* **13** (2021). <https://doi.org:10.3390/cancers13184520>
- 368 Drean, A., Lord, C. J. & Ashworth, A. PARP inhibitor combination therapy. *Crit Rev Oncol Hematol* **108**, 73-85 (2016). <https://doi.org:10.1016/j.critrevonc.2016.10.010>
- 369 Ji, Z. *et al.* p53 rescue through HDM2 antagonism suppresses melanoma growth and potentiates MEK inhibition. *J Invest Dermatol* **132**, 356-364 (2012). <https://doi.org:10.1038/jid.2011.313>
- 370 Shattuck-Brandt, R. L. *et al.* Metastatic Melanoma Patient-Derived Xenografts Respond to MDM2 Inhibition as a Single Agent or in Combination with BRAF/MEK Inhibition. *Clin Cancer Res* **26**, 3803-3818 (2020). <https://doi.org:10.1158/1078-0432.CCR-19-1895>
- 371 Ishizawa, J. *et al.* Predictive Gene Signatures Determine Tumor Sensitivity to MDM2 Inhibition. *Cancer Res* **78**, 2721-2731 (2018). <https://doi.org:10.1158/0008-5472.CAN-17-0949>

- 372 Saiki, A. Y. *et al.* Identifying the determinants of response to MDM2 inhibition. *Oncotarget* **6**, 7701-7712 (2015). <https://doi.org:10.18632/oncotarget.3116>
- 373 Avery-Kiejda, K. A. *et al.* P53 in human melanoma fails to regulate target genes associated with apoptosis and the cell cycle and may contribute to proliferation. *BMC Cancer* **11**, 203 (2011). <https://doi.org:10.1186/1471-2407-11-203>
- 374 Waldman, T., Kinzler, K. W. & Vogelstein, B. p21 is necessary for the p53-mediated G1 arrest in human cancer cells. *Cancer Res* **55**, 5187-5190 (1995).
- 375 Shamloo, B. & Usluer, S. p21 in Cancer Research. *Cancers (Basel)* **11** (2019). <https://doi.org:10.3390/cancers11081178>
- 376 Shangary, S. *et al.* Reactivation of p53 by a specific MDM2 antagonist (MI-43) leads to p21-mediated cell cycle arrest and selective cell death in colon cancer. *Mol Cancer Ther* **7**, 1533-1542 (2008). <https://doi.org:10.1158/1535-7163.MCT-08-0140>
- 377 Vilgelm, A. E. *et al.* MDM2 antagonists overcome intrinsic resistance to CDK4/6 inhibition by inducing p21. *Sci Transl Med* **11** (2019). <https://doi.org:10.1126/scitranslmed.aav7171>
- 378 Aliouat-Denis, C. M. *et al.* p53-independent regulation of p21Waf1/Cip1 expression and senescence by Chk2. *Mol Cancer Res* **3**, 627-634 (2005). <https://doi.org:10.1158/1541-7786.MCR-05-0121>
- 379 Georgakilas, A. G., Martin, O. A. & Bonner, W. M. p21: A Two-Faced Genome Guardian. *Trends Mol Med* **23**, 310-319 (2017). <https://doi.org:10.1016/j.molmed.2017.02.001>
- 380 Romanov, V. S., Pospelov, V. A. & Pospelova, T. V. Cyclin-dependent kinase inhibitor p21(Waf1): contemporary view on its role in senescence and oncogenesis. *Biochemistry (Mosc)* **77**, 575-584 (2012). <https://doi.org:10.1134/S000629791206003X>
- 381 Galanos, P. *et al.* Chronic p53-independent p21 expression causes genomic instability by deregulating replication licensing. *Nat Cell Biol* **18**, 777-789 (2016). <https://doi.org:10.1038/ncb3378>
- 382 Ji, Z. *et al.* Vemurafenib synergizes with nutlin-3 to deplete survivin and suppresses melanoma viability and tumor growth. *Clin Cancer Res* **19**, 4383-4391 (2013). <https://doi.org:10.1158/1078-0432.CCR-13-0074>
- 383 Wu, C. E. *et al.* ATM Dependent DUSP6 Modulation of p53 Involved in Synergistic Targeting of MAPK and p53 Pathways with Trametinib and MDM2 Inhibitors in Cutaneous Melanoma. *Cancers (Basel)* **11** (2018). <https://doi.org:10.3390/cancers11010003>
- 384 Saiki, A. Y. *et al.* MDM2 antagonists synergize broadly and robustly with compounds targeting fundamental oncogenic signaling pathways. *Oncotarget* **5**, 2030-2043 (2014). <https://doi.org:10.18632/oncotarget.1918>
- 385 Eroglu, Z. & Ribas, A. Combination therapy with BRAF and MEK inhibitors for melanoma: latest evidence and place in therapy. *Ther Adv Med Oncol* **8**, 48-56 (2016). <https://doi.org:10.1177/1758834015616934>
- 386 Vilgelm, A. E. *et al.* Mdm2 and aurora kinase a inhibitors synergize to block melanoma growth by driving apoptosis and immune clearance of tumor cells. *Cancer Res* **75**, 181-193 (2015). <https://doi.org:10.1158/0008-5472.CAN-14-2405>
- 387 Patel, A. *et al.* Targeting p63 Upregulation Abrogates Resistance to MAPK Inhibitors in Melanoma. *Cancer Res* **80**, 2676-2688 (2020). <https://doi.org:10.1158/0008-5472.CAN-19-3230>

- 388 Valentine, J. M., Kumar, S. & Moumen, A. A p53-independent role for the MDM2 antagonist Nutlin-3 in DNA damage response initiation. *BMC Cancer* **11**, 79 (2011). <https://doi.org:10.1186/1471-2407-11-79>
- 389 Ray, R. M., Bhattacharya, S. & Johnson, L. R. Mdm2 inhibition induces apoptosis in p53 deficient human colon cancer cells by activating p73- and E2F1-mediated expression of PUMA and Siva-1. *Apoptosis* **16**, 35-44 (2011). <https://doi.org:10.1007/s10495-010-0538-0>
- 390 Enge, M. *et al.* MDM2-dependent downregulation of p21 and hnRNP K provides a switch between apoptosis and growth arrest induced by pharmacologically activated p53. *Cancer Cell* **15**, 171-183 (2009). <https://doi.org:10.1016/j.ccr.2009.01.019>
- 391 Zhang, Z. *et al.* MDM2 is a negative regulator of p21WAF1/CIP1, independent of p53. *J Biol Chem* **279**, 16000-16006 (2004). <https://doi.org:10.1074/jbc.M312264200>
- 392 Mirzayans, R., Andrais, B., Scott, A. & Murray, D. New insights into p53 signaling and cancer cell response to DNA damage: implications for cancer therapy. *J Biomed Biotechnol* **2012**, 170325 (2012). <https://doi.org:10.1155/2012/170325>
- 393 Wang, J. *et al.* TAp73 is a downstream target of p53 in controlling the cellular defense against stress. *J Biol Chem* **282**, 29152-29162 (2007). <https://doi.org:10.1074/jbc.M703408200>
- 394 Chen, X., Zheng, Y., Zhu, J., Jiang, J. & Wang, J. p73 is transcriptionally regulated by DNA damage, p53, and p73. *Oncogene* **20**, 769-774 (2001). <https://doi.org:10.1038/sj.onc.1204149>
- 395 Flores, E. R. *et al.* p63 and p73 are required for p53-dependent apoptosis in response to DNA damage. *Nature* **416**, 560-564 (2002). <https://doi.org:10.1038/416560a>
- 396 Soussi, T. & Wiman, K. G. TP53: an oncogene in disguise. *Cell Death Differ* **22**, 1239-1249 (2015). <https://doi.org:10.1038/cdd.2015.53>
- 397 Bae, W. K. *et al.* TAp73 inhibits cell invasion and migration by directly activating KAI1 expression in colorectal carcinoma. *Cancer Lett* **415**, 106-116 (2018). <https://doi.org:10.1016/j.canlet.2017.12.002>
- 398 Stindt, M. H. *et al.* Functional interplay between MDM2, p63/p73 and mutant p53. *Oncogene* **34**, 4300-4310 (2015). <https://doi.org:10.1038/onc.2014.359>
- 399 Kasim, V. *et al.* Synergistic cooperation of MDM2 and E2F1 contributes to TAp73 transcriptional activity. *Biochem Biophys Res Commun* **449**, 319-326 (2014). <https://doi.org:10.1016/j.bbrc.2014.05.026>
- 400 de Gruijl, F. R., van Kranen, H. J. & Mullenders, L. H. UV-induced DNA damage, repair, mutations and oncogenic pathways in skin cancer. *J Photochem Photobiol B* **63**, 19-27 (2001). [https://doi.org:10.1016/s1011-1344\(01\)00199-3](https://doi.org:10.1016/s1011-1344(01)00199-3)
- 401 Kim, K. B. *et al.* Prevalence of Homologous Recombination Pathway Gene Mutations in Melanoma: Rationale for a New Targeted Therapeutic Approach. *J Invest Dermatol* **141**, 2028-2036 e2022 (2021). <https://doi.org:10.1016/j.jid.2021.01.024>
- 402 Fratangelo, F. *et al.* Effect of ABT-888 on the apoptosis, motility and invasiveness of BRAFi-resistant melanoma cells. *Int J Oncol* **53**, 1149-1159 (2018). <https://doi.org:10.3892/ijo.2018.4457>
- 403 Rodriguez, M. I. *et al.* PARP-1 regulates metastatic melanoma through modulation of vimentin-induced malignant transformation. *PLoS Genet* **9**, e1003531 (2013). <https://doi.org:10.1371/journal.pgen.1003531>

- 404 Lobbich, M. & Jeggo, P. A. The impact of a negligent G2/M checkpoint on genomic instability and cancer induction. *Nat Rev Cancer* **7**, 861-869 (2007). <https://doi.org:10.1038/nrc2248>
- 405 Slade, D. Mitotic functions of poly(ADP-ribose) polymerases. *Biochem Pharmacol* **167**, 33-43 (2019). <https://doi.org:10.1016/j.bcp.2019.03.028>
- 406 Slade, D. PARP and PARG inhibitors in cancer treatment. *Genes Dev* **34**, 360-394 (2020). <https://doi.org:10.1101/gad.334516.119>
- 407 Castedo, M. *et al.* Cell death by mitotic catastrophe: a molecular definition. *Oncogene* **23**, 2825-2837 (2004). <https://doi.org:10.1038/sj.onc.1207528>
- 408 Vogel, C., Kienitz, A., Hofmann, I., Muller, R. & Bastians, H. Crosstalk of the mitotic spindle assembly checkpoint with p53 to prevent polyploidy. *Oncogene* **23**, 6845-6853 (2004). <https://doi.org:10.1038/sj.onc.1207860>
- 409 Fridman, J. S. & Lowe, S. W. Control of apoptosis by p53. *Oncogene* **22**, 9030-9040 (2003). <https://doi.org:10.1038/sj.onc.1207116>
- 410 Bunz, F. *et al.* Requirement for p53 and p21 to sustain G2 arrest after DNA damage. *Science* **282**, 1497-1501 (1998). <https://doi.org:10.1126/science.282.5393.1497>
- 411 Al Bitar, S. & Gali-Muhtasib, H. The Role of the Cyclin Dependent Kinase Inhibitor p21(cip1/waf1) in Targeting Cancer: Molecular Mechanisms and Novel Therapeutics. *Cancers (Basel)* **11** (2019). <https://doi.org:10.3390/cancers11101475>
- 412 Karimian, A., Ahmadi, Y. & Yousefi, B. Multiple functions of p21 in cell cycle, apoptosis and transcriptional regulation after DNA damage. *DNA Repair (Amst)* **42**, 63-71 (2016). <https://doi.org:10.1016/j.dnarep.2016.04.008>
- 413 Sedelnikova, O. A., Pilch, D. R., Redon, C. & Bonner, W. M. Histone H2AX in DNA damage and repair. *Cancer Biol Ther* **2**, 233-235 (2003). <https://doi.org:10.4161/cbt.2.3.373>
- 414 Kuo, L. J. & Yang, L. X. Gamma-H2AX - a novel biomarker for DNA double-strand breaks. *In Vivo* **22**, 305-309 (2008).
- 415 Guleria, A. & Chandna, S. ATM kinase: Much more than a DNA damage responsive protein. *DNA Repair (Amst)* **39**, 1-20 (2016). <https://doi.org:10.1016/j.dnarep.2015.12.009>
- 416 Marechal, A. & Zou, L. DNA damage sensing by the ATM and ATR kinases. *Cold Spring Harb Perspect Biol* **5** (2013). <https://doi.org:10.1101/cshperspect.a012716>
- 417 Weston, V. J. *et al.* The PARP inhibitor olaparib induces significant killing of ATM-deficient lymphoid tumor cells in vitro and in vivo. *Blood* **116**, 4578-4587 (2010). <https://doi.org:10.1182/blood-2010-01-265769>
- 418 Schmitt, A. *et al.* ATM Deficiency Is Associated with Sensitivity to PARP1- and ATR Inhibitors in Lung Adenocarcinoma. *Cancer Res* **77**, 3040-3056 (2017). <https://doi.org:10.1158/0008-5472.CAN-16-3398>
- 419 Wang, C., Jette, N., Moussienko, D., Bebb, D. G. & Lees-Miller, S. P. ATM-Deficient Colorectal Cancer Cells Are Sensitive to the PARP Inhibitor Olaparib. *Transl Oncol* **10**, 190-196 (2017). <https://doi.org:10.1016/j.tranon.2017.01.007>
- 420 Shen, C. & Houghton, P. J. The mTOR pathway negatively controls ATM by up-regulating miRNAs. *Proc Natl Acad Sci U S A* **110**, 11869-11874 (2013). <https://doi.org:10.1073/pnas.1220898110>
- 421 Wang, B. *et al.* Targeting mTOR signaling overcomes acquired resistance to combined BRAF and MEK inhibition in BRAF-mutant melanoma. *Oncogene* **40**, 5590-5599 (2021). <https://doi.org:10.1038/s41388-021-01911-5>

- 422 Hickson, I. *et al.* Identification and characterization of a novel and specific inhibitor of the ataxia-telangiectasia mutated kinase ATM. *Cancer Res* **64**, 9152-9159 (2004). <https://doi.org:10.1158/0008-5472.CAN-04-2727>
- 423 Le, B. V., Podsiywalow-Bartnicka, P., Piwocka, K. & Skorski, T. Pre-Existing and Acquired Resistance to PARP Inhibitor-Induced Synthetic Lethality. *Cancers (Basel)* **14** (2022). <https://doi.org:10.3390/cancers14235795>
- 424 Li, H. *et al.* PARP inhibitor resistance: the underlying mechanisms and clinical implications. *Mol Cancer* **19**, 107 (2020). <https://doi.org:10.1186/s12943-020-01227-0>
- 425 Sun, C. *et al.* Rational combination therapy with PARP and MEK inhibitors capitalizes on therapeutic liabilities in RAS mutant cancers. *Sci Transl Med* **9** (2017). <https://doi.org:10.1126/scitranslmed.aal5148>
- 426 Maertens, O. *et al.* MAPK Pathway Suppression Unmasks Latent DNA Repair Defects and Confers a Chemical Synthetic Vulnerability in BRAF-, NRAS-, and NF1-Mutant Melanomas. *Cancer Discov* **9**, 526-545 (2019). <https://doi.org:10.1158/2159-8290.CD-18-0879>
- 427 Giudice, E. *et al.* PARP Inhibitors Resistance: Mechanisms and Perspectives. *Cancers (Basel)* **14** (2022). <https://doi.org:10.3390/cancers14061420>
- 428 Amaral, T. *et al.* The mitogen-activated protein kinase pathway in melanoma part I - Activation and primary resistance mechanisms to BRAF inhibition. *Eur J Cancer* **73**, 85-92 (2017). <https://doi.org:10.1016/j.ejca.2016.12.010>
- 429 Brough, R., Frankum, J. R., Costa-Cabral, S., Lord, C. J. & Ashworth, A. Searching for synthetic lethality in cancer. *Curr Opin Genet Dev* **21**, 34-41 (2011). <https://doi.org:10.1016/j.gde.2010.10.009>
- 430 Rezatabar, S. *et al.* RAS/MAPK signaling functions in oxidative stress, DNA damage response and cancer progression. *J Cell Physiol* **234**, 14951-14965 (2019). <https://doi.org:10.1002/jcp.28334>
- 431 Vakana, E. *et al.* LY3009120, a panRAF inhibitor, has significant anti-tumor activity in BRAF and KRAS mutant preclinical models of colorectal cancer. *Oncotarget* **8**, 9251-9266 (2017). <https://doi.org:10.18632/oncotarget.14002>
- 432 Beaumont, K. A. *et al.* Cell Cycle Phase-Specific Drug Resistance as an Escape Mechanism of Melanoma Cells. *J Invest Dermatol* **136**, 1479-1489 (2016). <https://doi.org:10.1016/j.jid.2016.02.805>
- 433 Keung, M. Y. T., Wu, Y. & Vadgama, J. V. PARP Inhibitors as a Therapeutic Agent for Homologous Recombination Deficiency in Breast Cancers. *J Clin Med* **8** (2019). <https://doi.org:10.3390/jcm8040435>
- 434 Yi, T. *et al.* Antitumor efficacy of PARP inhibitors in homologous recombination deficient carcinomas. *Int J Cancer* **145**, 1209-1220 (2019). <https://doi.org:10.1002/ijc.32143>
- 435 Kohn, E. C., Lee, J. M. & Ivy, S. P. The HRD Decision-Which PARP Inhibitor to Use for Whom and When. *Clin Cancer Res* **23**, 7155-7157 (2017). <https://doi.org:10.1158/1078-0432.CCR-17-2186>
- 436 Lotan, T. L. *et al.* Homologous recombination deficiency (HRD) score in germline BRCA2- versus ATM-altered prostate cancer. *Mod Pathol* **34**, 1185-1193 (2021). <https://doi.org:10.1038/s41379-020-00731-4>
- 437 O'Sullivan Coyne, G. *et al.* PARP Inhibitor Applicability: Detailed Assays for Homologous Recombination Repair Pathway Components. *Onco Targets Ther* **15**, 165-180 (2022). <https://doi.org:10.2147/OTT.S278092>
- 438 Thomas, A., Murai, J. & Pommier, Y. The evolving landscape of predictive biomarkers of response to PARP inhibitors. *J Clin Invest* **128**, 1727-1730 (2018). <https://doi.org:10.1172/JCI120388>

- 439 Makvandi, M. *et al.* A PET imaging agent for evaluating PARP-1 expression in ovarian cancer. *J Clin Invest* **128**, 2116-2126 (2018). <https://doi.org:10.1172/JCI97992>
- 440 Makvandi, M. *et al.* A Radiotracer Strategy to Quantify PARP-1 Expression In Vivo Provides a Biomarker That Can Enable Patient Selection for PARP Inhibitor Therapy. *Cancer Res* **76**, 4516-4524 (2016). <https://doi.org:10.1158/0008-5472.CAN-16-0416>
- 441 Sander Effron, S. *et al.* PARP-1 Expression Quantified by [(18)F]FluorThanatrace: A Biomarker of Response to PARP Inhibition Adjuvant to Radiation Therapy. *Cancer Biother Radiopharm* **32**, 9-15 (2017). <https://doi.org:10.1089/cbr.2016.2133>
- 442 Ossovskaya, V., Koo, I. C., Kaldjian, E. P., Alvares, C. & Sherman, B. M. Upregulation of Poly (ADP-Ribose) Polymerase-1 (PARP1) in Triple-Negative Breast Cancer and Other Primary Human Tumor Types. *Genes Cancer* **1**, 812-821 (2010). <https://doi.org:10.1177/1947601910383418>
- 443 Kupczyk, P. *et al.* PARP1 as a Marker of an Aggressive Clinical Phenotype in Cutaneous Melanoma-A Clinical and an In Vitro Study. *Cells* **10** (2021). <https://doi.org:10.3390/cells10020286>
- 444 Chow, J. P. *et al.* PARP1 is overexpressed in nasopharyngeal carcinoma and its inhibition enhances radiotherapy. *Mol Cancer Ther* **12**, 2517-2528 (2013). <https://doi.org:10.1158/1535-7163.MCT-13-0010>
- 445 Gajdzis, M. *et al.* The Prognostic Values of PARP-1 Expression in Uveal Melanoma. *Cells* **10** (2021). <https://doi.org:10.3390/cells10020285>
- 446 Choi, E. B. *et al.* PARP1 enhances lung adenocarcinoma metastasis by novel mechanisms independent of DNA repair. *Oncogene* **35**, 4569-4579 (2016). <https://doi.org:10.1038/onc.2016.3>
- 447 Ali, R. *et al.* Targeting PARP1 in XRCC1-Deficient Sporadic Invasive Breast Cancer or Preinvasive Ductal Carcinoma In Situ Induces Synthetic Lethality and Chemoprevention. *Cancer Res* **78**, 6818-6827 (2018). <https://doi.org:10.1158/0008-5472.CAN-18-0633>
- 448 Mou, K. *et al.* PARP1 Is a Prognostic Marker and Targets NFATc2 to Promote Carcinogenesis in Melanoma. *Genet Test Mol Biomarkers* **26**, 503-511 (2022). <https://doi.org:10.1089/gtmb.2021.0214>
- 449 Zhang, Z. *et al.* Association of expression of p53, livin, ERCC1, BRCA1 and PARP1 in epithelial ovarian cancer tissue with drug resistance and prognosis. *Pathol Res Pract* **216**, 152794 (2020). <https://doi.org:10.1016/j.prp.2019.152794>
- 450 Afzal, H. *et al.* PARP1: A potential biomarker for gastric cancer. *Pathol Res Pract* **215**, 152472 (2019). <https://doi.org:10.1016/j.prp.2019.152472>
- 451 Huang, Y.-H. *et al.* PARP1 as a prognostic biomarker for human cancers: a meta-analysis. *Biomarkers in Medicine* **15**, 1563-1578 (2021).

## 11. Appendix

### 11.1. *Accepted Publication I*

Lisa Marie Fröhlich, Elena Makino, Tobias Sinnberg, and Birgit Schitteck

**Enhanced expression of p21 promotes sensitivity of melanoma cells towards targeted therapies.**

Published in *Experimental Dermatology*, 2022, May 06; 31: 1243- 1252.

doi: 10.1111/exd.14585



Received: 8 November 2021 | Revised: 7 April 2022 | Accepted: 2 May 2022  
DOI: 10.1111/exd.14585

## RESEARCH ARTICLE

Experimental Dermatology WILEY

# Enhanced expression of p21 promotes sensitivity of melanoma cells towards targeted therapies

Lisa Marie Fröhlich | Elena Makino | Tobias Sinnberg | Birgit Schitteck

Division of Dermatoonology, Department of Dermatology, University of Tübingen, Tübingen, Germany

**Correspondence**

Birgit Schitteck, Division of Dermatoonology, Department of Dermatology, Eberhard-Karls-Universität Tübingen, Liebermeisterstr. 25, D - 72076 Tübingen, Germany.  
Email: [birgit.schitteck@uni-tuebingen.de](mailto:birgit.schitteck@uni-tuebingen.de)

**Funding information**

This work was supported by the Deutsche Forschungsgemeinschaft (DFG, German Research Foundation; SCHI 510/11-1) under Germany's Excellence Strategy—EXC 2180-390900677 to B. Schitteck

**Abstract**

Metastatic melanoma patients benefit from the approved targeted BRAF inhibitor (BRAFi) therapy. Despite the great progress in the therapeutic approach to combat metastatic melanoma, fast emerging drug resistance in patients limits its long-term efficacy. In this study, we aimed to unravel the role of the p53 target gene CDKN1A/p21 in the response of melanoma cells towards BRAFi. We show that p53 activation increases BRAFi sensitivity in a synergistic manner exclusively in cells with a high expression of CDKN1A/p21. In a similar way, high expression of p21 was associated with a better response towards the mouse double minute 2 inhibitor (MDM2i) compared to those with low p21 expression. Indeed, p21 knockdown decreased the sensitivity towards both targeted therapies. The results indicate that the sensitivity of melanoma cells towards targeted therapies (BRAFi and MDM2i) is dependent on the p21 protein level in the cells. In addition to that, we found that p53 negatively regulates p73 expression; however, p73 seems not to have an influence on p53 expression. These findings offer new potential strategies for the treatment improvement of melanoma patients with high basal p21 levels with BRAFi by increasing treatment efficacy using combination therapies with p53 activating substances, which are able to further increase p21 expression levels. Furthermore, the data suggest that the expression and induction level of p21 could be used as a predictive biomarker in melanoma patients to forecast the outcome of a treatment with p53 activating substances and BRAFi. All in all, this manuscript shows the distinct role of p53 family members and its impact on melanoma therapy. In future, individualized treatment regimens based on p21 basal and induction levels could help melanoma patients with limited treatment options.

**KEY WORDS**

biomarker, DNA damage, MAPK pathway, melanoma, p21, p53, p73, targeted therapy, therapy resistance

## 1 | INTRODUCTION

Melanoma is one of the most aggressive cancers still with a high mortality rate. Although the development of therapies targeting BRAF V600 mutations improved the prognosis of metastatic melanoma

patients compared to chemotherapy treatment, the majority of patients show a progressing disease even with the combination of BRAFi and MEK inhibitor (MEKi), and therefore, only a small subset of melanoma patients show a complete response after MAPK inhibitor (MAPKi) therapy.<sup>1-3</sup> Despite major research efforts, no explicit

This is an open access article under the terms of the [Creative Commons Attribution-NonCommercial-NoDerivs](https://creativecommons.org/licenses/by-nc-nd/4.0/) License, which permits use and distribution in any medium, provided the original work is properly cited, the use is non-commercial and no modifications or adaptations are made.

© 2022 The Authors. *Experimental Dermatology* published by John Wiley & Sons Ltd.

clinical breakthrough has yet been achieved to overcome the resistance towards targeted therapy.<sup>4,5</sup> In addition to targeted therapy with MAPKi, melanoma patients benefit from immunotherapy, such as the checkpoint inhibitors ipilimumab, nivolumab or pembrolizumab. However, the response rate and tolerability limit the success rate of immunotherapy in the treatment of metastatic melanoma.<sup>3,6</sup> Thus, novel molecular approaches to target therapy resistance in melanoma are urgently needed.

In many cancer types, a key player in the cellular response to DNA damage is the p53 transcription factor<sup>7,8</sup> which has in general a high potential to induce apoptosis.<sup>9</sup> p53 is the most frequently mutated tumour suppressor gene in human cancers leading to a defective DNA damage response. Interestingly, up to 80% of cutaneous human melanomas express wildtype p53, however, often with otherwise impaired function.<sup>10-12</sup> Frequent mechanisms of p53 inactivation in melanoma cells are deletions in the CDKN2A locus or the overexpression of the prominent p53 inhibitors murine double minute 2 and 4 (MDM2 and MDM4).<sup>13,14</sup> DNA-damaging agents, for example chemotherapeutics, disrupt the interaction between p53 and the negative regulator MDM2, leading to a stabilization of p53.<sup>15</sup> Increased abundance of p53 then triggers the transcription of a number of genes with a broad range of functions, including DNA repair, metabolism, cell cycle arrest and apoptosis.<sup>16-18</sup> Once activated, p53 either inhibits cell growth by activating p21 and other cell cycle regulators or induces apoptosis through proapoptotic targets such as Puma, Noxa and Bax and by this maintains genomic integrity.<sup>19</sup> p21 functions in cell cycle control, where an induction especially results in cell cycle arrest; however, repressed p21 can lead to a promotion of cell growth.<sup>20</sup>

Research focus was put on reactivation of wildtype p53 in melanoma as a parallel cancer therapeutic opportunity alongside BRAF V600E inhibition.<sup>21</sup> Nutlin-3 and AMG-232, antagonists of the MDM2-p53 interaction and small molecules that restore DNA binding and transcription activity of p53, are p53 activators.<sup>22</sup> However, despite numerous attempts to target the p53 signalling pathway, there are currently no successful treatments available in the clinic.<sup>23,24</sup> p53 activity is regulated by post-translational modifications and a complex network of interacting proteins, among those p73, which is rarely mutated in cancers. The p53 family member p73 shares high sequence homology with p53 at the amino acid level. p73 shares functional properties with p53, such as DNA damage-induced apoptosis,<sup>25</sup> and stress signals induce p73 by induction of p53.<sup>26</sup> TAp73, the full-length form of p73, was found capable of performing p53-like functions, including transactivation of many p53 target genes, such as p21 in cancer cell lines.<sup>27</sup> However, p73 isoforms can also have distinct roles in either promoting or repressing cancer cell growth. Indeed, we showed recently that melanoma cells, which developed resistance towards MAPKi, show an enhanced susceptibility to platinum-based drugs correlating with TAp73, but not p53 expression status.<sup>28</sup> Our data showed that a subgroup of

melanoma patients with acquired resistance to MAPKi treatment and low TAp73 expression can benefit from chemotherapy with platinum-based drugs as a second line therapy.

In this study, we wanted to unravel the distinct role of p53 and its target gene p21 in the response of melanoma cells towards targeted therapies, using BRAFi and MDM2i. Furthermore, our aim was to decipher the influence of p53 gene expression and activity on p73 and TAp73 expression. Despite the poor long-lasting clinical effectiveness of BRAFi and MAPKi as antimelanoma agents, advances in our understanding of p53 family member activity and their role in the response towards targeted therapy are of utmost importance.

## 2 | MATERIALS AND METHODS

### 2.1 | Cell culture

A375, SK-MEL19 and SK-MEL28 are human metastatic melanoma cell lines and were purchased by ATCC. The remaining cell lines were received from M. Herlyn and C. Krepler (Wistar Institute, Philadelphia, USA). 1205LU wildtype and p53 knockout cells were received from Carola Berking (Erlangen, Germany). The cell lines were cultured in RPMI 1640 medium containing 10% fetal bovine serum (Sigma Aldrich) and 1% penicillin and streptomycin. The BRAFi resistant cells were created as previously described.<sup>28</sup> Cell cultures were regularly tested for mycoplasma using the Venor GeM Classic Mycoplasma Detection Kit (Minerva Biolabs) and used no longer than 2 months upon thawing of the frozen stock.

### 2.2 | Viability analysis

For the analysis of cell viability, 4-Methylumbelliferyl heptanoate (MUH) assay was performed as previously described.<sup>29</sup> The following inhibitors were used as stated in the respective figure legends: vemurafenib (LC Laboratories), Nutlin-3 (SelleckChem/R&D Systems) and AMG-232 (Medchem Express). Nonlinear regression analysis and synergism analysis were performed with the help of Graphpad Prism.

### 2.3 | RNA isolation and RT-qPCR

The RNA isolation and RT-qPCR analysis were performed as previously described.<sup>28</sup> The normalization of target gene expression was performed with the help of the expression of actin. The relative expression was then normalized to the relative expression of the respective control group. RT-qPCR was performed with 96 block Lightcycler (Roche). These primer sequences were selected for RT-qPCR analysis:

Gene Name	Forward sequence	Reverse sequence
BAX	ATGTTTCTGACGGCACTTC	ATCAGTTCCGGCACCTTG
CDKN1A	TCACTGTCTTGACCCTTGTC	GGCGTTGGAGTGGTAGAAA
MDM2	CAGGCAAACCTCATCTTGACC	GCCATGTCTGCATCCTGTTA
TATP73	AGGGGACGCAGCGAAAC	TCCAGAGGTGCTCAAACGTG
TP73	CCTGTCATCCCTCCAACAC	TGCTGGATGCTGAAAAGTG
TP53	AGGCCTTGGAACCAAGGAT	GA CTGACCTTTTGGACTTCA

## 2.4 | Immunoblot analysis

The immunoblot analysis was done as described previously.<sup>29</sup> These primary antibodies were selected: anti- $\beta$ -Actin (CST # 4967), anti-MDM2 (sc-7918), anti-p21 Waf1/Cip1 (CST #2946), anti-p53 (DOI) (sc-126) and anti-p73 (BD #558787).

siRNA	Sense (5'-3')	Antisense (5'-3')
siCTR	ACAACAUUCAUAUAGCUGCCCCC	GGGGCAGCUAUAUGAAUGUUGU
si1TATP73	GCACCACGUUUGAGCACCU-dTdT	AGGUGCUAACGUGGUGC-dTdT
si2TATP73	GGAACCAGACAGCACCTACTT-dTdT	AAGTAGTGCTGCTGGTTCC-dTdT

siRNAs against p53 (sip53), MDM2 (siMDM2) and CDKN1A (siCKDN1A) were designed and purchased by siDESIGN Center of Dharmacon™.

## 2.6 | Adeno-viral infection

The p53 overexpression adenovirus was produced by Dr. Tobias Sinnberg according to the AdEasy XL adenoviral expression system (Stratgene) manufacturer's protocol. 24h after cells were seeded, they were infected with the virus particles that were added to the melanoma cell culture medium. After overnight incubation, the cells were washed 2 times with PBS and seeded for subsequent experiments.

## 2.7 | Plasmid transfection

The melanoma cells were transiently transfected with *CDKN1A* expressing plasmid (Origene RC201765) using Lipofectamine3000 (Thermo Fisher Scientific) according to the manufacturer's protocol as previously described.<sup>28</sup>

## 2.8 | Database and statistical analysis

Multiple t-test according to Holm Sidac method was applied for the statistical analysis with Graphpad Prism. The data were denoted

## 2.5 | Small interfering RNA (siRNA) transfection

Small interfering RNA transfection was performed with Lipofectamine RNAimax (Thermo Fisher Scientific) in accordance with the manufacturer's protocol as previously described.<sup>28</sup> These siRNAs were selected:

significant when  $p < 0.05$  and marked with asterisks (\*). Non-significant data were marked with "ns."

## 3 | RESULTS

### 3.1 | MDM2 inhibition reduces cell viability in a p21 dependent manner

First, we analysed the functional impact of MDM2 inhibition in BRAFi sensitive and resistant melanoma cells. We therefore treated sensitive (S) and BRAFi resistant (R) melanoma cells with inhibitors of the p53/MDM2 protein interaction—Nutlin-3 (Figure 1A) and AMG-232 (Figure 1B). MDM2 inhibition by Nutlin-3 or AMG-232 treatment reduces melanoma cell viability in a concentration-dependent manner irrespective of the TP53 mutational status of the melanoma cells (Table 1). In addition, BRAFi resistant melanoma cells underwent cell death similar to the sensitive parental cells after the treatment with Nutlin-3 or AMG-232 except for SK-MEL28 R cells which are more sensitive towards AMG-232 treatment (Figure 1A,B). Nutlin-3 was able to activate p53 in the melanoma cells as seen by enhanced expression of the p53 target transcripts *CDKN1A* (p21), *BAX* and *MDM2* in A375 and SK-MEL19 (Supplementary Figure 1A,B). In accordance with that, siRNA induced knockdown of MDM2 in A375 cells resulted in activation of p53 signalling on transcript and protein level (Supplementary Figure 1C,D), reduced melanoma cell viability (Supplementary Figure 1E) and increased the apoptosis level as well as the number of cells in the G2/M cell cycle phase (Supplementary Figure 1F).

TABLE 1 p53 mutational status in A375, SK-MEL19, 451Lu, SK-MEL28, Mel1617 and 1205Lu melanoma cell lines. Functional classification of p53 mutations are adapted from <http://mutantp53.broadinstitute.org/heatMap/login> (13.09.21)

	A375	SK-MEL19	451Lu	SK-MEL28	Mel1617	1205Lu
p53 status	Wildtype	N131K partial functional	Y220C non functional	L145R non functional	Wildtype	Wildtype

We noticed that the sensitivity towards the MDM2i Nutlin-3 and AMG-232 differed between the melanoma cell lines and did not correlate with the p53 mutational status. We therefore determined the inhibitory concentrations where 50% of the cells died (IC50) after Nutlin-3 and AMG-232 treatment. As shown in Figure 1A,B, A375 (p53<sup>wt</sup>) and SK-MEL19 (p53<sup>mut</sup>) cells were more sensitive towards MDM2i inhibition as 451Lu (p53<sup>mut</sup>), Mel1617 (p53<sup>wt</sup>) and SK-MEL28 (p53<sup>mut</sup>) cells. We termed them MDM2i sensitive and resistant cells, respectively. Sensitivity towards both MDM2i Nutlin-3 and AMG-232 was similar and did not significantly differ between the BRAFi sensitive and resistant cell line pairs. Since *CDKN1A* is known to be a major target gene of p53, we analysed p21 protein and transcript levels in the MDM2i sensitive and resistant melanoma cell lines. Surprisingly, A375 S and SK-MEL19 S (MDM2i sensitive) had high basal p21 protein levels, whereas the basal p21 protein level of 451Lu S, Mel1617 S and SK-MEL28 S (MDM2i resistant) was undetectable (Figure 1C). This correlated with a lower RNA expression of the p21 corresponding gene *CDKN1A* in MDM2i-resistant cells compared to MDM2i sensitive melanoma cell lines (Figure 1D). The corresponding BRAFi resistant cell lines show the same expression pattern (data not shown). These data strongly suggest that irrespective of the p53 mutational status high p21 levels are essential for a good response of melanoma cells towards MDM2i treatment.

### 3.2 | MDM2 inhibition increases BRAFi sensitivity in a synergistic manner only in MDM2i sensitive cells

Since our aim is to find effective treatments for BRAFi resistant melanoma patients, we focused on the following experiments in which we analysed the combinatorial effect of BRAFi and MDM2i on each two representative BRAFi R melanoma cell lines, which are either MDM2i sensitive (A375, SK-MEL19) or MDM2i resistant (451Lu, Mel1617). Interestingly, compared to the single treatment, combined treatment with the BRAFi vemurafenib and AMG-232 decreased the cell viability of MDM2i sensitive cell lines A375 R and SK-MEL19 R, but not of MDM2i resistant cell lines 451Lu R and Mel1617 R (Figure 2A). Combined treatment with vemurafenib and Nutlin-3 had a synergistic effect on MDM2i sensitive cells; however, the effect of combined vemurafenib and Nutlin-3 treatment only resulted in an additive effect in the MDM2i resistant cells (Figure 2B). Nutlin-3 as single treatment or in combination with vemurafenib induced p53 family signalling, which was detected by the enhanced expression of the p53 targets *CDKN1A* (p21), *BAX* and *MDM2* on transcript level in A375 and SK-MEL19 (Supplementary Figure 1A,B). Vemurafenib treatment alone did not show such a prominent and consistent effect on these targets. We were able to confirm these results with a

siRNA induced knockdown of MDM2 or the overexpression of p53 in A375 S cells (Supplementary Figure 1G-I). A knockdown of MDM2 via siRNA transfection enhanced the sensitivity of A375 S cells towards BRAFi treatment (Supplementary Figure 1G). Surprisingly, overexpression of p53 via transfection did not influence melanoma cell viability of A375 and 451Lu itself (Supplementary Figure 5H), but sensitized treatment naive and BRAFi resistant melanoma cells towards vemurafenib treatment (Supplementary Figure 1I). We then asked if the synergistic combinatorial effect of vemurafenib and MDM2i in MDM2i sensitive cell lines correlates with an induction of p21. Indeed, single Nutlin-3 and the combinatorial treatment of Nutlin-3 and vemurafenib treatment resulted in an induction of p21 in the MDM2i sensitive cell lines A375 and SK-MEL19. However, no p21 induction was observed in MDM2i resistant cell lines (Figure 2C). Furthermore, single Nutlin-3 and combined Nutlin-3 and vemurafenib treatment in A375 and SK-MEL19 cells resulted in a significant induction of *CDKN1A* gene transcripts (Supplementary Figure 1A,B). Together, these data indicate that the basal expression as well as the induction level of p21 correlates with the synergistic effect of BRAFi and MDM2i in melanoma cells.

### 3.3 | P21 mediates increased sensitivity towards targeted therapy with BRAFi and MDM2i

To determine whether the observed increased expression of p21 is responsible for sensitivity towards MDM2i, we first tested several agents known to induce p53 activity. P53 activation by either Nutlin-3 treatment or siRNA transfection against *MDM2* induces *CDKN1A*/p21 RNA (Supplementary Figure 1A,C) and protein (Figures 2C and Supplementary Figure 1D) expression in melanoma cells.

Next, we tested the functional effect of p21 on MDM2i sensitivity. For this, we used a melanoma cell line (1205Lu) in which p53 was knocked out by CRISPR/CAS9 and compared the results to the parental p53 wildtype cell line. Nutlin-3 treatment of 1205Lu p53 wildtype cells resulted in a clear reduction of cell viability, whereas the decrease in viable cells was less strong in 1205Lu p53 knockout cells (Figure 3A). Interestingly, Nutlin-3 treatment of 1205Lu cells showed a significant upregulation of p21 and MDM2 on transcript and protein level only in p53 wildtype cells, but not in 1205Lu cells, where p53 was knocked out (Figure 3B,C). Nutlin-3 treatment resulted in a downregulation of p73 and TAp73 on transcript level only in 1205Lu wildtype cells and a decrease in p73 protein levels in both p53 wildtype and knockout cells (Figure 3B,C). Most importantly, a knockdown of *CDKN1A*, the gene that encodes for p21, by siRNA transfection reduced the sensitivity of both treatment naive as well as BRAFi resistant A375 and BRAFi resistant SK-MEL19 cells

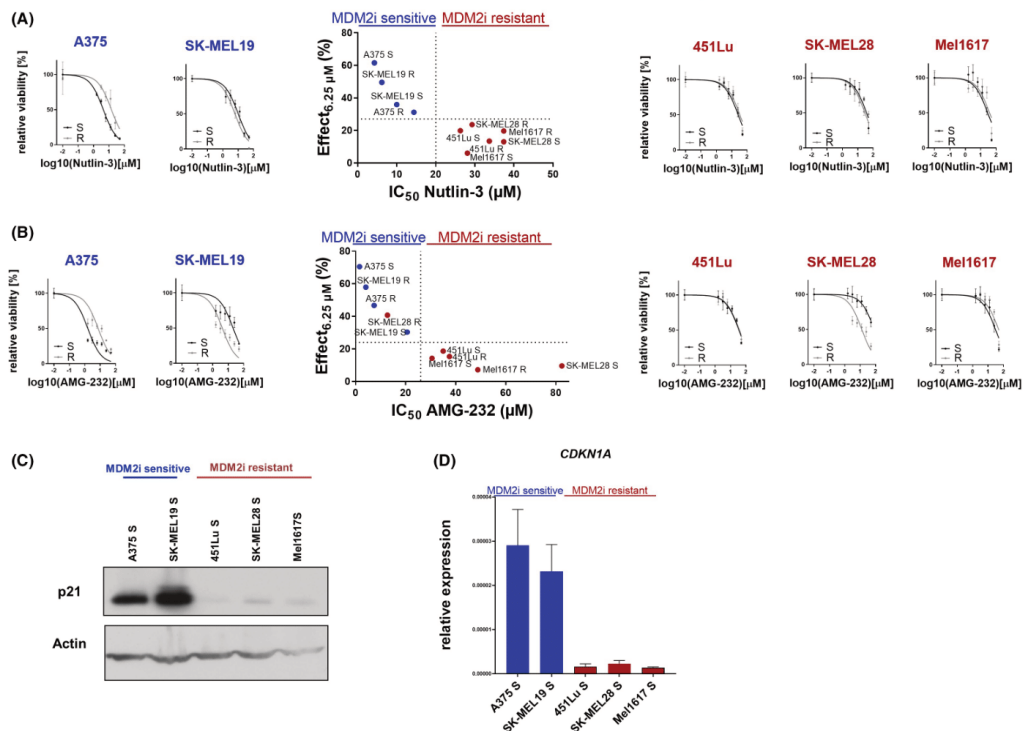


FIGURE 1 MDM2i efficiently reduces melanoma cell growth. (A–B) Vemurafenib sensitive (S) and vemurafenib resistant (R) melanoma cell lines were treated with different concentrations of Nutlin-3 (A) and AMG-232 (B) for 72 h (viability analysis in quintuplicates, mean  $\pm$  SD). IC<sub>50</sub> levels and inhibitory effect at 6.25  $\mu$ M of Nutlin-3 and AMG-232 treatment in the different melanoma cells were calculated using the cell viability data. (C) Immunoblot analysis was performed using melanoma cell lysates. (D) Relative RNA expression of the respective melanoma cell lines was determined using RT-qPCR

towards Nutlin-3 treatment (Figure 3E,I). In accordance with that, overexpression of *CDKN1A* resulted in a significant sensitization of these cells towards Nutlin-3 treatment (Figure 3F,J). Interestingly, downregulation of p21 reduced also the sensitivity towards the BRAFi vemurafenib in treatment naive A375 cells (Figure 3G,I). The effect of siRNA induced knockdown of *CDKN1A* on BRAFi resistant cells was not visible. However, induction of p21 protein level by overexpression of *CDKN1A* sensitized both treatment naive as well as BRAFi resistant A375 and BRAFi resistant SK-MEL19 melanoma cells towards vemurafenib treatment (Figure 3H,J). In summary, our data indicate that sensitivity towards targeted therapy with BRAFi or MDM2i is increased by high expression of *CDKN1A*/p21.

### 3.4 | P53 negatively regulates p73 expression

We noticed that siRNA induced p21 knockdown resulted in a decreased p53 protein expression and an increased p73 expression suggesting a cross-regulation of p53 and p73 expression (Figure 3D). Thus, we analysed the influence of p53 on p73 expression. p53

overexpression decreased the protein level of p73 in BRAFi sensitive and resistant melanoma cells, and vice versa, siRNA induced p53 knockdown increased total p73 protein level independent of p53 mutational status (Figure 4A). However, RNA expression of total *TP73* and *TATP73* did not show a significant alteration after p53 knockdown pointing to a posttranscriptional regulation of p73 expression by p53 (Figure 4B). In contrast, MDM2 inhibition by siRNA transfection reduced not only the abundance of p73 $\alpha$  on protein level, but also the total *TP73* and *TATP73* transcript level in A375 cells (Figure 4C). These data could be confirmed by Nutlin-3 treatment of A375 S and R cells (Supplementary Figure 1J). Interestingly, p73 seems not to have an influence on p53 expression since down- or upregulation of TAp73 expression did not affect p53 protein and transcript level (Figure 4D,E).

## 4 | DISCUSSION

This study made the important observation that melanoma cells differ in their sensitivity towards BRAFi and inhibitors of MDM2 depending on p21 protein levels in the cells. Furthermore, in accordance

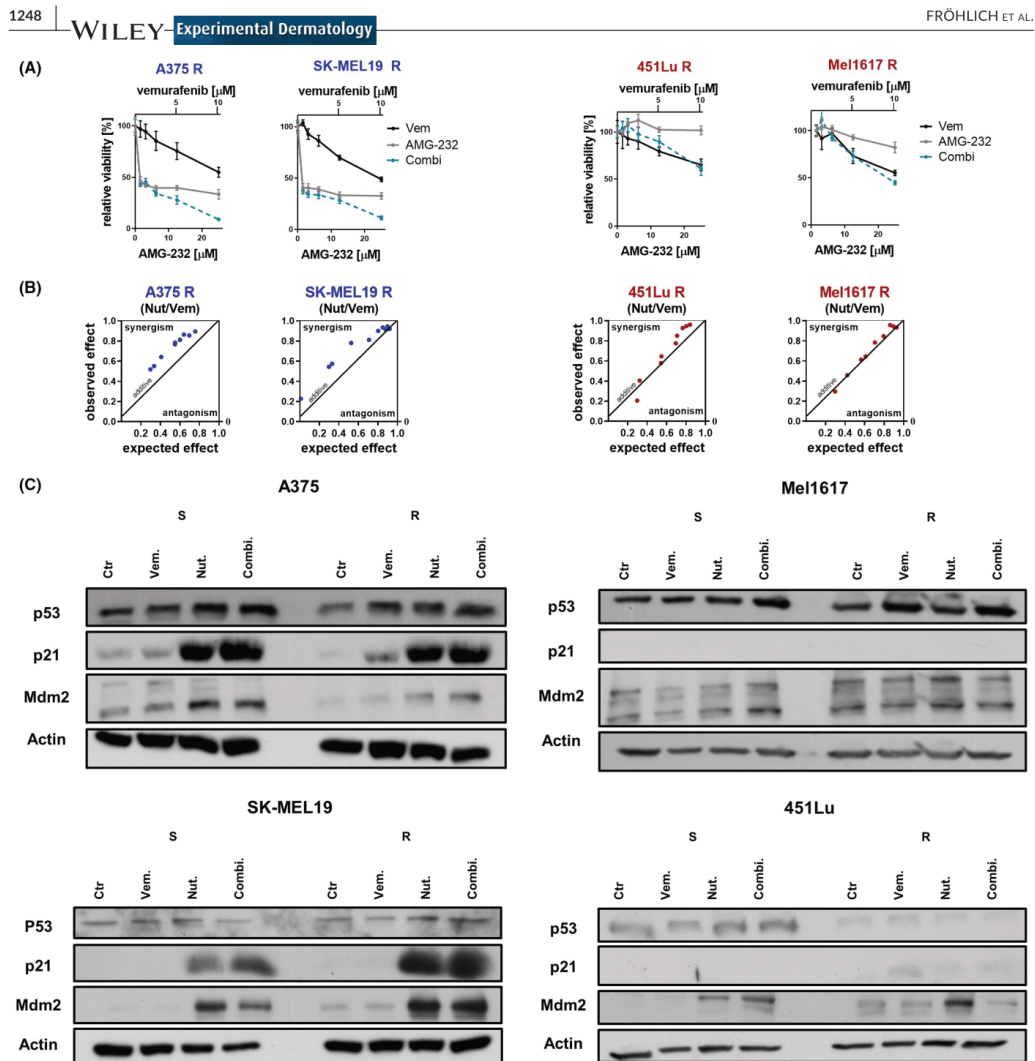
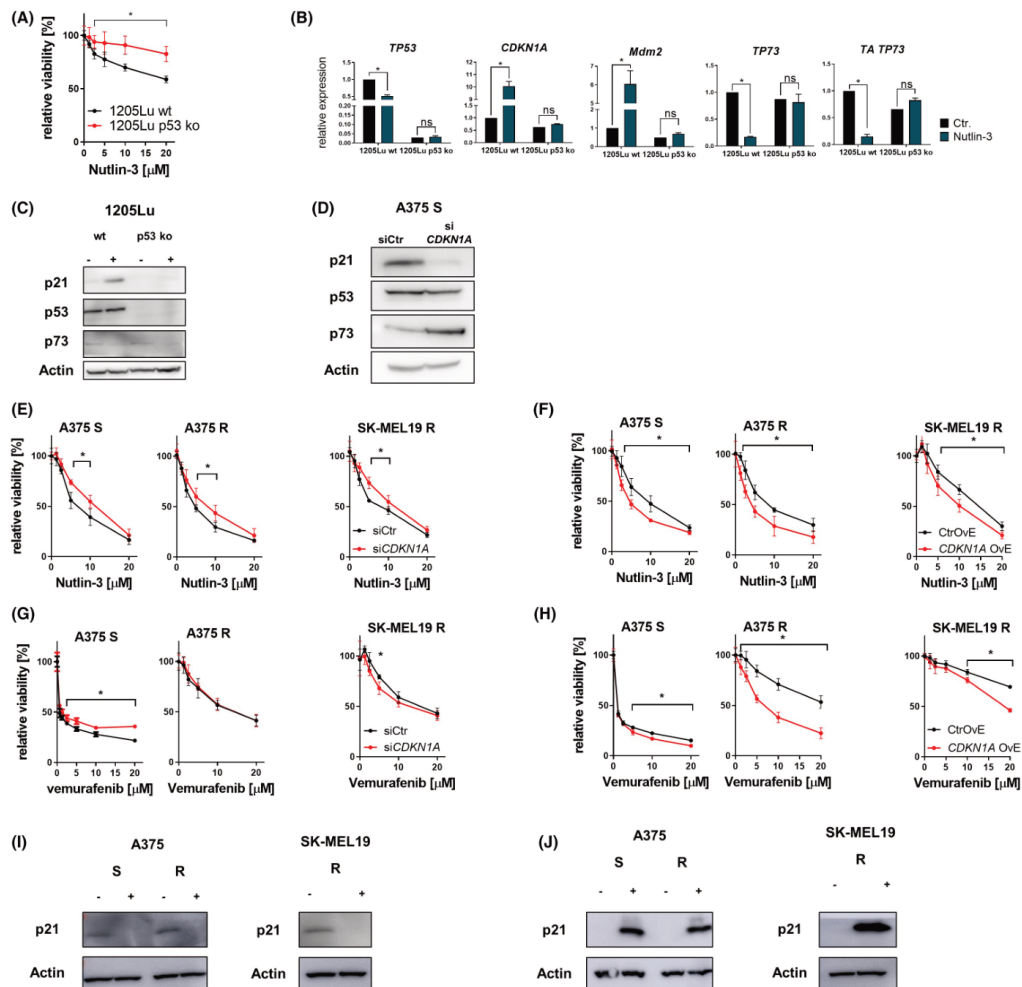


FIGURE 2 Combinational treatment of MDM2i and MAPKi reduces melanoma cell growth in a synergistic manner. (A) Viability assays were performed in the BRAFi resistant melanoma cells (R) which were treated with a combination of AMG-232 and vemurafenib (viability analysis in quintuplicates, mean  $\pm$  SD). (B) Isobologram analysis was performed using the data of cells treated with a combination of Nutlin-3 (Nut) and vemurafenib (Vem). (C) Immunoblot analysis was performed using the lysates of treatment naive and MAPKi resistant melanoma cells which remained untreated (Ctr.), were treated with vemurafenib (Vem), Nutlin-3 (Nut.), or with a combination of both drugs (Combi.)

with previous publications,<sup>30,31</sup> we were able to show that p53 activation in melanoma cells by either MDM2 inhibition with Nutlin-3 or AMG-232 or direct p53 activation using overexpression could sensitize both BRAFi sensitive and interestingly also BRAFi resistant melanoma cells to vemurafenib treatment in a synergistic manner in MDM2i sensitive cells lines. However, the combinational effect could not be observed in MDM2i-resistant cell lines, and we could show that the synergistic activity in MDM2i sensitive cell lines is dependent on p21 induction. In our previous study, we could show that

BRAFi resistant cells are more sensitive towards the chemotherapeutic agent cisplatin, and this is not mediated by p53 activation, but by a lower expression of the TAp73 isoform.<sup>28</sup> Therefore, our previous data and the results in this study indicate that the different p53 family members mediate distinct sensitivities towards targeted therapies or DNA-damaging substances.

Together with findings of other recent papers,<sup>32</sup> we found that in all melanoma cell lines used and irrespective of their p53 mutational or BRAFi sensitive or resistant status, treatment with the MDM2i



**FIGURE 3** p21 plays a crucial role in the response of MDM2i and MAPKi treatment of melanoma cells. (A) Viability analysis was performed after the treatment of 1205Lu wt and 1205Lu p53 ko cells with Nutlin-3 for 72 h (viability analysis in quintuplicates, mean  $\pm$  SD). (B) Relative RNA expression of TP53 and its target genes in 1205Lu wt and 1205Lu p53 ko cells was determined by RT-qPCR. The samples were collected 24 h after the treatment with 5  $\mu$ M Nutlin-3 or remained untreated (Ctr.; analysis in triplicates, mean  $\pm$  SD). (C) Immunoblot analysis was performed using 1205Lu wt and 1205Lu p53 ko melanoma cell lysates which were collected 24 h after the treatment with 5  $\mu$ M Nutlin-3 (+) or remained untreated (-). (D) Immunoblot analysis was performed using A375 S melanoma cell lysates which were collected 48 h after the transfection of siRNA against CDKN1A (siCDKN1A) or control siRNA (siCtr). (E-H) Viability analysis was performed after the treatment of A375 S and R as well as SK-MEL19 S cells with Nutlin-3 (E, F) or vemurafenib (G, H) for 72 h. CDKN1A knockdown (siCDKN1A) and control siRNA transfected cells (siCtr) or CDKN1A overexpression (CDKN1A OVE) and control overexpression (ctrOVE) transfected cells were used. The treatment started 24 h after the transfection process (viability analysis in quintuplicates, mean  $\pm$  SD). (I-J) Immunoblot analysis was performed using the lysates of melanoma cell lines used in (E-H). The samples were collected 24 h after the transfection process of siCtr (-) and siCDKN1A (+) (I) or ctrOVE (-) and CDKN1A OVE (+) (J).

Nutlin-3 and AMG-232 resulted in a decrease in cell viability. In contrast to an ectopically induced expression and accumulation of p53, the reduction of intrinsic p53 level via siRNA or specific knockout

of p53 did not influence the basal p53 signalling activity, as well as melanoma cell viability or vemurafenib sensitivity.<sup>33</sup> Further publications support these findings by showing no effect on p53 target

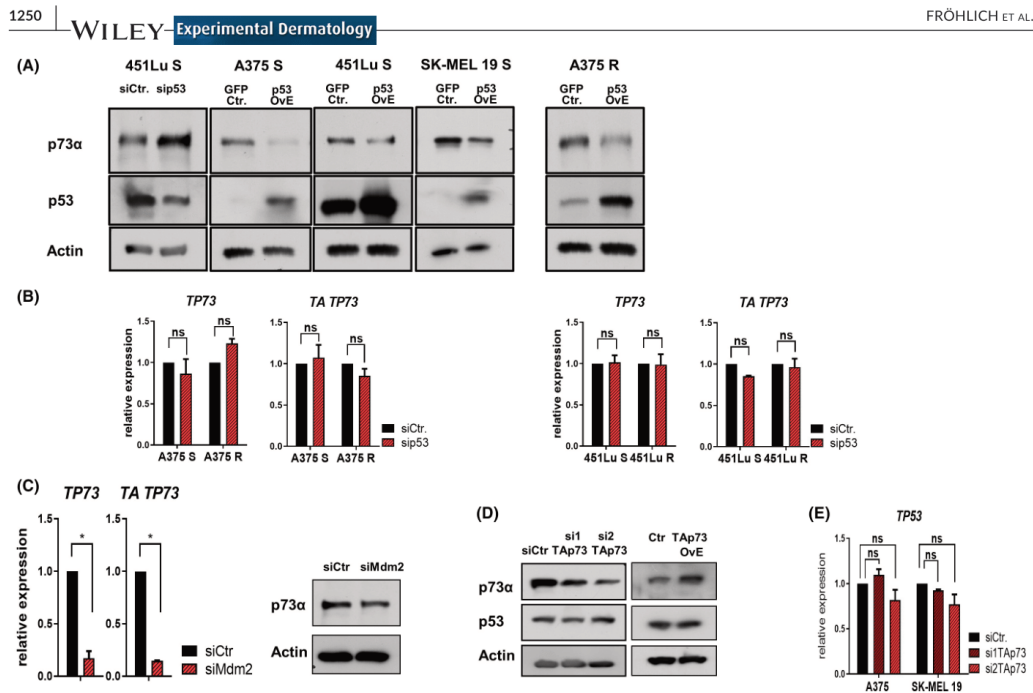


**FIGURE 4** p53 negatively regulates p73 expression. (A) Immunoblot analysis was performed using the melanoma cell lysates which were collected 48 h after the transfection of siRNA against p53 (sip53) or control siRNA (siCtr) as well as after the adenoviral infection of p53 overexpression plasmid (p53Ove) or the correspondent control plasmid (GFP Ctr). (B-C) Relative RNA expression of TP73 and its specific isoform TATP73 was determined by RT-qPCR. The samples were collected 24 h after the transfection of siRNA against TP53 (sip53) (B) or the siRNA against MDM2 (siMdm2) (C) as well as 24 h after the transfection of control siRNA (siCtr) (analysis in triplicates, mean  $\pm$  SD). Immunoblot analysis was performed using the A375 melanoma cell lysates which were collected 48 h after the transfection of siRNA against MDM2 (siMdm2) and control siRNA (Ctr). "ns" is defined non-significant. (D) Immunoblot analysis was performed using lysates of BRAFi resistant (R) SK-MEL19 melanoma cells which were collected 48 h after the transfection of Ha-Tap73 $\alpha$  expressing plasmid (p73Ove) or pcDNA control-plasmid (Ctr) or lysates of treatment naive (S) SK-MEL19 cells which were collected 48 h after the transfection with siRNA against TATP73 (si1Tap73 or si2Tap73) or after the transfection with control siRNA (siCtr) (analysis in triplicates, mean  $\pm$  SD). (E) Relative RNA expression of TP53 after treatment naive A375 and SK-MEL19 cell lines was determined by RT-qPCR. The correspondent samples were collected 24 h after the transfection with siRNAs against Tap73 (si1Tap73 or si2Tap73) or after the transfection with control siRNA (siCtr); analysis in triplicates, mean  $\pm$  SD

gene transcription after knockdown of p53. These findings suggest that the basal p53 signalling activity is markedly suppressed in melanoma cells.

In our study, we showed that p21 plays a crucial role in the sensitivity of melanoma cells not only towards BRAFi, but also towards MDM2i. In accordance with previous publications, we pointed out that MDM2 inhibition results in an induction of p53 and its target genes, such as p21.<sup>34</sup> Furthermore, we found that p21 is essential for the effect of MDM2i in melanoma cells, as a siRNA induced knockdown lead to a reduced sensitivity of treatment naive as well as BRAFi resistant A375 and BRAFi resistant SK-MEL19 melanoma cells towards Nutlin-3 treatment. In accordance with that, induction of p21 by *CDKN1A* overexpression resulted in a clear sensitization of these cells towards Nutlin-3 treatment. This study revealed that high basal p21 levels correlate with a higher sensitivity of melanoma cells towards MDM2i. High p21 levels lead to an accumulation of

A375 S cells in G1 phase, which possibly makes them more sensitive to p53 mediated apoptosis.<sup>35</sup> In addition to that, we found that p53 activation, for example by Nutlin-3 treatment, influences the BRAFi treatment effect. P53 accumulation and activation resulted in an induction of the p53 target gene *CDKN1A* and a decrease in p73 expression, which ultimately lead to a Nutlin-3 induced sensitization of the BRAFi resistant melanoma cells to vemurafenib treatment. With these findings, we are able to confirm previous publications that state that a combination of Nutlin-3 treatment with BRAFi results in a synergistic reduction of melanoma cell viability in vitro.<sup>30-32</sup> Furthermore, we could show for the first time that the combined MDM2i and BRAFi treatment had a synergistic effect on MDM2i sensitive cell lines, whereas the effect of combined MDM2i and BRAFi treatment only resulted in an additive effect in MDM2i resistant cell lines and that MDM2i sensitivity is determined by basal expression and induction level of p21. By this, p21 expression could

be used as a prognostic biomarker for the treatment response of melanoma patients towards BRAFi and MDM2i.

To unravel the complex interplay of p53 with p73 in BRAFi sensitivity we determined the crosstalk of both p53 family members. In our study, we show that modulating p53 level by either overexpression or downregulation negatively influenced protein level of p73, but not p73 transcription pointing to a p53 mediated posttranscriptional regulation of p73 expression. However, Nutlin-3 treatment or MDM2 knock-down could reduce the total TP73 and TATP73 transcript as well as p73 $\alpha$  protein level in TP53 wild type cells. Previous papers could show that p53 directly interacts with the TAp73 promoter and thereby activate TAp73 expression, which in particular occurs upon cellular stress. This ultimately leads to an apoptotic response.<sup>36,37</sup> Interestingly, although the crosstalk between p53 and p73 has been extensively studied,<sup>38,39</sup> no mechanism of direct reduction of p73 protein level by p53 overexpression of MDM2 inhibition has been published before. The observed effect of Nutlin-3 or siRNA mediated MDM2 blockage on TAp73 protein level is possibly mediated by p53 activation. Besides the direct inhibitory interaction of MDM2 and p73 on protein level, MDM2 was also shown to induce TATP73 transcription,<sup>40</sup> which would fit to the findings of this present study. Surprisingly, TAp73 levels do not alter the transcription or protein level of p53 and its downstream signalling in A375 and SK-MEL19 cells, which points to p53 independent, but TAp73 dependent molecular mechanisms.

In summary, the results of this study show that p21 has a distinct role in determining the sensitivity towards BRAFi and MDM2i. The p21 expression and induction level could be used as a biomarker in melanoma patients to dissect them for a combined treatment with p53 activating substances and BRAFi. Also, drugs that activate p21 could serve as a potential amplifier to targeted therapeutics in the treatment strategy. This could sensitize BRAFi-resistant melanoma patients for the p53 activating substances in combination with MAPKi pointing to an individualized treatment regimen based on p21 basal and induction level in future.

#### AUTHOR CONTRIBUTIONS

L.M.F., E.M. and B.S. designed the experiments and wrote the manuscript, with critical input from T.S. Western blot and RT-qPCR analysis, cell viability assays, and transfections and analyses were done by L.M.F. and E.M.

#### ACKNOWLEDGEMENTS

Part of the study has been published as a PhD thesis by the author Elena Makino.<sup>41</sup> Open Access funding enabled and organized by Projekt DEAL.

#### CONFLICT OF INTEREST

The authors declare no competing financial interests.

#### DATA AVAILABILITY STATEMENT

The datasets used and/or analysed during the current study are available from the corresponding author on reasonable request.

#### REFERENCES

- Jenkins RW, Fisher DE. Treatment of advanced melanoma in 2020 and beyond. *J Invest Dermatol*. 2021;141(1):23-31. doi:10.1016/j.jid.2020.03.943
- Rizos H, Menzies AM, Pupo GM, et al. BRAF inhibitor resistance mechanisms in metastatic melanoma: spectrum and clinical impact. *Clin Cancer Res*. 2014;20(7):1965-1977. doi:10.1158/1078-0432.CCR-13-3122
- Schadendorf D, van Akkooi ACJ, Berking C, et al. Melanoma. *Lancet*. 2018;392(10151):971-984. doi:10.1016/S0140-6736(18)31559-9
- Czarnecka AM, Bartnik E, Fiedorowicz M, Rutkowski P. Targeted therapy in melanoma and mechanisms of resistance. *Int J Mol Sci*. 2020;21(13):4576. doi:10.3390/ijms21134576
- Patel M, Eckburg A, Gantiwala S, et al. Resistance to molecularly targeted therapies in melanoma. *Cancers (Basel)*. 2021;13(5):1115. doi:10.3390/cancers13051115
- Steininger J, Gellrich FF, Schulz A, Westphal D, Beisert S, Meier F. Systemic therapy of metastatic melanoma: on the road to cure. *Cancers (Basel)*. 2021;13(6):1430. doi:10.3390/cancers13061430
- Paek AL, Liu JC, Loewer A, Forrester WC, Lahav G. Cell-to-cell variation in p53 dynamics leads to fractional killing. *Cell*. 2016;165(3):631-642. doi:10.1016/j.cell.2016.03.025
- Vazquez A, Bond EE, Levine AJ, Bond GL. The genetics of the p53 pathway, apoptosis and cancer therapy. *Nat Rev Drug Discov*. 2008;7:979-987. doi:10.1038/nrd2656
- Fridman JS, Lowe SW. Control of apoptosis by p53. *Oncogene*. 2003;22(56):9030-9040. doi:10.1038/sj.onc.1207116
- Hayward NK, Wilmott JS, Waddell N, et al. Whole-genome landscapes of major melanoma subtypes. *Nature*. 2017;545(7653):175-180. doi:10.1038/nature22071
- Hodis E, Watson IR, Kryukov GV, et al. A landscape of driver mutations in melanoma. *Cell*. 2012;150(2):251-263. doi:10.1016/j.cell.2012.06.024
- Zhang T, Dutton-Regester K, Brown KM, Hayward NK. The genomic landscape of cutaneous melanoma. *Pigment Cell Melanoma Res*. 2016;29(3):266-283. doi:10.1111/pcmr.12459
- Wang P, Yu J, Zhang L. The nuclear function of p53 is required for PUMA-mediated apoptosis induced by DNA damage. *Proc Natl Acad Sci USA*. 2007;104(10):4054-4059. doi:10.1073/pnas.0700020104
- Yu J, Wang Z, Kinzler KW, Vogelstein B, Zhang L. PUMA mediates the apoptotic response to p53 in colorectal cancer cells. *Proc Natl Acad Sci USA*. 2003;100(4):1931-1936. doi:10.1073/pnas.2627984100
- Haupt Y, Maya R, Kazanietz A, Oren M. Mdm2 promotes the rapid degradation of p53. *Nature*. 1997;387(6630):296-299. doi:10.1038/387296a0
- Wade M, Wang YV, Wahl GM. The p53 orchestra: Mdm2 and Mdmx set the tone. *Trends Cell Biol*. 2010;20(5):299-309. doi:10.1016/j.tcb.2010.01.009
- Gannon HS, Jones SN. Using mouse models to explore MDM-p53 signaling in development, cell growth, and tumorigenesis. *Genes Cancer*. 2012;3(3-4):209-218. doi:10.1177/1947601912455324
- Riley T, Sontag E, Chen P, Levine A. Transcriptional control of human p53-regulated genes. *Nat Rev Mol Cell Biol*. 2008;9(5):402-412. doi:10.1038/nrm2395
- Vogelstein B, Lane D, Levine AJ. Surfing the p53 network. *Nature*. 2000;408(6810):307-310. doi:10.1038/35042675
- Gartel AL, Radhakrishnan SK. Lost in transcription: p21 repression, mechanisms, and consequences. *Cancer Res*. 2005;65(10):3980-3985. doi:10.1158/0008-5472.CAN-04-3995
- Yu J, Zhang L, Hwang PM, Kinzler KW, Vogelstein B. PUMA induces the rapid apoptosis of colorectal cancer cells. *Mol Cell*. 2001;7(3):673-682. doi:10.1016/s1097-2765(01)00213-1
- Hsieh CC, Shen CH. The potential of targeting P53 and HSP90 overcoming acquired MAPKi-resistant melanoma. *Curr Treat Options Oncol*. 2019;20(3):22. doi:10.1007/s11864-019-0622-9

23. Khoo KH, Verma CS, Lane DP. Drugging the p53 pathway: understanding the route to clinical efficacy. *Nat Rev Drug Discov.* 2014;13(3):217-236. doi:10.1038/nrd4236
24. Cheok CF, Verma CS, Baselga J, Lane DP. Translating p53 into the clinic. *Nat Rev Clin Oncol.* 2011;8(1):25-37. doi:10.1038/nrclinonc.2010.174
25. Talos F, Nemajerova A, Flores ER, Petrenko O, Moll UM. p73 suppresses polyploidy and aneuploidy in the absence of functional p53. *Mol Cell.* 2007;27(4):647-659. doi:10.1016/j.molcel.2007.06.036
26. Moll UM, Slade N. p63 and p73: roles in development and tumor formation. *Mol Cancer Res.* 2004;2(7):371-386.
27. Wang C, Teo CR, Sabapathy K. p53-related transcription targets of TAp73 in cancer cells-Bona fide or distorted reality? *Int J Mol Sci.* 2020;21(4):1346. doi:10.3390/ijms21041346
28. Makino E, Gutmann V, Kosnopfel C, et al. Melanoma cells resistant towards MAPK inhibitors exhibit reduced TAp73 expression mediating enhanced sensitivity to platinum-based drugs. *Cell Death Dis.* 2018;9(9):930. doi:10.1038/s41419-018-0952-8
29. Sinnberg T, Makino E, Krueger MA, et al. A nexus consisting of Beta-catenin and Stat3 attenuates BRAF inhibitor efficacy and mediates acquired resistance to vemurafenib. *EBioMedicine.* 2016;8:132-149. doi:10.1016/j.ebiom.2016.04.037
30. Ji Z, Kumar R, Taylor M, et al. Vemurafenib synergizes with nutlin-3 to deplete survivin and suppresses melanoma viability and tumor growth. *Clin Cancer Res.* 2013;19(16):4383-4391. doi:10.1158/1078-0432.CCR-13-0074
31. Ji Z, Njauw CN, Taylor M, Neel V, Flaherty KT, Tsao H. p53 rescue through HDM2 antagonism suppresses melanoma growth and potentiates MEK inhibition. *J Invest Dermatol.* 2012;132(2):356-364. doi:10.1038/jid.2011.313
32. Shattuck-Brandt RL, Chen SC, Murray E, et al. Metastatic melanoma patient-derived xenografts respond to MDM2 inhibition as a single agent or in combination with BRAF/MEK inhibition. *Clin Cancer Res.* 2020;26(14):3803-3818. doi:10.1158/1078-0432.CCR-19-1895
33. Avery-Kiejda KA, Bowden NA, Croft AJ, et al. P53 in human melanoma fails to regulate target genes associated with apoptosis and the cell cycle and may contribute to proliferation. *BMC Cancer.* 2011;11:203. doi:10.1186/1471-2407-11-203
34. Vilgelm AE, Saleh N, Shattuck-Brandt R, et al. MDM2 antagonists overcome intrinsic resistance to CDK4/6 inhibition by inducing p21. *Sci Transl Med.* 2019;11(505):eaav7171. doi:10.1126/scitranslmed.aav7171
35. Shamloo B, Usluer S. p21 in cancer research. *Cancers (Basel).* 2019;11(8):1178. doi:10.3390/cancers11081178
36. Wang J, Liu YX, Hande MP, Wong AC, Jin YJ, Yin Y. TAp73 is a downstream target of p53 in controlling the cellular defense against stress. *J Biol Chem.* 2007;282(40):29152-29162. doi:10.1074/jbc.M703408200
37. Chen X, Zheng Y, Zhu J, Jiang J, Wang J. p73 is transcriptionally regulated by DNA damage, p53, and p73. *Oncogene.* 2001;20(6):769-774. doi:10.1038/sj.onc.1204149
38. Murray-Zmijewski F, Lane DP, Bourdon JC. p53/p63/p73 isoforms: an orchestra of isoforms to harmonise cell differentiation and response to stress. *Cell Death Differ.* 2006;13(6):962-972. doi:10.1038/sj.cdd.4401914
39. Stindt MH, Muller PA, Ludwig RL, Kehroesser S, Dotsch V, Vousden KH. Functional interplay between MDM2, p63/p73 and mutant p53. *Oncogene.* 2015;34(33):4300-4310. doi:10.1038/onc.2014.359
40. Kasim V, Huang C, Zhang J, et al. Synergistic cooperation of MDM2 and E2F1 contributes to TAp73 transcriptional activity. *Biochem Biophys Res Commun.* 2014;449(3):319-326. doi:10.1016/j.bbrc.2014.05.026
41. Makino E. The influence of nuclear nodal points on targeted and cytostatic treatment response of metastatic melanoma. Dissertation; 228.

#### SUPPORTING INFORMATION

Additional supporting information may be found in the online version of the article at the publisher's website.

**How to cite this article:** Fröhlich LM, Makino E, Sinnberg T, Schitteck B. Enhanced expression of p21 promotes sensitivity of melanoma cells towards targeted therapies. *Exp Dermatol.* 2022;31:1243-1252. doi: [10.1111/exd.14585](https://doi.org/10.1111/exd.14585)

**1 Supplementary figure 1**

2 **a-b** Relative gene expression of TP53 and its target genes CDKN1A, MDM2 and BAX in A375 S/R (**a**)  
3 and SK-MEL19 S/R (**b**) were analysed. The RT-qPCR samples were collected after the treatment with  
4 5  $\mu$ M vemurafenib, (Vem.), 5  $\mu$ M Nutlin-3 (Nutlin-3) or after the combined treatment (Combi.). The  
5 correspondent untreated cell samples were used as control (Ctr.) (analysis in triplicates, mean  $\pm$  SD). **c**  
6 Relative gene expressions of MDM2, TP53 and its target gene CDKN1A were analysed in A375 S cells.  
7 The samples were collected 24h after the transfection of siRNA against MDM2 (siMDM2) or control  
8 siRNA (siCtr) (analysis in triplicates, mean  $\pm$  SD). **d** Immunoblot analysis was performed using lysates  
9 of treatment naïve A375 cells which were collected 48 h after the transfection of siRNA against MDM2  
10 (siMDM2) or of non-silencing control siRNA (siCtr.). **e** Relative viability was calculated in A375 S  
11 cells which were collected 96 h after the transfection of siRNA against MDM2 (siMDM2) and control  
12 siRNA (siCtr). **f** Relative distribution of sub-G1 phase and G2/M phase cells was detected by cell cycle  
13 analysis. The assay was performed 96 h after the transfection of siRNA against MDM2 (siMDM2) or  
14 non-silencing control siRNA (Ctr.). **g** Viability analysis was performed after the treatment A375 S cells.  
15 MDM2 knock-down (siMDM2) and control siRNA transfected cells (siCtr) were used. The vemurafenib  
16 treatment started 24 h after the transfection process for 72 h (viability analysis in quintuplicates, mean  
17  $\pm$  SD). **h** Relative viability of the cells was calculated (viability analysis in quintuplicates, mean  $\pm$  SD).  
18 **i** Viability analysis was performed after the treatment of the correspondent infected cells with up to 20  
19  $\mu$ M vemurafenib for 72 h. The treatment was started 24 h after the infection (viability analysis in  
20 quintuplicates, mean  $\pm$  SD). **j** Relative gene expressions of TP73 and TATP73 were analysed in A375  
21 S and R cells. The samples were collected 24h after the treatment with 5  $\mu$ M Nutlin-3 or remained  
22 untreated (Ctrl.) (analysis in triplicates, mean  $\pm$  SD).

23

24

25

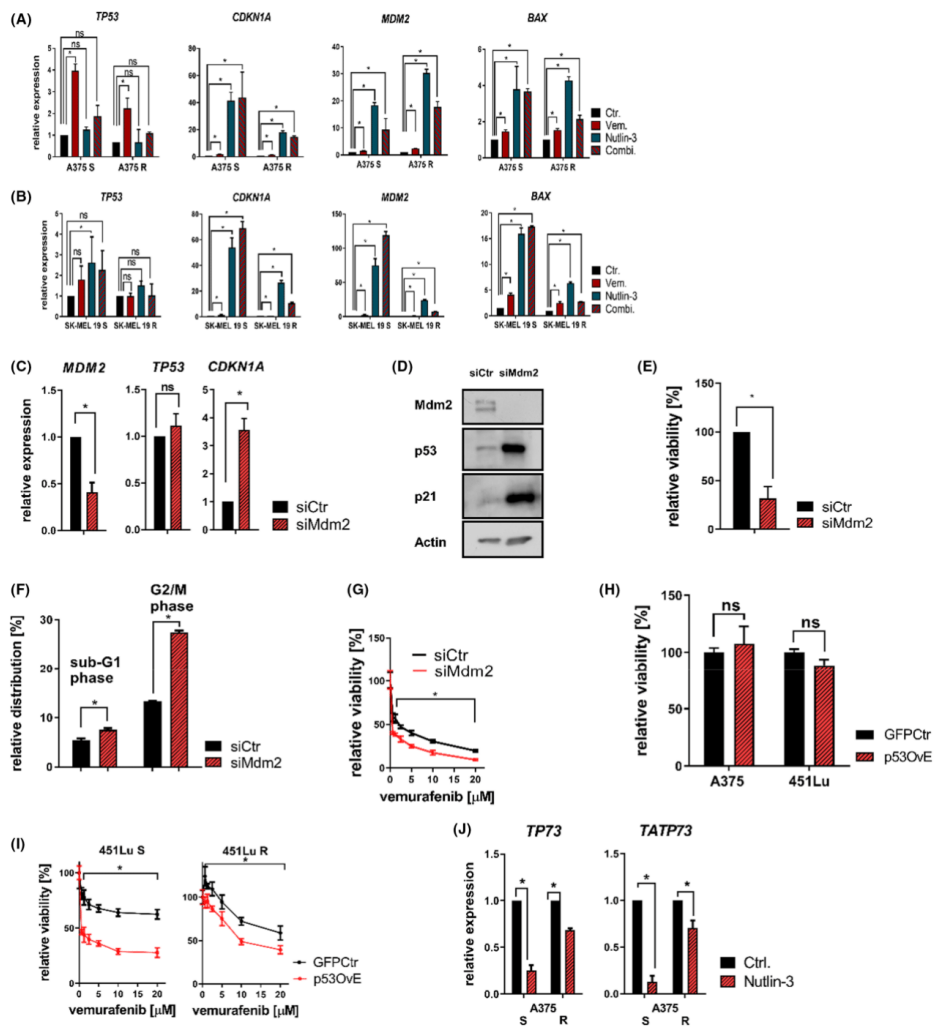


**Table 1**

p53 mutational status in A375, SK-MEL19, 451Lu, SK-MEL28, Mel1617 and 1205Lu melanoma cell lines. Functional classification of p53 mutations are adapted from <http://mutantp53.broadinstitute.org/heatMap/login> (13.09.21)

	A375	SK-MEL19	451Lu	SK-MEL28	Mel1617	1205LU
p53 status	wildtype	N131K partial functional	Y220C non functional	L145R non functional	wildtype	wildtype

## **11.2. Accepted Publication II**

Lisa Marie Fröhlich, Heike Niessner, Birgit Sauer, Sofie Kämereit, Eftychia Chatziioannou, Simon Riel, Tobias Sinnberg , and Birgit Schitteck

**PARP inhibitors effectively reduce MAPK inhibitor resistant melanoma cell growth and synergize with MAPK inhibitors through a synthetic lethal interaction *in vitro* and *in vivo*.**

Published in Cancer Research Communications, 2023, September 05; 3 (9): 1743–1755.

Doi: <https://doi.org/10.1158/2767-9764.CRC-23-0101>

RESEARCH ARTICLE <https://doi.org/10.1158/2767-9764.CRC-23-0101>

OPEN ACCESS

# PARP Inhibitors Effectively Reduce MAPK Inhibitor Resistant Melanoma Cell Growth and Synergize with MAPK Inhibitors through a Synthetic Lethal Interaction *In Vitro* and *In Vivo*

Lisa Marie Fröhlich<sup>1</sup>, Heike Niessner<sup>1</sup>, Birgit Sauer<sup>1</sup>, Sofie Kämereit<sup>1</sup>, Eftychia Chatziioannou<sup>1</sup>, Simon Riel<sup>2</sup>, Tobias Sinnberg<sup>1,3</sup>, and Birgit Schitteck<sup>1,4</sup>

## ABSTRACT

The efficacy of targeting the MAPK signaling pathway in patients with melanoma is limited by the rapid development of resistance mechanisms that result in disease relapse. In this article, we focus on targeting the DNA repair pathway as an antimelanoma therapy, especially in MAPK inhibitor resistant melanoma cells using PARP inhibitors. We found that MAPK inhibitor resistant melanoma cells are particularly sensitive to PARP inhibitor treatment due to a lower basal expression of the DNA damage sensor ataxia-telangiectasia mutated (ATM). As a consequence, MAPK inhibitor resistant melanoma cells have decreased homologous recombination repair activity leading to a reduced repair of double-strand breaks caused by the PARP inhibitors. We validated the clinical relevance of our findings by ATM expression analysis in biopsies from patients with melanoma before and after development of resistance to MAPK inhibitors. Furthermore, we show that inhibition of the MAPK pathway induces a homologous recombination

repair deficient phenotype in melanoma cells irrespective of their MAPK inhibitor sensitivity status. MAPK inhibition results in a synthetic lethal interaction of a combinatorial treatment with PARP inhibitors, which significantly reduces melanoma cell growth *in vitro* and *in vivo*. In conclusion, this study shows that PARP inhibitor treatment is a valuable therapy option for patients with melanoma, either as a single treatment or as a combination with MAPK inhibitors depending on ATM expression.

**Significance:** We show that MAPK inhibitor resistant melanoma cells exhibit low ATM expression increasing their sensitivity toward PARP inhibitors and that a combination of MAPK/PARP inhibitors act synthetically lethal in melanoma cells. Our study shows that PARP inhibitor treatment is a valuable therapy option for patients with melanoma, either as a single treatment or as a combination with MAPK inhibitors depending on ATM expression, which could serve as a novel biomarker for treatment response.

## Introduction

Melanoma cells typically have a high mutational load due to accumulation of unrepaired UV radiation-associated DNA damage (1). Therefore, efficient repair of DNA damage is of fundamental importance for genomic integrity and play a critical role in cancer development and progression. Interestingly, cancer

cells are more susceptible to inhibition of DNA damage repair (DDR) compared with noncancerous cells making this pathway an attractive target in cancer therapy especially for patients who suffer from acquired resistance toward targeted drugs (2). Up to 50% of patients with melanoma have a genetic mutation in the *BRAF* gene leading to a hyperactivation of the MAPK signaling pathway and thus benefit from therapy with MAPK inhibitors (MAPKi; ref. 3). However, long-term treatment results in acquired resistance to MAPKi, which limits the benefit of the therapy (4). Interestingly, it still remains unknown whether melanoma cells resistant to MAPKi therapy can be targeted by modulating the DDR.

PARPs are essential in the immediate response to DNA damage. PARP is involved in early steps of the base excision repair, and its inhibition via PARP inhibitors (PARPi) results in the inability to repair the damaged base. In addition, PARPi prevent the dissociation of PARP from damaged DNA leading to PARP trapping and thereby double-strand break (DSB) formation, which is mainly responsible for the cytotoxic effect of PARPi (5). A synthetic lethal interaction of PARPi in tumors with a genetic mutation in homologous recombination repair (HRR) genes makes these patients particularly sensitive to PARPi (6, 7). On the basis of this knowledge, several clinical trials are on the way

<sup>1</sup>Division of Dermatocology, Department of Dermatology, University of Tübingen, Tübingen, Germany. <sup>2</sup>Department of Dermatology, University of Tübingen, Tübingen, Germany. <sup>3</sup>Department of Dermatology, Venereology and Allergology, Charité Universitätsmedizin Berlin, Berlin, Germany. <sup>4</sup>Cluster of Excellence iFIT (EXC 2180) "Image-Guided and Functionally Instructed Tumor Therapies," University of Tübingen, Tübingen, Germany.

**Corresponding Author:** Birgit Schitteck, University of Tübingen, Liebermeisterstr. 25, Tübingen 72076, Germany. Phone: 4970-7129-80832; E-mail: [birgit.schitteck@uni-tuebingen.de](mailto:birgit.schitteck@uni-tuebingen.de)

doi: 10.1158/2767-9764.CRC-23-0101

This open access article is distributed under the Creative Commons Attribution 4.0 International (CC BY 4.0) license.

© 2023 The Authors; Published by the American Association for Cancer Research

Fröhlich et al.

using PARPi in patients with cancer with a HRR deficiency (HRD) including patients with melanoma (8–10).

Interestingly, inhibition of the MAPK pathway in treatment-naïve melanoma cells was recently shown by us and others to suppress the expression of HRR pathway genes leading to a HRD phenotype (11, 12). This suggests that combined treatment of melanoma cells with PARPi and MAPKi is effective in killing these cells and first preliminary investigations showed a synergistic reduction of cancer cell viability of PARPi in combination with MAPKi (12, 13). However, the molecular mechanisms of synergistic killing of PARPi and MAPKi in treatment-naïve melanoma cells and the effectiveness of PARPi as a monotherapy or in combination with MAPKi in melanoma cells with acquired resistance toward MAPKi is still unknown.

The aim of this study was to decipher whether PARPi therapy can be an appropriate treatment strategy for patients with melanoma and to identify the molecular mechanisms of PARPi sensitivity. In addition, we wanted to unravel whether there are differences in PARPi sensitivity in melanoma cells with an acquired resistance toward MAPKi in comparison with treatment-naïve cells. Finally, we aimed to analyze a potential synergistic effect of PARPi with MAPKi in melanoma cells which are either sensitive or resistant toward MAPKi treatment. Our aim was to unravel which patients with melanoma specifically can benefit from PARPi treatment alone or in combination with MAPKi and to identify biomarkers for treatment response.

## Materials and Methods

### Cell Culture

The human metastatic melanoma cell lines A375, SKMel28, and HT-144 were purchased from ATCC. The human patient-derived xenograft (PDX) cells were received from T. Sinnberg and H. Niessner. The remaining cells were received from M. Herlyn (Wistar Institute, Philadelphia, PA). The BRAF inhibitor (BRAFi) and MEK inhibitor (MEKi) resistant cells were created as described previously (14). BRAFi resistant (R) cell lines were cultured with 2  $\mu\text{mol/L}$  vemurafenib, BRAFi plus MEKi resistant (RR) cell lines were cultured with 2  $\mu\text{mol/L}$  vemurafenib and 5  $\text{nmol/L}$  trametinib. All cell lines were cultured in RPMI640 medium containing 10% FBS (Sigma-Aldrich F9665) and 1% penicillin and streptomycin (Gibco 11548876) at 37°C and 5%  $\text{CO}_2$ . The cell lines were regularly tested for *Mycoplasma* using the Venor GeM Classic *Mycoplasma* Detection Kit (Minerva Biolabs 11-1025; last test: November 2022) and used no longer than 2 months upon thawing of the frozen stock. Cell lines were authenticated by short tandem repeat profile analysis (Microsynth; last authentication: November 2022). Primary human fibroblasts were isolated from human foreskin after routinely circumcision from the Loretto Clinic Tübingen upon informed consent of the patients as described previously (15).

### Viability Analysis and Inhibitors

Cell viability was analyzed with the 4-Methylumbelliferyl heptanoate (MUH) assay as described previously (16). A total of  $1 \times 10^3$  melanoma cells or  $5 \times 10^3$  fibroblasts were seeded the day before treatment started. Cells were treated with the following inhibitors: vemurafenib (BRAF inhibitor, Medchemexpress HY-12057), trametinib (MEK inhibitor, Biomol 16292-250), LY3009120 (panRAF inhibitor, Medchemexpress HY-12558), olaparib (PARP inhibitor, Medchemexpress HY-10162), or talazoparib (PARP inhibitor, Medchemexpress HY-16106). Experiments were performed in quintuplicates.

### Cell-cycle Analysis

A total of  $2 \times 10^5$  melanoma cells per cavity of a 6-well plate were seeded 24 hours before treatment start with 2  $\mu\text{mol/L}$  talazoparib for the indicated timepoints. Cells were permeabilized in 80% cold ethanol for 1 hour and resuspended in PBS containing 100  $\mu\text{g/mL}$  RNaseA (Applchem) and 50  $\mu\text{g/mL}$  Propidium Iodide (Sigma-Aldrich P4864) for 30 minutes. LSRII FACS (BCD Biosciences) was used for the cell-cycle experiment. For cell-cycle sorting, cells were treated with 5  $\mu\text{mol/L}$  vemurafenib or remained untreated. A total of 24 hours after the treatment start, cells were harvested and stained with Hoechst (1:20,000, Thermo Fisher Scientific H3570) for 10 minutes and then sorted according to their cell-cycle phase in  $G_1$ -phase, S-phase, and  $G_2$ -M-phase. For the sorting of the cells, FACS Aria (BD Biosciences) was used. FACSDiva software (BD Biosciences) was used for the analysis of the distribution of the cells in the different cell-cycle phases. FloJo\_10 was used to visualize the data.

### Apoptosis Assay

Apoptosis assay was performed with the Incucyte Caspase-3/7 Dye for apoptosis (Sartorius 4440) according to the manufacturer's protocol. Briefly,  $5 \times 10^3$  cells were seeded into 96-well plate cavities. A total of 24 hours after seeding, cells were treated with 5  $\mu\text{mol/L}$  talazoparib, or remained untreated. Simultaneously, the Caspase-3/7 dye diluted 1:1,000 in cell culture medium was added to the cells. Using the Incucyte SX1, phase contrast and green channels were selected and nine images per well were taken to cover the entire well with an average scan interval of 2 hours for a total of 48 hours. Green fluorescence positive cells were quantified.

### Spheroid Assay

Spheroid assay was performed as described previously (11). For this, 250 cells in 25  $\mu\text{L}$  medium were grown in hanging drops for 10 days. The formed spheroids were then reseeded on a 12-well plate in medium containing 1.2  $\text{mg/mL}$  collagen I (Matrix Biosciences, 50105). Spheroids were treated on day 0 with 5  $\mu\text{mol/L}$  talazoparib, 2.5  $\mu\text{mol/L}$  vemurafenib, a combination of both drugs, or remained untreated. Between 5 and 15 spheroids per treatment group were included in the analysis. Spheroid sizes were quantified using ImageJ.

### Colony Formation Assay

Colony formation assay was performed as described previously (16). A total of 750 cells were seeded and 24 hours later treated with 2  $\mu\text{mol/L}$  talazoparib, 2  $\mu\text{mol/L}$  vemurafenib, a combination of both drugs, or remained untreated. Seven days after treatment start, cells were fixed in 4% formalin, stained with 3% crystal violet solution (Sigma-Aldrich, HT90132) in 80% methanol for 2 hours, and colonies were counted.

### RNA Isolation and qRT-PCR

RNA isolation was performed with the help of the Nucleospin RNA Kit (Macherey-Nagel 740955) according to the manufacturer's protocol. RNA isolation of mouse tumor material was performed with NucleoSpin totalRNA formalin-fixed paraffin-embedded (FFPE; Macherey-Nagel 740969) according to the manufacturer's protocol. The cDNA was produced and qRT-PCR was performed as described previously (14). qRT-PCR was performed with the Lightcycler 96 Instrument (Roche). The primer sequences are depicted in Table 1.

Actin served as a housekeeping gene. PCR profiler array was performed as described previously (11). RT<sup>2</sup> Profiler PCR Array Human DNA Repair and

Downloaded from <http://ascrjournals.org/cancercommunication/article-pdf/3/9/1743/3382329/crc-23-0101.pdf> by University of Tuebingen user on 07 September 2023

## PARP Inhibitors as an Effective Treatment for Melanoma

TABLE 1 Primers used in this project

Gene name	Forward sequence	Reverse sequence
<i>CDKN1A</i>	TCACTGTCTTGTACCCCTGTGTC	GGCGTTTGGAGTGGTAGAAA
<i>ATM</i>	TGTTCCAGGACACGAAGGGAGA	CAGGGTCTCAGCACTATGGGA
<i>BRCA1</i>	TTGTTGATGTGGAGGAGCAA	GATCCAGGTAAGGGTTCC
<i>BRCA2</i>	GAAAATCAAGAAAATCCTTAAAGGCT	GTAATCGGCTCTAAAGAAACATGATG
<i>RAD51</i>	GGTGAAGGAAAGCCATGTA	GGGTCTGGTGTCTGTGT
<i>EXO1</i>	TCGGATCTCTAGCTTTGGCTG	AGCTGTCTGCACATTCTAGCC
<i>Actin</i>	CACCATTGGCAATGAGCGGTTT	AGGCTTTGCGGATGCCACGT

p53 Signaling Pathway (Qiagen PAHS-042) were used. Cells were treated with 5  $\mu\text{mol/L}$  talazoparib for 24 hours or remained untreated. Experiments were performed in triplicates.

### Comet Assay

The Comet Assay Kit (Abcam, ab238545) was used for analysis of DNA damage and performed according to the manufacturer's protocol. A total of 1,500 cells were seeded on each cavity of the 3-well object slide. The cells were treated with 15  $\mu\text{mol/L}$  talazoparib, 5  $\mu\text{mol/L}$  vemurafenib, a combination of both drugs, or remained untreated. TBE electrophoresis was performed at 2 V/cm for 20 minutes. For the analysis of the comets, the software OpenComet was used (17, 18). The tail moment was calculated by using the formula: tail moment = tail length  $\times$  tail DNA %, where the tail length is defined as the length of the tail in pixels and the tail DNA % is defined as the tail DNA content as a percentage of comet DNA content.

### Migration and Invasion Assay

Boyden chamber-based migration and matrigel invasion assay was performed as described previously (19). A total of  $8 \times 10^5$  cells were seeded onto the transwell insert and 10 minutes after the seeding process, cells were treated with talazoparib, or remained untreated. Experiments were performed in triplicates.

### IHC and Immunofluorescence Staining

FFPE tissue sections of metastatic melanoma samples were deparaffinized and prepared as described previously (11). For IHC staining, ataxia-telangiectasia mutated (ATM) antibody (ab32420, 1:50) was used with Fast Red Substrate (Thermo Fisher Scientific Lab Vision Liquid Fast-Red Substrate System), and a counterstain with hematoxylin and eosin was performed. For the analysis of patient material, written informed consent from the patients was obtained. The studies were conducted in accordance with the Declaration of Helsinki and approved by the Ethics Commission Tübingen, Germany (approval number 866/2021B02). For immunofluorescence staining of ATM,  $5 \times 10^4$  cells were seeded into each well of an 8-well chamber slide (Falcon 354118). On the next day, cells were fixed with 4% formalin for 10 minutes. The following primary antibodies were used for immunofluorescence staining: anti-ATM (ab32420, 1:250), anti-pH2AX (Ser139; Merck, JBW301, 1:500), anti-p21 Waf1/Cip1 (DCS60; CST2946, 1:50). After overnight incubation of the first antibody at 4°C, the secondary antibodies were added for 1 hour at room temperature. For ATM staining, the secondary antibody Cy3 Donkey Anti-Rabbit IgG (711-166-152, Jackson ImmunoResearch, 1:250), and for pH2AX and p21 the Alexa Fluor 488 Donkey Anti-Mouse IgG (715-546-151, Jackson ImmunoResearch, 1:250) was used. DAPI staining (Invitrogen, NucBlue fixed cell stain Ready-Probes reagent) or Hoechst33342 (Invitrogen) were used to stain the

nuclei. Quantification of the IHC was performed by counting the cells with the help of ImageJ. Quantification of the immunofluorescence was performed with the Zen blue Version 2.6 software. For this, a total of 10 images with on average 25 cells per image for each group were analyzed. The red fluorescence intensity per cell was analyzed.

### Immunoblot Assay

Immunoblot analysis was performed as described previously (16). For studying the PARP trapping effect of the PARPi, isolation of the nuclear soluble and chromatin bound fraction was performed using the Subcellular Protein Fractionation Kit for Cultured Cells (Thermo Fisher Scientific 78840) according to the manufacturer's protocol. Cells were therefore treated with 0.005% Methyl methane sulfonate (MMS, Thermo Fisher Scientific, 156890050) and 2  $\mu\text{mol/L}$  talazoparib. The following primary antibodies were used for immunoblot analysis: anti-p21 Waf1/Cip1 (DCS60; Cell Signaling Technology 2946, 1:1,000), anti-pH2AX (Ser139; Merck, JBW301, 1:500), anti- $\beta$ -Actin (Cell Signaling Technology 4967, 1:2,000), anti-p53 (DOI; sc-126, 1:500), anti-ATM (D2E2; Cell Signaling Technology 2873, 1:1,000), anti-PARP (Cell Signaling Technology 9542, 1:1,000), and anti-H2A.X (Cell Signaling Technology 2595, 1:1,000). The following secondary antibodies were used: anti-mouse IgG, horseradish peroxidase (HRP)-linked (Cell Signaling Technology 7076) and anti-rabbit IgG, HRP-linked (Cell Signaling Technology 7074).

### Xenograft Mouse Experiment

The animal experiments were approved and performed in compliance with the requirements of the German Animal Welfare Act and approved by local authorities (Regierungspräsidium Tübingen, HT1-18). The mice were randomized into the different treatment groups based on gender and age. A total of  $1 \times 10^6$  melanoma cells (A375 S, A375 R) in 50  $\mu\text{L}$  sterile PBS (Sigma-Aldrich D8537) and 50  $\mu\text{L}$  Matrigel (Corning 354234) were subcutaneously injected into the right flank of NSG mice. The inhibitors talazoparib and vemurafenib were dissolved in 10% DMSO (PanReac AppliChem A3672), 40% PEG300 (Medchemexpress HY-Y0873), 5% Tween80 (Sigma-Aldrich P1754), and 45% PBS. After a palpable tumor size of 25  $\text{mm}^3$ , the treatment with 2 mg/kg/day talazoparib (A375 R), or 1 mg/kg/day talazoparib (A375 S), 25 mg/kg/day vemurafenib (A375 S), or a combination of 1 mg/kg/day talazoparib and 25 mg/kg/day vemurafenib (A375 S) via oral gavage started. The control mice received the solvent without inhibitors. The mice were treated daily for 14 days. The tumor was measured every second day. After 14 days, if the tumor exceeded a size of 1,000  $\text{mm}^3$ , or the tumor ulcerated, the mice were euthanized, and the tumor was removed for further analysis. The tumor volume was calculated with the formula:  $V_{\text{tumor}} = 0.5 \times \text{width}^2 \times \text{length}$ .

Fröhlich et al.

### Statistical Analysis

All experiments were statistically analyzed using GraphPad Prism version 9.1.2. Data that are statistically significant ( $P < 0.05$ ) were labeled with asterisks (\*,  $P < 0.05$ ; \*\*,  $P < 0.01$ ; \*\*\*,  $P < 0.001$ ; and \*\*\*\*,  $P < 0.0001$ ). Unless otherwise stated, statistical analysis was performed by unpaired *t* test when two groups were compared with each other, and one-way ANOVA was performed when multiple groups were compared with each other. For the normalized intensity of ATM levels of patients with melanoma before and after MAPK inhibitor resistance, the GSE data provided by Gene Expression Omnibus (GEO; GSE50509 and GSE61992) were used (20–23). Paired Wilcoxon test was performed for the statistical analysis of the GEO data. For the analysis of the MUH cell viability assay, nonlinear regression analysis was performed. When comparing two MUH curves with each other, comparison of fits of the nonlinear regression was performed. Synergism analysis was performed by calculating the combined index (CI) values of each treatment ratio and drug concentration using the software compusyn (<https://www.combosyn.com/>); with  $CI < 1$  synergistic,  $CI \geq 1$  additive). In detail, the observed effect of each single treatment and the combined treatment were used. The compusyn software then calculated the CI value using the measured treatment effect of the single treatments versus the combined treatment. The compusyn software calculated the CI value for each treatment ratio used. The calculated CI values were then added in a graphic in respect of the treatment ratio. Protein expression of immunoblot experiments was analyzed with ImageJ 1.53a.

### Data Availability

The data generated in this study are available upon request from the corresponding author. ATM mRNA expression profile data analyzed in this study were obtained from GEO at GSE50509 and GSE61992.

## Results

### BRAF<sup>i</sup> Resistant Melanoma Cells are Highly Susceptible to PARPi Treatment

To analyze whether PARPi treatment affects acquired resistance to MAPKi, we tested the sensitivity of the PARPi olaparib and talazoparib in melanoma cell line pairs that are either sensitive (S) or resistant (R) toward the BRAF<sup>i</sup> vemurafenib. Interestingly, the R cells were significantly more sensitive to both PARPi (Fig. 1A). Next, we tested the sensitivity to PARPi of a PDX from a patient with melanoma who developed resistance toward the BRAF<sup>i</sup> vemurafenib and dabrafenib. The cells of this patient were highly sensitive toward the PARPi olaparib and talazoparib (Fig. 1A). Most importantly, treatment with talazoparib almost completely prevented growth of human A375 R melanoma cells in NSG mice. The tumor volume over time of mice treated with talazoparib was significantly reduced from day 7 on compared with the solvent-treated control mice (Fig. 1B). The final tumor size of the mice treated with talazoparib was also significantly lower compared with the solvent-treated control mice (Fig. 1C). In addition, the tumors at the end of the experiment in the talazoparib-treated mice were macroscopically smaller than the solvent-treated control mice (Fig. 1D). These data indicate that BRAF<sup>i</sup> resistant melanoma cells can be treated with PARPi as a single agent.

### PARPi Treatment Induces p53-associated Proapoptotic Genes and Cell Death in BRAF<sup>i</sup> Resistant Melanoma Cells

To decipher the molecular mechanism underlying the high sensitivity of BRAF<sup>i</sup> R cells toward PARPi, we tested their effect on melanoma progression and

cell-cycle arrest induction. Interestingly, treatment of A375 R cells with the PARPi talazoparib for 24 hours significantly decreased their migratory and invasive ability (Fig. 2A). Furthermore, cell-cycle analysis revealed an initial induction of G<sub>2</sub>-M arrest that transitioned to apoptosis, as seen by the appearance of a subG<sub>1</sub> peak in talazoparib-treated BRAF<sup>i</sup> R cells (Fig. 2B). Apoptosis induction by talazoparib was confirmed by measuring the amount of activated caspase 3/7 over time (Fig. 2C). As apoptosis induction is often accompanied by activation of the p53 signaling pathway, we performed a PCR profiler array for genes involved in the p53 signaling pathway. Indeed, genes important in p53-mediated cell-cycle arrest and apoptosis induction, such as FOXO3, SESN2, BAX, APAF1, CDKN1A, MDM2, and CDKN2A were upregulated after talazoparib treatment of A375 R cells (Fig. 2D; Supplementary Table S1). In particular, both RNA and protein expression of p21/CDKN1A were significantly induced in talazoparib-treated BRAF<sup>i</sup> R cells (Fig. 2E and F). This PARPi-dependent upregulation of p21/CDKN1A was also confirmed in the talazoparib-treated mouse tumors (Supplementary Fig. S1A). These data suggest that PARPi treatment induces G<sub>2</sub>-M arrest and subsequent activation of apoptosis by p53-associated induction of proapoptotic genes.

### MAPKi Resistant Melanoma Cells Exhibit Low Expression of the DNA DSB Sensor ATM

We found that talazoparib treatment of A375 R cells clearly induced phosphorylation of the histone variant H2A.X (pH2AX) at position serine 139 indicating induction of DNA damage (Fig. 3A). This was also observed in the A375 R tumors of talazoparib-treated mice (Supplementary Fig. S1B). Because the PARP trapping and thereby the induction of DSB is the main mechanism of cellular toxicity of PARPi (24), we tested whether PARPi treatment leads to a higher PARP trapping effect in MAPKi resistant cells. For this, we performed a Western blot analysis, in which we analyzed PARP levels bound to chromatin, and thus, trapped PARP after talazoparib treatment and after short-time treatment with methyl methanesulfonate to induce DNA damage. As expected, higher chromatin bound PARP levels were observed compared with untreated control cells (Fig. 3B). However, no difference between trapped PARP and thus the PARP trapping efficacy in MAPKi resistant cells compared with their sensitive counterparts was seen. Therefore, we proposed that the PARP trapping efficacy is not higher in MAPKi resistant cells compared with their treatment-naïve counterpart. To gain further insight into the high PARPi sensitivity of BRAF<sup>i</sup> R melanoma cells compared with their treatment naïve, sensitive counterparts, we performed a PCR Profiler Array for human DNA repair genes. Interestingly, we found that in A375 R cells, ATM in particular was downregulated (Fig. 3C; Supplementary Table S1). ATM is a gene important for DNA DSB sensing and for early steps of the DNA damage repair. We confirmed the data by immunoblot analysis (Fig. 3D), qPCR (Fig. 3E), and immunofluorescence staining (Supplementary Fig. S1C) in several matching pairs of S and R melanoma cell lines. The data indicate that RNA and protein expression of ATM is downregulated in BRAF<sup>i</sup> R cells compared with their sensitive counterparts. Moreover, IHC of matched biopsies from one patient before and after BRAF<sup>i</sup> resistance development showed a clear downregulation of ATM protein levels in the MAPKi resistant tumor compared with the treatment-naïve tumor (Fig. 3F). Downregulation of ATM in MAPKi resistant melanomas compared with the treatment-naïve tumors was confirmed by database analysis of mRNA sequencing data from matched melanoma samples before and after either BRAF<sup>i</sup> resistance or BRAF<sup>i</sup>/MEKi dual resistance development published by Hugo and colleagues (21–23). ATM mRNA levels were significantly reduced in MAPKi resistant melanoma samples compared with samples of the same patient

Downloaded from <http://ascrjournals.org/cancercommunication/article-pdf/3/9/1743/3382329/crc-23-0101.pdf> by University of Tuebingen user on 07 September 2023

## PARP Inhibitors as an Effective Treatment for Melanoma

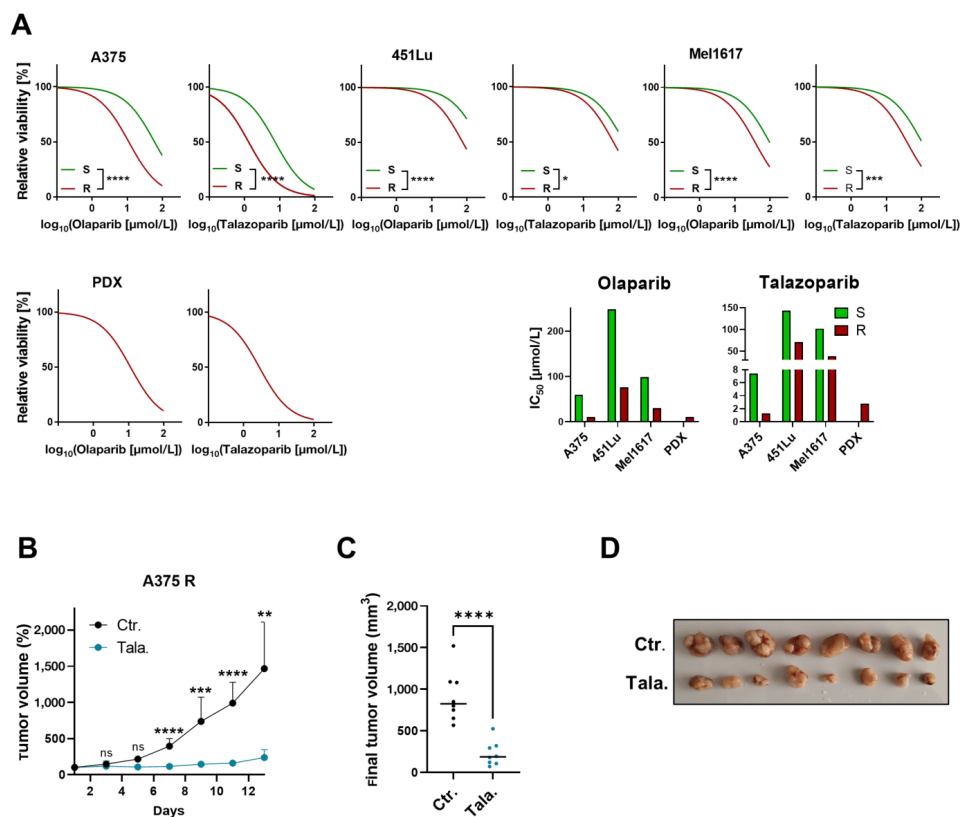


**FIGURE 1** MAPKi resistant melanoma cells are highly susceptible to PARPi treatment. **A**, MUH cell viability assay of vemurafenib sensitive (S) and resistant (R) melanoma cell lines as well as PDX R cells treated with different concentrations of PARPi (olaparib and talazoparib) starting at 100  $\mu\text{mol/L}$  for 72 hours. Comparison of fits of the nonlinear regression was performed to analyze statistical differences between S and R cells.  $\text{IC}_{50}$  levels are shown. **B**, NSG mice were treated with 2 mg/kg/day talazoparib (Tala.) or the same solvent without talazoparib (Ctr.). The xenograft tumor volume in percent compared with treatment start over time is shown. **C**, The final tumor volume of the individual mice is depicted. Multiple *t* test was used to compare the control (Ctr.) group to the talazoparib (Tala.) group. **D**, Representative pictures of the excised tumors are illustrated.

before the onset of MAPKi resistance (Supplementary Fig. S1D). To study the importance of ATM to PARPi treatment in melanoma on a functional level, we used the human melanoma cell line HT-144, that has the homozygous mutation p.W2845\* in the ATM gene, resulting in a truncated and thereby inefficient ATM protein. Interestingly, the MUH analysis showed that the ATM-deficient cells are also sensitive to talazoparib treatment (Fig. 3G) and that inhibition of ATM by the ATM inhibitor Ku-55933 is more effective in A375 S cells than the corresponding R cells (Fig. 3H). Most strikingly, downregulation of ATM in A375 S cells via treatment with low concentrations of Ku-55933 sensitized the cells significantly to talazoparib treatment (Fig. 3I). Taken together, these data suggest that BRAFi R cells are more susceptible to PARPi therapy because of lower ATM levels and consequently an inefficient sensing of DNA DSBs.

### Synergistic Killing of Melanoma Cells by a Combination of MAPKi and PARPi

Next, we tested whether combined treatment of MAPKi resistant melanoma cells with PARPi and MAPKi increases the effectiveness compared with the monotherapy. Treatment of A375 R cells with talazoparib and the BRAFi vemurafenib did not increase cell death induction compared with talazoparib treatment alone (Fig. 4A; Supplementary Fig. S2A). However, a combination of talazoparib and the MEKi trametinib resulted in a synergistic reduction of melanoma cell viability, as indicated by the low CI values (Fig. 4B; Supplementary Fig. S2A). Consistent with these data, a combination of talazoparib and the panRAF inhibitor (panRAFi) LY3009120 had a synergistic cytotoxic effect on BRAF/MEKi double-resistant A375 melanoma cells (A375 RR; Fig. 4C;

Fröhlich et al.

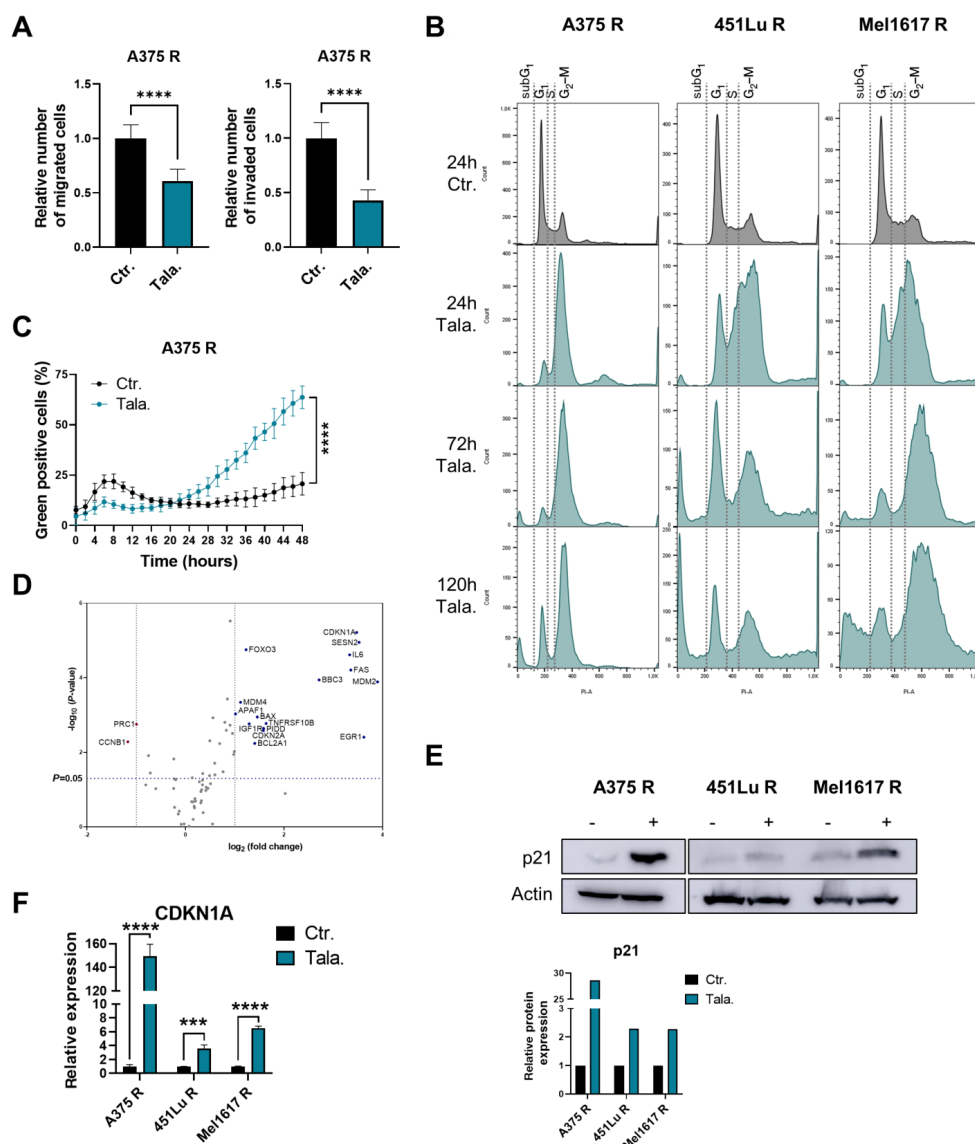


**FIGURE 2** PARPi treatment induces p53-associated proapoptotic genes and cell death in BRAF<sup>i</sup> resistant melanoma cells. **A**, Migration and Invasion assay using A375 R cells that were treated with 5  $\mu\text{mol/L}$  talazoparib (Tala.) for 24 hours or remained untreated (Ctrl.) is shown. The relative number of migrated (left) or invaded (right) cells is shown. Unpaired *t* test was performed to compare the Ctrl. with Tala. group. **B**, Cell-cycle analysis was performed in A375 R, 451Lu R, and Mel1617 R cells after treatment with 2  $\mu\text{mol/L}$  talazoparib (Tala.) for 24, 72, or 120 hours. Untreated cells (Ctrl.) served as a control. **C**, Incucyte Caspase-3/7 Dye for apoptosis was used to trace cell death activation after (Continued on the following page.)

Downloaded from [http://ascrjournals.org/cancerscommunication/article-pdf/3\(9\)/1743/382329/crc-23-0101.pdf](http://ascrjournals.org/cancerscommunication/article-pdf/3(9)/1743/382329/crc-23-0101.pdf) by University of Tuebingen user on 07 September 2023

## PARP Inhibitors as an Effective Treatment for Melanoma

(Continued) treatment of 5  $\mu\text{mol/L}$  talazoparib (Tala.) for up to 48 hours compared with untreated cells (Ctr.). The percentage of green fluorescence positive cells is shown. Unpaired *t* test was performed to compare the Ctr. with Tala. group. **D**, RT<sup>2</sup> Profiler PCR Array Human p53 Signaling Pathway was performed in A375 R cells that were treated with 5  $\mu\text{mol/L}$  talazoparib for 24 hours or remained untreated. log<sub>2</sub> fold changed in the expression of the corresponding genes between the talazoparib treated group and the control group as well as the log<sub>10</sub> *P* values of the respective gene expression changes are shown in the volcano plot. Technical triplicates were performed. **E**, Immunoblot analysis of A375 R, 451Lu R, and Mel1617 R cells treated with 5  $\mu\text{mol/L}$  talazoparib (+) for 24 hours or untreated (-). Relative protein expression is shown. **F**, Relative gene expression of CDKN1A after 5  $\mu\text{mol/L}$  talazoparib (Tala.) treatment for 24 hours or untreated A375 R, 451Lu R, and Mel1617 R cells. Unpaired *t* test was performed to compare the Ctr. with Tala. group.

Supplementary Fig. S2B). These data indicate that patients with MAPKi resistant melanoma may benefit from a combination of PARPi and MEKi or panRAFi in case of a MEKi resistance.

Next, we asked whether a combination of MAPKi and PARPi would be effective in MAPKi sensitive melanoma cells as a potential additional initial treatment for patients with melanoma. For this, we treated SKMel28 S and A375 S cells either with olaparib, talazoparib, vemurafenib, or the combination of a PARPi and the BRAFi. As shown in Fig. 4D, the combination treatment synergistically reduced the growth of the S melanoma cells (see also Supplementary Fig. S2C and S2D). The different combination treatments led also to a significant lower cytotoxicity in primary human fibroblasts compared with A375 melanoma cells (Supplementary Fig. S2E). The combination treatment was also very efficient in killing melanoma cells cultivated in three dimensions, as it significantly decreased the growth of melanoma cells in spheroids (Fig. 4E). Moreover, the combination treatment significantly reduced the colony formation ability of SKMel28 S and A375 S cells (Fig. 4F). Most strikingly, the combination treatment of vemurafenib and talazoparib completely inhibited growth of A375 S cells *in vivo* (Fig. 4G and H). The tumor volume over time of mice treated with the combination was significantly reduced compared with the tumor volume over time of the solvent-treated control mice. The final tumor size of the mice treated with the combination of BRAFi and PARPi was also significantly lower compared with the tumor size of mice treated solely with vemurafenib or talazoparib. In summary, we demonstrated that a combination of PARPi and MAPKi synergistically reduces the growth of BRAFi sensitive, BRAFi resistant, as well as BRAFi/MEKi double-resistant melanoma cells *in vitro* and *in vivo*.

### Synthetic Lethality Elicits Synergism in the Combination of MAPKi with PARPi

To analyze the molecular mechanism of the synergistic effect of PARPi and MAPKi, we determined the extent of DNA damage induction by talazoparib, vemurafenib, or the combination treatment using pH2AX staining of A375 S cells. As shown in Fig. 5A, talazoparib induced DNA damage to a high extent, in contrast to vemurafenib. Interestingly, the combination of talazoparib and vemurafenib did not result in an increase of pH2AX staining extent compared with the single treatments (Fig. 5A). Consistent with that, a comet assay showed no increase in DNA damage of the combined treatment of talazoparib and vemurafenib compared to each single treatment (Fig. 5B). On the basis of these results, we postulated that the synergistic effect of combining PARPi and MAPKi initially does not enhance DNA damage in melanoma cells, but that MAPKi treatment possibly results in the inability to repair the DNA damage induced by PARPi treatment.

Therefore, we analyzed gene expression of the important HRR genes BRCA1, BRCA2, RAD51, and EXO1 after MAPKi treatment in MAPKi S, R, and RR A375 melanoma cells. Interestingly, treatment with the BRAFi vemurafenib, the MEKi trametinib, or the panRAFi LY3009120 resulted in a significant downregulation

of these genes in MAPKi sensitive cells, whereas the respective effective MAPKi treatment downregulated these HRR genes in R or RR cells: the MEKi and the panRAFi in R cells and the panRAFi in RR cells (Fig. 5C). To exclude the possibility that the downregulation of HRR genes was solely due to G<sub>1</sub> cell-cycle arrest induced by vemurafenib, we checked RNA expression of HRR genes in sorted vemurafenib-treated cells that were either in G<sub>1</sub>- or G<sub>2</sub>-M-phase and compared them to the respective untreated cells in G<sub>1</sub>- or G<sub>2</sub>-M-phase. Cells treated with vemurafenib showed decreased HRR gene expression, regardless of cell-cycle phase they were in (Supplementary Fig. S2F). These data indicate that downregulation of the MAPK signaling pathway by the respective MAPKi results in an HRD phenotype in melanoma cells and is therefore synthetically lethal in combination with PARPi.

### Discussion

In this work, we show that PARPi therapy could be an effective treatment option for patients with both MAPKi sensitive as well as MAPKi resistant melanoma as a monotherapy or in combination with MAPKi. We demonstrate that a diverse array of MAPKi induce an HRD phenotype and thus act synthetic lethal in combination with PARPi in MAPKi sensitive and resistant melanoma cells *in vitro* and *in vivo*.

We found lower ATM expression in MAPKi resistant cells and saw higher sensitivity of these cells to PARP inhibitor therapy. Because ATM is known to be an important sensor to activate HRR upon DNA DSBs, our hypothesis is that the higher sensitivity of MAPKi resistant cells to PARPi is explained by lower ATM levels, and thus lower repair of DNA DSBs by HRR. In addition, we found a combination effect between MAPKi and PARPi. This combination effect can be explained by the fact that suppression of the MAPK signaling pathway leads to downregulation of essential HRR genes, such as BRCA1, BRCA2, RAD51, or EXO1. Therefore, BRAF mutant cells treated with MAPK inhibitors are very sensitive to PARP inhibitors due to the downregulation of HRR gene expression. Interestingly, we have been able to detect this combination effect not only in MAPKi sensitive but also in MAPKi resistant cells. We assume that downregulation of ATM decreases the sensing of the DSB, and additional treatment with the MEKi trametinib, or the panRAFi LY3009120 leads to a further decrease in HRR activity, making these cells even more sensitive to PARPi treatment.

Consistent with other publications, we found that cell viability in established melanoma cell lines as well as PDX melanoma cells and PDX melanoma mouse models was clearly reduced by PARPi treatment, especially by talazoparib, a PARPi with high PARP trapping activity (25). We were able to discover that MAPKi resistant melanoma cells are more sensitive to PARPi treatment compared with their treatment-naïve counterparts. Furthermore, we show for the first time that MAPKi resistant melanoma cell lines and patient material have decreased ATM expression, and this confers sensitivity to PARPi treatment. ATM, the most upstream DDR kinase of HRR, acts as a DSB sensor and is

Fröhlich et al.

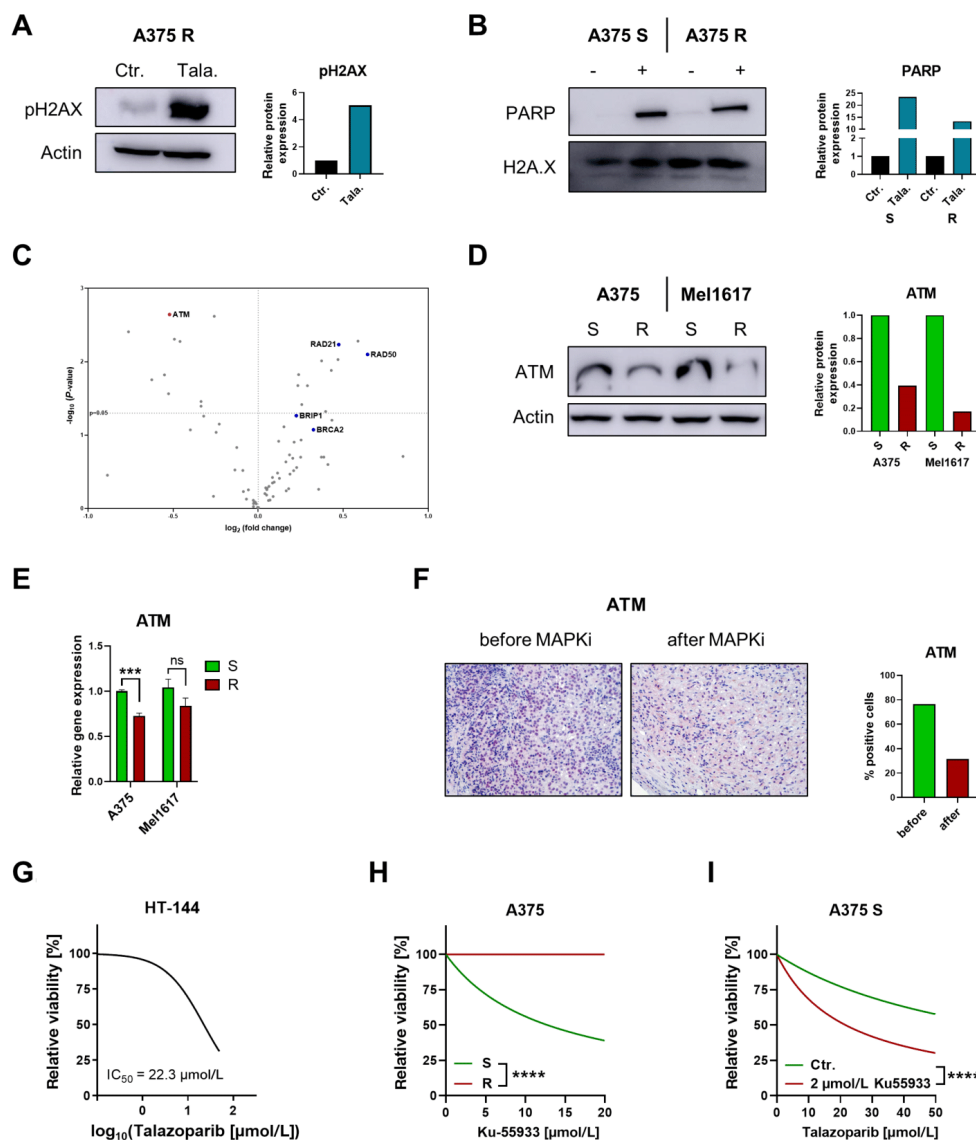


**FIGURE 3** MAPKi resistant cells show decreased ATM expression. **A**, Immunoblot analysis of A375 R cells treated with 5  $\mu\text{mol/L}$  talazoparib (Tala.) for 24 hours or untreated (Ctr.). Relative protein expression is shown. Actin control was reused from Fig. 2E as the Western blots were performed in the same experiment. **B**, Immunoblot analysis of chromatin bound fraction of A375 S and R cells after the treatment with 0.005% MMS and 2  $\mu\text{mol/L}$  talazoparib (+) for 6 hours or untreated cells (-). Relative protein expression is shown. **C**, RT<sup>2</sup> Profiler PCR Array Human DNA Repair was performed in A375 S versus R.  $\log_2$  fold change in the expression of the corresponding genes of R compared with S cells as well as the  $\log_{10}$  P values of the respective gene expression changes are shown in the volcano plot. Technical triplicates were performed. (Continued on the following page.)

## PARP Inhibitors as an Effective Treatment for Melanoma

(Continued) **D**, Immunoblot analysis of A375 and Mel1617 S and R cells. Relative protein expression is shown. **E**, Relative ATM gene expression of A375 and Mel1617 S and R is shown. Unpaired *t* test was performed to compare the Ctr. with Tala. group. **F**, IHC of paraffin-embedded tumors of a patient before and after MAPKi resistance stained for ATM. 10X magnification was used. Quantification of the ATM positive cells was performed and % ATM positive cells is shown. **G**, MUH cell viability assay of HT-144 melanoma cell line treated with different concentrations of talazoparib (Tala.) starting at 50  $\mu\text{mol/L}$  for 72 hours.  $\text{IC}_{50}$  level is shown. **H**, MUH cell viability assay of A375 S and R cells treated with different concentrations of Ku-55933 (Ku.) for 72 hours. Comparison of fits of the nonlinear regression was performed to analyze statistical differences between S and R cells. **I**, MUH cell viability assay of A375 S cells treated with different concentrations of talazoparib for 72 hours. Cells were additionally treated with a stable concentration of 2  $\mu\text{mol/L}$  Ku-55933 or remained untreated. Comparison of fits of the nonlinear regression was performed to analyze statistical differences between cells treated with Ku-55933 or untreated cells.

recruited and triggered by the MRN complex (26). Activation of ATM results in phosphorylation of crucial proteins, such as BRCA1 and thereby triggers the repair of the DSB via HRR (27). Indeed, several studies have shown that ATM-deficient cancer cells have impaired HRR by inefficient sensing and therefore are particularly susceptible to PARPi treatment (28–30). Also, phase II clinical trials checking the efficacy of PARPi treatment in patients with cancer with among others somatic or germline ATM gene mutations, are currently underway (NCT04042831, NCT03344965, NCT02286687, NCT04030559), even for patients with melanoma (NCT03925350, NCT04633902). Combining our results with previously published data, we hypothesize, that paradoxical hyperactivation of the MAPK signaling pathway, a frequent MAPKi resistance mechanism, upregulates the mTOR signaling pathway, and as a consequence negatively regulates ATM expression (31, 32). Furthermore, downregulation of the Tap73 isoform in MAPKi resistant melanoma cells might have an influence on ATM expression (14). However, we cannot exclude the possibility that other factors associated with MAPKi resistance also have an impact on the increased PARPi sensitivity of MAPKi resistant melanoma cells.

We demonstrated that MAPKi resistant melanoma cells did not respond to inhibition of ATM by Ku-55933, whereas the inhibitor showed marked cytotoxicity in MAPKi sensitive cells. This suggests that downregulation of ATM during the emergence of MAPKi resistance causes MAPKi resistant cells to lose their dependence to ATM signaling compared with MAPKi sensitive cells. This goes in line with a publication showing that ATM-deficient cells do not respond to the ATM inhibitor Ku-55933 (33). Taken together, we conclude that especially the difficult-to-treat patients with melanoma that developed MAPKi treatment resistance may benefit from PARPi treatment, and that ATM might be a promising biomarker for treatment response.

We found that PARPi treatment significantly decreased the migratory and invasive potential of melanoma cells. Further publications support our data by showing that PARPi lead to suppression of migration, invasion, and colonization of distal organs of metastatic melanoma cells (34, 35). These findings suggest that PARPi treatment could not only lead to a shrinkage of the primary tumor, but also reduce the metastatic potential of melanoma cells. In agreement with other studies, we could show that DNA damage induction by PARPi treatment of melanoma cells leads to clear G<sub>2</sub>-M-phase arrest and subsequent induction of apoptosis (25, 35). Cell death was mainly mediated by p53-associated activation of proapoptotic genes and massive induction of p21. p53-dependent p21 activation is known to be crucial for G<sub>2</sub>-M checkpoint arrest following DNA damage (36–38). This eventually led to mitotic catastrophe and apoptosis, resulting in cancer cell death (39, 40).

Numerous preclinical and clinical studies have been looking at the use of PARPi in combination with chemotherapy, ionizing radiation, or immunotherapies (8,

41, 42). However, the potential of combining PARPi with targeted therapies, especially with MAPKi, is still unknown. Previously, another group and ours were able to decipher that suppressing the MAPK pathway downregulates HRR gene expression in MAPKi sensitive melanoma cells via the transcription factor ELK1, but the HRR regulation in MAPKi resistant cells remains unknown (11, 12). Therefore, we used a MEKi to suppress the MAPK signaling pathway in BRAFi resistant melanoma cell lines, and a panRAFi in BRAFi/MEKi double-resistant melanoma cells, that has proven to suppress the MAPK signaling pathway in BRAFi/MEKi double-resistant cancers (43, 44). We were able to show that downregulation of the MAPK signaling pathway specifically induces an HRD phenotype by suppressing the important HRR genes BRCA1, BRCA2, RAD51, and EXO1. Because the MAPK signaling pathway is mainly responsible for cell growth, we assume that an activation of it, and thus a faster cell division also requires a higher HRR activity, and therefore the HRR genes are regulated via the MAPK signaling pathway (45).

Most strikingly and in line with other publications, we demonstrated that PARPi in combination with MAPKi show a synergistic cytotoxicity in melanoma cells both *in vitro* and *in vivo* (12, 13). MAPKi results in an HRD phenotype and the combination with PARPi leads to a synergistic synthetic lethal interaction of both therapies. Taken together, we propose that patients with treatment-naïve BRAF-mutated melanoma would benefit from a combination treatment with BRAFi and PARPi as resistance quickly develops in the majority of MAPKi single treated patients. BRAFi/MEKi pretreated and thereby double-resistant patients as well as MEKi single resistant patients may benefit from a combination therapy of panRAFi and PARPi. However, we found that the combination of talazoparib with vemurafenib has significantly higher toxicity *in vitro* on primary human fibroblasts as the MEKi or panRAFi. Therefore, a potential toxicity may limit the clinical translation of the combination therapy. To mitigate a potential toxicity of the combination treatment, we propose to use in clinical studies talazoparib in combination with MEKi or panRAFi. Consistent with this, preliminary data from a phase I clinical trial in which solid tumors with Ras pathway alterations were treated with the PARPi olaparib and the MEKi selumetinib showed no grade 4 adverse events and were generally well tolerated (46).

With this project, we support the concept that not only BRCA-mutated patients benefit from PARPi therapy, but also non-BRCA1-mutant tumors that have BRCAness and thus a HRD phenotype may be treated with and benefit from PARPi treatment (47–49). There are currently numerous clinical trials underway focusing on the efficacy of PARPi therapy on HRD cancers, including patients with melanoma (NCT03207347, NCT03925350, NCT04633902, NCT05482074, NCT04187833, NCT05169437). Olaparib has even been approved for patients with HRD prostate cancer with a mutation in at least one of 14 HRR-related genes (50). However, these involve patients that carry a

Fröhlich et al.

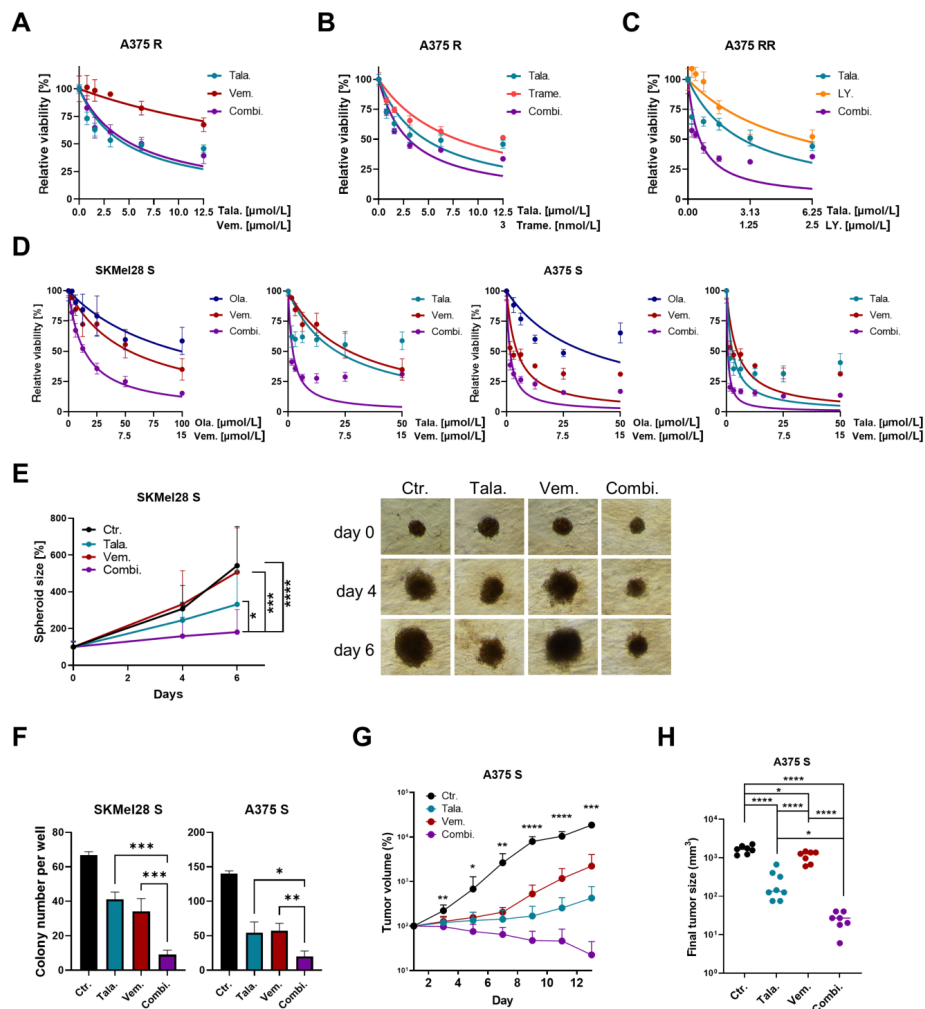


**FIGURE 4** Synthetic lethality elicits synergism in the combination of MAPKi with PARPi. MUH cell viability assay of A375 R or A375 RR cells treated with different concentrations of talazoparib (Tala.), vemurafenib (Vem.), trametinib (Trame.), LY3009120 (LY.) or a combination of these drugs (Combi.) for 72 hours. **A**, **B**, **C** MUH cell viability assay of A375 and SKMel28 S cells treated with different concentrations of olaparib (Ola.), talazoparib (Tala.), vemurafenib (Vem.) or a combination of these drugs (Combi.) for 72 hours. **D**, **E** MUH cell viability assay of A375 and SKMel28 S cells treated with different concentrations of olaparib (Ola.), talazoparib (Tala.), vemurafenib (Vem.) or a combination of these drugs (Combi.) in collagen for 6 days or remained untreated. The total size of the spheroids was quantified and multiple *t* test was performed to compare the groups at day 6. Representative pictures of the spheroids are shown. **F**, Colony formation of SKMel28 S and A375 S was analyzed after the treatment with 2  $\mu\text{mol/L}$  talazoparib (Tala.), 2  $\mu\text{mol/L}$  vemurafenib (Vem.), a combination of both drugs (Combi.) for 7 days or untreated cells (Ctr.). The number of colonies per well was counted. One-way ANOVA was used to compare each group with each other. **G**, NSG mice were treated with control vehicle (Ctr.), 1 mg/kg/day talazoparib (Tala.), 25 mg/kg/day (Vem.), or a combination of both inhibitors (Combi.). The xenograft tumor volume in percent compared with treatment start over time is shown. Multiple *t* test was used to compare the Ctr. group with the Combi. group. **H**, The final tumor volume of the individual mice of G is depicted. Multiple *t* test was used to compare the different groups with each other.

## PARP Inhibitors as an Effective Treatment for Melanoma

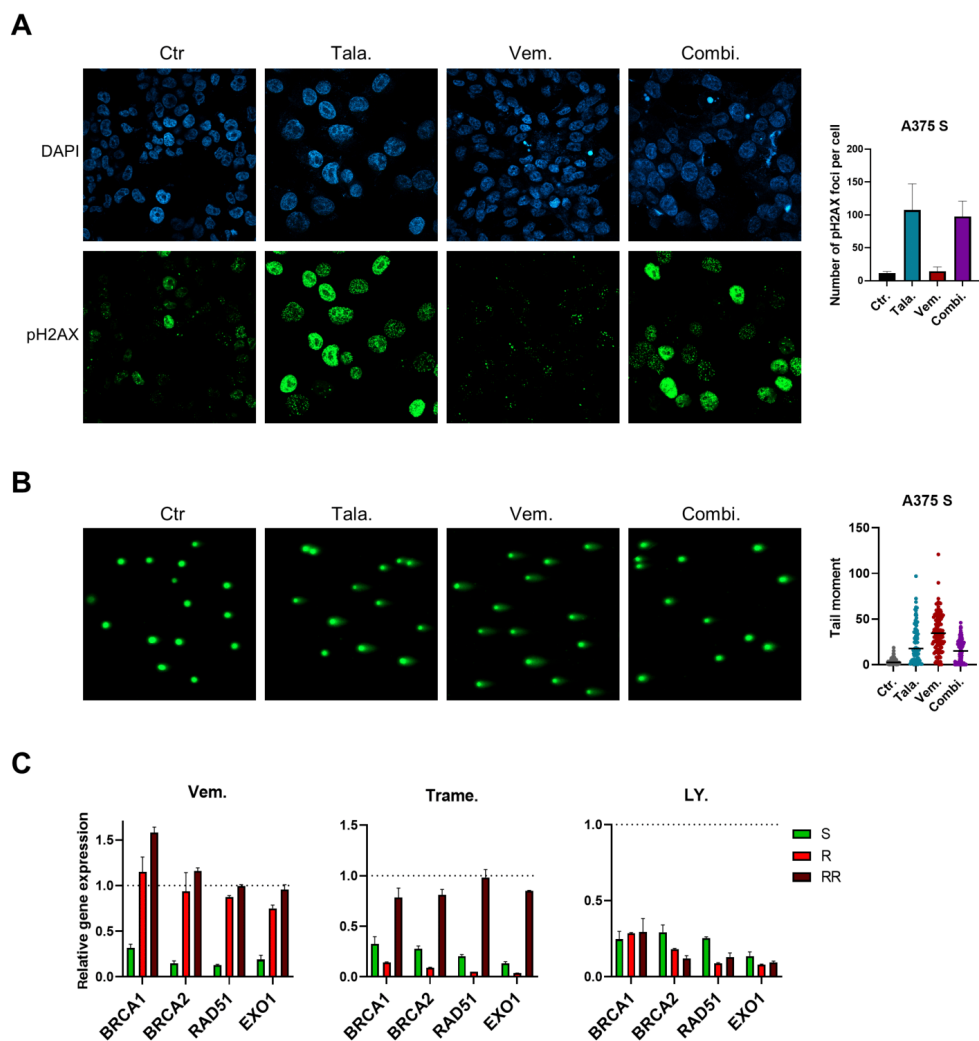


**FIGURE 5** MAPKi induce HRD phenotype and thereby act synthetic lethal in combination with PARPi. **A**, Immunofluorescence of A375 S cells that were treated with 5  $\mu\text{mol/L}$  talazoparib (Tala.), 5  $\mu\text{mol/L}$  vemurafenib (Vem.), or a combination of both inhibitors (Combi.) for 24 hours, or remained untreated (Ctr.). Green: pH2AX, blue: DAPI. 40X magnification was used. Number of pH2AX foci per cell was counted and one-way ANOVA was performed to analyze the differences between the groups. **B**, Comet Assay was performed using A375 S cells that were treated with either 15  $\mu\text{mol/L}$  talazoparib (Tala.), 5  $\mu\text{mol/L}$  vemurafenib (Vem.), a combination of both drugs (Combi.) for 24 hours or remained untreated (Ctr.). Green: DNA. 10X magnification was used. **C**, RNA expression of MAPKi sensitive (S), vemurafenib resistant (R), or vemurafenib and trametinib double-resistant (RR) A375 cells after the treatment with 5  $\mu\text{mol/L}$  vemurafenib (Vem.), 10 nmol/L trametinib (Trame.), or 5  $\mu\text{mol/L}$  LY3009120 (LY.) for 24 hours. The relative gene expression of the treated cells compared with the control group is shown.

Downloaded from [http://aacrjournals.org/cancerrescommun/article-pdf/3\(9\)/1743/382329/crc-23-0101.pdf](http://aacrjournals.org/cancerrescommun/article-pdf/3(9)/1743/382329/crc-23-0101.pdf) by University of Tuebingen user on 07 September 2023

**Fröhlich et al.**

mutation in one of the HRR genes. Our data are consistent with the outcome of another study indicating that patients do not necessarily have to have a mutation in the HRR pathway to respond well to PARPi treatment, but that suppression of the MAPK pathway with targeted therapy leads to reduced HRR gene expression inducing an HRD phenotype (12).

In summary, our study indicates that PARPi should not be limited to the treatment of patients with somatic or germline mutations in the HRR pathway, but that a combined treatment of melanoma patients with PARPi and MAPKi induces synthetic lethality by inducing a HRD phenotype and stops tumor growth.

**Authors' Disclosures**

H. Niessner reports grants from Novartis and Pascoe outside the submitted work. T. Sinnberg reports grants from Novartis, Skyline-Dx, Neracare, and Pascoe outside the submitted work. No disclosures were reported by the other authors.

**Authors' Contributions**

**L.M. Fröhlich:** Conceptualization, data curation, validation, investigation, visualization, methodology, writing-original draft, writing-review and editing.

**H. Niessner:** Data curation, validation, investigation, writing-review and editing. **B. Sauer:** Data curation, methodology. **S. Kämereit:** Data curation, methodology. **E. Chatzioannou:** Data curation, investigation, methodology. **S. Riel:** Data curation, validation, visualization, methodology. **T. Sinnberg:** Data curation, validation, investigation, writing-review and editing. **B. Schittek:** Conceptualization, supervision, funding acquisition, writing-original draft, writing-review and editing.

**Acknowledgments**

The FACS sorting experiment was performed with the kind help of Wolfgang Kempf. Mona Eisele helped performing toxicity experiments.

Financial support: This work was supported by the Deutsche Forschungsgemeinschaft (DFG, German Research Foundation; SCHI 510/12-1) under Germany's Excellence Strategy—EXC2180-390900677 to B. Schittek.

**Note**

Supplementary data for this article are available at Cancer Research Communications Online (<https://aacrjournals.org/cancerrescommun/>).

Received March 01, 2023; revised May 03, 2023; accepted July 27, 2023; published first September 05, 2023.

**References**

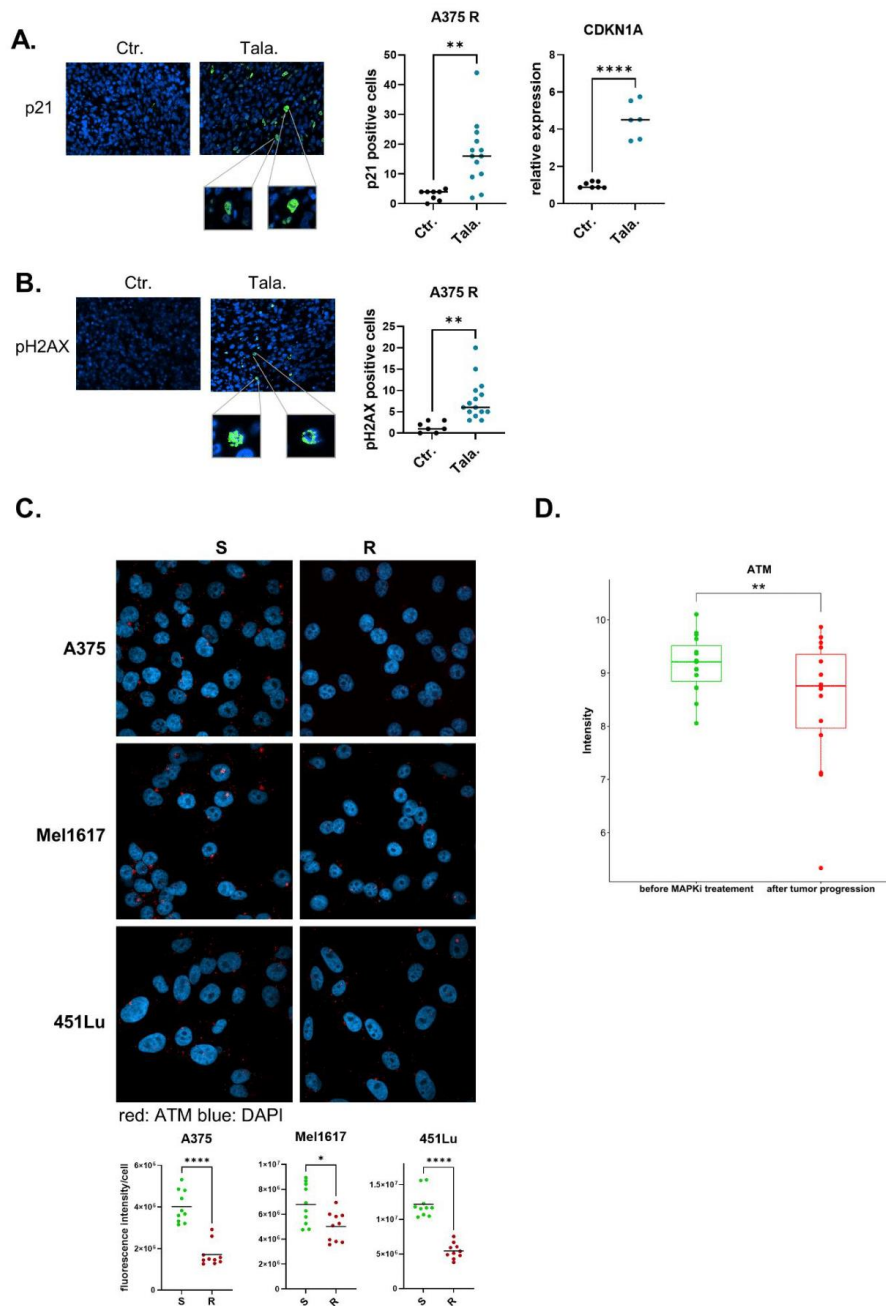
- de Gruij FR, van Kranen HJ, Mullenders LH. UV-induced DNA damage, repair, mutations and oncogenic pathways in skin cancer. *J Photochem Photobiol B* 2001;63: 19-27.
- Brown JS, O'Carrigan B, Jackson SP, Yap TA. Targeting DNA repair in cancer: beyond PARP inhibitors. *Cancer Discov* 2017;7: 20-37.
- Cheng Y, Zhang G, Li G. Targeting MAPK pathway in melanoma therapy. *Cancer Metastasis Rev* 2013;32: 567-84.
- Czarnecka AM, Bartnik E, Fiedorowicz M, Rutkowski P. Targeted therapy in melanoma and mechanisms of resistance. *Int J Mol Sci* 2020;21: 4576.
- Pommier Y, O'Connor MJ, de Bono J. Laying a trap to kill cancer cells: PARP inhibitors and their mechanisms of action. *Sci Transl Med* 2016;8: 362ps17.
- Lord CJ, Ashworth A. PARP inhibitors: synthetic lethality in the clinic. *Science* 2017;355: 1152-8.
- O'Neil NJ, Bailey ML, Hieter P. Synthetic lethality and cancer. *Nat Rev Genet* 2017;18: 613-23.
- Rose M, Burgess JT, O'Byrne K, Richard DJ, Bolderson E. PARP inhibitors: clinical relevance, mechanisms of action and tumor resistance. *Front Cell Dev Biol* 2020;8: 564601.
- Chan WY, Brown LJ, Reid L, Joshua AM. PARP inhibitors in melanoma—expanding therapeutic option? *Cancers* 2021;13: 4520.
- Maresca L, Stecca B, Carrassa L. Novel therapeutic approaches with DNA damage response inhibitors for melanoma treatment. *Cells* 2022;11: 1466.
- Makino E, Fröhlich LM, Sinnberg T, Kosnopfel C, Sauer B, Garbe C, et al. Targeting Rad51 as a strategy for the treatment of melanoma cells resistant to MAPK pathway inhibition. *Cell Death Dis* 2020;11: 581.
- Maertens O, Kuzmickas R, Manchester HE, Emerson CE, Gavin AG, Guild CJ, et al. MAPK pathway suppression unmasks latent DNA repair defects and confers a chemical synthetic vulnerability in BRAF-, NRAS-, and NFI-mutant melanomas. *Cancer Discov* 2019;9: 526-45.
- Sun CY, Fang Y, Yin J, Chen J, Ju ZL, Zhang D, et al. Rational combination therapy with PARP and MEK inhibitors capitalizes on therapeutic liabilities in RAS mutant cancers. *Sci Transl Med* 2017;9: eaal5148.
- Makino E, Gutmann V, Kosnopfel C, Niessner H, Forschner A, Garbe C, et al. Melanoma cells resistant towards MAPK inhibitors exhibit reduced TAP73 expression mediating enhanced sensitivity to platinum-based drugs. *Cell Death Dis* 2018;9: 930.
- Bitschar K, Sauer B, Focken J, Dehmer H, Moos S, Konnerth M, et al. Lgdunin amplifies innate immune responses in the skin in synergy with host- and microbiota-derived factors. *Nat Commun* 2019;10: 2730.
- Sinnberg T, Makino E, Krueger MA, Velic A, Macek B, Rothbauer U, et al. A nexus consisting of Beta-catenin and Stat3 attenuates BRAF inhibitor efficacy and mediates acquired resistance to vemurafenib. *EBioMedicine* 2016;8: 132-49.
- Gyori BM, Venkatachalam G, Thiagarajan PS, Hsu D, Clement MV. Corrigendum to OpenComet: an automated tool for comet assay image analysis [Redox Biol. Volume Pages 457-465]. *Redox Biol* 2021;40: 101876.
- Gyori BM, Venkatachalam G, Thiagarajan PS, Hsu D, Clement MV. OpenComet: an automated tool for comet assay image analysis. *Redox Biol* 2014;2: 457-65.
- Kosnopfel C, Sinnberg T, Sauer B, Busch C, Niessner H, Schmitt A, et al. YB-1 expression and phosphorylation regulate tumorigenicity and invasiveness in melanoma by influencing EMT. *Mol Cancer Res* 2018;16: 1149-60.
- Hugo W, Shi H, Sun L, Piva M, Song C, Kong X, et al. Non-genomic and immune evolution of melanoma acquiring MAPK1 resistance. *Cell* 2015;162: 1271-85.
- Long GV, Fung C, Menzies AM, Pupo GM, Carlino MS, Hyman J, et al. Increased MAPK reactivation in early resistance to dabrafenib/trametinib combination therapy of BRAF-mutant metastatic melanoma. *Nat Commun* 2014;5: 5694.
- Rizos H, Menzies AM, Pupo GM, Carlino MS, Fung C, Hyman J, et al. BRAF inhibitor resistance mechanisms in metastatic melanoma: spectrum and clinical impact. *Clin Cancer Res* 2014;20: 1965-77.
- Gopal YN, Rizos H, Chen G, Deng W, Frederick DT, Cooper ZA, et al. Inhibition of mTORC1/2 overcomes resistance to MAPK pathway inhibitors mediated by PGClalpha and oxidative phosphorylation in melanoma. *Cancer Res* 2014;74: 7037-47.
- Krastev DB, Wicks AJ, Lord CJ. PARP inhibitors – trapped in a toxic love affair. *Cancer Res* 2021;81: 5605-7.

## PARP Inhibitors as an Effective Treatment for Melanoma

25. Kim KB, Sorocanu L, de Semir D, Millis SZ, Ross J, Vosoughi E, et al. Prevalence of homologous recombination pathway gene mutations in melanoma: rationale for a new targeted therapeutic approach. *J Invest Dermatol* 2021;141: 2028-36.
26. Guleria A, Chandna S. ATM kinase: much more than a DNA damage responsive protein. *DNA Repair* 2016;39: 1-20.
27. Marechal A, Zou L. DNA damage sensing by the ATM and ATR kinases. *Cold Spring Harb Perspect Biol* 2013;5: a012716.
28. Weston VJ, Oldreive CE, Skowronska A, Oscier DG, Pratt G, Dyer MJS, et al. The PARP inhibitor olaparib induces significant killing of ATM-deficient lymphoid tumor cells *in vitro* and *in vivo*. *Blood* 2010;116: 4578-87.
29. Schmitt A, Knittel G, Welcker D, Yang TP, George J, Nowak M, et al. ATM deficiency is associated with sensitivity to PARP1 and ATR inhibitors in lung adenocarcinoma. *Cancer Res* 2017;77: 3040-56.
30. Wang C, Jette N, Moussienko D, Bebb DG, Lees-Miller SP. ATM-deficient colorectal cancer cells are sensitive to the PARP inhibitor olaparib. *Transl Oncol* 2017;10: 190-6.
31. Shen C, Houghton PJ. The mTOR pathway negatively controls ATM by up-regulating miRNAs. *Proc Natl Acad Sci U S A* 2013;110: 11869-74.
32. Wang B, Zhang W, Zhang G, Kwong L, Lu H, Tan J, et al. Targeting mTOR signaling overcomes acquired resistance to combined BRAF and MEK inhibition in BRAF-mutant melanoma. *Oncogene* 2021;40: 5590-9.
33. Hickson I, Zhao Y, Richardson CJ, Green SJ, Martin NM, Orr AI, et al. Identification and characterization of a novel and specific inhibitor of the ataxia-telangiectasia mutated kinase ATM. *Cancer Res* 2004;64: 9152-9.
34. Rodriguez MI, Peralta-Leal A, O'Valle F, Rodriguez-Vargas JM, Gonzalez-Flores A, Majuelos-Melguizo J, et al. PARP-1 regulates metastatic melanoma through modulation of vimentin-induced malignant transformation. *PLoS Genet* 2013;9: e1003531.
35. Fratangelo F, Camerlingo R, Carriero MV, Pirozzi G, Palmieri G, Gentilcore G, et al. Effect of ABT-888 on the apoptosis, motility and invasiveness of BRAF1-resistant melanoma cells. *Int J Oncol* 2018;53: 1149-59.
36. Karimian A, Ahmadi Y, Yousefi B. Multiple functions of p21 in cell cycle, apoptosis and transcriptional regulation after DNA damage. *DNA Repair* 2016;42: 63-71.
37. Bunz F, Dutriaux A, Lengauer C, Waldman T, Zhou S, Brown JP, et al. Requirement for p53 and p21 to sustain G(2) arrest after DNA damage. *Science* 1998;282: 1497-501.
38. Al Bitar S, Gali-Muhtasib H. The role of the cyclin dependent kinase inhibitor p21(cip1/waf1) in targeting cancer: molecular mechanisms and novel therapeutics. *Cancers* 2019;11: 1475.
39. Slade D. PARP and PARG inhibitors in cancer treatment. *Genes Dev* 2020;34: 360-94.
40. Fridman JS, Lowe SW. Control of apoptosis by p53. *Oncogene* 2003;22: 9030-40.
41. Dreon A, Lord CJ, Ashworth A. PARP inhibitor combination therapy. *Crit Rev Oncol Hemat* 2016;108: 73-85.
42. Min A, Im SA. PARP inhibitors as therapeutics: beyond modulation of PARylation. *Cancers* 2020;12: 394.
43. Peng SB, Henry JR, Kaufman MD, Lu WP, Smith BD, Vogeti S, et al. Inhibition of RAF isoforms and active dimers by LY3009120 leads to anti-tumor activities in RAS or BRAF mutant cancers. *Cancer Cell* 2015;28: 384-98.
44. Vakana E, Pratt S, Blosser W, Dowless M, Simpson N, Yuan XJ, et al. LY3009120, a panRAF inhibitor, has significant anti-tumor activity in BRAF and KRAS mutant preclinical models of colorectal cancer. *Oncotarget* 2017;8: 9251-66.
45. Zhang W, Liu HT. MAPK signal pathways in the regulation of cell proliferation in mammalian cells. *Cell Res* 2002;12: 9-18.
46. Kurnit KC, Meric-Bernstam F, Hess K, Coleman RL, Bhosale P, Savelieva K, et al. Phase I dose escalation of olaparib (PARP inhibitor) and selumetinib (MEK inhibitor) combination in solid tumors with Ras pathway alterations [abstract]. In: Proceedings of the American Association for Cancer Research Annual Meeting 2019; 2019 Mar 29-Apr 3; Atlanta, GA, Philadelphia (PA): AACR; Cancer Res 2019;79(13 Suppl):Abstract nr CTO20.
47. Keung MYT, Wu YY, Vadgama JV. PARP inhibitors as a therapeutic agent for homologous recombination deficiency in breast cancers. *J Clin Med* 2019;8: 435.
48. Yi TJ, Feng Y, Sundaram R, Tie Y, Zheng H, Qian YP, et al. Antitumor efficacy of PARP inhibitors in homologous recombination deficient carcinomas. *Int J Cancer* 2019;145: 1209-20.
49. Kohn EC, Lee JM, Ivy SP. The HRD decision-which PARP inhibitor to use for whom and when. *Clin Cancer Res* 2017;23: 7155-7.
50. Lotan TL, Kaur HB, Salles DC, Murali S, Schaeffer EM, Lanchbury JS, et al. Homologous recombination deficiency (HRD) score in germline BRCA2- versus ATM-altered prostate cancer. *Mod Pathol* 2021;34: 1185-93.

Downloaded from <http://acrjournals.org/cancerrescommunit/article-pdf/39/17/143/3362329/crc-23-0101.pdf> by University of Tuebingen user on 07 September 2023

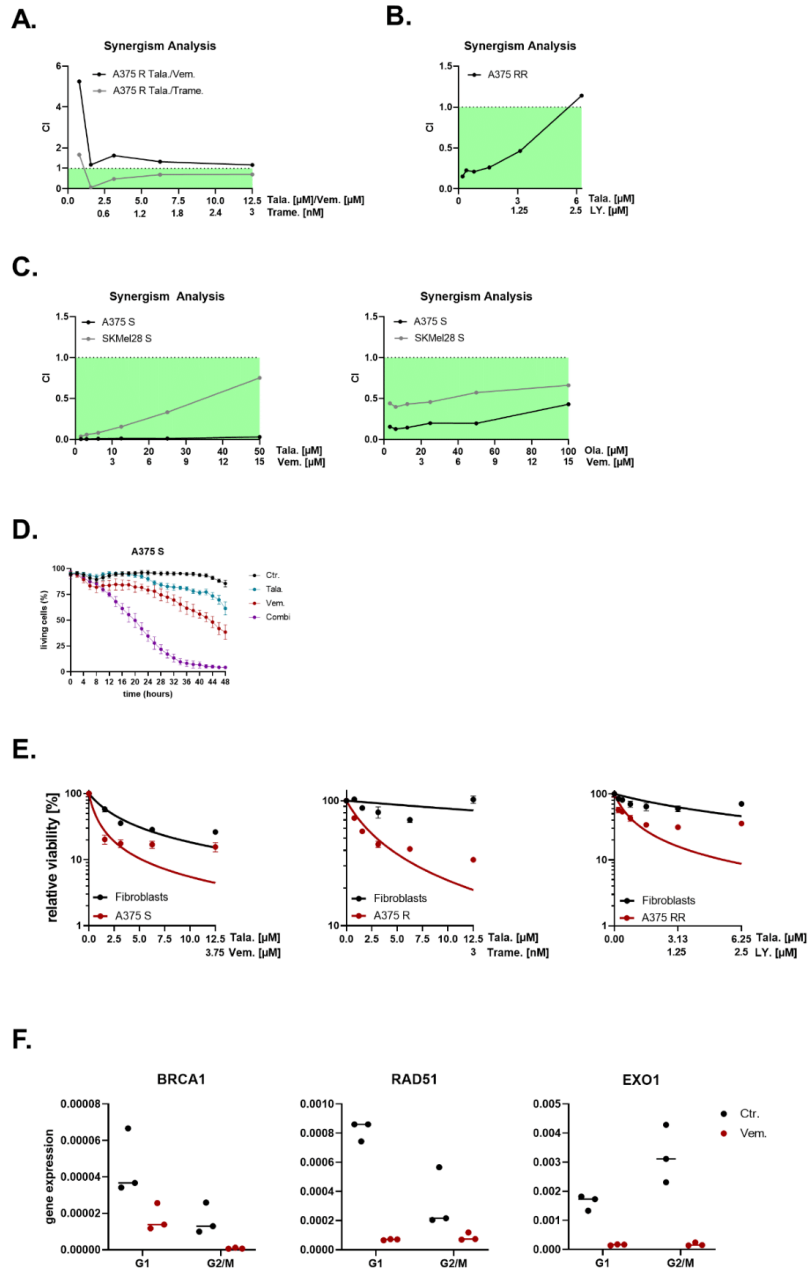
Supplementary Figure S1:



**Supplementary Figure S1: PARPi treatment in melanoma cells.**

**A.-B.** Immunofluorescence of p21 (**A.**) and pH2AX (**B.**) of the mouse tumors from Figure 1D. Green: p21/pH2AX. Blue: DAPI. Number of p21/pH2AX positive cells per image section is shown. 20x magnification was used. **C.** Immunofluorescence of ATM in 451Lu, A375, and Mel1617 S and R cells was performed. Red: ATM, blue: Hoechst. 40X magnification was used. 10 images with on average 25 cells per image were analysed. The fluorescence intensity per cell is shown. **D.** Normalized ATM RNA expression levels of melanoma patients before MAPKi treatment and after tumor progression. The data were obtained from the databases GSE50509 and GSE61992.

Supplementary Figure S2:



**Supplementary Figure S2: Synergistic interaction of PARPi and MAPKi treatment.**

**A.-C.** Synergism analysis was performed using the data of Figure 4A (**A.**), Figure 4B (**A.**), Figure 4C (**B.**), and Figure 4D (**C.**) treated with combinations of olaparib (Ola.), talazoparib (Tala.), vemurafenib (Vem.), trametinib (Trame.), or LY3009120 (LY.) for 72. Synergism analysis was analyzed using the combosyn software. The calculated combined index (CI) values reflect the degree of the combined treatment with: synergistic effect =  $0 < CI < 1$ , and additive effect =  $CI \geq 1$  **D.** A375 S cells were treated with 5  $\mu$ M talazoparib (Tala.), 5  $\mu$ M vemurafenib (Vem.), or a combination of both drugs (Combi.) for 48h or remained untreated (Ctr.). Every 2 hours pictures of the cells were taken with the Incucyte SX1 system. Incucyte advanced label-free classification analysis software was used to calculate the percent of living cells. **E.** MUH cell viability assay of primary human fibroblasts treated with different concentrations of the PARPi talazoparib (Tala.) and the BRAFi vemurafenib (Vem.), the MEKi trametinib (Trame.), or the panRAFi LY3009120 (LY.) for 72h. A375 melanoma cells (S for Tala.+Vem., R for Tala.+Trame, and RR for Tala.+LY.) from Figure 4A-D were used for comparison. **F.** A375 S cells were sorted in the different cell cycle phases. RNA expression of either in G1 or in G2/M phase treated with 5  $\mu$ M vemurafenib (Vem.) or untreated (Ctr.).

**RT2 Profiler™ PCR Array Human p53 Signaling Pathway  
and Human DNA Repair Pathway**

**All data points from Figure 2D are listed in this table**

Gene Name	log2 normalized value	-log10(p value t test)
APAF1	1.01288514	3.03072004
ATM	0.79597297	2.80654904
ATR	0.69150819	2.23571029
BAX	1.45448513	2.94940022
BBC3	2.70787411	3.94357563
BCL2	0.1885916	0.76014342
BCL2A1	1.40286804	2.24135978
BID	-0.03158801	0.08121413
BIRC5	-0.60607268	1.02814909
BRCA1	0.34388587	1.25673688
BRCA2	0.55483672	2.92635927
BTG2	4.75035273	3.76500639
CASP2	0.13388339	1.31962833
CASP9	0.49191802	2.31161177
CCNE1	0.12114984	0.67818994
CCNG1	0.82569546	2.59260708
CCNH	0.31001825	0.95116633
CDC25A	0.17364958	0.5560912
CDC25C	-0.7171246	1.44636402
CDK1	-0.80846531	1.12758229
CDK4	0.34716198	1.43223185
CDKN1A	3.47005108	5.21461411
CDKN2A	1.57688571	2.58521764
CHEK1	-0.23946711	1.82365861
CHEK2	-0.2024955	1.2681825
CRADD	0.90554543	5.52184126
DNMT1	0.34069674	1.1293568
E2F1	-0.7544001	1.9121389
E2F3	0.32542563	0.99821605
EGFR	0.97583067	1.94353697
EGR1	3.61750964	2.40750054
EI24	0.41125555	0.97870277
FADD	-0.09084605	0.07115044
FAS	3.35282209	4.20887029
FOXO3	1.22723035	4.7526781
GADD45A	4.35747682	3.06680363
HDAC1	-0.12902245	0.42382616
HK2	0.19936324	0.69321056
IGF1R	1.28928696	2.76526008
IL6	3.32788221	4.61671204
JUN	0.98949122	2.02168509
KAT2B	0.76078978	1.4811485
MCL1	0.84725785	3.43024913
MDM2	3.89393966	3.89134033
MDM4	1.11403672	3.34272582
MLH1	0.27939648	1.21249789
MSH2	-0.22368926	1.28778335
MYC	0.95193819	2.50773956

---

NF1	0.41732484	1.06497322
NFKB1	0.58955381	1.70811409
PCNA	0.15243966	0.20379407
PIDD	1.58150844	2.64245848
PRC1	-0.99712831	
PRKCA	0.18026627	0.51114691
PTEN	0.90193859	2.72885259
PTTG1	-0.24214845	1.03095071
RB1	0.15043346	0.67124915
RELA	0.59493449	1.39890688
SESN2	3.51946064	4.94962545
SIAH1	0.32001619	0.70385322
SIRT1	-0.15013943	0.34629973
STAT1	0.50494921	1.16047572
TNF	2.02101161	0.89864347
TNFRSF10B	1.63378521	2.77455764
TNFRSF10D	0.54647548	0.07915007
TP53	0.48466694	1.37704499
TP53BP2	0.30865781	0.6467659
TP73	0.35706867	0.38348081
TRAF2	0.06887054	0.02005464
TSC1	0.45156138	1.03578854
WT1	-0.22493917	0.52652156

**RT2 Profiler<sup>TM</sup> PCR Array Human p53 Signaling Pathway  
and Human DNA Repair Pathway****All data points from Figure 3C are listed in this table**

Gene Name	log2 normalized value	-log10(p value t test)
APEX1	-0.12597014	0.83190298
APEX2	-0.02771635	0.02742257
ATM	-0.52083166	2.64336295
ATR	-0.02724114	0.06841827
ATXN3	-0.49239969	2.30738537
BRCA1	0.08428122	0.34871756
BRCA2	0.32521336	1.07440348
BRIP1	0.22415027	1.26487664
CCNH	0.00155365	0.01499298
CCNO	0.41023358	0.60030278
CDK7	0.17931079	0.27128133
DDB1	-0.13641789	0.5262517
DDB2	0.23364096	1.6760862
DMC1	0.18417736	0.73218233
ERCC1	-0.76209597	2.40760987
ERCC2	0.4338778	1.20403399
ERCC3	-0.33561686	1.39491467
ERCC4	0.03980503	0.20440295
ERCC5	0.28955406	1.67395149
ERCC6	0.58669917	2.28091943
ERCC8	-0.33585548	1.45898667
EXO1	0.16304651	0.63621499
FEN1	0.08802402	0.16499339
LIG1	0.22619472	0.55956094
LIG3	-0.45942325	2.27657783
LIG4	0.05194111	0.27754675
MGMT	0.04955337	0.18465428
MLH1	-0.01117357	0.06559986
MMS19	-0.25796279	2.61966912
MPG	-0.02832823	0.0693097
MRE11	0.04458263	0.28184589
MSH2	0.12040794	0.91721372
MSH3	0.18691541	0.46956364
MSH5	0.09410385	0.36121342
MSH6	-0.02303999	0.09079098
MUTYH	-0.02861803	0.11382699
NEIL1	-0.39853044	1.07178698
NEIL2	0.39667568	1.32203889
NEIL3	0.3729834	2.01187331
NTHL1	-0.31986432	1.25987464
OGG1	0.21169022	0.90490347
PARP1	-0.24729656	1.03914251
PARP2	0.1139778	0.48434723
PARP3	0.85148107	0.71014355
PMS1	0.43031985	1.88208644
PMS2	-0.06879938	0.12934189
PNKP1	0.05136902	0.2578199
POLB	0.46962075	2.02942533
POLD3	-0.02324612	0.07894762

---

POLL	-0.26287698	0.16753936
PRKDC	-0.62508201	1.75479334
RAD18	0.08423095	0.42430549
RAD21	0.47330119	2.23355101
RAD23A	0.35563714	0.2625226
RAD23B	0.20862337	0.51663953
RAD50	0.64344583	2.09964765
RAD51	0.37188149	0.70161828
RAD51C	0.12479489	0.41229901
RAD51D	0.20359113	0.68549977
RAD52	-0.09002701	0.51930038
RAD54L	-0.08682054	0.23265457
RFC1	-0.02204358	0.07727411
RPA1	0.15186564	1.11430211
RPA3	0.23805789	1.82495344
SLK	0.06364554	0.30242927
SMUG1	0.06108438	0.11120688
TDG	-0.5508043	1.82155905
TOP3A	-0.22887078	1.15118181
TREX1	0.06974728	0.11678777
UNG	-0.00304141	0.01723906
XAB2	-0.05743238	0.25537759
XPA	-0.88595039	0.45463073
XPC	0.16515434	0.242071
XRCC1	-0.52676542	1.56438563
XRCC2	0.24998614	0.70083339
XRCC3	0.38598401	0.70169397
XRCC4	0.25651006	1.41736369
XRCC5	-0.01672993	0.08729448
XRCC6	0.25225234	0.93440668

### **11.3. Submitted Publication I**

Lisa Marie Fröhlich and Birgit Schitteck

**PARP1 expression predict PARP inhibitor sensitivity and correlates with metastatic potential and overall survival in melanoma.**

Submitted to International Journal of Cancer

1 **PARP1 expression predicts PARP inhibitor sensitivity and**  
2 **correlates with metastatic potential and overall survival in**  
3 **melanoma**

4

5 Lisa Marie Fröhlich<sup>1</sup> and Birgit Schitteck<sup>1,2</sup>

6

7 <sup>1</sup> Division of Dermatooncology, Department of Dermatology, University of Tübingen,  
8 Tübingen, Germany

9 <sup>2</sup>Cluster of Excellence iFIT (EXC 2180) "Image-Guided and Functionally Instructed  
10 Tumor Therapies", University of Tübingen, Germany

11

12 Running Title: PARP1 predicts PARP inhibitor sensitivity

13 Keywords: PARP inhibitors, PARP1, melanoma, biomarker

14 Correspondence: Birgit Schitteck, Division of Dermatooncology, Department of  
15 Dermatology, University of Tübingen, Liebermeisterstr. 25, D -72076 Tübingen,  
16 Germany. Email: [birgit.schitteck@uni-tuebingen.de](mailto:birgit.schitteck@uni-tuebingen.de), phone: +497071/2980832

17

18 List of Abbreviations:

BER	base excision repair
DSB	double strand break
HRD	HRR deficiency
HRR	homologous recombination repair
MAPK	mitogen-activated protein kinase
NAD <sup>+</sup>	nicotinamide adenine dinucleotide
PARP	poly (ADP-ribose) polymerase
PARPi	PARP inhibitor

19

20 Article category: Molecular Cancer Biology

21

22 Novelty and Impact: This study shows the importance of PARP1 as a potential  
23 biomarker to predict the response to PARPi therapy in melanoma. In addition, we  
24 demonstrate that melanomas with high PARP1 expression levels show increased  
25 metastatic potential, as well as decreased overall survival. With this, we suggest, that  
26 especially the late stage metastasized melanoma patients might profit from PARPi  
27 therapy.

28

**29 Abstract**

30 Metastatic melanoma is still a difficult-to-treat cancer type due to its frequent resistance  
31 mechanisms to targeted and immunotherapy. Therefore, we aimed to unravel novel  
32 therapeutic strategies for melanoma patients. Preclinical and clinical studies show that  
33 melanoma patients may benefit from a treatment with poly (ADP-ribose) polymerase  
34 (PARP) inhibitors (PARPi).

35 In this study, we focus on PARP1 as a potential biomarker to predict the response of  
36 melanoma cells to PARPi therapy. We found that melanoma cells with high basal  
37 PARP1 gene expression exhibit significantly increased cell death after PARPi  
38 treatment due to higher PARP1 trapping compared to melanoma cells with low PARP1  
39 gene expression. In addition, we could demonstrate that PARP1 expression levels are  
40 low in non-malignant skin cells, and metastatic melanomas show considerably higher  
41 PARP1 levels compared to primary melanomas. Also, PARP1 expression levels  
42 positively correlated with the invasiveness of melanoma cells. Most strikingly, we found  
43 that high PARP1 levels correlate with worse overall survival of late stage metastasized  
44 melanoma patients.

45 In conclusion, we show that PARP1 might act as a biomarker to predict the response  
46 to PARPi therapy, and that in particular the late stage metastasized melanoma patients  
47 are especially sensitive to PARPi therapy due to elevated PARP1 gene expression.  
48 Also, our data suggest that the PARPi cytotoxicity primarily will affect the high PARP1  
49 expressing melanoma cells, rather than the low PARP1 expressing non-malignant skin  
50 cells resulting in only low side effects.

51

**52 Introduction**

53 Malignant melanoma, a skin cancer arising from mutated melanocytes, is a very  
54 aggressive tumor and patients have poor prognosis because of a high potential for  
55 metastasis to distant organs <sup>1</sup>. At the moment, patients with mutated mitogen-activated  
56 protein kinase (MAPK) signalling pathway profit from a combination therapy of BRAF  
57 inhibitors and MEK inhibitors <sup>2</sup>. Despite the good efficacy of the targeted therapy,  
58 several molecular mechanisms that lead to acquired resistance after long-term  
59 treatment restrict the positive outcome <sup>3</sup>. Melanoma patients also benefit from  
60 checkpoint inhibitors; however, the success of immunotherapy is limited due to  
61 tolerability and response rate issues <sup>4</sup>. Therefore, it is of major importance to  
62 investigate possible new therapeutic options for melanoma patients.

63 Poly (ADP-ribose) polymerase (PARP) inhibitors (PARPi) are the first FDA and EMA  
64 approved anti-cancer drugs to directly target the DNA damage response. PARP1 is a  
65 major regulator of the DNA repair mechanism termed base excision repair (BER). By  
66 acting as nicotinamide adenine dinucleotide (NAD<sup>+</sup>) analogue, PARPi block the  
67 PARylation process of PARP1, which results in inefficient BER. Moreover, PARP1 can  
68 no longer auto-PARylate itself, resulting in stalled replication forks by the inability of  
69 PARP1 to dissociate from the DNA and ultimately the induction of double strand breaks  
70 (DSB), which exert the major cytotoxic function of PARPi therapy. This phenomenon  
71 is termed as PARP trapping effect <sup>5</sup>.

72 In our previous recent study, we showed that PARPi effectively reduce the growth of  
73 MAPK inhibitor resistant melanoma cells and synergize with MAPK inhibitors through  
74 a synthetic lethal interaction highlighting the importance of PARPi treatment for  
75 melanoma patients in a clinical setting <sup>6</sup>. Furthermore, patients with a homologous  
76 recombination repair (HRR) deficiency (HRD), and thereby the inefficiency to repair  
77 DSB, particularly profit from PARPi therapy <sup>7</sup>. However, additional biomarkers might  
78 even further predict the response to PARPi therapy, independent of HRD. Therefore,  
79 we aimed to unravel the influence of PARP1 expression levels in melanoma cells on  
80 PARPi therapy response. Furthermore, we wanted to find out whether PARP1  
81 expression levels might have an impact on melanoma progression and prognosis.

**82 Materials and Methods****83 Cell Culture**

84 The human melanoma cell lines A375 (RRID:CVCL\_0132) and SKMel28  
85 (RRID:CVCL\_0526) were purchased from ATCC. The remaining cells WM3211  
86 (RRID:CVCL\_6797), WM793 (RRID:CVCL\_8787), WM1552 (RRID:CVCL\_6472),  
87 Mel1617 (RRID:CVCL\_DG51), 1205Lu (RRID:CVCL\_5239), WM3248  
88 (RRID:CVCL\_6798), BLM (RRID:CVCL\_7035), and SKMel19 (RRID:CVCL\_6025)  
89 were received from M. Herlyn (Wistar institute, Philadelphia, USA). All cell lines were  
90 cultured in RPMI1640 medium (Gibco, 21875034) containing 10% fetal bovine serum  
91 (Sigma-Aldrich, F9665) and 1% penicillin and streptomycin (Gibco, 11548876) at 37°C  
92 and 5% CO<sub>2</sub>. The cell lines were regularly tested for mycoplasma contamination using  
93 the Venor GeM Classic Mycoplasma Detection Kit (Minderva Biolabs, 11-1025) and  
94 were authenticated by STR profile analysis (Microsynth). Primary human fibroblasts  
95 were isolated from human foreskin after routinely circumcision from the Loretto Clinic  
96 Tübingen upon informed consent of the patients as previously described<sup>8</sup>. Fibroblast  
97 isolation from human foreskin was approved by the ethics committee of the medical  
98 faculty of the University Tübingen (654/2014BO2) and performed according to the  
99 principles of the Declaration of Helsinki.

**100 Viability Analysis and Inhibitors**

101 Cell viability was analysed with the 4-methylumbelliferyl heptanoate (MUH) assay as  
102 previously described<sup>6</sup>. Cells were treated with talazoparib (Medchemexpress,  
103 HY16106) or olaparib (Medchemexpress, HY-10162) for 72h. Experiments were  
104 performed in technical quintuplicates.

**105 RNA Isolation and RT-qPCR**

106 RNA isolation was performed with the help of the Nucleospin<sup>®</sup> RNA Kit (Macherey-  
107 Nagel 740955) according to the manufacturer's protocol. The cDNA was produced and  
108 RT-qPCR was performed as previously described<sup>6</sup>. RT-qPCR was performed with the  
109 Lightcycler<sup>®</sup> 96 Instrument (Roche). The following primer sequences were used:  
110 PARP1 forward: CCAAGCCAGTTCAGGACCTCAT, PARP1 reverse:  
111 GGATCTGCCTTTTGCTCAGCTTC. Actin forward:  
112 CACCATTGGCAATGAGCGGTTC, Actin reverse: AGGTCTTTGCGGATGTCCACGT.  
113 Actin served as a housekeeping gene. Experiments were performed in technical  
114 triplicates.

**115 Immunoblot Assay**

116 Immunoblot analysis was performed as previously described <sup>6</sup>. Isolation of the  
117 chromatin bound fraction was performed using the Subcellular Protein Fractionation  
118 Kit for Cultured Cells (Thermofisher Scientific™, 78840) according to the  
119 manufacturer's protocol. Cells were treated with 0.005% methyl methane sulfonate  
120 (MMS, Thermofisher Scientific™, 156890050) to recruit PARP1 to the DNA and 2 μM  
121 talazoparib for 6h. The following primary antibodies were used: anti-PARP (CST 9542,  
122 1:1000) and anti-H2A.X (CST 2595, 1:1000). The following secondary antibodies were  
123 used: anti-mouse IgG, HRP-linked (CST 7076, 1:2000), anti-rabbit IgG, and HRP-  
124 linked (CST 7074, 1:2000).

**125 Transfection**

126 The melanoma cells A375 and SKMel28 were transiently transfected with either siRNA  
127 against PARP1 or with a PARP1 expressing plasmid (Origene, RC207085). The  
128 following siRNAs against PARP1 (siPARP1, Dharmacon, D-006656-02-0005) was  
129 used. For the transfection of the siRNA against PARP1, Lipofectamine RNAimax  
130 (Thermofisher Scientific™, 13778075) and for the PARP1 expressing plasmid,  
131 Lipofectamine3000 (Thermofisher Scientific™, L3000150) was used according to the  
132 manufacturer's protocol and as previously described <sup>6</sup>. 24h after the transfection  
133 process, cells were either harvested for RNA gene expression analysis or reseeded  
134 into 96 well plates for further MUH analysis.

**135 Migration and Invasion Assay**

136 Boyden chamber-based migration and matrigel invasion assay was performed as  
137 previously described <sup>6</sup>.  $8 \times 10^5$  cells were seeded onto the transwell inserts and 24h  
138 after the seeding, migrated or invaded cells were fixed and stained. Experiments were  
139 performed in triplicates and 9 images per group were quantified.

**140 Database Analysis**

141 The Kaplan-Meier curve of the TCGA SKCM 470 database of melanoma patients was  
142 generated with R2 Genomics Analysis and Visualization Platform (<https://r2.amc.nl>).  
143 The median was used to divide the patients into high PARP1 expression and low  
144 PARP1 expression and a survival curve for each group with a cut-off at 10 years was  
145 plotted. The GSE112509 dataset was used to compare the PARP1 gene expression  
146 between melanocytic nevi and primary melanomas and the GSE8401 as well as the  
147 TCGA SKCM 375 dataset was used to compare the PARP1 gene expression between

148 primary and metastatic melanomas. For correlation analysis of the respective datasets  
149 the DepMap portal was used (<https://depmap.org/portal/>). For analysis of the  
150 metastatic potential and the penetrance, the MetMap 500 dataset was utilized.  
151 Penetrance was defined as the percentage of mice detected with the cell line after  
152 cancer cell injection<sup>9</sup>. For the PARP1 gene expression, the DepMap Public 23Q2  
153 dataset was used and for the talazoparib and olaparib drug sensitivity, the PRISM  
154 Repurposing 19Q4 dataset was utilized.

#### 155 **Statistical Analysis**

156 All experiments were statistically analysed using GraphPad Prism version 9.1.2. Data  
157 that are statistically significant ( $p < 0.05$ ) were labelled with asterisks (\* for  $p < 0.05$ , \*\* for  
158  $p < 0.01$ , \*\*\* for  $p < 0.001$ , and \*\*\*\* for  $p < 0.0001$ ). Unless otherwise stated, statistical  
159 analysis was performed by unpaired t-test when two groups were compared to each  
160 other. For the analysis of the correlation between two datasets, a simple linear  
161 regression model was used. For the analysis of survival curves the R2 platform was  
162 used to compare the high PARP1 expression and low PARP1 expression groups. The  
163 median was used to divide high PARP1 expression and low PARP1 expression groups  
164 and a log rank test was performed to check for significant differences in the overall  
165 survival of the two groups.

166

167 **Results**

168 **PARP1 expression levels are predictive for overall survival and PARPi response**  
169 **in melanoma**

170 To analyse the potential role of PARP1 as a biomarker in melanoma, we correlated  
171 overall survival of melanoma patients with PARP1 expression levels in their tumors.  
172 Interestingly, overall survival analysis showed a significant difference in the prognosis  
173 of melanoma patients depending on PARP1 expression levels. Melanoma patients with  
174 high PARP1 expression have a significant lower overall survival probability compared  
175 to patients with low PARP1 expression (Figure 1A). We then split these patients into  
176 early stage patients without metastasis (stage 0-II) and late stage patients suffering  
177 from metastasis (stage III-IV). Interestingly, while no significant difference in overall  
178 survival between high and low PARP1 expressing patients in stage 0-II melanoma  
179 patients was seen, metastasized patients in stages III-IV with high PARP1 expression  
180 levels show significant worse outcome than late stage patients with low PARP1  
181 expression levels (Figure 1B, 1C).

182 To unravel the influence of PARP1 expression on PARPi response, we performed cell  
183 viability assays after PARPi treatment (olaparib or talazoparib) of melanoma cells,  
184 which express PARP1 at different levels. Indeed, a significant correlation between  
185 PARP1 RNA expression and PARPi sensitivity could be detected, with cells having  
186 high PARP1 expression showing a significantly better response to PARPi therapy  
187 (Figure 1D). Consistent with this, analysis of a correlation between the PRISM  
188 Repurposing 19Q4 and DepMap Public 23Q2 dataset checking for the drug sensitivity  
189 (olaparib and talazoparib) and PARP1 gene expression of various melanoma cells in  
190 vitro validated our results (Supplementary Figure S1A, S1B). RT-qPCR analysis  
191 revealed that fibroblasts show significant lower PARP1 gene expression levels  
192 compared to metastatic melanoma cells. In addition, we found an increase in PARP1  
193 gene expression between melanoma cells in radial growth phase (RGP), vertical  
194 growth phase (VGP) and metastatic melanoma cells (Figure 1E). In line with this, we  
195 could demonstrate that melanocytic nevi show significant reduced PARP1 gene  
196 expression levels compared to primary melanoma cells (Figure 1F).

197 To conclude, we found that in melanoma patients high PARP1 gene expression  
198 correlates with worse overall survival, especially in the metastasized patients and that  
199 the sensitivity towards PARPi positively correlates with PARP1 gene expression in  
200 melanoma patients and in melanoma cell lines. These data implicate, that especially

201 late stage metastasized patients with high PARP1 gene expression levels would profit  
202 from PARPi therapy with limited side effects on low PARP1 expressing benign cells.

### 203 **PARP1 trapping after PARPi treatment induces melanoma cell death**

204 Since the main cytotoxicity of PARPi therapy is known to be dependent on PARP  
205 trapping and thereby the induction of DSB, we were interested, if PARP1 expression  
206 levels correlate with trapped PARP1. Indeed, cells with high PARP1 gene expression  
207 and thereby increased PARPi sensitivity, such as A375 (see Figure 1D), show clearly  
208 enhanced chromatin bound PARP after talazoparib treatment, whereas cells with low  
209 PARP1 gene expression and thereby reduced PARPi sensitivity, such as SKMel28  
210 (see Figure 1D), do not show this effect (Figure 2A). To support the hypothesis, that  
211 PARPi therapy induces higher PARP trapping and thereby more DSB in high PARP1  
212 expressing cells, we performed siRNA induced knockdown of PARP1 in A375 cells  
213 and subsequently treated them with PARPi. Strikingly, in high PARP1 expressing A375  
214 cells, the knockdown of PARP1 significantly desensitized these cells to olaparib and  
215 talazoparib treatment (Figure 2B, Supplementary Figure S1C). Vice versa, an  
216 upregulation of PARP1 expression via plasmid transfection led to a clear sensitization  
217 of low PARP1 expressing SKMel28 cells to olaparib and talazoparib treatment (Figure  
218 2C, Supplementary Figure S1D).

219 These data indicate that PARP1 expression correlate with a higher PARP trapping  
220 effect after PARPi therapy and a higher killing efficiency.

### 221 **PARP1 expression level correlates with metastatic potential of melanoma cells**

222 To analyse the influence of PARP1 expression on the metastasis potential of  
223 melanoma cells, we analysed PARP1 gene expression in primary versus metastatic  
224 melanoma samples in two datasets. Interestingly, we found a significant lower RNA  
225 expression of PARP1 in the primary melanoma group compared to the metastatic  
226 melanoma group (Figure 3A). When analysing the role of PARP1 in metastasis  
227 formation and metastatic penetrance of melanoma cells line, a trend was observed,  
228 confirming that PARP1 might positively influence the metastatic potential of  
229 melanomas (Figure 3B, 3C).

230 Furthermore, we checked for differences in the migratory and invasive potential of high  
231 PARP1 expressing A375 and low PARP1 expressing SKMel28 cells. As expected, the  
232 migratory and invasive potential of high PARP1 expressing A375 melanoma cells was

233 significantly enhanced compared to low PARP1 expressing SKMel28 melanoma cells  
234 (Figure 3D, 3E).

235 Taken together, we show that high PARP1 gene expression levels correlate with  
236 increased metastatic potential and penetrance of melanoma cells and enhanced  
237 migratory and invasive capacity.

238

**239 Discussion**

240 This study shows the importance of basal PARP1 gene expression on sensitivity  
241 towards PARPi therapy. Elevated PARP1 levels were associated with higher PARP1  
242 trapping after PARPi treatment leading to high cytotoxicity in these cells. Upregulation  
243 of PARP1 sensitized low PARP1 expressing cells to PARPi therapy, and vice versa,  
244 downregulation of PARP1 desensitized high PARP1 expressing melanoma cells to  
245 PARPi treatment. We found that melanoma cells show significantly increased PARP1  
246 gene expression levels compared to non-malignant skin cells. Moreover, our data  
247 revealed that high PARP1 expression levels positively correlate with the metastatic  
248 and invasive potential of melanoma cells. Most strikingly, we were able to show that  
249 high PARP1 levels are associated with worse overall survival exclusively in late stage  
250 melanoma patients.

251 Currently, PARPi are FDA approved for the treatment of HRD cancers <sup>10</sup>. Our data  
252 indicate that that elevated PARP1 levels result in increased PARP trapping by PARP  
253 inhibitors, and thereby higher cytotoxicity. Consistent with another study, we here show  
254 that PARP1 therefore could serve as a useful biomarker to forecast PARPi response  
255 in cancer patients <sup>11,12</sup>. We therefore propose that, in addition to testing the HRD status  
256 of patients before receiving PARPi therapy, PARP1 gene expression levels should be  
257 analysed to further predict PARPi therapy success.

258 In this study we demonstrate, that PARP1 expression levels correlate with increased  
259 invasiveness and metastatic potential of melanoma cells. These results go in line with  
260 many further publications stating that PARP1 activates metastatic features in  
261 melanoma cells and thereby acts as a marker of an aggressive clinical phenotype <sup>13-</sup>  
262 <sup>16</sup>. Interestingly, together with other publications, we additionally found that PARP1  
263 gene expression is significantly increased in melanomas compared to non-malignant  
264 skin cells, such as fibroblasts or melanocytic nevi <sup>16</sup>. With this, we suggest that  
265 undesirable side effects of PARPi therapy targeting non-cancerous cells should be  
266 comparably low.

267 Our data indicate, that PARP1 is associated with a worse overall survival of melanoma  
268 patients. Indeed, various other publications demonstrated that high PARP1 expressing  
269 cancer patients showed poor overall survival, and vice versa, low PARP1 expression  
270 correlated with significant better overall survival <sup>13,16-20</sup>. To our knowledge, this is the  
271 first publication to show that the decreased survival probability of high PARP1  
272 expressing cancers is dependent on the tumor stage, and that only in late stage

273 metastatic melanoma patients (stage III-IV), a significant difference in overall survival  
274 between low and high PARP1 expressing patients is evident.

275 Taken together, our study reveals that PARP1 might be an effective biomarker to  
276 forecast PARPi response. We suggest that patients with late stage metastatic  
277 melanoma should be screened for PARP1 gene expression. Patients who exhibit high  
278 PARP1 gene expression should additionally be screened for HRD, as we expect a poor  
279 overall survival. We suggest that patients with high PARP1 expression and an HRD  
280 should receive PARPi therapy. Together with our previous results, we propose that  
281 patients displaying high PARP1 levels but are proficient in HRR should profit from a  
282 combination of PARPi therapy plus MAPKi therapy, since MAPKi therapy in BRAF  
283 mutated melanoma cell lines induces an HRD phenotype and thereby act synthetic  
284 lethal in combination (see graphical abstract) <sup>6</sup>.

285

286 Author Contributions: B. Schitteck: Conceptualization, Funding acquisition,  
287 Investigation, Methodology, Supervision, Writing – original draft. L.M. Fröhlich:  
288 Conceptualization, Wet lab experiments, Formal Analysis, Investigation, Methodology,  
289 Visualization, Writing – original draft.

290 Conflict of Interest: The authors declare no potential conflict of interests.

291 Data Availability Statement: The data generated in this study are available upon  
292 request from the corresponding author. The following publicly available databases  
293 were used: TCGA SKCM 470 rsem, TCGA SKCM 375 rsem, GSE112509, GSE8401,  
294 MetMap 500, DepMap Public 23Q2 and PRISM Repurposing 19Q4.

295 Funding: This work was supported by the Deutsche Forschungsgemeinschaft (DFG,  
296 German Research Foundation; SCHI 510/12–1) under Germany's Excellence  
297 Strategy—EXC2180–390900677 to B. Schitteck.

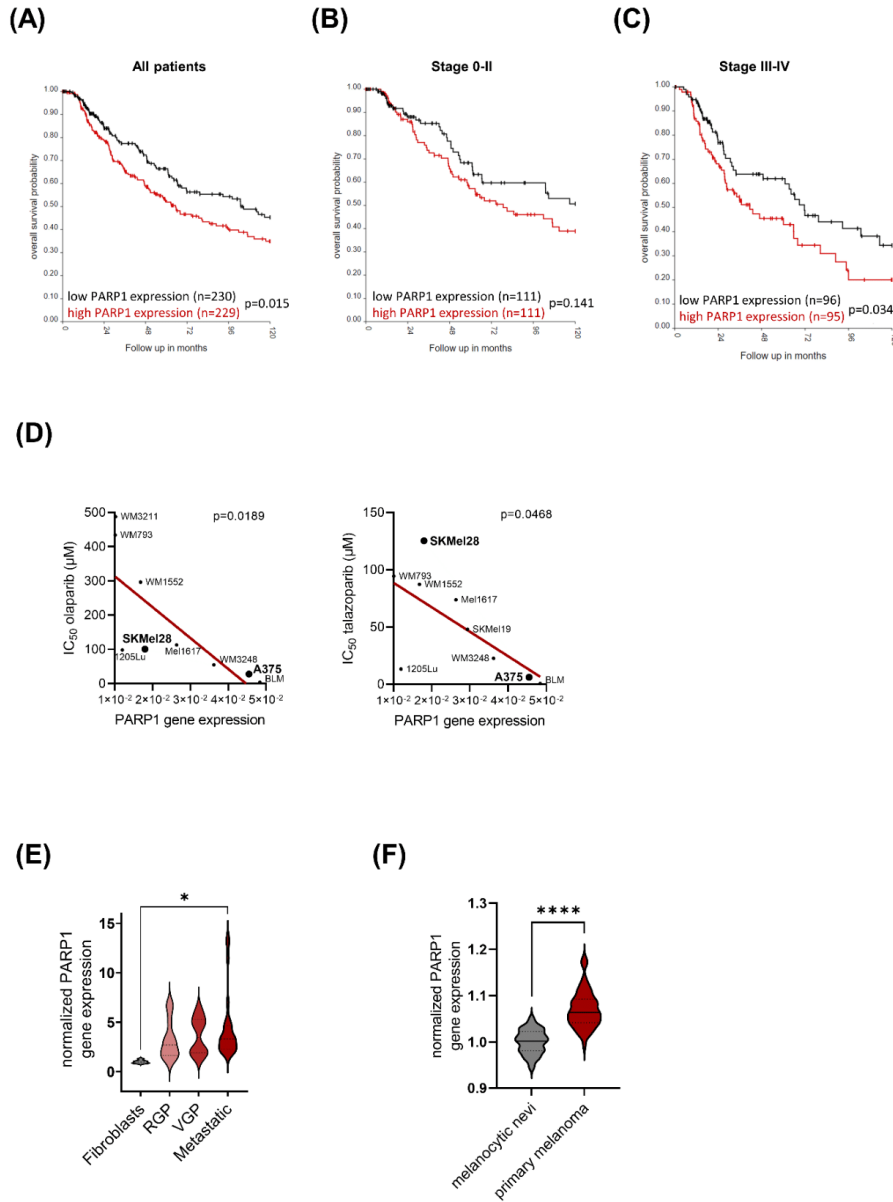
298 **References**

- 299 1. Gray-Schopfer V, Wellbrock C, Marais R. Melanoma biology and new targeted  
300 therapy. *Nature*. Feb 22 2007;445(7130):851-7. doi:10.1038/nature05661
- 301 2. Flaherty KT, Infante JR, Daud A, et al. Combined BRAF and MEK inhibition in  
302 melanoma with BRAF V600 mutations. *N Engl J Med*. Nov 1 2012;367(18):1694-703.  
303 doi:10.1056/NEJMoa1210093
- 304 3. Czarnecka AM, Bartnik E, Fiedorowicz M, Rutkowski P. Targeted Therapy in  
305 Melanoma and Mechanisms of Resistance. *Int J Mol Sci*. Jun 27  
306 2020;21(13)doi:10.3390/ijms21134576
- 307 4. Jenkins RW, Fisher DE. Treatment of Advanced Melanoma in 2020 and  
308 Beyond. *J Invest Dermatol*. Jan 2021;141(1):23-31. doi:10.1016/j.jid.2020.03.943
- 309 5. Rose M, Burgess JT, O'Byrne K, Richard DJ, Bolderson E. PARP Inhibitors:  
310 Clinical Relevance, Mechanisms of Action and Tumor Resistance. *Front Cell Dev Biol*.  
311 2020;8:564601. doi:10.3389/fcell.2020.564601
- 312 6. Froehlich LM, Niessner H, Sauer B, et al. PARP inhibitors effectively reduce  
313 MAPK inhibitor resistant melanoma cell growth and synergize with MAPK inhibitors  
314 through a synthetic lethal interaction in vitro and in vivo. *Cancer Research*  
315 *Communications*.
- 316 7. Yap TA, Sandhu SK, Carden CP, de Bono JS. Poly(ADP-ribose) polymerase  
317 (PARP) inhibitors: Exploiting a synthetic lethal strategy in the clinic. *CA Cancer J Clin*.  
318 Jan-Feb 2011;61(1):31-49. doi:10.3322/caac.20095
- 319 8. Bitschar K, Sauer B, Focken J, et al. Lugdunin amplifies innate immune  
320 responses in the skin in synergy with host- and microbiota-derived factors. *Nat*  
321 *Commun*. Jun 21 2019;10(1):2730. doi:10.1038/s41467-019-10646-7
- 322 9. Jin X, Demere Z, Nair K, et al. A metastasis map of human cancer cell lines.  
323 *Nature*. Dec 2020;588(7837):331-336. doi:10.1038/s41586-020-2969-2
- 324 10. O'Sullivan Coyne G, Karlovich C, Wilsker D, et al. PARP Inhibitor Applicability:  
325 Detailed Assays for Homologous Recombination Repair Pathway Components. *Onco*  
326 *Targets Ther*. 2022;15:165-180. doi:10.2147/OTT.S278092
- 327 11. Makvandi M, Xu K, Lieberman BP, et al. A Radiotracer Strategy to Quantify  
328 PARP-1 Expression In Vivo Provides a Biomarker That Can Enable Patient Selection  
329 for PARP Inhibitor Therapy. *Cancer Res*. Aug 1 2016;76(15):4516-24.  
330 doi:10.1158/0008-5472.CAN-16-0416
- 331 12. Sander Efron S, Makvandi M, Lin L, et al. PARP-1 Expression Quantified by  
332 [(18)F]FluorThanatrace: A Biomarker of Response to PARP Inhibition Adjuvant to  
333 Radiation Therapy. *Cancer Biother Radiopharm*. Feb 2017;32(1):9-15.  
334 doi:10.1089/cbr.2016.2133
- 335 13. Gajdzis M, Theocharis S, Klijanienko J, et al. The Prognostic Values of PARP-  
336 1 Expression in Uveal Melanoma. *Cells*. Jan 31 2021;10(2)doi:10.3390/cells10020285
- 337 14. Rodriguez MI, Peralta-Leal A, O'Valle F, et al. PARP-1 regulates metastatic  
338 melanoma through modulation of vimentin-induced malignant transformation. *Plos*  
339 *Genet*. Jun 2013;9(6):e1003531. doi:10.1371/journal.pgen.1003531
- 340 15. Kupczyk P, Simiczjew A, Marczuk J, et al. PARP1 as a Marker of an  
341 Aggressive Clinical Phenotype in Cutaneous Melanoma-A Clinical and an In Vitro  
342 Study. *Cells*. Jan 31 2021;10(2)doi:10.3390/cells10020286
- 343 16. Mou K, Zhou Y, Mu X, Zhang J, Wang L, Ge R. PARP1 Is a Prognostic Marker  
344 and Targets NFATc2 to Promote Carcinogenesis in Melanoma. *Genet Test Mol*  
345 *Biomarkers*. Nov 2022;26(11):503-511. doi:10.1089/gtmb.2021.0214

- 346 17. Zhang Z, Dou X, Yang H, et al. Association of expression of p53, livin, ERCC1,  
347 BRCA1 and PARP1 in epithelial ovarian cancer tissue with drug resistance and  
348 prognosis. *Pathol Res Pract*. Feb 2020;216(2):152794. doi:10.1016/j.prp.2019.152794  
349 18. Huang YH, Yin SJ, Gong YY, et al. PARP1 as a prognostic biomarker for human  
350 cancers: a meta-analysis. *Biomark Med*. Nov 2021;15(16):1563-1578.  
351 doi:10.2217/bmm-2020-0891  
352 19. Afzal H, Yousaf S, Rahman F, et al. PARP1: A potential biomarker for gastric  
353 cancer. *Pathol Res Pract*. Aug 2019;215(8):152472. doi:10.1016/j.prp.2019.152472  
354 20. Donizy P, Wu CL, Mull J, et al. Up-Regulation of PARP1 Expression Significantly  
355 Correlated with Poor Survival in Mucosal Melanomas. *Cells*. May 5  
356 2020;9(5)doi:10.3390/cells9051135  
357  
358

359 **Figures:**

**Figure 1: PARP1 levels are predictive for overall survival and PARPi response in melanoma**



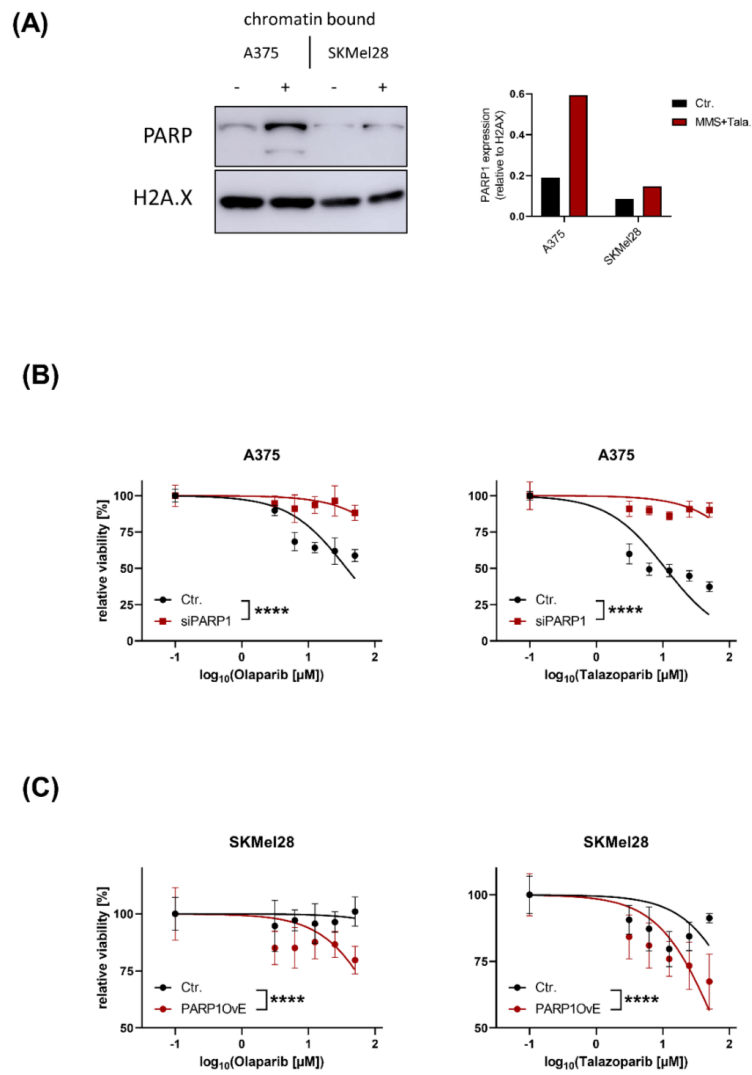
360

361 **Figure 1: PARP1 levels are predictive for overall survival and PARPi response in**  
362 **melanoma**

363 **(A-C)** Kaplan Meier curve of overall survival of 459 melanoma patients **(A)** of the TCGA  
364 SKCM 470 dataset divided into stage 0, I, Ia, Ib, IIa, IIb, IIc **(B)** and stage III, IIIa, IIIb,  
365 IIIC, and IV **(C)** grouped into high and low PARP1 expression. Median was used to  
366 define the cutoff between high and low PARP1 expression. R2 was used to plot the  
367 graph and perform statistical analysis. **(D)** MUH cell viability assay was performed after  
368 treatment of melanoma cells with different concentrations of olaparib or talazoparib for  
369 72h. IC<sub>50</sub> was calculated. PARP1 gene expression of the respective cells is shown.  
370 The correlation between the IC<sub>50</sub> levels and the PARP1 expression was analysed using  
371 the simple linear regression model. **(E)** Gene expression of PARP1 of 6 fibroblasts, 12  
372 melanoma cells in radial growth phase (RGP), 6 melanoma cells in vertical growth  
373 phase (VGP) and 27 metastatic melanoma cells is shown. Unpaired t-test was used to  
374 compare the two groups. **(F)** GSE112509 dataset was used to compare PARP1 gene  
375 expression between 23 melanocytic nevi and 57 primary melanomas. Unpaired t-test  
376 was used to compare the two groups.

377

**Figure 2: PARP1 trapping of PARPi treatment induces melanoma cell death**



378

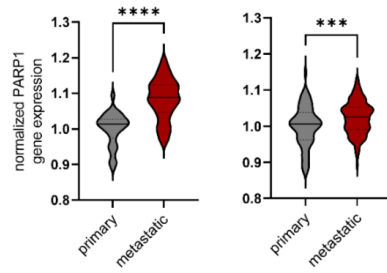
379

380

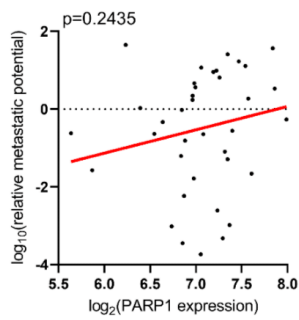
381 **Figure 2: PARP1 trapping after PARPi treatment induces melanoma cell death**  
382 **(A)** Immunoblot analysis of chromatin bound fraction of A375 and SKMel28 cells after  
383 the treatment with 0.005% MMS plus 2  $\mu$ M talazoparib (+) or untreated cells (-) for 6 h.  
384 **(B)-(C)** MUH cell viability assay of SKMel28 and A375 melanoma cell lines treated with  
385 different concentrations of PARPi (olaparib and talazoparib) for 72 h. PARP1  
386 knockdown (siPARP1) and control (Ctr.) cells (**(B)**) or PARP1 overexpression  
387 (PARP1OvE) and control (Ctr.) (**(C)**) transfected cells were used. The treatment started  
388 24 h after the transfection process. Comparison of fits of the nonlinear regression was  
389 performed to analyse statistical differences between the untransfected and transfected  
390 cells.  
391

**Figure 3: PARP1 expression levels correlate with invasiveness and metastatic potential of melanoma cells**

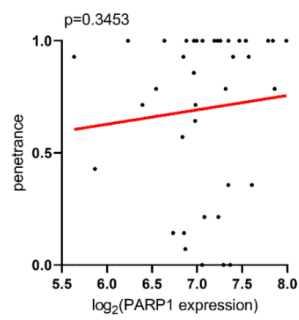
(A)



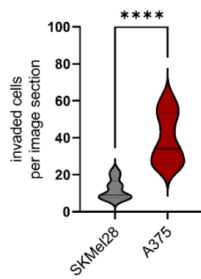
(B)



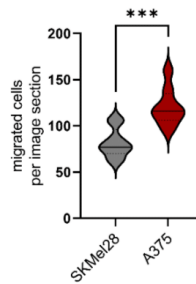
(C)



(D)



(E)



392

393

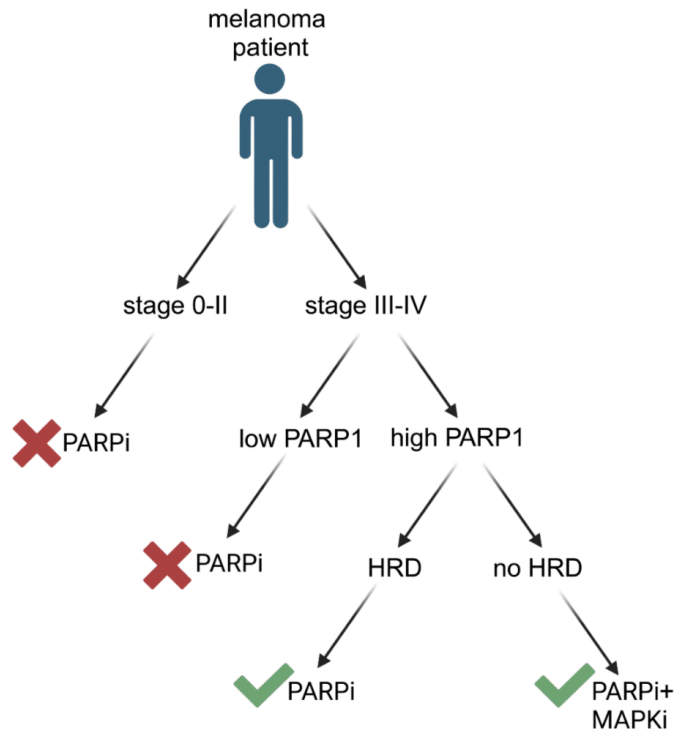
394

395 **Figure 3: PARP1 expression levels correlate with invasiveness and metastatic**  
396 **potential of melanoma cells**

397 **(A)** GSE8401 dataset (left) and TCGA SKCM 375 (right) was used to compare PARP1  
398 gene expression between 23 primary melanomas and 57 metastatic melanomas (left)  
399 or 65 primary melanomas and 266 metastatic melanomas (right). Unpaired t-test was  
400 used to compare the two groups. **(B)** The relative metastatic potential in brain, lung,  
401 liver, bone, and kidney using the MetMap 500 data compared to PARP1 expression  
402 using the DepMap Public 23Q2 of melanoma cells is shown. The correlation between  
403 the relative metastatic potential and the PARP1 expression was analysed using the  
404 simple linear regression model. **(C)** The penetrance in brain, lung, liver, bone, and  
405 kidney using the MetMap 500 data compared to PARP1 expression using the DepMap  
406 Public 23Q2 is shown. The correlation between the penetrance and the PARP1  
407 expression was analysed using the simple linear regression model. **(D)-(E)** Migration  
408 and invasion assay using SKMel28 and A375 cells. The number of invaded **((D))** or  
409 migrated **((E))** cells per image section is shown. 9 images per group were analysed.  
410 Unpaired t-test was performed to compare the two groups.

411

Graphical Abstract

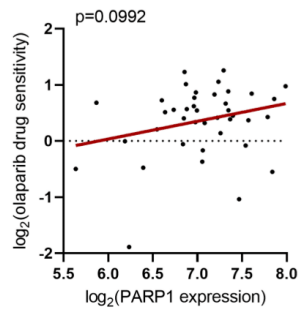


412

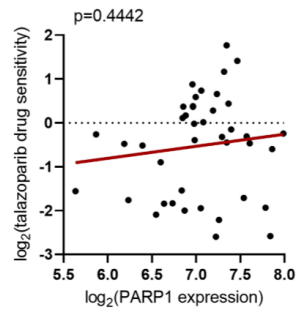
413

## Supplementary Figure S1

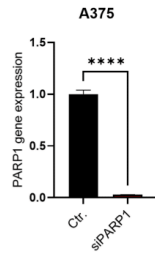
(A)



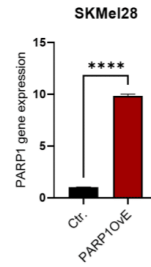
(B)



(C)



(D)



**Supplementary Figure 1:**

**(A)-(B)** PARPi drug sensitivity using the PRISM Repurposing 19Q4 data compared to PARP1 expression using the DepMap Public 23Q2 is shown. The correlation between olaparib (**(A)**) or talazoparib (**(B)**) drug sensitivity and the PARP1 expression was analysed using the simple linear regression model. **(C)-(D)** Relative gene expression of A375 cells after the transfection of siRNA against PARP1 (siPARP1) or control (Ctr.) **(C)** and of SKMel28 cells after the transfection of the PARP1 expressing plasmid (PARP1OvE) or control (Ctr.) **(D)**. Cells were harvested 24h after the transfection process. T-test was used to compare the two groups.

## 12. Acknowledgments

I would like to express my sincere gratitude to Birgit Schitteck for giving me the opportunity to work on this project and pursue PhD thesis in her lab. Thank you, Birgit, for always giving me the autonomy to concentrate on the projects that fascinated me the most. Additionally, I am immensely appreciative of the enjoyable company outings, whether kayaking, visiting the Wilhelma, or playing minigolf!

I am also deeply thankful to Lukas Flatz and his exceptional working group for fostering an excellent working atmosphere in our labs and offices.

A special thank goes out to all lab members that supported me in countless ways during my PhD journey. Jule, your daily companionship in the lab and the delightful hours we spent biking in the forest meant the world to me. Tobias, your invaluable support, and brilliant ideas when I faced challenges were true lifesavers. Heike, thank you for taking care of my mouse experiments during the times when I was bored at home having corona. Your willingness to lend a listening ear has been a tremendous source of comfort. Kathrin H., Efi, Sofie, and Mona, your assistance with lab work and data for my publications has been incredibly valuable. Kathrin S., the weekends spent in the lab were more enjoyable with your presence, and our memorable road bike tour and the delicious Germknödel will always be cherished. To Ana, Madeleine, Lena, Jasmin, and everyone else who accompanied me during my time here, my PhD years wouldn't have been the same without you all!

Last but not least, I want to express my heartfelt thanks to my family and friends who have been steadfast pillars of support throughout my entire PhD journey. Thank you for lifting my spirits during moments of frustration when experiments didn't go as planned. Mama, your constant listening ear, positive feedback, and valuable advice were of utmost importance. Papa, your wisdom in reminding me that work isn't everything and that relaxation is essential has been invaluable. I truly couldn't have made it this far without both of you! Michi, thank you for proofreading my manuscripts, even when you're not familiar with the subject matter. Basti, your patience in enduring my complaints, providing distractions when I was feeling frustrated, and your constant support in general have been a blessing beyond words.